

# **Investigation of three accessory subunits of complex I from *Yarrowia lipolytica***

## **Dissertation**

zur Erlangung des Doktorgrades  
der Naturwissenschaften

vorgelegt beim Fachbereich Biochemie, Chemie und Pharmazie  
der Johann Wolfgang Goethe Universität  
in Frankfurt am Main

von

**Krzysztof Dobrynin**

aus Lodz, Polen

Frankfurt am Main 2010

(D30)



Von Fachbereich Biochemie, Chemie und Pharmazie der  
Goethe Universität als Dissertation angenommen.

Dekan : Prof. Dr. D. Steinhilber

Gutachter : Prof. Dr. B. Ludwig  
Prof. Dr. U. Brandt

Datum der Disputation : 24.06.2010

---

**Teile der vorliegenden Arbeit wurden veröffentlicht:**

A. Abdrakhmanova, K. Dobrynin, K. Zwicker, S. Kerscher and U. Brandt. ‘Rhodanese is tightly associated with complex I from *Yarrowia lipolytica*, but not required for iron-sulfur cluster assembly’. *FEBS Letters*, 579 (2005) 6781–6785

K. Dobrynin, A. Abdrakhmanova, S. Richers, S. Kerscher and U. Brandt. ‘Complex I from *Yarrowia lipolytica* contains two different acyl carrier proteins’. *Biochimica et Biophysica Acta* 1797 (2010) 152–159

Die vorliegende Arbeit wurde in der Zeit von Januar 2005 bis Juni 2009 im Gustav-Emden Zentrum der Biologischen Chemie, Molekulare Bioenergetik, des Universitätsklinikums der Goethe Universität in Frankfurt am Main unter Anleitung von Prof. Dr. Ulrich Brandt durchgeführt.

## ACKNOWLEDGEMENTS

I sincerely thank Prof. Ulrich Brandt for giving me opportunity to work in the Molecular Bioenergetics lab, for providing financial support and necessary research facilities. His excellent scientific supervision, advice and continuous support made it possible to complete this work.

I am grateful to Prof. Bernd Ludwig for taking the responsibility of external supervision.

I would like to thank Dr. Stefan Kerscher for scientific support in the molecular biology field and for outstanding scientific guidance throughout this project.

I would also like to thank:

Prof. Dr. Hermann Schägger and Dr. Ilka Wittig for scientific discussions and helpful suggestions to the electrophoresis and protein chemistry field

Dr. Volker Zickermann for introducing me to the world of complex I purification procedures

Dr. Klaus Zwicker for recording EPR spectra of complex I mutants

Dr. Sebastian Richers for performing the HPLC analysis of mitochondrial phospholipids

Dr. Albina Abdrakhmanova for support at first stages of my project

Dr. Alexander Galkin and Dr. Maja Tocilescu for stimulating discussions and valuable suggestions, as well as for being dear friends

Dr. Martina Ding for help with translation of the summary into German language  
Dipl.-Ing. Gudrun Beyer for valuable hints in the molecular biology field

Andrea Duchene, Karin Siegmund and Ilka Siebels for excellent technical assistance

Andrea Böttcher for being always ready to cope with IT problems

Lena Schmidt for great organisational skills and warm personality

I am very thankful to all group members for creating a nice working atmosphere.

Last, but not least, I would like to thank Blanka for being always there. We made it together!

Finally, I am grateful to my parents and my brother for continuous support and for having faith in me.



*Pracę dedykuję rodzicom i Grzesiowi...*





---

**INDEX OF CONTENTS**

INDEX OF CONTENTS .....	I
1. INTRODUCTION .....	1
1.1 Mitochondrial respiratory chain .....	1
1.2 NADH:ubiquinone oxidoreductase .....	4
1.3 Accessory subunits .....	7
1.4 Biogenesis of complex I.....	10
1.5 Complex I from <i>Yarrowia lipolytica</i> .....	11
1.6 Acyl carrier proteins.....	12
1.6.1 Fatty acid synthesis .....	16
1.6.2 Significance of ACPs in biosynthetic pathways other than FAS .....	19
1.6.3 Mitochondrial acyl carrier proteins.....	20
1.6.4 Mitochondrial fatty acid synthesis .....	21
1.6.5 Mitochondrial acyl carrier protein as complex I subunit.....	22
1.7 Thiosulfate sulfurtransferase (rhodanese).....	24
1.8 Goals of the study.....	27
2 MATERIALS AND METHODS.....	29
2.1 Materials.....	29
2.1.1 Chemicals .....	29
2.1.2 Phospholipid standards (Sigma).....	30
2.1.3 Inhibitors.....	30
2.1.4 Media and solutions .....	30
2.1.5 Strains .....	32
2.1.6 Plasmids.....	34
2.1.7 Enzymes.....	35
2.1.8 Antibodies.....	36
2.1.9 Instruments .....	37
2.1.10 Software .....	39

---

2.2	Methods of Molecular Biology.....	41
2.2.1	Deletion strains.....	41
2.2.2	DNA gel electrophoresis.....	41
2.2.3	Fill-in reaction of 5`-overhang .....	41
2.2.4	DNA-vector dephosphorylation .....	41
2.2.5	Phosphorylation of PCR-products .....	42
2.2.6	DNA extraction from agarose gels.....	42
2.2.7	Ligation.....	42
2.2.8	Preparation of electro-competent <i>Escherichia coli</i> cells .....	42
2.2.9	Transformation into <i>Escherichia coli</i> (electro-competent cells).....	42
2.2.10	Preparation of plasmid-DNA from <i>Escherichia coli</i> .....	42
2.2.11	DNA sequencing .....	43
2.2.12	Polymerase chain reaction (PCR) .....	43
2.2.13	Generation of point mutations.....	43
2.2.14	Southern blot .....	43
2.2.15	<sup>32</sup> P DNA labelling .....	44
2.2.16	Hybridisation of radio actively labelled DNA probes .....	44
2.2.17	Transformation of <i>Y. lipolytica</i> .....	44
2.2.18	Isolation of total DNA of <i>Y. lipolytica</i> .....	45
2.2.19	Sporulation.....	45
2.3	Methods of Protein Chemistry.....	46
2.3.1	Growth of <i>Y. lipolytica</i> .....	46
2.3.2	Preparation of intact mitochondria.....	46
2.3.3	Preparation of mitochondrial membranes in small amounts .....	47
2.3.4	Protein quantification.....	47
2.3.5	Mitochondrial fractionation.....	47
2.3.6	Localization of ACPM1-strepII and ACPM2-flag in mitochondria .....	
	by western blot analysis .....	48
2.3.7	StrepII-tag detection with streptavidin .....	48
2.3.8	Doubled SDS-polyacrylamide gel electrophoresis (dSDS-PAGE) .....	49

2.3.9	Two-dimensional blue-native SDS polyacrylamide gel electrophoresis (2D-BN/SDS PAGE).....	49
2.3.10	Silver-staining of 2D-SDS gels .....	49
2.3.11	Staining with nitro blue tetrazolium (NBT) .....	50
2.3.12	Measurement of NADH:HAR oxidoreductase activity .....	50
2.3.13	Measurement of complex I catalytic activity .....	50
2.3.14	Measurement of rhodanese activity .....	51
2.3.15	Purification of complex I.....	51
2.3.16	Reactivation of purified complex I .....	51
2.3.17	EPR-spectra .....	52
2.3.18	Protein analysis with the matrix assisted laser desorption ionization time of flight mass spectrometry (MALDI-TOF-MS).....	52
2.3.19	Sequence analysis.....	53
2.4	The phospholipid composition of mitochondria.....	53
2.4.1	Extraction of phospholipids for the TLC analysis .....	53
2.4.2	Thin layer chromatography (TLC).....	54
2.4.3	Extraction of phospholipids for HPLC analysis.....	54
2.4.4	Phospholipid analysis of <i>acpm2Δ</i> and <i>acpm2Δ::pS88A</i> with HPLC .....	54
2.4.5	Mass spectrometry of phospholipids .....	55
3	RESULTS.....	57
3.1	Acyl carrier proteins.....	57
3.1.1	Generation of ACPM deletion strains.....	57
3.1.2	Generation of strains with exchanged serines binding the phosphopantethein moiety ....	61
3.1.3	The tagged versions of ACPMs .....	63
3.1.4	Consequence of the deletion of ACPM1 and ACPM2 genes.....	65
3.1.5	The mitochondrial lipid composition analysed by thin layer chromatography.....	70
3.1.6	The mitochondrial lipid composition analysed by HPLC .....	71
3.1.7	Identification of mitochondrial phospholipids with MALDI-TOF-MS .....	74
3.1.8	ACPM1 and ACPM2 are <i>bona fide</i> subunits of <i>Y. lipolytica</i> complex I.....	76
3.1.9	Sub-mitochondrial localization of ACPM1 and ACPM2.....	79

---

3.2	Exploration of the <i>st1</i> subunit of complex I from <i>Y. lipolytica</i> .....	81
3.2.1	Identification of a rhodanese-like protein in purified complex I .....	81
3.2.2	Generation of the <i>st1</i> deletion strain ( <i>st1Δ</i> ).....	84
3.2.3	Complementation of <i>st1Δ</i> strain with a plasmid carrying <i>st1-strepII</i> .....	87
3.2.4	Purified <i>Y. lipolytica</i> complex I displays rhodanese activity .....	89
3.2.5	The rhodanese deletion strain.....	89
4	DISCUSSION .....	95
4.1	Acyl carrier proteins.....	95
4.2	Rhodanese .....	102
4.3	Biosynthetic module of complex I - link between ACPMs and <i>st1</i> subunit .....	106
5	SUMMARY .....	109
6	OUTLOOK .....	111
7	AUSFÜHRLICHE DEUTSCHSPRACHIGE ZUSAMMENFASSUNG.....	113
7.1	Komplex I .....	113
7.2	Acyl-Carrier-Proteine.....	113
7.3	Rhodanese (Thiosulfat:Cyanid Sulfurtransferase) .....	114
7.4	Zielsetzungen .....	115
7.5	Ergebnisse .....	115
7.6	Fazit.....	119
7.7	Ausblick .....	120
8	REFERENCES .....	121
9	APPENDIX .....	139
9.1	Gene maps.....	139
9.1.1	The <i>st1</i> gene encoding the rhodanese .....	139
9.1.2	The ACPM1 gene locus .....	142
9.1.3	The ACPM2 gene locus .....	144
9.2	Oligonucleotides.....	146
9.2.1	Oligonucleotides for the <i>st1</i> gene.....	146
9.2.2	Oligonucleotides for ACPM1 gene.....	147
9.2.3	Oligonucleotides for the ACPM2 gene.....	148

9.2.4	Oligonucleotides for ACPM1 and ACPM2 genes swap strategy .....	149
9.2.5	Oligonucleotides for <i>URA3</i> gene .....	149
9.3	Complex I subunits of <i>Yarrowia lipolytica</i> .....	150
9.4	Protein alignments .....	153
9.4.1	Alignment of ACPs from different species .....	153
9.4.2	Alignment of ACPM1 and ACPM2 subunits from <i>Y. lipolytica</i> .....	154
9.4.3	Alignment of the st1 subunit .....	154
9.4.4	Alignment of <i>S. cerevisiae</i> and <i>Y. lipolytica</i> mitochondrial FASII enzymes.....	158
9.5	The mass spectrometric analysis of mitochondrial phospholipids .....	165
9.6	Chemical Structures .....	169
9.6.1	Complex I Inhibitors .....	169
9.6.2	Fatty Acid Synthase Inhibitor.....	169
9.6.3	Phospholipids .....	169
9.6.4	Cofactors.....	170
9.6.5	Other Structures.....	171
10	ABBREVIATIONS .....	173
11	LIST OF FIGURES .....	177
12	LIST OF TABLES.....	181
13	CURRICULUM VITAE .....	183



# 1. INTRODUCTION

## 1.1 *Mitochondrial respiratory chain*

The mitochondrial electron transport chain (ETC) is a part of the oxidative phosphorylation (OXPHOS) metabolic pathway. Its components catalyze the transfer of electrons from nicotinamide adenine dinucleotide (NADH) or succinate produced in catabolic pathways onto molecular oxygen. The key constituents of the pathway (*Figure 1.1*) include four multi-subunit protein complexes embedded in the inner mitochondrial membrane (IMM):

- NADH:ubiquinone oxidoreductase (complex I),
- succinate:ubiquinone oxidoreductase (complex II),
- ubiquinol:cytochrome *c* oxidoreductase (complex III),
- cytochrome *c* oxidase (complex IV),

and the mobile electron carriers

- ubiquinone (Q),
- cytochrome *c*.

Most electrons enter the ETC through complex I, which oxidizes NADH. The electrons travel then over a number of redox centers such as iron-sulfur clusters (in complexes I, II and III), hemes (in complexes II, III and IV) and flavins (flavin mononucleotide (FMN) or flavin adenine dinucleotide (FAD) in complexes I and II). An alternative electron entry side is constituted by the succinate:ubiquinone oxidoreductase or complex II, which is a member of both, the ETC and the citric acid cycle. The electron transfer is coupled to a vectorial proton translocation across the inner mitochondrial membrane performed by complex I, III and IV. The proton translocation creates a chemiosmotic potential, which is utilized by the F<sub>1</sub>F<sub>0</sub>-ATP synthase (complex V) for the regeneration of ATP from adenosine diphosphate (ADP) [1].

Mitochondria from different organisms contain up to four alternative dehydrogenases [2] and a non-heme alternative oxidase [3;4] in addition to the main components of the ETC.

These simple enzymes catalyze the same redox reaction as their multi-subunit counterparts complex I and IV, respectively, though they are not able to pump protons.

A fraction of the electrons travelling through the ETC never manage to reduce molecular oxygen to water at complex IV. Instead, about 1% of the electrons escape at the level of complexes I and III reducing oxygen incompletely [5;6] thereby yielding reactive oxygen species (ROS) such as the superoxide anion ( $O_2^{\cdot-}$ ). These highly reactive molecules play an important role in cellular signaling; however, its excessive production leads to oxidative stress and eventually to the cell damage.

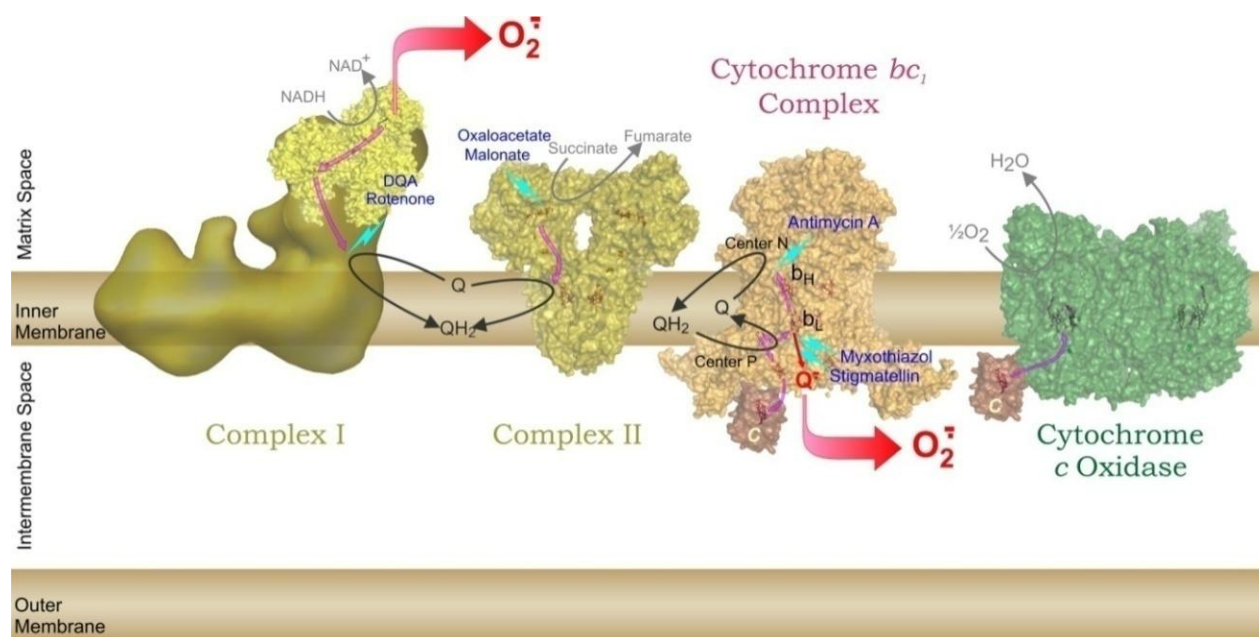


**Figure 1.1 Schematic representation of the mitochondrial electron transfer chain**

A representation of the three dimensional structures of respiratory chain complexes I-IV embedded in the IMM is shown. Complex I is the only member of the ETC for which only the structure of the hydrophilic part is available. Substrates and products of the enzymatic reactions are shown in grey; inhibitors of the enzymes in blue. The black arrows indicate pathways of the quinone accepting electrons from complex I or II and delivering them to complex III. Violet arrows show the electron transfer pathways inside of the complexes and the solid red arrows indicate sites of the reactive oxygen species production at complexes I and III. Reprinted from [7]

The knowledge of three-dimensional structures, catalytic and regulatory properties of the respiratory chain complexes are of medical significance, since they are involved in the development of numerous human pathologies [8;9]. The detailed crystal structures for complex II [10], complex III [11;12] and complex IV [13;14] have already been obtained,



whereas the structure of complex V [15] is only partially available. Although complex I was first purified from bovine heart mitochondria almost 50 years ago [16], its detailed molecular structure is just partially emerging [17], and its mechanism is still elusive.

In the IMM the respiratory chain complexes are organized into larger assemblies called supercomplexes or respirasomes (*Figure 1.2A*) [18]. General functional advantages of respirasomes are catalytic enhancement, substrate channelling, sequestration of reactive intermediates, and structural stabilization of the individual complexes. These supercomplexes, formed by complexes I, III and IV, seem to interact with each other to form even larger supramolecular structures (*Figure 1.2B*) named "respiratory strings" [19]. Likewise, complex V monomers form dimers (*Figure 1.2C*) and assemble into a network of oligomeric ATP synthase that has been shown to stabilise and crucially modulate the tubular cristae morphology (*Figure 1.2D*) [20;21].

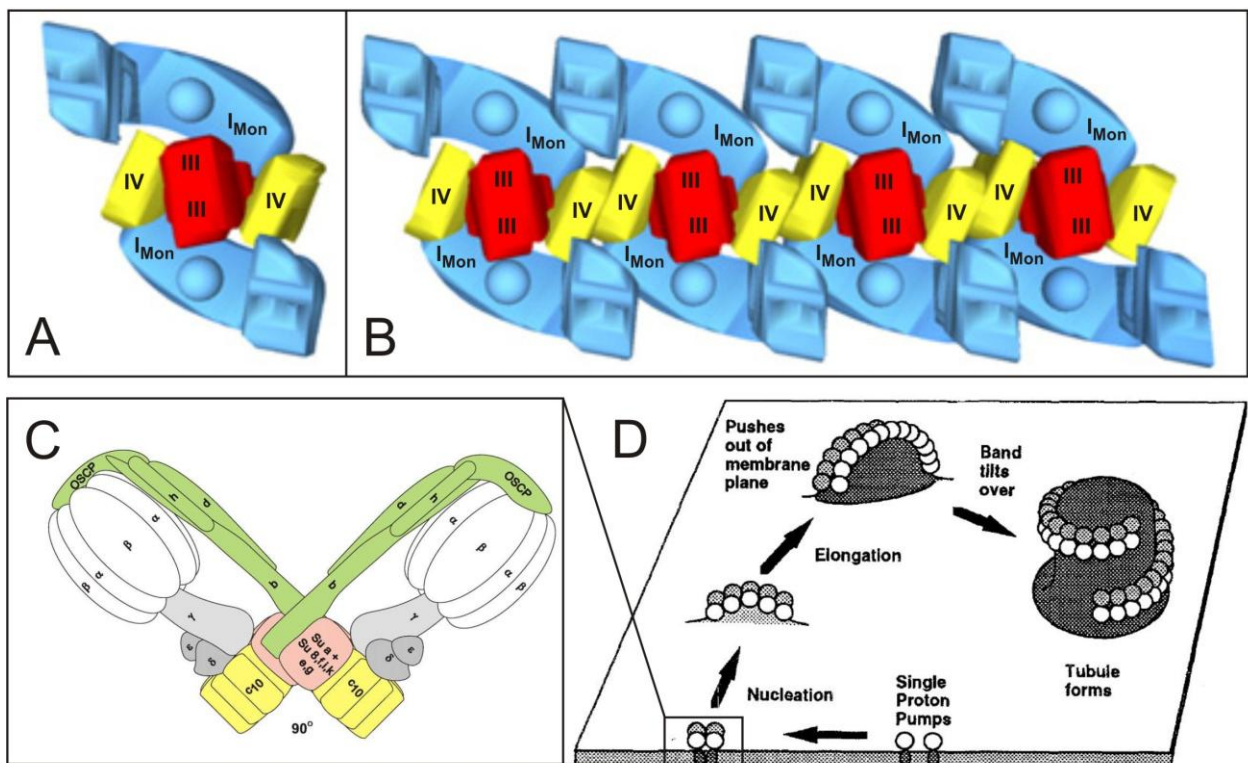


**Figure 1.2** *Supramolecular molecular structures of the respiratory chain complexes*

The respiratory supercomplexes composed of complexes I, III and IV (A) seem to interact with each other to form larger assemblies called 'respiratory strings' (B). Adapted from [22]; ATPase synthase dimers (C), reprinted from [23], oligomerise and take part in the modulation of the mitochondrial cristae morphology (D). Reprinted from [24].

---

## 1.2 NADH:ubiquinone oxidoreductase

Complex I (NADH:ubiquinone oxidoreductase, EC 1.6.5.3), the first electron transferring protein complex of the mitochondrial respiratory chain, is one of the largest and most complicated membrane bound protein complexes known [25]. It catalyses the transfer of two electrons from NADH to ubiquinone, which is coupled to the translocation of four protons across the inner mitochondrial membrane [26]. The redox reaction can be summarized as follows:  $\text{NADH} + \text{ubiquinone} + 5\text{H}^+_{\text{Matrix}} \rightarrow \text{NAD}^+ + \text{ubiquinol} + 4\text{H}^+_{\text{Intermembrane space}}$ .

Almost all organisms possess complex I, however, in the fermenting yeasts *Saccharomyces* and *Kluyveromyces* complex I is absent [27-29] and alternative mitochondrial NADH:Q oxidoreductases [30] are the only enzymes feeding reducing equivalents from NADH into the electron transport chain. Moreover, a number of organisms like plants and some protists contain both complex I and alternative dehydrogenase [31;32]. Many mutations are known in complex I subunit genes that are associated with heritable diseases, including Parkinson's disease, Leber's hereditary optic neuropathy (LHON) and Leigh Syndrome [33;34].

Depending on the organism, eukaryotic complex I contains up to 45 subunits as in the first studied and still best characterised enzyme from bovine heart mitochondria [35], resulting in a total molecular mass of ~ 1,000 kDa [35;36]. Other eukaryotic model organisms used for complex I studies include the yeast *Y. lipolytica* [37], the fungus *N. crassa* [38], the green alga *Chlamydomonas reinhardtii* [39], and the plants *Arabidopsis thaliana* and *Sativa oryza* [40]. A simpler form of the proton-pumping NADH:ubiquinone oxidoreductase exhibiting a molecular mass of about 550 kDa exists in bacteria. 14 genes organized in a single *nuo* or *nqo* operon<sup>1</sup> [41] encode the hydrophilic and hydrophobic subunits of bacterial complex I [42] (*Table 9.18*, appendix). Recently, an additional subunit (Nqo15) was shown to co-purify with the bacterial core enzyme from *Thermus thermophilus*. This subunit is not encoded in the same operon and seems to be only present in the closest relatives of *T. thermophilus* [43].

Homologues of the bacterial subunits make up the core of mitochondrial complex I from mammals and fungi (*Table 9.18*, appendix) and are sufficient to perform all

bioenergetic functions. Sequence analysis reveals that these 14 ‘central’ subunits fall into two categories. Seven subunits ND1-6 and NDL4 are highly hydrophobic and are predicted to contain 57 transmembrane helices embedded in the IMM. Except for some plants, algae, and protists, they are encoded by the mitochondrial genome in most eukaryotes. The remaining seven hydrophilic peptides (75-kDa 51-kDa, 49-kDa, 30-kDa, 24-kDa, TYKY, PSST) are nuclear coded and contain binding motifs for all known redox prosthetic groups: NADH, flavin mononucleotide (FMN) and iron-sulfur clusters. This part of the complex is responsible for the dehydrogenase and ubiquinone reduction activity [44]. One FMN is non-covalently bound to the 51-kDa subunit and is the entry point for electron transfer from NADH via several iron-sulfur clusters [45;46] to ubiquinone. Results from different studies suggest the presence of eight to nine iron-sulfur clusters (6-7 [4Fe-4S] and 2 [2Fe-2S]) in complex I (*Figure 1.3*).

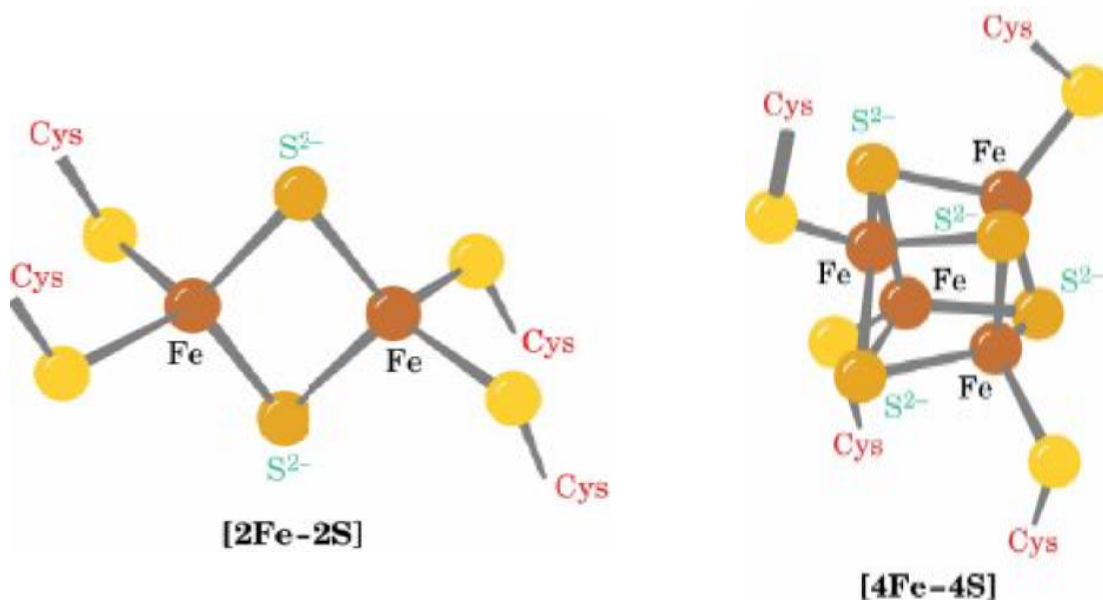


**Figure 1.3 Schematic representation of a binuclear and a tetranuclear iron-sulfur cluster**

Typically, iron-sulfur clusters are co-ordinated by sulfur atoms from four liganding cysteine residues (yellow). Acid-labile sulfur atoms are shown as orange spheres. Iron atoms are shown as red spheres. Figure adapted from [47].

<sup>1</sup> *nqo* for NADH:quinone oxidoreductase and *nuo* for NADH:ubiquinone oxidoreductase.

In the recently released bacterial X-ray structure of the peripheral arm of complex I from *T. thermophilus* (Figure 1.4A) [17] nine clusters designated N1a, N1b, N2, N3, N4, N5, N6a, N6b, N7 were present (Figure 1.4B). Similarly, all nine clusters were identified in *Escherichia coli* complex I [48]. Eukaryotic complex I possesses usually eight iron-sulfur clusters, but only six of them N1a, N1b, N2, N3, N4, N5 were detectable in bovine heart complex I [49] and only four clusters N1-N4 in *Neurospora crassa* [50]. The assignment of the EPR signals to particular clusters is still a matter of debate [51;52].

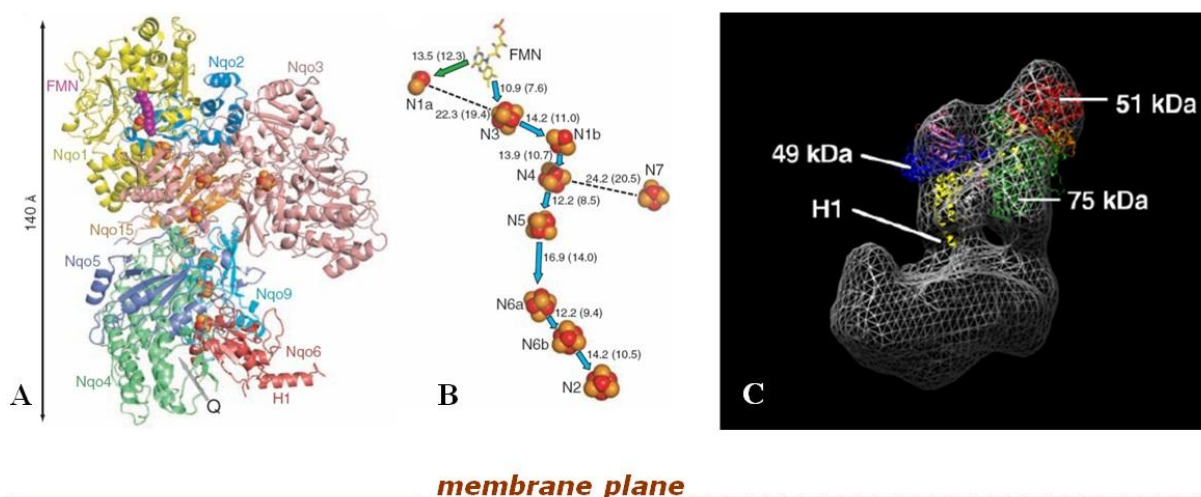


**Figure 1.4 Structure of the hydrophilic domain of complex I from *T. thermophilus* and electron microscopic reconstruction of *Y. lipolytica* enzyme**

The orientation of the X-ray structure of the peripheral domain from *T. thermophilus* (A) with respect to the membrane arm is a matter of current discussion. In the orientation proposed by [17] (A) the subunit Nqo4 (49-kDa) reaches the membrane arm and the H1 helix of the PSST subunit extends in the direction of the membrane distal part of the enzyme. In this orientation, arrangement of iron-sulfur clusters in the peripheral arm is perpendicular to the membrane (B) [17]. Nevertheless, increasing amount of evidence favors the orientation of the peripheral arm with iron-sulfur clusters arranged more parallel to the mitochondrial membrane [53] and H1 helix extending towards the membrane arm. Fitting of the bacterial X-ray structure (A) into the 3D reconstruction of complex I from *Y. lipolytica* in the orientation proposed by [53] is shown in (C).

The hydrophilic subunits of the peripheral part of the complex stand more or less perpendicular on one end of the intrinsic membrane arm and point toward the matrix side in mitochondria and to the cytoplasm in bacteria. This orientation results in an L-shaped particle [54-58] as revealed by electron microscopy studies from different eukaryotic and prokaryotic sources. A 3D-reconstruction of complex I from *Y. lipolytica* [53] represents this

characteristic complex I shape (*Figure 1.4C*), here fitted with the atomic structure of the hydrophilic part of the bacterial enzyme homologue from *T. thermophilus* (*Figure 1.4A*).

Phylogenetic studies of the central complex I subunits revealed similarity to different types of hydrogenases [59;60] and three functional modules of complex I were defined: the N module, comprising the electron entry site, the Q module or electron output module and the P module, responsible for proton translocation across the inner mitochondrial membrane. The N module comprises the 75-kDa, 51-kDa and 24-kDa, which are related to the  $\alpha$  and  $\gamma$  subunits of  $\text{NAD}^+$ -reducing hydrogenases [61]. These subunits contain redox cofactors, which transfer electrons from NADH via FMN to a wire of iron sulfur-clusters [45;46]. The Q module is composed of the 49-kDa, 30-kDa, PSST and TYKY subunits and mediates the transfer of electrons from the N module, via three further iron-sulfur clusters to ubiquinone. The 49-kDa subunit and the PSST subunits display homology to the large and small subunits, respectively, of water-soluble [NiFe] hydrogenases [62;63]. In *E. coli*, the 30-kDa subunit is fused to the 49-kDa subunit [42]. The P module is composed of seven, mitochondrially encoded and membrane-embedded subunits, ND1-ND6 and NDL4. Homology studies have shown that subunits ND2/ND4/ND5 are members of a family of proteins also comprising the *mrp* (multiple resistance and pH adaptation) type  $\text{Na}^+/\text{H}^+$  antiporters known for *Bacillus subtilis* and other bacteria [64;65]. These antiporters are commonly found in bacteria. It seems likely that the ion translocation functions of the *mrp* proteins were retained by homologous complex I subunits embedded in the membrane. Despite of the availability of the bacterial X-ray structure of the peripheral arm (*Figure 1.4A*) [17], the topology of membrane arm proton-pumping elements is still for the most part unclear [66]. Thus, the mechanism of coupling between electron transport and proton-pumping activity remains still elusive.

### ***1.3 Accessory subunits***

Over the course of evolution the minimal set of 14 ‘central’ subunits that make up the prokaryotic complex I was extended significantly by nuclear coded accessory subunits in eukaryotes. The function of accessory subunits is largely unknown, however certain insights

to the role of the subunits and their assignment to different parts of complex I has been achieved by analysing subcomplexes (*Figure 1.5*).

Purified bovine complex I was shown to dissociate upon treatment with non-denaturing detergents and chaotropes [67;68]. Using the detergent lauryldimethylamine oxide (LDAO), followed by ion-exchange chromatography, the bovine complex I was resolved into subcomplexes I $\alpha$  and I $\beta$  (*Figure 1.5*) [67;69]. Subcomplex I $\beta$  represents the major portion of the membrane part of complex I. Upon prolonged incubation in LDAO, fraction I $\alpha$  releases the predominantly hydrophilic subcomplex I $\lambda$  [70], which together with I $\beta$  is known as the hydrophobic protein (HP) [71]. The subcomplex I $\lambda$  can be further subdivided into the soluble, catalytically active flavoprotein subcomplex (FP) (*Figure 1.5*) comprising the FMN molecule, the NADH binding site, one [2Fe-2S] and one [4Fe-4S] cluster [72-74]. Also, a subcomplex referred to as the iron-protein (IP) composed of the 75-kDa, 49-kDa, 30-kDa, TYKY and PSST subunits was isolated [75].

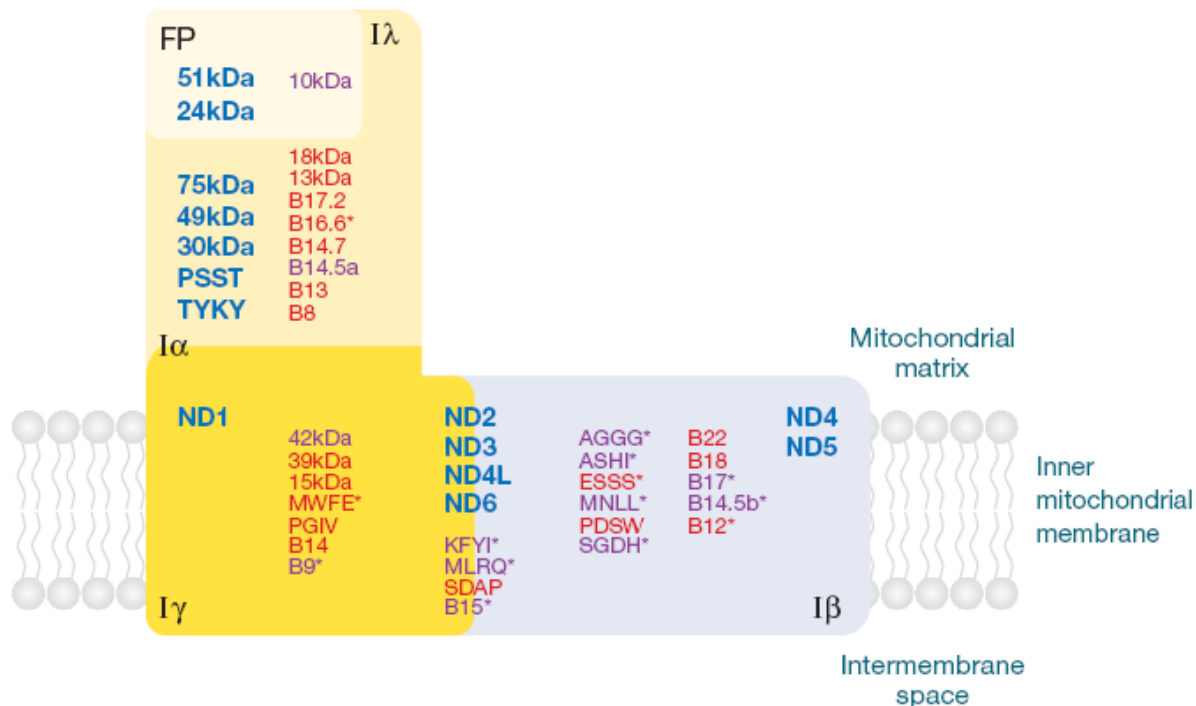


**Figure 1.5 Subcomplexes and subunits of bovine heart complex I**

Flavoprotein (FP) is a component of I $\lambda$  (light yellow), and I $\alpha$  essentially is a combination of I $\lambda$  and I $\gamma$  (yellow). I $\beta$  (blue gray) forms the major part of the membrane integral arm of complex I. Central subunits are in blue, accessory subunits found in all eukaryotic complexes are in red, and *Metazoa* specific subunits are in purple. Subunits marked with an asterisk are predicted to contain a single transmembrane domain [35]. Reprinted from [25].

Analysis of the subcomplexes by gel electrophoresis, Edman degradation and mass spectrometry [36] provided further information about the subunits. Some of them exhibit remarkable sequence similarities to other proteins. Depending on the organism the number of accessory subunits can be as high as 31 in bovine complex I (*Figure 1.5*) [35]; 18 accessory subunits have clear orthologs in mitochondria from all other lineages studied. With the exception of the fermenting yeast *S. cerevisiae*, which lacks not only the mitochondrial but also all nuclear genes of complex I [27] with the notable exception of the orthologue of mitochondrial acyl-carrier protein (SDAP). The type and number of the remaining up to 13 accessory subunits varies among species. The plant-specific subunits include isoforms of  $\gamma$ -type carbonic anhydrase [76]. These proteins form a distinct domain attached to the membrane arm, which confers an additional catalytic function to complex I [77].

Four accessory subunits contain several conserved cysteines (*Table 9.18*, appendix), thus it was proposed that these proteins may be involved in iron-sulfur cluster assembly [39;78]. Moreover, the NMR structure of the human subunit B8 revealed a  $\text{Fe}_2\text{S}_2$  ferredoxin fold similar to the one found in thioredoxin [79]. Subunit B14.7 exhibits some homology to components of the translocase of the inner membrane [69;80] and is therefore considered a member of the TIM17/22 family [69]. cAMP-dependent phosphorylation of several accessory subunits including ESSS, MWFE [81], 42-kDa subunit [82] and other post-translational modifications of complex I were observed. The 42-kDa subunit has some homology to bacterial deoxyribonucleotide kinase [83]. Subunit B16.6 [84] in mammals is identical to GRIM-19 (gene associated with retinoid-interferon induced mortality), an apoptosis-inducing factor [85;86]. GRIM-19 knockout mice are deficient for complex I assembly [87], but it remains unclear whether the presence of this protein in complex I is directly related to its proapoptotic function. It should be noted that subunit B16.6, but not its characteristic “death domain” of GRIM-19, is also conserved in fungi. Subunit B17.2 was first identified as DAP13 (a differentiation-associated protein) by an expression screen in proliferating human erythroid cells [88], but the link to complex I function is unclear. Subunit B17.2 is one of three accessory (*Table 9.18*, appendix) and two central complex I subunits (49 kDa and TYKY) that form tyrosine nitrates when mitochondria are incubated with peroxynitrite [89]. NADPH, which does not participate in the redox chemistry of

---

complex I is tightly bound as a cofactor to the 39-kDa subunit [90;91]. The sequence of this protein exhibits homologies to the family of short-chain dehydrogenases and contains a conserved NADPH-binding motif [64;92]. Some insight into functional characteristics of several accessory subunits has been obtained, but the significance of most of these findings is still unclear.

#### ***1.4 Biogenesis of complex I***

The eukaryotic complex I biogenesis is a complicated process, which requires a coordinated expression of nuclear and mitochondrial genomes. Nuclear-coded subunits destined for the mitochondria are synthesized in the cytosol and are directed to the matrix by the N-terminal presequence, which is subsequently cleaved off [93]. As for other respiratory chain complexes, it has been speculated that several accessory subunits are involved in organization of complex I assembly. This process has been the subject of several studies carried out on eukaryotic organisms like *N. crassa* and the green algae *C. reinhardtii* [94-96]. In *N. crassa* it has been shown that the peripheral arm and the membrane arm are formed independently [97]. Mutants lacking one of the nuclear encoded subunits of the peripheral arm were unable to assemble the hydrophilic arm but accumulated the membrane part of the enzyme. The absence of only the acyl carrier protein of complex I affected assembly of the membrane arm [98]. Similarly, the absence of mitochondrially encoded subunits of the membrane part did not prevent assembly of the hydrophilic arm. Both parts of the enzyme were shown to be assembly intermediates. In *N. crassa* the 49-kDa, 30-kDa, TYKY and PSST subunits are essential for association of the hydrophilic part [99]. For assembly of the membrane arm, subunits ND1-ND4, ND4L and ND6 are required and, interestingly, ND5 is not [99].

In bovine complex I, 14 subunits are classified as single transmembrane domain (STMD) proteins (*Table 9.18*, appendix). By readily inserting into the mitochondrial inner membrane, these proteins could promote and organize assembly of the mitochondrially encoded subunits by interacting with their highly hydrophobic transmembrane segments and then remain attached to the complex [37]. It is known that the hydrophobic arm is formed by association of two assembly intermediates which contain complex I-specific assembly



factors, called CIA30 and CIA84. These proteins are not components of mature complex I, but are essential for assembly of the membrane arm in *N. crassa* [100]. In human cells only a homolog of CIA30 could be found [101], but also another possible complex I chaperone, namely prohibitin, was identified [102].

Several findings suggest distinct assembly pathways of complex I in different organisms. In *N. crassa*, the AQDQ homologue is not essential for complex I assembly [103], whereas in human cells, mutations in the gene encoding this protein (*NDUFS4*) did affect complex I assembly [104]. It may be speculated that the biogenesis of complex I in different species occurs in different ways and may depend on its specific subunit composition. Despite of some progress made in complex I biogenesis studies, the picture emerging is still rather incomplete and not yet consistent.

### ***1.5 Complex I from Yarrowia lipolytica***

*Y. lipolytica* is a greatly advantageous model system for the structural and functional analysis of mitochondrial complex I [3]. The respiratory chain of this fast growing, non-pathogenic, obligate aerobic *Ascomycetes* yeast [105;106] is more similar to the respiratory chain in mammals than to that in fermentative yeasts like *S. cerevisiae*. In contrast to *S. cerevisiae* that does not contain complex I, *Y. lipolytica* features a permanently high content of mitochondria with constitutive expression of stable complex I. The completely sequenced genome of *Y. lipolytica* and a comprehensive set of well-developed genetic tools [3] made it possible to efficiently create mutations in complex I subunit genes. The generation of an internal version of the alternative dehydrogenase (NDH2i) [107-109] allowed for the survival of complex I deletion strains.

So far, 14 central and 26 accessory subunits have been identified in *Y. lipolytica* complex I (*Figure 1.6*), (*Table 9.18*, appendix), adding up a total mass of about 950 kDa [37;110]. All redox prosthetic groups NADH, FMN and eight iron-sulfur clusters (6 [4Fe-4S] and 2 [2Fe-2S]) are present, although only five, N1-N5 can be detected by EPR spectroscopy [58;111]. Three accessory subunits exhibit similarities to enzymes known from fatty acid metabolism and carry cofactors not involved in complex I electron transfer activity. The 39-kDa subunit possesses a tightly bound NADPH cofactor proposed to be involved in

stabilization of the multiprotein complex [91]. Moreover, *Y. lipolytica* complex I contains two pantetheine-4'phosphate cofactors bound to two different mitochondrial acyl carrier proteins (ACPMs).

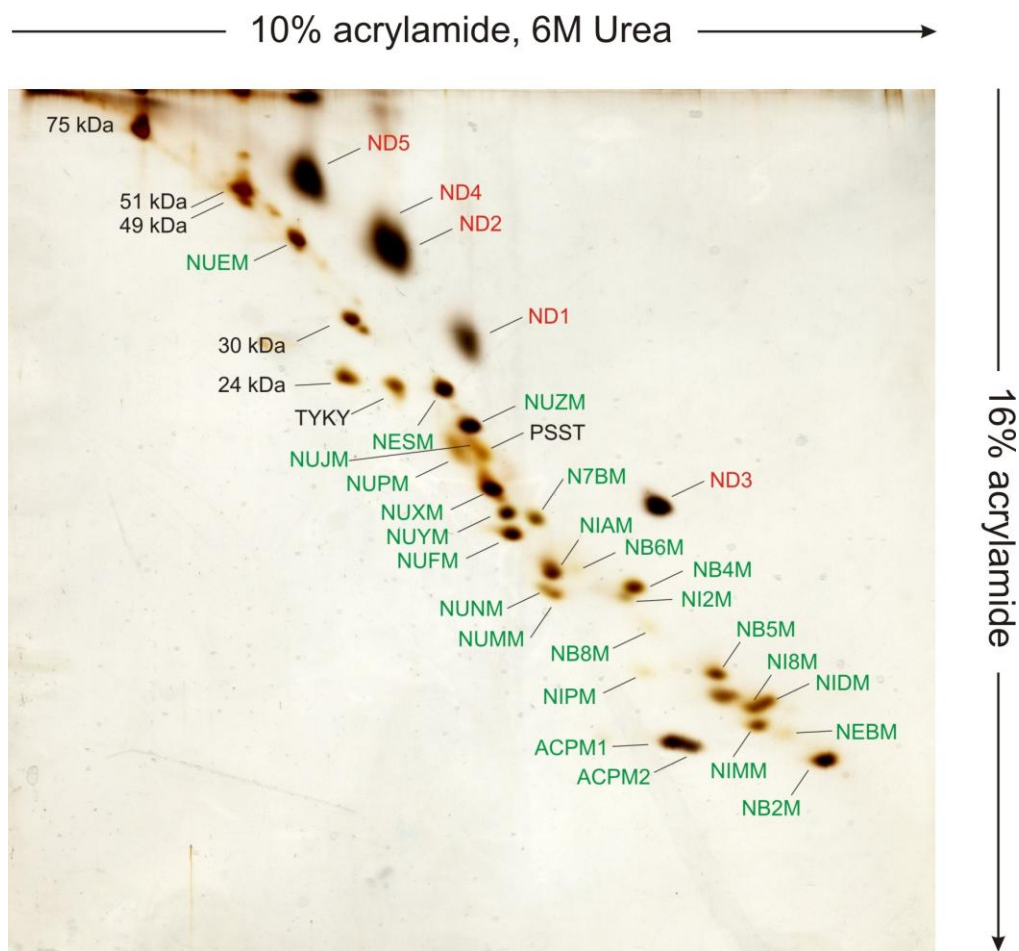


**Figure 1.6** The dSDS-PAGE of purified complex I from *Y. lipolytica*

Silver-stained doubled sodium dodecylsulfate-polyacrylamide gel electrophoresis (dSDS-PAGE) of a complex I crystal. The seven central, nuclear-coded subunits are labelled in black using bovine nomenclature and five of the seven central, mitochondrially coded subunits in red. Spots that could be assigned to the individual accessory subunits by mass spectrometry are labelled in green using the *Y. lipolytica* nomenclature.

### 1.6 Acyl carrier proteins

Acyl carrier proteins (ACPs) are small (~10 kDa) acidic proteins that play a central role in fatty acid synthesis (FAS) (Figure 1.7). These abundant proteins are essential cofactors shuttling fatty acid chain intermediates along components of the FAS pathway. More than

300 different ACP structures are available in the Protein Data Bank, of which the best characterized remains the *Escherichia coli* ACP [112]. ACPs are composed of a common four  $\alpha$ -helical bundle with a right-handed twist and a long structured loop connecting helices  $\alpha 1$  and  $\alpha 2$  (Figure 1.7A).

The *apo*-ACP is inactive and is post-translationally converted to an active *holo* form by *holo*-(ACP) synthase (AcpS) that transfers the pantetheine-4'-phosphate (PP) group from coenzyme A (CoA) to a highly conserved serine residue situated at the beginning of helix  $\alpha 2$  [113] (Figure 1.7A). This group is attached to ACP through a phosphodiester bond and serves as a platform for sulfhydryl bound acyl intermediates during fatty acid synthesis (Figure 1.8). NMR studies showed that a PP moiety lacking the acyl chain does not interact with the protein and is exposed to the solvent [114;115]. As soon as poorly water-soluble acyl chain is anchored to the PP cofactor, the acyl rest is accommodated in a plastic, hydrophobic cleft located in the vicinity of phosphopantethylated serine and flanked by helices  $\alpha 2$  and  $\alpha 3$  (Figure 1.7C). The reactive part of the growing fatty acyl chain including the thioester bond and groups at positions 1 to 3 is shielded by the ACP protein moiety. Since exposed fatty acids can be recognised by enzymes not belonging to the FAS and can be diverted for instance to fatty acid degradation ( $\beta$  oxidation) or regulatory signalling pathways, clearly protection is required for efficient progress of the fatty acid biosynthesis [116].

ACPs possess well conserved amino acid sequences (Table 1.1, Figure 9.4, appendix), especially in the vicinity of the PP-binding serine, as well as a highly conserved cluster of negatively charged residues on helix  $\alpha 2$  (Figure 1.7B). The so called 'universal recognition helix' is thought to be responsible for specific interactions with other FAS enzymes [117-122], which induces conformational changes in the ACP structure. Consequently, a protected fatty acid is released to the active site of a partner enzyme (Figure 1.7D) and finally, the modified substrate is reburied in the hydrophobic fold of the ACP. An interaction of *E. coli* ACP with the FASII enoyl reductase (Fab I) was captured in a 3D x-ray crystallographic structure [112].

Species, enzyme, NCBI accession	<i>Y. lipolytica</i> ACPM1		<i>Y. lipolytica</i> ACPM2		Subcellular location
	Similarity (%)	Identity (%)	Similarity (%)	Identity (%)	
<i>Y. lipolytica</i> ACPM1 (Q6c926)	(100)	(100)	81	63	Complex I
<i>H. influenzae</i> ACP (Q4qp33)	82	58	n.a. <sup>2</sup>	n.a.	Cytoplasm
<i>Y. lipolytica</i> ACPM2 (Q6c7x2)	81	63	(100)	(100)	Complex I
<i>S. pombe</i> ACP1 (Q10217)	80	68	66	48	Complex I
<i>E. coli</i> ACP (P0a6a8)	80	58	65	47	Cytoplasm
<i>H. pylori</i> ACP (Q1ctw7)	79	54	n.a.	n.a.	Cytoplasm
<i>A. thaliana</i> mtACP2 (O80800)	77	50	79	48	Matrix [123]
<i>T. guttata</i> ACP (B5G0K6)	77	44	70	43	Complex I
<i>N. crassa</i> ACPM (P11943)	76	64	68	53	Complex I
<i>A. thaliana</i> mtACP1 (P53665)	75	55	60	39	Matrix [123], Complex I
<i>C. reinhardtii</i> ACP1 (132151)	75	55	n.a.	n.a.	Mitochondria
<i>T. thermophilus</i> ACP (Q5SL79)	72	46	n.a.	n.a.	Cytoplasm
<i>S. cerevisiae</i> ACP1 (P32463)	70	52	69	43	Cytoplasm
<i>S. salar</i> ACPM (B5RI61)	70	46	55	34	Complex I
<i>H. sapiens</i> NDUFAB1	69	42	60	36	Complex I
<i>A. thaliana</i> mtACP3 (Q9fgj4)	68	45	n.a.	n.a.	Mitochondria
<i>O. sativa</i> ACP (O3g0352800)	64	47	n.a.	n.a.	Mitochondria
<i>M. musculus</i> ACPM (Q9cr21)	64	41	72	44	Complex I
<i>B. taurus</i> SDAP (P52505)	64	41	59	39	Complex I, Matrix [124]
<i>D. discoideum</i> AB1 (Q54e22)	62	40	61	36	Complex I
<i>D. melanogaster</i> ACPM (Q94519)	n.a.	n.a.	69	43	Complex I
<i>M. capsulatus</i> ACP (Q60616)	n.a.	n.a.	67	52	Cytoplasm
<i>P. troglodytes</i> ACP (Q0mqc3)	n.a.	n.a.	60	36	Complex I
<i>G. gorilla</i> ACP (Q0mqc2)	n.a.	n.a.	60	36	Complex I
<i>P. abelii</i> ACP (Q0mqc1)	n.a.	n.a.	60	36	Complex I

See next page for description.

<sup>2</sup> no significant similarity found.

**Table 1.1. Similarity and identity scores for pairwise comparisons between *Y. lipolytica* ACPM1 or ACPM2 and ACP from other organisms**

(previous page) The alignments were created using the GAP programme from the HUSAR ([genius.embnet.dkfz-heidelberg.de](http://genius.embnet.dkfz-heidelberg.de)) program package in standard mode. The probability of mitochondrial import was calculated using MitoProt II software (<http://ihg.gsf.de/ihg/mitoprot.html>).

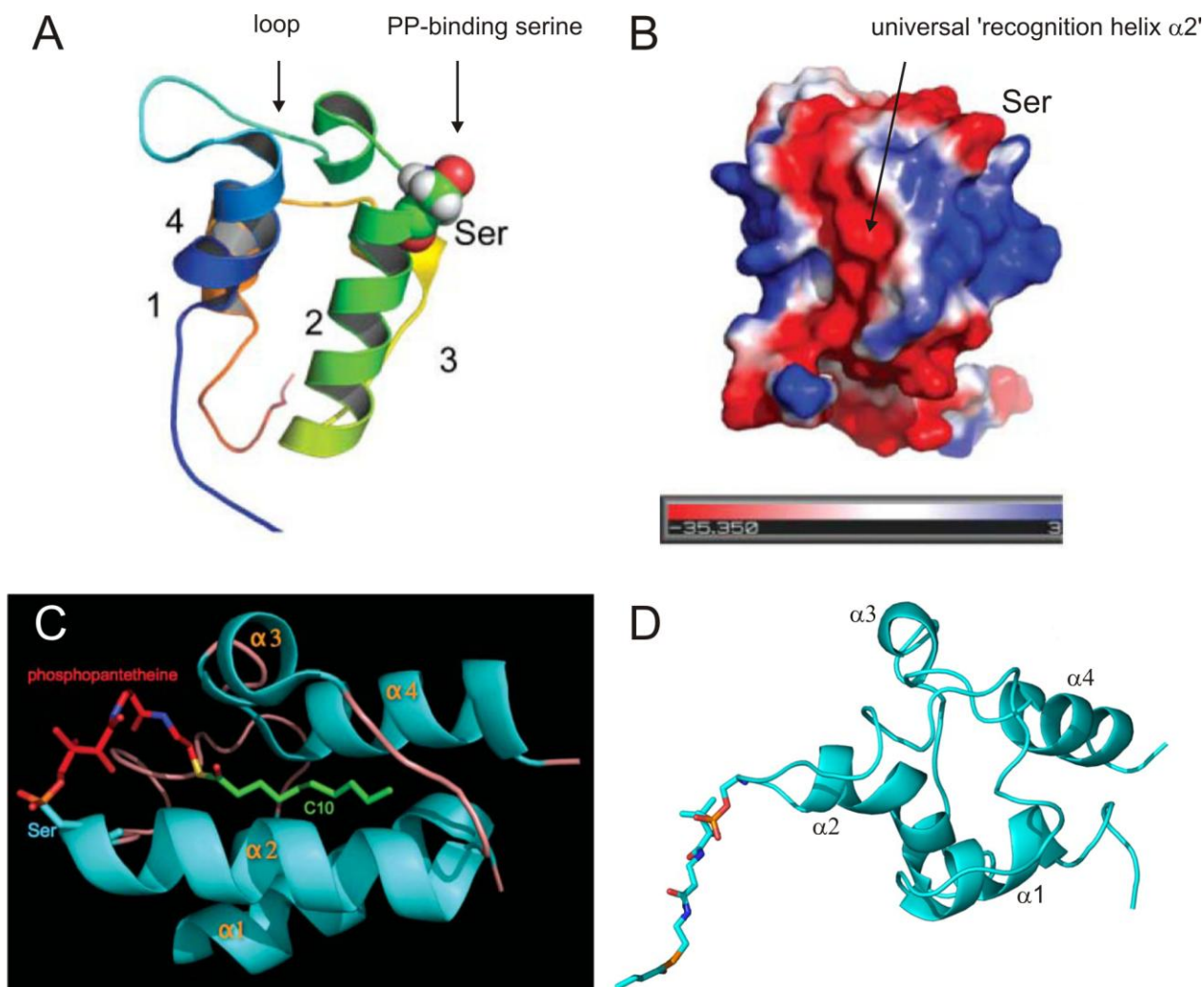


**Figure 1.7 The acyl carrier protein structure**

(A) The ribbon diagram of the rat FAS ACP domain (2PNG), colored blue to red, corresponding to N to C termini [117;125]. The post-translationally modified serine residue on helix  $\alpha 2$  is shown; (B) The surface electrostatic potential colored from red (negative) to blue (positive). Red-colored area running vertically in the structure comprise the universal 'recognition helix'; (C) The x-ray crystallographic structure of ACP-decanoyl thioester buried in the hydrophobic pocket. The pantetheine-4'-phosphate moiety is shown in red and the decanoyl moiety in green; (A, B, C) Adapted from [126]; (D) The conformation adopted by the butyryl-ACP after delivering the substrate into the active site of a partner enzyme. The phosphopantetheine-binding serine-36 (*E. coli* nomenclature) and the thioester bond is shown in orange. Adapted from [112].

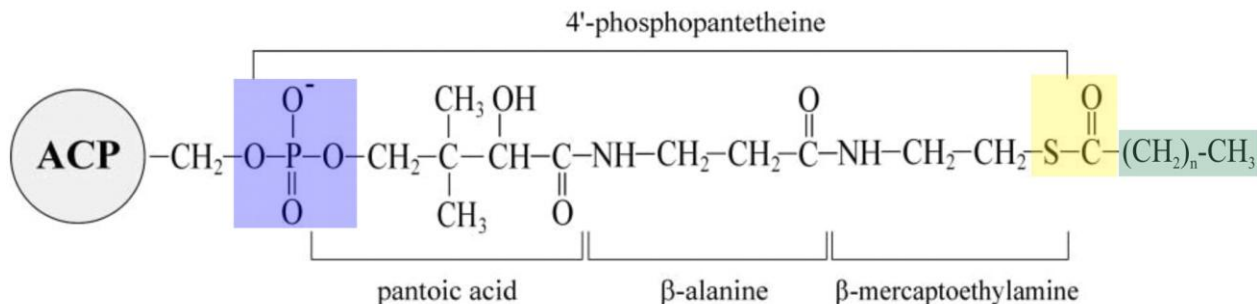


**Figure 1.8 Structural formula for the pantetheine-4'-phosphate-ACP**

The pantetheine-4'-phosphate (PP) group is composed of the pantoic acid, β-alanine and β-mercaptoethylamine. The PP is covalently bound from the side of pantoic acid to the conserved serine residue of the ACP protein over the phosphodiester bond (highlighted in blue) and on the side of β-mercaptoethylamine to the acyl chain over the thioester bond (highlighted in yellow). The alkyl group of the acyl chain is denoted with  $-(\text{CH}_2)_n-\text{CH}_3$  and is highlighted in green. Adapted from [116].

### 1.6.1 Fatty acid synthesis

Fatty acid synthesis is a central metabolic pathway that entails the iterative elongation of fatty acid chains through a set of chemical reactions conserved in all kingdoms of life (*Figure 1.9*). Despite the conserved reaction pathway, where ACP plays a central role, the molecular architectures of FAS systems differ considerably. Whereas in most plants, bacteria and organelles of bacterial origin (plant chloroplasts and mitochondria) synthesis is carried out by sets of individual enzymes known as the FAS type II [127-129], eukaryotes have evolved large, architecturally diverse, multifunctional synthases referred to as FAS type I [130;131]. The FAS type I complex is present in the cytosol of eukaryotes [132;133] and is composed of one or two giant polypeptides [134] containing all necessary enzymes for fatty acid synthesis (*Figure 1.9*). In this type of FAS the ACP-like domain is bound to other enzymes by means of two flexible protein linkers (*Figure 1.10B*). All enzymes of FAS are nuclear coded, with the exception of two ACPs from *Cryptomonas* algae and a β-Keto-Acyl-ACP-synthase from red algae, which are encoded by the plastidal genome [135;136].

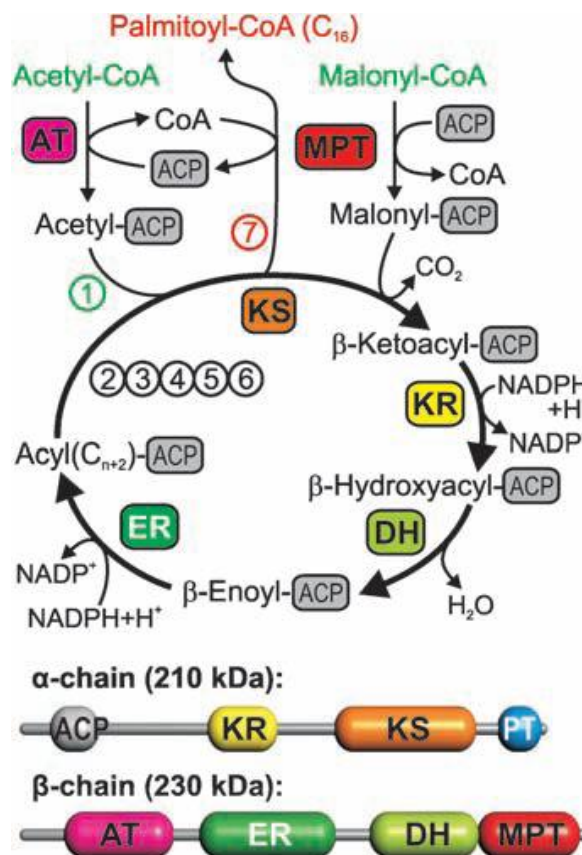


**Figure 1.9 Reaction sequence in fatty acid synthesis**

All catalytic domains necessary for *de novo* fatty acid synthesis are found on one multidomain polypeptide chains in mammals or on two in fungi. FAS involves the transfer of activated acetyl and malonyl substrates from coenzyme A (CoA) to the pantetheine-4'-phosphate prosthetic group of acyl carrier protein (ACP) via acetyl transferase (AT) and malonyl/palmitoyl transferase (MPT). Ketoacyl synthase (KS) condenses them by malonyl decarboxylation to acetoacetyl-ACP, which is further modified at the  $\beta$ -carbon position by ketoacyl reductase (KR), dehydratase (DH), and enoyl reductase (ER) to yield butyryl-ACP. These reactions are repeated six times, resulting in the sequential incorporation of seven two-carbon units. In fungi, the palmitoyl end product is transferred back from ACP to CoA by MPT [137], whereas in the mammalian system, the fatty acid is released from ACP by a thioesterase [131].

The fungal and mammalian FAS, although both are classified as type I are structurally highly diverse. Fungal FAS is a huge, barrel-shaped, 2.6-megadalton  $\alpha_6\beta_6$  heterododecameric complex (Figure 1.10A) [138] with two reaction chambers, each containing three full sets of active sites (Figure 1.10B). In contrast, mammalian fatty acid synthase is a 540 kDa x-shaped  $\alpha_2$  homodimer containing a full set of catalytic sites present in each of two semicircular reaction chambers on both sides of the molecule [131;139] (Figure 1.10C).

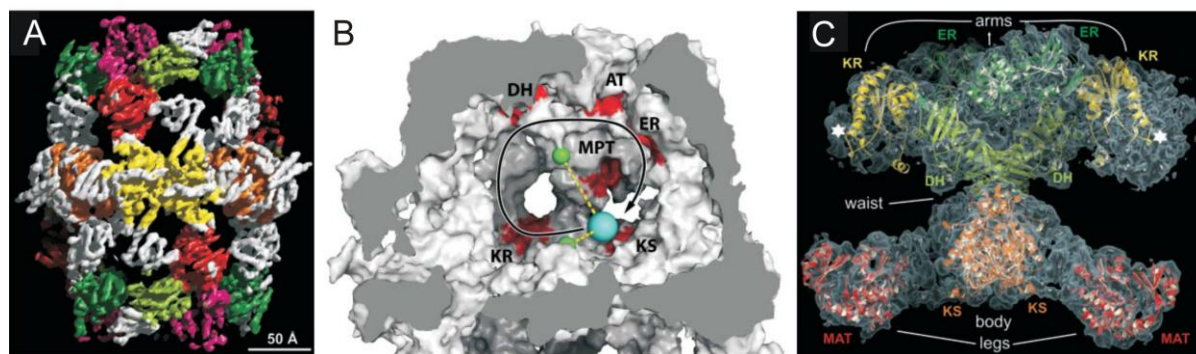


**Figure 1.10 Structure of type I fatty acid synthase complexes**

(A) Overall structure of fungal FAS I contain six complete sets of active sites distributed on  $6\alpha$  and  $6\beta$  chains: KR (yellow), KS (orange), ER (dark green), AT (magenta), DH (light green), PTT (red). Reprinted from [138]; (B) Cross section of a reaction chamber of the fungal FAS I complex. ACP (cyan) guided by elastic protein linkers (yellow) is channelled into circular path, which increases the concentration of the ACP in the area where active sites (red) are distributed. Reprinted from [140]; (C) Homodimer structure of mammalian FAS I complex. White stars indicate the suggested attachment regions for ACP and thioesterase (TE). Reprinted from [139];

FAS I is usually considered to be a more efficient biosynthetic machine because the enzymatic activities are fused into a single polypeptide template and the intermediates do not diffuse away from the complex. However, FAS I can only synthesize a narrow spectrum of fatty acids, predominantly palmitate, destined for membrane biogenesis and energy storage [130]. In contrast, FAS II is capable of producing a diversity of products for cellular metabolism. Not only different chain lengths are produced, but also unsaturated fatty acids, iso- and anteisobranched-chain fatty acids, and hydroxyl fatty acids. This enormous diversity of products is possible because the ACP intermediates in the pathway are diffusible entities that can be diverted into other biosynthetic pathways [128].



### 1.6.2 Significance of ACPs in biosynthetic pathways other than FAS

In addition to fatty acid synthesis, ACPs are also involved in many other reactions that require acyl transfer steps such as synthesis of polyketide [141] and peptide antibiotics [142;143], biotin precursor [144], membrane-derived oligosaccharides [145], acyl transfer to glycerol-3-phosphate and monoacylglycerol-3-phosphate [146], acylation of toxins [147]. ACPs also function as essential cofactor in the lipoylation of pyruvate and  $\beta$ -ketoglutarate dehydrogenase complexes [148].

Moreover, ACP from *Mycobacterium tuberculosis* (Figure 1.11A) is able to produce mycolic acids that are extremely long-chain (C70 - C90)  $\alpha$ -alkyl,  $\beta$ -hydroxy fatty acids [149](Figure 1.11B). This bacterium has developed an ACP with a unique C-terminal extension consisting of more than 50% of hydrophobic residues, which can fold and guide very long-chain acyl intermediates during biosynthesis [149].

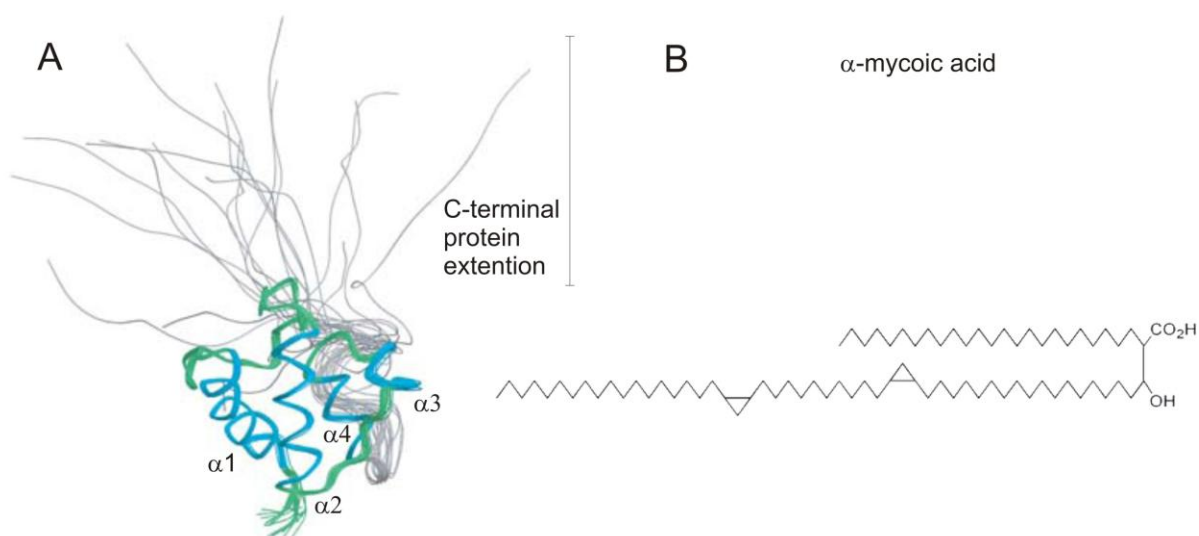


**Figure 1.11 Superimposed NMR structures of ACP from *Mycobacterium tuberculosis***

(A) *M. tuberculosis* ACP shuttles very long-chain hydrophobic substrates, which are stabilised during the synthesis and transport by an unfolded C-terminal protein extension (grey). *M. tuberculosis* possesses such an extension in addition to the typical ACP four-helix core structure (blue and green). Adapted from [128]; (B) An example of a long-chain  $\alpha$ -mycolic acid - a structural component of the cell wall of the bacterium *M. tuberculosis*. Adapted from [149].

### 1.6.3 Mitochondrial acyl carrier proteins

One or several ACPs of the bacterial FAS type II have been found in mitochondria of several species, including *N. crassa* [150;151], bovine heart [152] and *A. thaliana* [153]. These proteins are denoted ACPM for “AcyCarrier Protein, Mitochondrial”. Mitochondria of *N. crassa* were found to contain a protein which was labelled with [<sup>14</sup>C] pantothenic acid and carried an acyl group [150]. Evidence for a covalently attached pantetheine-4'-phosphate in bovine ACPM [152] was obtained by electrospray mass spectrometry, before and after incubation of the protein at alkaline pH conditions. So far, only two ACPM structures, structurally highly related to their bacterial counterparts are available: The human structure solved by NMR [154] (Figure 1.12A) and a structure from parasitic protozoan *Toxoplasma gondii* solved by x-ray crystallography [155] (Figure 1.12B).

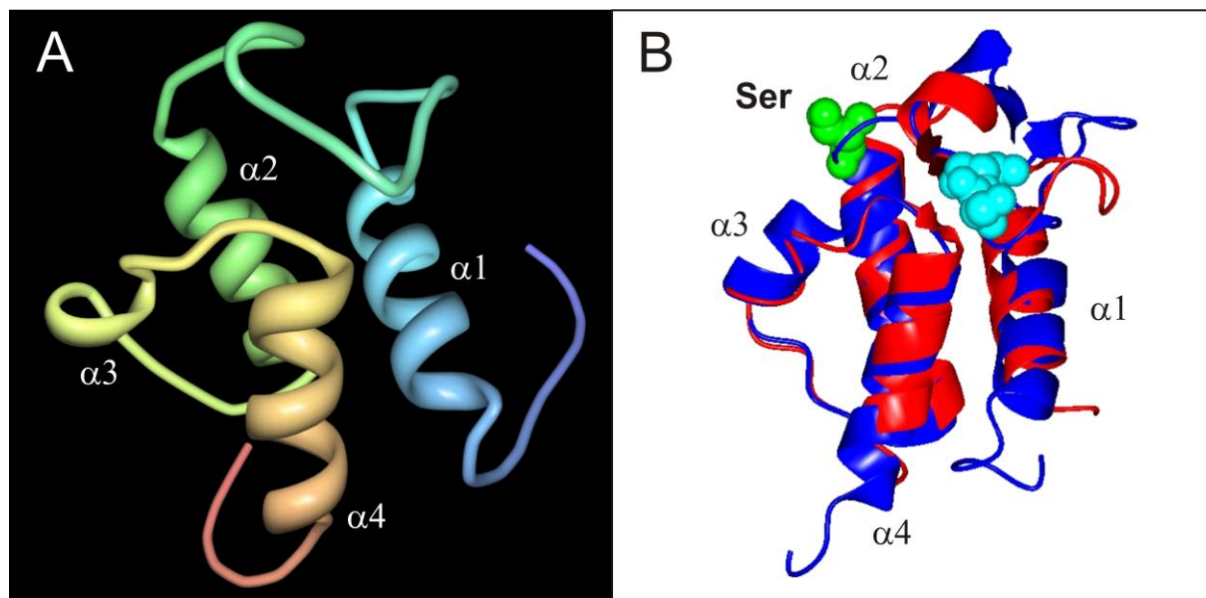


**Figure 1.12 Structures of the mitochondrial acyl carrier proteins**

Mitochondrial ACPs are highly related to the known bacterial structures. (A) NMR structure of human ACPM colored blue to red, corresponding to N to C termini [154]. This figure was prepared using the PDB Protein Workshop 3.4 software [156]; (B) An x-ray structure of the apo-ACPM from *Toxoplasma gondii* (blue) by [155] superimposed with bacterial apo-ACP x-ray structure of *E. coli* (red) [157]. *T. gondii* does not contain the highly conserved pantetheine-4' phosphate-binding serine residue, which is located at the beginning of the helix  $\alpha 2$  in most organisms including *E. coli* (green). Instead, *T. gondii* ACPM possesses two directly neighboring serines (cyan) situated on the loop connecting helices  $\alpha 1$  and  $\alpha 2$ . Structures were superimposed using CCP4 Molecular Graphics software [158].

### 1.6.4 Mitochondrial fatty acid synthesis

Following discovery and identification of ACPMs, further studies showed that mitochondria contain all necessary enzymes for fatty acid biosynthesis and that they are able to synthesize short-chain fatty acids [159;160] (9.4.4, appendix). Yeast deletion mutants lacking one of the mitochondrial FAS components: ACPM,  $\beta$ -Ketoacyl-ACP synthase or mitochondrial  $\beta$ -Ketoacyl-ACP reductase develop a pleiotropic respiratory deficient phenotype. These mutants are unable to grow on non-fermentable carbon sources, such as glycerol or lactate and switch from respiration to fermentation [98;161]. An explanation was provided by postulating that ACPM is involved in the synthesis of octanoic acid as a precursor for lipoic acid synthesis (*Figure 1.13*) in pea [162], *A. thaliana* [163], *N. crassa* [164;165] and *S. cerevisiae* [166]. Lipoic acid is an important sulfur containing prosthetic group of some mitochondrial enzymes such as the pyruvate dehydrogenase (PDH) and  $\alpha$ -ketoglutarate dehydrogenase (KGDH) complexes [148;167].

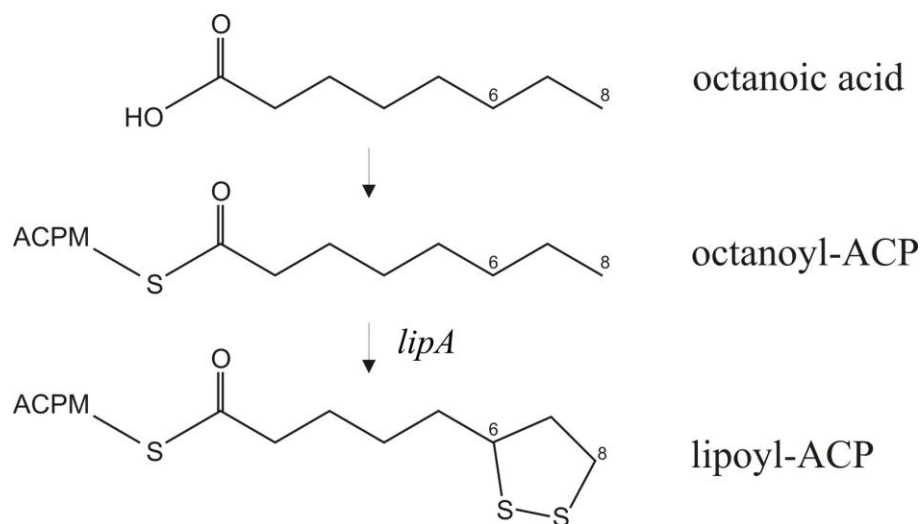


**Figure 1.13** Reaction sequence of lipoic acid synthesis in mitochondria

The ACPM was postulated to be involved in the synthesis of octanoic acid, which is further modified by lipoyl synthase (*lipA*) by inserting sulfur atoms at unactivated carbons at position 6 and 8 in the lipoic acid synthesis. Subsequently, the *lipB* and *lipA* lipoyl ligases transfer lipoyl groups to the E2 subunits of the pyruvate dehydrogenase (PDH) and  $\alpha$ -ketoglutarate dehydrogenase (KGDH) complexes [168;169]. The scheme is adapted from a model proposed for the endogenous lipoic acid biosynthesis pathways operating in *E. coli* [170].

---

Moreover, there is evidence for synthesis of longer fatty acids in mitochondria [162;163]. It was speculated that this activity plays a vital role, most likely for repair of mitochondrial lipids [159].

Recently, two distinct links between mitochondrial FAS and RNA processing have been discovered in vertebrates and yeast, respectively. In vertebrates, the mitochondrial 3-hydroxyacyl-ACP dehydratase and the RPP14 subunit of RNase P are encoded by the same bicistronic transcript in an evolutionarily conserved arrangement that is unusual for eukaryotes [171]. In yeast, defects in mitochondrial FAS result in inefficient RNase P cleavage in the organelle [172]. Hypothetically, the intersection of mitochondrial FAS and RNA processing has been maintained throughout evolution as a means to regulate mitochondrial function relative to the nutritional state of the cell [173].

### **1.6.5 Mitochondrial acyl carrier protein as complex I subunit**

Several groups demonstrated that mitochondrial ACP is tightly associated with complex I in some species [152;174], whereas in others, it is found as a free, soluble protein [123]. Furthermore, mitochondrial ACP appears to be essential for structural and functional integrity of complex I [175]. The number of mitochondrial acyl carrier proteins in eucaryotes ranges from one to three. Typically however two isoforms are found [175].

In *N. crassa*, one ACPM has been found that is a subunit of complex I [151]. Its disruption results in a defect in assembly of the peripheral arm and improper assembly of the membrane part, but no effects on complexes III or IV were observed [98]. The lysophospholipid content of mitochondrial membranes was increased. In contrast, the yeast *S. cerevisiae* lacks complex I and its ACPM is located in the mitochondrial matrix. In this yeast, deletion of *ACPM* leads to loss of lipoic acid synthesis and eventually to a pleiotropic respiratory deficient phenotype [98].

Similarly, depletion of ACPM by RNAi in *Trypanosoma brucei* and in human cell lines lead to defect in mitochondrial fatty acid and lipoic acid synthesis [176], which consequently caused reduction of activity of PDH and KGDH complexes. Concomitantly, the ACPM depletion lead to a drastic decrease in complex I activity and membrane potential, as

well as to changes in mitochondrial morphology [4]. Furthermore, decreased amounts of phosphatidylinositol and phosphatidylethanolamine were reported.

Of the ACPM from bovine heart mitochondria identified originally as complex I subunit SDAP [152] only a small fraction is associated with complex I. Most of the ACPM is found as a soluble (matrix) protein and is therefore available to carry the intermediates of type II fatty acid synthesis [124]. In *A. thaliana*, which expresses three mitochondrial ACPs [123], no significant amount of ACPM is found in complex I as determined by BN-PAGE, instead, as in bovine mitochondria, the proteins appear to exist predominantly as soluble matrix proteins.

---

## 1.7 Thiosulfate sulfurtransferase (rhodanese)

Sulfurtransferases are ubiquitous enzymes found in all living organisms, from bacteria to man [177]. In mammals, two closely related enzymes are present, namely thiosulfate:cyanide sulfurtransferase (TST, EC 2.8.1.1), also referred to as rhodanese, and 3-mercaptopyruvate:cyanide sulfurtransferase (MST, EC 2.8.1.2). Both are located predominantly in mitochondria [178]. In vitro, thiosulfate sulfurtransferase (TST) catalyses the transfer of a sulfane sulfur atom from thiosulfate to cyanide yielding thiocyanate and sulfite (Figure 1.14).

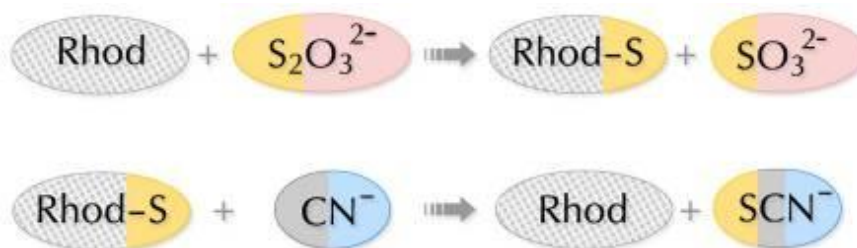


**Figure 1.14** Scheme representing the sulfur-transfer reaction catalyzed by rhodanese

The thiosulfate sulfurtransferase (TST) catalyses the transfer of a sulfane sulfur atom from thiosulfate to cyanide yielding thiocyanate and sulfite. The catalysis occurs via a double displacement mechanism involving the transient formation of a persulfide-containing intermediate (Rhod-S), in which the transferring sulfur is bound to the invariant catalytic cysteine residue. Reprinted from [177].

3-Mercaptopyruvate sulfurtransferase (MST) is able to catalyse the same reaction but shows higher affinity for 3-mercaptopyruvate as sulfur donor [179]. Substrate specificities seem to correlate with characteristic active site loop motifs: the five amino acids immediately downstream of the active site cysteine comprise one or two positively charged residues in TSTs, but not in MSTs [177]. Sulfur transfer occurs by a double displacement mechanism that involves formation of a persulfide containing intermediate with an invariant catalytic cysteine residue [177].

X-ray structures have been solved for TST from bovine liver [180] and *Azotobacter vinelandii* (Figure 1.15) [181]. Comparative studies have revealed a large superfamily that

includes proteins with a single rhodanese domain (e.g., many bacterial and plant enzymes), proteins with tandem repeats of rhodanese domains where only the C-terminal domain is catalytically active (e.g. *A. vinelandii* and mammalian TST and MST) and proteins in which a rhodanese domain, typically lacking the active site cysteine, is fused to other domains (e.g., the dual specific phosphatase Cdc25) [177] (*Figure 9.6* and *Figure 9.7*, appendix). While it is generally assumed that tandem domain repeat enzymes make the most significant contribution to cellular sulfurtransferase activity, it has been demonstrated that GlpE from *E. coli*, a representative of the single domain enzymes, is active in vitro [182;183]. Multiple copies of sulfurtransferase are found in the genome of some archaeobacteria, eubacteria, plants and vertebrates, including mammals and birds. Only a subset of them is predicted to be targeted to mitochondria using the MitoProtII [184] algorithm (*Table 3.3*, results).

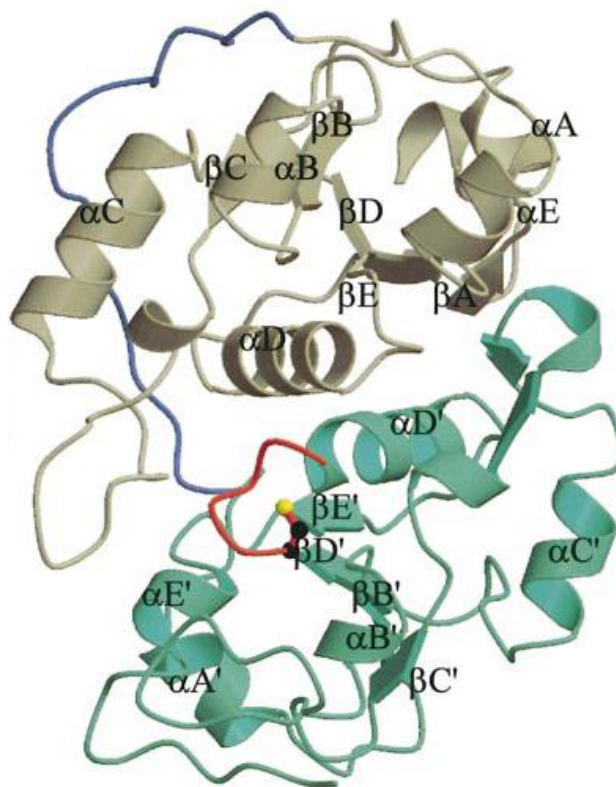


**Figure 1.15 Overall structure of *A. vinelandii* rhodanese**

Ribbon representation of RhdA. The N- and C-terminal domains (brown and green, respectively), the linker peptide (blue). The secondary structure elements of each domain are labelled with letters following the scheme proposed for bovine rhodanese [180]. A single quote indicates elements of the C-terminal domains. The active-site loop is shown in red; the catalytic residue, Cys230, is represented in ball and stick. The drawings were prepared with the programs MOLSCRIPT [185] and Raster3D [186]. Reprinted from [181].

---

The biological roles of TST and MST are largely speculative, because their *in vivo* substrates remain unknown. Proposed functions include cyanide detoxification [187], maintenance of the sulfane pool [188], selenium metabolism [189] and thiamine biosynthesis [190]. Due to its ability to transfer sulfur atoms and its mitochondrial localization it has also been suggested that rhodanese may be involved in the formation of iron-sulfur clusters [191]. It has been reported that rhodanese can form complexes through disulfide bonds with membrane-bound enzymes and it was speculated that rhodanese may regulate mitochondrial oxidative phosphorylation by controlling the status of iron-sulfur clusters of respiratory chain enzymes [191]. *In vitro*, rhodanese has been shown to catalyse sulfur transfer to bovine kidney succinate dehydrogenase [192], to spinach ferredoxin [193] and to the iron-sulfur protein fragment of bovine heart complex I, thereby promoting its NADH dehydrogenase activity [194]. The activity of bovine rhodanese may be regulated by protein kinases/phosphatases [195]. According to this model, phosphorylation leads to loss of rhodanese activity and converts the enzyme into a protein sulfurase, which may extract 'labile' sulfur from iron-sulfur clusters of the respiratory chain.



### ***1.8 Goals of the study***

NADH:ubiquinone oxidoreductase (complex I) from *Y. lipolytica* contains at least 26 “accessory” subunits however the significance of most of them remains unknown. The aim of this study was to characterize the role of three accessory subunits of complex I recently identified: two mitochondrial acyl carrier proteins, ACPM1 and ACPM2 and a sulfurtransferase (st1) subunit.

Significance of both ACPMs in the structural integrity and activity of complex I was evaluated. In order to distinguish whether the activity of ACPMs or their presence as structural components of complex I is important for proper complex I assembly and function, the phosphopantetheine-binding serine residues of ACPMs were mutated. Furthermore, effects of the deletion and the point mutation on the respiratory chain complexes assembly and activity were checked. Since ACPMs has been postulated to take part in the mitochondrial fatty acid synthesis, mitochondrial lipid composition of the strain lacking the pantetheine-4'-phosphate cofactor and completely deprived of ACPM was determined. Previous reports suggested localization of ACPMs in the mitochondrial matrix, which triggered the idea of verification of the submitochondrial distribution of ACPMs in *Y. lipolytica*.

A protein exhibiting rhodanese (thiosulfate:cyanide sulfurtransferase) activity associated with a homogeneous complex I preparation was suspected to play a role in the iron-sulfur cluster assembly. Complex I assembly and activity, whereas assembly of its iron-sulfur clusters in *Y. lipolytica* strain deprived of rhodanese was assayed.



## 2 MATERIALS AND METHODS

### 2.1 *Materials*

#### 2.1.1 **Chemicals**

Chemiluminescent Peroxidase Substrate-1 (Sigma), Ethanol (J.T. Baker, Deventer-Netherlands); bovine serum albumin (BSA) (Biolabs, New England); n-dodecyl- $\beta$ -D-maltoside (Biomol Feinchemikalien GmbH, Hamburg- Germany); DEAE Bio-Gel A Agarose (Biorad Laboratories GmbH, München- Germany); Chelating Sepharose (Pharmacia Biotech AB, Uppsala-Sweden); Agar; bactoPTMP yeast extract, Trypton, selected peptone 140 (Gibco BRL Life Technologies, Paisley-United Kingdom); YNB (Difco Laboratories, Sparks, MD, USA); boric acid, phenol, developer, fixing and developing solutions and X-ray films (Kodak BioMax MR, Rochester, New York); acetone, ammonium peroxosulfate, chloroform acetic acid, Folin-Ciocalteus-Phenol reagent, isoamyl alcohol, isopropanol, HCl, trichlorine acetic acid (Merck, Darmstadt-Germany); ammonium sulphate, EDTA, glass pearls (0.25 – 0.5 mm), KCl, KOH,  $\text{KH}_2\text{PO}_4$ , sodium acetate, sodium citrate, NaCl, NaOH,  $\text{NiSO}_4$ ,  $\text{NaH}_2\text{PO}_4$ , saccharose, nucleotides, Ni-NTA Fast Flow Sepharose (Pharmacia); acrylamide, bisacrylamide, Coomassie-Blue G-250, urea, polyethylene glycol (PEG) 4000, dodecylsulphate Na-salt (SDS), Tricine, agarose, amino caproic acid, amino acids, ampicilline, DMSO, ethidium bromide, glucose, glycerol (Pharmacia); hexaammine ruthenium(III) chloride (HAR), Hepes, KCN, lithium acetate, mercaptoethanol, Mops, methanol, d-NADH, NADH,  $\text{NaN}_3$ , nystatine, PMSF, Taq DNA polymerase, TEMED, Tris, asolectin, oligonucleotides (Sigma Chemie GmbH, Deisenhofen- Germany), Bio-Beads SM-2 (Bio-Rad), asolectin (Fluka); oligonucleotides (ARK Scientific GmbH Biosystems, Darmstadt-Germany) or (MWG-Biotech Ebersberg- Germany), potassium thiosulfate, potassium, thiosulfate cyanide, nitroblue tertazolium (Sigma), zymolyase 20T (ICN Biomedicals), bovine rhodanese (Sigma).

---

### 2.1.2 Phospholipid standards (Sigma)

1,1',2,2'-tetraoleoyl cardiolipin	(CL)
1,2-dipalmitoyl- <i>sn</i> -glycero-3-phosphoethanolamine	(PE)
L- $\alpha$ -phosphatidylinositol (soy bean)	(PI)
1,2-dipalmitoyl- <i>sn</i> -glycero-3-phosphocholine	(PC)
1,2-dipalmitoyl- <i>sn</i> -glycero-3-phosphate	(PA)
L- $\alpha$ -lysophosphatidylethanolamine (egg, chicken)	(LPE)
L- $\alpha$ -lysophosphatidylinositol (soy bean)	(LPI)
1-palmitoyl-2-hydroxy- <i>sn</i> -glycero-3-phosphocholine	(LPC)
1-palmitoyl-2-hydroxy- <i>sn</i> -glycero-3-phosphate	(LPA)

### 2.1.3 Inhibitors

2-decyl-4-quinazolinyl amine (DQA) was a generous gift from Aventis CropScience, Biochemical Research, Frankfurt am Main, Germany; rotenone was purchased from Sigma Chemie GmbH, Deisenhofen, Germany.

### 2.1.4 Media and solutions

#### Media for *Escherichia coli*:

LB-media: 1 % NaCl, 0.5 % Yeast Extract, 1 % Bactotryptone, pH 7.5 (1.5 % agar for plates)

SOC-media: 0.5 % Yeast Extract, 2 % Bactotryptone, 10 mM NaCl, 2.5 mM KCl, 10 mM MgCl<sub>2</sub>, 10 mM MgSO<sub>4</sub>, 20 mM glucose

#### Media for *Yarrowia lipolytica*:

Sporulation (minimal) medium (CSM): 0.7 % Yeast Nitrogen Base w/o (NH<sub>4</sub>)<sub>2</sub>SO<sub>4</sub> and amino acids, 0.5 % (NH<sub>4</sub>)<sub>2</sub>SO<sub>4</sub>, 50 mM sodium citrate

YPD-complete medium: 2 % Bacto™Pepton, 1 % Yeast Extract, 2 % glucose

Permanent culture medium: YPD-media + 40 % glycerol

Minimal synthetic defined medium (S): 1.7 % Yeast Nitrogen Base w/o (NH<sub>4</sub>)<sub>2</sub>SO<sub>4</sub> and amino acids, 5 % (NH<sub>4</sub>)<sub>2</sub>SO<sub>4</sub>, pH 5.0 were prepared as a 10 X stock solution and sterile filtrated. Carbon source (0.4 % acetate or 2 % glucose) were prepared as 2 X stock solution, autoclaved and added to 10 X S-media. Depending on the type of selection one or several of the following components were added: 130 μM histidine, 200 μM lysine, 460 μM leucine, 180 μM uracil.

Buffers and solutions:

10 X TAE-buffer: 400 mM Tris / acetate, 10 mM EDTA, pH 8.3

TE: 10 mM Tris / HCl, 1 mM EDTA, pH 8.0

20 X SSC-buffer: 3 M NaCl. 0.3 M sodium citrate, pH 7.0

One step buffer (freshly prepared): 45 % PEG4000, 0.1 M lithium acetate pH 6.0, 100 mM dithiothreitol, 250 μg/ml salmon sperm DNA as carrier

IPG buffer (Sigma)

Rehydration buffer: 8 M urea, 1.5 % Triton X-100, 10 mg/ml DTE 0.5 % IPG Buffer and a trace of bromphenol blue

SDS equilibration buffer: containing 50 mM Tris-HCl pH 8.8, 6M urea, 30 % glycerol, 4 % SDS, 10 mg/ml DTE and a trace of bromphenol blue

Molybdenum Blue Spray Reagent (Sigma)

## 2.1.5 Strains

*Escherichia coli* competent cells

Strain	Genotype
XL1-Blue	<i>recA1 endA1yrA96 thi-1 hsdR17 supE44</i> <i>relA1 lac</i> [F' <i>proAB lacI<sup>q</sup>ZΔM15 Tn10 (Tet<sup>r</sup>)</i> ]
XL10-Gold	<i>recA1 endA1 gyrA96 thi-1 hsdR17 supE44</i> <i>relA1 lac</i> [F' <i>proAB lacI<sup>q</sup>ZΔM15 Tn10 (Tet<sup>r</sup>)</i> ]

*Yarrowia lipolytica*

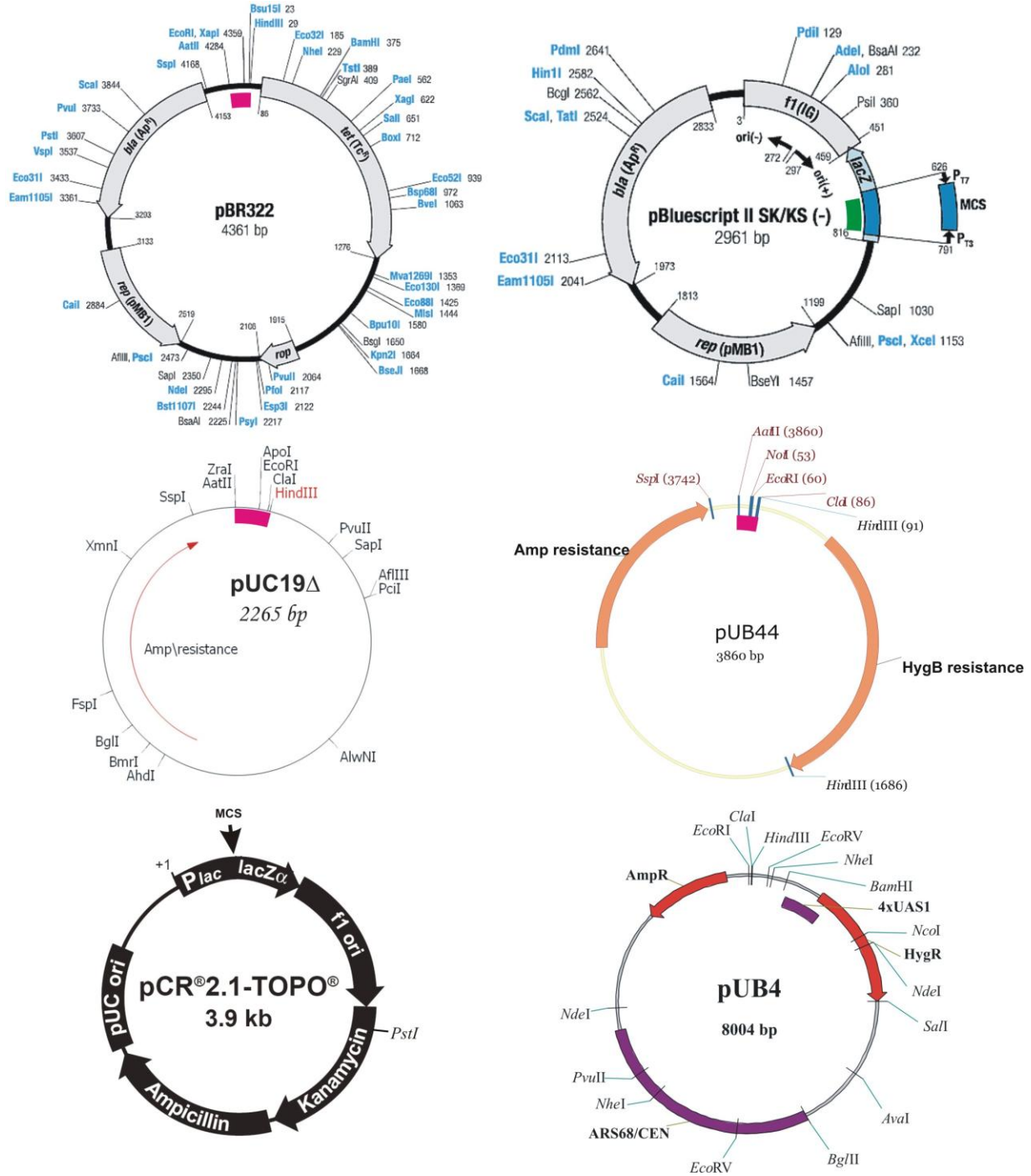
Strain	Genotype
PIPO	<i>30Htg pop-in-pop-out MatA, ura3-302, leu2-270, lys11-23</i>
GB10	<i>30Htg2 MatB NDH2i ura3-302 leu2-270 lys11-23</i>
GB14	<i>NUCM-Htg2, NDH2i, ura3-302, leu2-270, lys11-23/+, his1/+</i>
<i>acpm1Δ,</i> <i>acpm1Δ,</i> pACPM1-stepII	<i>30Htg2 MatA ndh2i acpm1:URA3-302, pACPM1-stepII</i> <i>leu2-270 lys11-23</i>
<i>acpm2Δ,acpm2</i> <i>Δ,</i> pACPM2-flag	<i>30Htg2 MatB ndh2i acpm2:URA3-302, pACPM2-flag leu2-270 lys11-23</i>
<i>acpm1Δ</i>	lethal
<i>acpm2Δ</i>	<i>30Htg2 MatB ndh2i acpm2:URA3-302 leu2-270 lys11-23</i>

---

<i>acpm1</i> Δ, <i>acpm1</i> Δ, pACPM1	<i>30Htg2 MatA ndh2i acpm1:URA3-302, pACPM1 leu2-270 lys11-23</i>
<i>acpm2</i> Δ, <i>acpm2</i> Δ, pACPM2	<i>30Htg2 MatB ndh2i acpm2:URA3-302, pACPM2 leu2-270 lys11-23</i>
<i>acpm1</i> Δ, <i>acpm1</i> Δ, pACPM1-S66A	lethal
<i>acpm2</i> Δ, <i>acpm2</i> Δ, pACPM2- S88A	<i>30Htg2 MatA ndh2i acpm2:URA3-302, pACPM2-S88A leu2-270 lys11-23</i>
<i>st1</i> Δ,pst1-strepII	<i>30Htg2 MatB ndh2i st1:URA3-302,pst1-strepII leu2-270 lys11-23</i>
<i>st1</i> Δ	<i>30Htg2 MatB ndh2i st1:URA3-302 leu2-270 lys11-23</i>
<i>st1</i> Δ, <i>st1</i> Δ, pst1	<i>30Htg2 MatA ndh2i st1:URA3-302,pst1 leu2-270 lys11-23</i>
<i>nubm</i> Δ	<i>30Htg2 MatB ndh2i nubm:URA3-302 leu2-270 lys11-23</i>
E129	<i>MatA, URA3-302, leu2-270, lys11-23</i>

---

## 2.1.6 Plasmids



See next page for description.



**Figure 2.1 Maps of plasmids**

(previous page) The pUC19 $\Delta$  vector was constructed by replacing the *AatII/HindIII* fragment of pBluescript SK- (marked in green) with the *AatII/HindIII* fragment of pBR322 (magenta), thereby replacing the polylinker with region that contains the unique *EcoRI* and *Clal* sites of pUC19 $\Delta$ . Vector pUB44 was constructed by cloning the hygromycin B resistance gene into the *HindIII* site (marked in red) of pUC19 $\Delta$ , and introducing a *NotI* site by site-directed mutagenesis, immediately adjacent to the *EcoRI* site. The pUB4 vector was derived from the pINA443 vector [105] as described in [196]. The representations of vectors pUB4 and pUB44 were prepared by Dr. Stefan Kerscher using software VectorNTI Advance 9.0; pUC19 $\Delta$  using Clone Manager Professional 9.0; pCR2.1 was adapted from Invitrogen (Groningen, The Netherlands); pBR322 and pBluescriptSK- were reprinted from Fermentas Life Sciences (St. Leon-Rot, Germany). Indicated locations of genes: ampicillin (*Ap<sup>R</sup>*), hygromycin (*Hyg<sup>R</sup>*) kanamycin, tetracycline (*Tc<sup>R</sup>*) resistance genes, origin of replication (*ori*, *rep*), *lac* promoter (*Plac*),  $\beta$ -galactosidase encoding fragment used for blue-white screening (*lacZ $\alpha$* ), multiple cloning site (MCS), the autonomous replication sequence (ARS68/CEN), the upstream activating sequence (4xUAS1) and gene coding for the Rop protein promoting conversion of the unstable RNA I - RNA II complex to a stable complex and serving to decrease copy number (*rop*). Recognition sites of restriction enzymes are indicated on most plasmids. Additionally, a *PstI* restriction site was introduced into plasmid pCR2.1 by site-directed mutagenesis.

**2.1.7 Enzymes**

Taq DNA polymerase (Sigma), Phusion DNA polymerase (Finnzymes), T4-ligase (Invitrogen), restriction enzymes (New England BioLabs)

## 2.1.8 Antibodies

### Primary antibodies

antibody	Specificity	provenience
30C10 G1	NUBM (51-kDa)	
42A10 G1	NUCM (49-kDa), internal epitop 31 PIPSGALGQKVPHV 45	Dr. Volker Zickermann Frankfurt am Main Germany
37G12 G1	NUEM (39-kDa), internal epitop 263 VRHIELPKALYQAYTKATQAI 284	
30C12 G1	NESM	
Monoclonal ANTI- FLAG <sup>®</sup> M2	1 DYKDDDDK 8	Sigma Germany
Monoclonal QIexpress <sup>®</sup> Strep- tag <sup>®</sup>	1 SAWSHQPFEK 10	QIAGEN, Germany
StrepMAB-Classic conjugated to horseradish peroxidase	1 SAWSHQPFEK 10	IBA, Germany
Aco1C-3 rabbit antiserum	yeast aconitase	Prof. Dr. Roland Lill, Marburg, Germany
$\alpha$ -hexokinase rabbit antiserum	SRKGSMAADVPRDLLC	Sigma-Genosys, USA

### Secondary antibody

Anti-Maus IgG (Fc Specific) Peroxidase conjugate developed in goat (Sigma, Germany)

### 2.1.9 Instruments

#### Centrifuges:

Heraeus Biofuge A (Osterode, Germany)

Heraeus Labofuge 400 (Osterode, Germany)

Heraeus Minifuge GL (Osterode, Germany)

Heraeus Cryofuge 8500i (Osterode, Germany)

Heraeus Megafuge 1.0 RS (Osterode, Germany)

Cooled centrifuge J2-21, Beckman Instruments GmbH (München, Germany)

Ultracentrifuge L7-65 and L8-70M, Beckman Instruments GmbH (Germany)

#### Spectrophotometer:

UV 300 Shimadzu (Düsseldorf, Germany)

U-3210 Hitachi (Düsseldorf, Germany)

MultiSpec-1501, Shimadzu (Düsseldorf, Germany)

SPECTRAMax PLUS<sup>384</sup>, Molecular Devices GmbH (Ismaning, Germany)

#### Thermocycler:

DNA Thermal Cycler 480, Perkin Elmer (Weiterstadt, Germany)

GeneAmp<sup>®</sup> PCR System 2400, Perkin Elmer (Weiterstadt, Germany)

cyclone<sup>®</sup> gradient, Peqlab, Biotechnologie GmbH (Erlangen, Germany)

#### Electroporation:

*E. coli* Pulser Bio-Rad (Hercules, USA)

#### DNA Sequencer:

ABI PRISM<sup>™</sup> 310 Genetic Analyzer, Perkin-Elmer (Weiterstadt, Germany)

#### Sonifier:

B 15 Sonifier / Cell Disrupter, Branson (Danbury, UK)

#### EPR-Spectrometer:

ESP 300 E, Bruker (Germany) with continuous flow cryostat ESR 900,

Tubney Woods Abingdon (Oxon, UK)

---

EPR-tubes:

Quartz glass Nr: 707-SQ-250M (length: 250 mm, diameter: 4 mm), Rototec Spintec (Biebesheim, Germany)

Phospholipid HPLC system:

Inline solvent degasser L-7612, VWR International GmbH (Darmstadt, Germany)  
pump L-7100 (with low pressure dosing unit), VWR  
high pressure active mixer for L-7100, VWR  
autosampler L-7200 (100 µL loop; 500 µL syringe), VWR  
column oven L-7360 (coolable), VWR  
diode array detector L-7455, VWR  
evaporative light scattering detector Sedex 75, Sedere (Alfortville, France)  
fraction collector SF-3120 Advantec, (Dublin, USA)  
controlling interface D-7000 VWR  
controlling software D-7000 HSM VWR

Protein HPLC system:

119UV/UV-Vis Detector, L-4000/L-4200 equipped with Intelligent Inert Pump L-6210 and D-2500 Chromato-Integrator, Merck, Germany.

Columns

TSKgel G 4000 SW filtration column (210.5 mm × 600 mm), TosoHaas GmbH (Stuttgart, Germany)

TSKgel 3000 SW filtration column (75 mm x 600 mm), TosoHaas GmbH (Stuttgart, Germany)

RP-HPLC column: Hibar RT 250-4, LiChospher 100, RP 18 (5 µm), with pre-column LiChospher 100 RP-18 (5µm), (Merck, Germany)

Other instruments:

10 l Fermenter, Biostat E; Braun (Melsungen, Germany)  
Bead-Beater glass pearls mill, Biospec (Bartlesville, USA)  
Cell-Desintegrator-C, Bernd Euler (Frankfurt/Main, Germany)  
BioLogic HR Workstation, Bio-Rad Laboratories GmbH (München, Germany)  
Photo camera MP4 land camera, Polaroid  
Hybridisations oven HB-1D, Techne (Wertheim, Germany)  
Microscope, Leitz (Wetzlar, Germany)  
Membrane, Millipore GmbH (Eschborn, Germany)  
Rotary concentrator Rotavapor-R (Büchi Glasapparatefabrik, Flawil, Switzerland)  
ChemiDoc XRS System, Bio-rad laboratories (Milan, Italy)  
MALDI-TOF mass spectrometer Voyager De Pro (Applied Biosystems, USA)  
Isoelectric focussing Rotofor<sup>®</sup> System, Bio-Rad Laboratories GmbH (Germany)

**2.1.10 Software**DNA and protein analysis software:

Mac Vector 3.5, IBI  
VectorNTI Advance 9.0 (InfosMax, USA)  
Clone Manager Professional 9.0 (Scientific & Educational Software, USA)  
HIBIO DNASIS<sup>™</sup> for Windows<sup>®</sup> Version 2, Hitachi Software Engineering Co., Ltd  
Husar (DKFZ, Heidelberg, Germany)  
CLUSTALW (EMBL-EBI, Heidelberg, Germany)  
MitoProt II (<http://ihg2.helmholtz-muenchen.de/ihg/mitoprot.html>)  
Hydrophobicity plots, Molecular toolkit, Colorado State University, USA  
(<http://www.vivo.colostate.edu/molkit/hydropathy/index.html>)  
Transmembrane helices prediction software HMMTOP (<http://www.enzim.hu/hmmtop/>) and TMHMM (<http://www.cbs.dtu.dk/services/TMHMM/>).  
Sequence Navigator (Applied Biosystems, USA)  
Sequencing Analysis (Applied Biosystems, USA)  
BCM Search Launcher (Baylor College of Medicine, USA)

---

Mascot (Matrix Science Ltd., London)

Protein Prospector (Mirrors at [UCL-Ludwig](#), UK / [Ludwig Institute Melbourne](#)  
(Australia))

PROWL (ProteoMetrics, USA)

SOFTmax PRO, Molecular Devices GmbH (Ismaning, Germany)

Other software:

Microsoft Office Package

## **2.2 Methods of Molecular Biology**

### **2.2.1 Deletion strains**

The haploid deletion strains of the *st1* and ACPM subunits of complex I from *Y. lipolytica* were generated using the one-step transformation method as described in [197]. The open reading frame (ORF) of the gene was replaced by URA3 reporter gene. A fragment of the gene in which the ORF had been replaced by URA3 gene was transformed into the haploid GB strain. Subsequently a strain carrying the appropriate markers on minimal media plates was selected. Finally, the selected clones were checked by PCR and Southern Blotting.

### **2.2.2 DNA gel electrophoresis**

The DNA was separated according to standard procedures [198] in the presence of 0.5 µg/ml ethidium bromide. Depending on the expected DNA fragment length agarose concentrations from 0.6 – 2.0 % in 1×TAE buffer were used. If the DNA fragments were extracted from the gel, TEA buffer with extra additive was used (UV-safe TAE, MWG-Biotech, Ebersberg). DNA molecular weight standards: 1 kb Ladder, 100 bp Ladder plus (MBI Fermentas, St. Leon-Rot).

### **2.2.3 Fill-in reaction of 5'-overhang**

The DNA blunt-ends were made with large fragments of *E. coli* DNA-polymerase I (Klenow-polymerase, New England Biolabs GmbH, Schwalbach/Taunus) as described in [198].

### **2.2.4 DNA-vector dephosphorylation**

To avoid self-ligation of empty vectors the DNA ends were dephosphorylated with SAP (Shrimp Alkaline Phosphatase, Boeringer Mannheim, Mannheim).

---

### **2.2.5 Phosphorylation of PCR-products**

To allow for ligation of PCR products it was necessary that both fragment ends were phosphorylated. For this purpose T4 polynucleotide kinase (New England Biolabs) as described by Ausubel [199]. Alternatively, primers rather than DNA fragments were phosphorylated before PCR.

### **2.2.6 DNA extraction from agarose gels**

The DNA extractions from agarose gels were performed using the “Easy Pure Kit” (Biozym Diagnostic GmbH, Hess. Oldendorf) or the QIAprep® Gel Extraction Kit (Qiagen).

### **2.2.7 Ligation**

The T4 DNA-ligase (Gibco BRL Life Technologies) was used in the provided buffer to ligate DNA fragments. Usually ligation was carried out over night at 14°C.

### **2.2.8 Preparation of electro-competent *Escherichia coli* cells**

The electro-competent *E. coli* cells were made according the procedure described in “Current Protocols in Molecular Biology” [199]. Transformation efficiency was up to  $7 \times 10^9$  colonies/ $\mu\text{g}$  DNA.

### **2.2.9 Transformation into *Escherichia coli* (electro-competent cells)**

The transformation of plasmids (with Amp<sup>R</sup> gene) into *E. coli* electro competent cells took place in an *E. coli* Pulser (Biorad) as described in “Current protocols in Molecular Biology” [199]. Transformants were then streaked out and grown over night on LB solid medium in the presence of ampicillin (50  $\mu\text{g}/\text{ml}$ ).

### **2.2.10 Preparation of plasmid-DNA from *Escherichia coli***

The plasmid-DNA was prepared according to [200] from a small volume of over night cultures (1.5-3 ml). Plasmid DNA for sequencing was prepared using the QIAprep® Spin Miniprep Kit (Qiagen).



### **2.2.11 DNA sequencing**

The double-strand DNA was used as template for sequencing. The sequencing reaction was run using the “ABI Prism dye terminator cycle sequencing kit” (Perkin Elmer, Weiterstadt). Sequencing was performed with an ABI Prism Automated Sequencer type ABI 310.

### **2.2.12 Polymerase chain reaction (PCR)**

10 ng of plasmid-DNA resp. 100 ng of genomic DNA, 5 µl of both oligonucleotides (5 µM), 5 µl of 10X reaction buffer provided by the manufacturer were combined in a total reaction volume of 50 µl. To avoid dimerisation of oligonucleotides as well as non-specific binding of oligonucleotides to matrix DNA manual “hot-start” was applied. Used polymerases were: Taq DNA polymerase, Taq2000™ DNA polymerase, Pfu DNA polymerase and PfuTurbo™ DNA polymerase from Stratagene (Heidelberg) as well as Taq DNA polymerase from Sigma Chemie GmbH (Deisenhofen).

### **2.2.13 Generation of point mutations**

The shuttle-vector pUB4 (*Figure 2.1*) carrying a 4.91 kb insert coding for the NUEM gene was used as template for site directed mutagenesis. Point mutation was introduced by PCR with the “QuikChange™ site-directed mutagenesis kit” (Stratagene, Heidelberg). After amplification of the insert-containing plasmid using phosphorylated primers the reaction mixture was digested with *DpnI* to eliminate methylated template plasmid. Phosphorylated PCR products were ligated and transformed into electro-competent cells. To check the presence of the desired mutation and the absence of inadvertent sequence changes, the complete ORF of the mutagenised gene was sequenced and compared to the wild type ORF.

### **2.2.14 Southern blot**

The digested DNA (genomic DNA: 500 ng; plasmid DNA: 50 ng) was separated using agarose gel electrophoresis (1 %). The DNA was transferred over night onto Hybond N<sup>+</sup>-membrane (Amersham, Braunschweig). Covalent crosslink of DNA to the membrane was achieved by UV-light irradiation (Stratalinker, Stratagene, Heidelberg).

---

### **2.2.15 <sup>32</sup>P DNA labelling**

The DNA fragments were labelled with [ $\alpha$ -<sup>32</sup>P] dCTP (25  $\mu$ Ci for 25 ng DNA) using the “Random primer labelling – Prime-It<sup>®</sup>II” Kit (Stratagene, Heidelberg). The rate of radioactive labelling was checked by pipetting 3  $\mu$ l of 1:100 diluted reaction mixtures onto two filter sheets (Whatman DE 81 ion exchange paper, Whatman International Ltd., Maidstone, England). One of the filters was washed two times for 5 minutes with 2  $\times$  SSC buffer and subsequently washed for 5 minutes in cold ethanol. To estimate incorporation of the radioactive label, count rates of both filters were controlled after drying using a Geiger counter.

### **2.2.16 Hybridisation of radio actively labelled DNA probes**

The hybridisation took place in a rotating glass tube using a thermostatted hybridisation oven (HB-1D, Techne). The membranes were pre-hybridised for 15 minutes at 68°C followed by a main hybridisation period of 60 min at 68°C in “QuikHyb<sup>®</sup>” hybridisation solution (Stratagene, Heidelberg). For the main hybridisation, <sup>32</sup>P-labelled DNA fragment was added together with 100  $\mu$ l (10 mg/ml) salmon sperm DNA. Subsequently, blots were washed four times (2  $\times$  15 min with 2  $\times$  SSC, 0.1 % SDS; 2  $\times$  15 min with 0.1  $\times$  SSC, 0.1 % SDS) to remove non-specifically bound radioactive probe. Blots were exposed to Kodak X-Omat AR films with an amplifier-sheet over night at –80°C.

### **2.2.17 Transformation of *Y. lipolytica***

The *Y. lipolytica* cells were transformed according to the method of [197]. A single colony was taken from a fresh plate. Alternatively, cells from 0.5 ml of an over night culture in complete medium were spun down. The cells were dispersed by vortexing for 1 min in 100  $\mu$ l of freshly prepared one step buffer (45 % PEG4000, 0.1 M lithium acetate pH 6.0, 100 mM dithiothreitol, 250  $\mu$ g/ml salmon sperm DNA as carrier). Subsequently the mixture was incubated for 1 h at 39°C and was spread on well dried selection plates. Transformants could be observed after 3 days incubation at 28°C.

**2.2.18 Isolation of total DNA of *Y. lipolytica***

The total DNA isolation was performed according to the “rapid isolation of yeast chromosomal DNA” protocol described in “Current Protocols in Molecular Biology” [199]. Plasmid DNA was obtained by transformation of 100 ng of total DNA into *E. coli* competent cells.

**2.2.19 Sporulation**

The cells were grown in the minimal synthetic medium (2.1.4) complemented with leucine and lysine for 4 days at 23°C. Isolated spores were treated with nystatin (1 mg/ml); subsequently, selection of haploid organisms was carried out. Finally, obtained clones were checked by PCR.

---

## 2.3 Methods of Protein Chemistry

### 2.3.1 Growth of *Y. lipolytica*

The *Y. lipolytica* parental strains were grown in YPD medium at 28°C in rotatory flasks. One colony of *Y. lipolytica* from an agarose YPD plate was taken for a 1 l pre-culture and shaken in a flask for 18 - 24 hours. Subsequently, the pre-culture was used to inoculate a 10 l fermenter (Biostat E; Braun, Melsungen). The fermentation lasted 14 - 18 hours. The yield was up to 90 g cells / 1 l (wet weight).

The mutant strains were grown by fermentation in 10 l of YPD medium. The medium of the pre-culture depended on the plasmid. In the case of pUB4 YPD containing 100 mg/l hygromycin B was used. The fermentation was inoculated in a 10 l fermenter with 1 l of pre-culture. The pre-cultures were shaken in flask for 24 hours and fermentation took another 24 hours. Even in the absence of selective pressure during fermentation, no substantial loss of plasmid was observed.

### 2.3.2 Preparation of intact mitochondria

The intact mitochondria from *Y. lipolytica* were prepared essentially by the enzymatic digestion method described in [201]. *Y. lipolytica* cells were harvested at early logarithmic stage (OD~3-4), washed twice in ice cold water, resuspended (0.1 g wet cells/ml) at room temperature in 50 mM Tris-HCl buffer (pH 8.6) supplemented with 5 mM dithiothreitol and incubated for 10 min, diluted with water and washed twice again. After the last centrifugation the weakened cells were resuspended (0.1 g wet cells/ml) in 1.2 M sorbitol and 10 mM HEPES-KOH, pH 7.5 and 3-4 mg/ml zymolyase 20T (from *Arthrobacter luteus*, ICN Biomedicals) was added to digest the cell wall. The formation of spheroplasts was monitored spectrophotometrically and usually 10-15 min of incubation at 30°C was enough to complete the digestion. After that, 0.2 mM Pefablock SC was added, the spheroplast suspension was rapidly cooled, centrifuged at 500-600 g for 10 min and the pellet was resuspended and washed twice in the same buffer containing 4 mg/ml fatty acid free BSA. The pellet of the last centrifugation was resuspended in grinding buffer (20 mM Tris-HCl, pH 7.3, 0.4 M

mannitol, 0.5 mM EDTA and 4 mg/ml BSA, fatty acid free). Spheroblasts were disrupted by 20 gentle strokes in a loosely fitting Dounce homogenizer. The suspension was diluted twice with isolation buffer (20 mM Tris-HCl, pH 7.3, 0.6 M mannitol, 0.5 mM EDTA and 4 mg/ml BSA) and centrifuged at 2000g for 10 min. The supernatant was collected and centrifuged once more at 7000g for 20 min, the pellet was resuspended with a smaller volume of isolation buffer and centrifuged again. The mitochondria were resuspended in 500-700  $\mu$ l of isolation buffer.

### **2.3.3 Preparation of mitochondrial membranes in small amounts**

The freshly harvested cells (4 - 8 g) were used at a 1:1:1 cells to buffer to glass beads ratio (same as in 2.3.2). Cell breakage was achieved by vortexing in a Falcon tube for 10  $\times$  1 min and intermittent cooling in ice for one minute. Centrifugations and further steps were the same as in 2.3.2.

### **2.3.4 Protein quantification**

The protein determination was done according to the procedure in [202], as modified in [203]. Calibration was carried out with 0.1 – 2.0 mg/ml bovine serum albumin (BSA).

### **2.3.5 Mitochondrial fractionation**

The intact mitochondria corresponding to 500  $\mu$ g of protein determined according to a standard protocol [202] were suspended in 170  $\mu$ l 1 mM EDTA, 20 mM Na<sup>+</sup>/Mops pH 7.2, subjected to 3 cycles of freezing and thawing using liquid nitrogen and centrifuged for 1 h at 100,000 g. The supernatant was transferred to another tube and 80  $\mu$ l of gel loading buffer I (0.03 % Serva Blue G, freshly added 6 % 2-mercaptoethanol, 30 % glycerol, 12 % SDS, 150 mM Tris-Cl pH 7.0) was added. The pellet was resuspended in 250  $\mu$ l gel loading buffer I/3 (buffer I diluted 3 times in water). The final protein concentration of the supernatant and pellet samples was 2 mg/ml. Also a sample of total mitochondria with the same protein concentration was prepared.

---

### **2.3.6 Localization of ACPM1-strepII and ACPM2-flag in mitochondria by western blot analysis**

To investigate protein expression and localization of ACPMs, solubilized fractions of soluble and membranous parts of mitochondria were resolved on a Tricine-SDS-PAGE [204]. A semidry immunoblotting procedure was applied using polyvinylidene difluoride membranes (Immobilon TMP, Millipore). Gel-blotting paper was incubated in blotting-buffer (cathode buffer: 300 mM 6-aminocaproic acid, 30 mM Tris, pH 9.2; anode buffer: 300 mM Tris, 100 mM Tricine, pH 8.7). Gels were blotted over night at 50 mA and 20 V. After blotting, membranes were incubated for 30 minutes in PBS buffer containing 0.5% (w/v) Tween20. After washing in PBS (270 mM NaCl, 5 mM KCl, 15 mM Na<sub>2</sub>HPO<sub>4</sub>, 3 mM KH<sub>2</sub>PO<sub>4</sub>, pH 7.5) with 0.1% (w/v) Tween20 buffer once for 15 minutes and twice for 5 minutes, membranes were incubated with antiserum diluted in PBS buffer with 0.1% (w/v) Tween20. For ACPM1-strepII protein detection membrane was probed for 40 min with mouse monoclonal strepII-tag antibody (Qiagen) diluted 1:5,000. Secondary antibodies anti-mouse IgG peroxidase conjugated were diluted 1:500,000 and incubated for 30 min; ACPM2-flag was detected with anti-flag polyclonal antibodies. All secondary antibodies subsequently used were anti-rabbit IgG peroxidase conjugated, diluted 1:500,000 and incubated for 30 min. Antiserum against aconitase was diluted 1:4,000 and incubated for 2.5 hours; hexokinase antiserum was diluted 1:10,000 and incubated for 20 h; NESM antiserum was diluted 1:15 and incubated for 20 min. All antibodies were purchased from Sigma unless indicated otherwise. Proteins were detected by enhanced chemiluminescent peroxidase substrate (ECL) from Sigma. The washed membrane was incubated for 1 minute with a 1:1, (v/v) mixture of ECL-1 solution, containing 2.5 mM luminol, 450 μM coumaric acid, and ECL-2 solution, containing 0.03% hydrogen peroxide. The peroxidase oxidises luminol in the presence of hydrogen peroxide. Light emission occurring during luminol oxidation was detected by placing the blot in contact with an X-ray film (Kodak BioMax MR Film).

### **2.3.7 StrepII-tag detection with streptavidin**

The transfer of proteins from the polyacrylamide gel to the blotting membrane was carried out according to the procedure described in 2.3.6. After blotting, membranes were incubated

for 60 minutes in room temperature in PBS buffer containing 0.5% (w/v) Tween20 and 2 µg/ml avidin. After washing in PBS (270 mM NaCl, 5 mM KCl, 15 mM Na<sub>2</sub>HPO<sub>4</sub>, 3 mM KH<sub>2</sub>PO<sub>4</sub>, pH 7.5) with 0.1% (w/v) Tween20 buffer once for 15 minutes and twice for 5 minutes, membranes were incubated for 60 min at room temperature with streptavidin conjugated with alkaline phosphatase diluted 1:1000 in PBS buffer with 0.1% (w/v) Tween20. After another three 5 min washing cycles in PBS with 0.1% (w/v) Tween20 buffer membranes were rinsed with water and developed in a solution of one tablet of 5-bromo-4-chloro-3-indolyl phosphate/ nitro blue tetrazolium (BCIP/ NBT) freshly dissolved in 10 ml water. Membranes were incubated until bands were visible and the reaction was stopped either with water or 100 mM EDTA pH 7.2. Avidin, streptavidin and BCIP/ NBT tablets were purchased at Sigma.

### **2.3.8 Doubled SDS-polyacrylamide gel electrophoresis (dSDS-PAGE)**

Tricine dSDS-PAGE was used to separate the subunits of complex I from *Y. lipolytica* and was performed as described [205]. Briefly, lanes from 1D-gels (10% polyacrylamide, 6M urea) were incubated in acidic solution containing 100 mM Tris, 150 mM HCl, pH 2 for 30 min and analysed by SDS-PAGE as a second dimension using 16% polyacrylamide. The 2D-gels were stained with Coomassie blue G 250 or silver.

### **2.3.9 Two-dimensional blue-native SDS polyacrylamide gel electrophoresis (2D-BN/SDS PAGE)**

Native protein complexes were separated in the first dimension using BN-PAGE [206]. 500 µg of total protein was solubilised with 3 g/g digitonin and 500 mM amino caproic acid. The resulting solubilised mitochondrial membranes were put on 4-13% gradient gels. Gel stripes containing proteins were excised and incubated in 1% SDS solution for 30 min. Proteins were separated in the second dimension using 16% polyacrylamide SDS-PAGE.

### **2.3.10 Silver-staining of 2D-SDS gels**

After electrophoresis the gel was incubated for 15 minutes in fixation solution, which consisted of 50% methanol and 10% acetic acid. Subsequently the gel was incubated in

---

0,005% sodiumthiosulfate-pentahydrate. The gel was washed in H<sub>2</sub>O and incubated in 0.1% silver nitrate (w/v) for 30 minutes. Subsequently the gel was briefly washed in H<sub>2</sub>O and developed in freshly prepared developer: 2% (w/v) sodium bicarbonate in 100 ml H<sub>2</sub>O plus 100  $\mu$ L 36.5% formaldehyde. The development reaction was stopped by adding 100 ml of 50 mM EDTA solution.

### **2.3.11 Staining with nitro blue tetrazolium (NBT)**

NBT-staining was used to detect the NADH activity of complex I in BN-PAGE. The non-fixed gel was incubated in a solution containing 3 mM NBT and 120  $\mu$ M NADH for 5 minutes. In order to stop the reaction, the gel was incubated in 50 % methanol and 10 % acetic acid.

### **2.3.12 Measurement of NADH:HAR oxidoreductase activity**

Detergent- and inhibitor-insensitive NADH:HAR [HAR: hexa-ammine-ruthenium(III) chloride] oxidoreductase activity was measured using a Shimadzu MultiSpec-1501 or a Molecular Devices SPECTRAmax PLUS<sup>384</sup> spectrophotometer by following NADH-oxidation at 340 minus 400 nm ( $\epsilon=6.22 \text{ mM}^{-1}\text{cm}^{-1}$ ). Assays were performed in the presence of 200  $\mu$ M NADH and 2 mM HAR, in 20 mM Na<sup>+</sup>/Hepes, pH 8.0, 2 mM NaN<sub>3</sub> at 30°C [207]. This activity depends only on the presence of FMN and probably FeS cluster N3 [208]. The reaction was started by the addition of 50  $\mu$ g (total protein) of unsealed mitochondrial membranes.

### **2.3.13 Measurement of complex I catalytic activity**

For measurement of complex I activity, dNADH was used as electron donor, and the ubiquinone analogue DBQ was used as electron acceptor. dNADH:DBQ oxidoreductase activity at 60  $\mu$ M DBQ and 100  $\mu$ M dNADH was measured using a Shimadzu MultiSpec-1501 or a Molecular Devices SPECTRAmax PLUS<sup>384</sup> spectrophotometer by following dNADH-oxidation at 340 minus 400 nm ( $\epsilon=6.22 \text{ mM}^{-1}\text{cm}^{-1}$ ) at 30°C in 20 mM Na-MOPS pH 7.2 buffer containing 50 mM NaCl and 2 mM KCN. The reaction was started by adding mitochondrial membranes equivalent to a final concentration of 30 to 50  $\mu$ g of protein/ml.



### 2.3.14 Measurement of rhodanese activity

Rhodanese activity was assayed according to the procedure reported by Sörbo [209;209] and Westley [210;210], with minor modifications. The reaction mixture contained 50 mM KCN, 50 mM sodium thiosulfate, 50mM Bis/Tris buffer, pH 7.0 and 1 µg/µl of purified complex I. An equal amount of enzyme inactivated by addition of 15% formaldehyde was used as blank. The reaction was followed for up to 70 min at 25°C. 70 µl aliquots of the reaction mixture were taken every 10 min and stopped by the addition of 32,5 µl 15% formaldehyde and 97,5 µl ferric nitrate, Fe(NO<sub>3</sub>)<sub>3</sub>. The final volume was 200 µl. The resulting thiocyanate complex was measured at 460 nm using a Molecular Devices SPECTRAMax PLUS<sup>384</sup> spectrophotometer. One unit of rhodanese was defined as the amount of enzyme that catalyses transfer of one micromole sulfur from cyanide onto thiocyanate per minute under these conditions. Specific activity (mU/mg) was calculated using an  $\epsilon_{460}$  of 1600 6.22 mM<sup>-1</sup>cm<sup>-1</sup> per mole of SCN<sup>-</sup>.

### 2.3.15 Purification of complex I

Complex I was purified from isolated mitochondrial membranes that were solubilised with n-dodecyl-β-D-maltoside as described [211] with slight modifications. Purification was achieved by Ni<sup>2+</sup>-affinity chromatography with a modest reduction of the imidazole concentration from 60 mM to 55 mM in the equilibration and washing buffer and subsequent gel filtration using a TSK4000 column.

### 2.3.16 Reactivation of purified complex I

In its natural environment, complex I is embedded in a lipid bilayer. Most of these lipids are lost during protein purification, resulting in significant loss of catalytic activity. To reactivate dNADH:DBQ oxidoreductase activity of complex I, asolectin was added (total soy bean extract with 20 % lecithin) in a 1:1 (w/w) protein-to-lipid ratio. The asolectin solution was 10 mg/ml solubilised by 1.6 % OG in 1 mM KP<sub>i</sub> and 25 mM K<sub>2</sub>SO<sub>4</sub> pH 7.2.

---

### **2.3.17 EPR-spectra**

Low temperature EPR spectra were obtained with a Bruker ESP 300E spectrometer equipped with a liquid helium continuous flow cryostat, ESR 900 from Oxford Instruments. Samples were mixed with NADH in the EPR tube and frozen in liquid nitrogen after 30 seconds reaction time. Spectra were recorded at 12 K or at 40 K with the following instrument settings: microwave frequency 9.475 GHz, microwave power 1 mW, modulation amplitude 0.64 mT. Under these conditions spectra show contributions from clusters N1, N2, N3 and N4. Spectra were recorded and analyzed by Dr. Klaus Zwicker.

### **2.3.18 Protein analysis with the matrix assisted laser desorption ionization time of flight mass spectrometry (MALDI-TOF-MS)**

Stained protein spots were excised from dSDS polyacrylamide gels and treated following the protocol of [212]. The proteins were cleaved with trypsin (12.5 ng/μl) in digestion buffer containing 25 mM ammonium hydrogen carbonate, 5 mM CaCl<sub>2</sub> at 37°C over night.

Spectra were recorded in the positive ion mode with a Voyager De Pro MALDI-TOF mass spectrometer (Applied Biosystems, Germany). The samples were deposited on preparative plates by the fast evaporation method. DHB (2,5-dihydroxybenzoic acid) or HCCA (4-hydroxy- $\alpha$ -cyano-cinnamic acid) from Sigma were used as a matrix. Spectra were calibrated internally using bovine trypsin autolysis products ( $m/z$  805.4167 and 2163.0567) or, if necessary, externally using a reference peptide mixture of bradykinin, angiotensin II, insulin (oxidized B chain), adrenocorticotrophic hormone (ProteoMass Peptide MALDI-MS Calibration Kit, Sigma) covering the  $m/z$  757.3997-3494.6513 range. MALDI spectra were analysed by the Mascot software package (Matrix Science Ltd., London), Prowl software package (ProteoMetrics, LLC, New York, USA). Mass spectrometric analysis of the proteins was performed by Dr. Albina Abdrakhmanova.

### **2.3.19 Sequence analysis**

DNA and protein sequences were analyzed using the Vector NTI (Informax) software. Homology searches of mammalian and fungal databases were done using the BLAST server at <http://www.ncbi.nlm.nih.gov/BLAST/>. Alignments of fungal and mammalian proteins were generated using the program CLUSTALW at <http://www.ebi.ac.uk/clustalw/index.html>. Searches of the NCBI conserved domains database [213] were performed at the NCBI server ([www.ncbi.nlm.nih.gov/structure/cdd/wrpsb.cgi](http://www.ncbi.nlm.nih.gov/structure/cdd/wrpsb.cgi)).

## ***2.4 The phospholipid composition of mitochondria***

Mitochondrial lipids were analyzed using thin layer chromatography (TLC) and high performance liquid chromatography (HPLC) and subsequently identified with mass spectrometry (MALDI-TOF). The HPLC and MALDI-TOF phospholipid analysis was performed by Sebastian Richers, Max-Planck-Institute for Biophysics, Frankfurt am Main.

### **2.4.1 Extraction of phospholipids for the TLC analysis**

Mitochondrial membrane (prepared as described in 2.3.3) extracts from strain GB10, *acpm2Δ* and *acpm2Δ::pS88A* were used for TLC analysis. Extraction was carried out according to the method of [214]. An equivalent of 100 μg protein was mixed with 2.5 ml methanol and 1.25 ml chloroform in a glass tube, vortexed for 2 min and incubated on ice for 15 min. Following, 1.25 ml chloroform and 1.25 ml water was added and mixed. The organic (lower) and water (upper) phase separate and precipitated proteins and nucleic acids gather between the phases. To accelerate the separation process, centrifugation at 1000 rpm for 10 min in Heraeus Megafuge 1.0 RS (Osterode, Germany) was applied. The organic phase, containing extracted phospholipids, was transferred to another glass tube and removed on a rotary concentrator Rotavapor-R (Büchi Glasapparatefabrik, Flawil, Switzerland) under reduced pressure at 30°C. After evaporation the total lipid sample was taken up in a small volume of approx. 100 μl chloroform-methanol 2 : 1.

---

### 2.4.2 Thin layer chromatography (TLC)

Extracted phospholipids (25 µl) were applied to the TLC sheets covered with silica gel 60 F<sub>254</sub> (Merck, Darmstadt, Germany) step wise 5 x 5 µl dried in between steps. TLC sheets were developed with a liquid phase containing 190 ml chloroform, 70 ml methanol, 18 ml water, 20 ml acetic acid, 80 ml acetone and visualised either with Molybdenum Blue Spray Reagent (Sigma) or by means of Typhoon 9400 Variable Mode Imager (Amersham Biosciences, Little Chalfont, UK). Images of the TLC sheets containing fluorescent dye F<sub>254</sub> were recorded in the fluorescent mode PMT 300V, at normal sensitivity 520 BP40 in the blue laser light at 488 nm.

### 2.4.3 Extraction of phospholipids for HPLC analysis

For the phospholipids extraction four different starting materials: *Y. lipolytica* cells, mitochondrial membranes, intact mitochondria and sucrose gradient purified intact mitochondria [215] from strains GB10, *acpm2Δ* and *acpm2Δ::pS88A* and the *nubmΔ* were used. Phospholipid composition of extracted samples was determined using a High Performance Liquid Chromatography (HPLC) analysis lipids were extracted according to the method of [216] with two modifications. After mixing the 50 µl sample with 950 µl chloroform/methanol (2/1, v/v), the phase separation was induced by the addition of 200 µl HCl<sub>(aq)</sub> (0.1 M) instead of the original recommended salt solutions. Furthermore two additional cycles of washing of the aqueous phase with the organic phase increased the yield. The combined organic phases were dried and redissolved in chloroform/methanol (4/1, v/v).

### 2.4.4 Phospholipid analysis of *acpm2Δ* and *acpm2Δ::pS88A* with HPLC

The phospholipids were separated by normal phase chromatography with a solvent system of chloroform/methanol/water/ammonia based on the method described by [217]. An evaporative light scattering detector Sedex 75 (Sedere, France) supplied with 3.3 bar nitrogen and heated to 80 °C detected the phospholipids. Phospholipids were quantified by external calibration with commercially available standards: 1,1',2,2'-tetraoleoyl cardiolipin (CL); 1,2-dipalmitoyl-*sn*-glycero-3-phosphoethanolamine (PE); L- $\alpha$ -phosphatidylinositol (PI), (soy bean); 1,2-dipalmitoyl-*sn*-glycero-3-phosphate (PA); 1,2-dipalmitoyl-*sn*-glycero-3-

phosphocholine (PC); L- $\alpha$ -lysophosphatidylethanolamine (egg, chicken), (LPE); L- $\alpha$ -lysophosphatidylinositol (soy bean), (LPI); 1-palmitoyl-2-hydroxy-*sn*-glycero-3-phosphate (LPA); 1-palmitoyl-2-hydroxy-*sn*-glycero-3-phosphocholine (LPC), (all from Sigma).

#### **2.4.5 Mass spectrometry of phospholipids**

Matrix-assisted laser desorption ionization time-of-flight (MALDI-TOF) mass spectrometry was used to identify the type of phospholipid headgroup and the fatty acid composition. Samples of phospholipid extracts were used directly, while the collected HPLC fractions were dried in a speed vac and redissolved in 4  $\mu$ L 19:1 (v/v) chloroform-methanol solution to change the solvent and increase the concentration. About 2  $\mu$ L of the sample were slowly added to MALDI target spots. The fast evaporation of the organic solution under the air stream of the fume hood allowed the addition of this relative large volume compared to the spot size. Despite the chloroform content of the solutions, plastic tips were used with a Gilson pipette to avoid scratching the target with glass. After the samples had dried completely, 0.3  $\mu$ L of matrix solution (0.5 M 2,5-dihydroxybenzoic acid in methanol with 2% (v/v) formic acid) were added to the spots. The dried target was inserted into the MALDI-TOF mass spectrometer and samples were analyzed in the range of 0-2000 m/z. Using the negative charged mode greatly simplifies the spectrum and allows the detection of other phospholipids even in the presence of phosphatidyl choline. Detectability of phospholipids and quality of spectra was largely depending on the laser energy which was optimal at around 55 %. Typically the resulting spectra of 200 laser shots were acquired and summed up. Phospholipid mixtures containing Dipalmitoyl-Glycero-Phosphate and Tetraoleoyl-Cardiolipin 0.1 g/L were used as external calibration standards in close vicinity to the sample spots. The monoisotopic masses of their single deprotonated ions containing over all a single negative charge were used for linear calibration. The  $[M-H]^-$  masses are 647.47 m/z for Dipalmitoyl-Glycero-Phosphate and 1456.03 m/z for Tetraoleoyl-Cardiolipin.



## 3 RESULTS

### 3.1 *Acyl carrier proteins*

#### 3.1.1 Generation of ACPM deletion strains

Using the sequences from the Genolevures website (<http://cbi.labri.fr/Genolevures/index.php>), the *ACPM* homologues YALI0D14850g (*ACPM1*) and YALI0D24629g (*ACPM2*) were identified. 2.70 kb of genomic DNA comprising the complete *ACPM1* open reading frame (two exons) and 0.97 kb of 5' and 0.96 kb of 3' flanking DNA was amplified with primers<sup>3</sup> *acpm1f* and *acpm1r* (Figure 3.1a). 3.60 kb of genomic DNA, comprising the complete *ACPM2* open reading frame (three exons) and 1.20 kb of 5' and 0.66 kb of 3' flanking DNA, was amplified using primers *acpm2f* and *acpm2r* (Figure 3.1b). Both PCR products were made using Taq DNA polymerase and genomic DNA from *Y. lipolytica* strain<sup>4</sup> E129 and cloned into plasmid<sup>5</sup> pCR2.1 (Figure 3.1a). Deletion strains for the ACPM subunits of complex I from *Y. lipolytica* were generated by homologous recombination using the one-step transformation method as described [197]. Deletion alleles in which the *ACPM* ORFs are replaced with the *URA3* marker gene were created as follows: First, genomic DNA fragments were transferred into the single *EcoRI* site of vector pUC19Δ (Figure 3.1d, e). Then, the *ACPM1* construct was gapped by PCR, using primers *acpm1Sall* and *acpm1BamHI*, thereby removing the ORF together with 143 bp of 5' flanking sequence and 22 bp of 3' flanking sequence. Similarly, the *ACPM2* construct was gapped by PCR, using primers *acpm2Sall* and *acpm2BamHI*, thereby removing the ORF together with 16 bp of 5' flanking sequence and 4 bp of 3' flanking sequence. The PCR products were digested with *BamHI* and *Sall* and ligated with the *Y. lipolytica URA3* marker gene as a 1.7 kb *BamHI/Sall* fragment, such that the orientation of the marker was opposite to the original ORFs (Figure 3.1c, f, g). Then, the hygromycin B resistance gene was cloned into the *HindIII* site and the *NotI* site, immediately adjacent to the *EcoRI* site was introduced by site-directed mutagenesis

<sup>3</sup> For gene maps see 9.1.2 and 9.1.3, appendix and for the list of primers see 9.2.2 and 9.2.3, appendix.

<sup>4</sup> Genotypes of all strains are listed in 2.1.5, materials and methods.

<sup>5</sup> See maps of plasmids in 2.1.6, materials and methods.

in both vectors (*Figure 3.1i, j*). Thereby, vectors pUB44 containing deletion constructs of each *ACPM* gene were created.

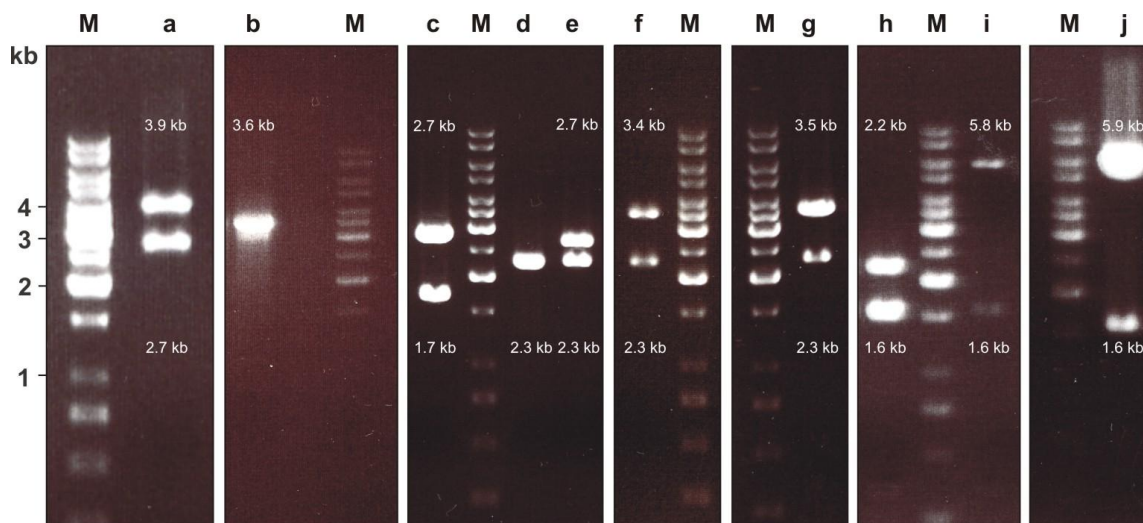


**Figure 3.1 Generation of *ACPM* deletion constructs**

(a) The pCR2.1 vector of 3.9 kb containing the *acpm1* insert of 2.7 kb digested with *EcoRI* restriction enzyme. (b) The *acpm2* fragment of 3.6 kb produced by PCR using primers *acpm2f* and *acpm2r*. (c) The *URA3* ORF insert of 1.7 kb excised from pBlueScript SK- vector of 2.7 kb using *BamHI* and *Sall* restriction enzymes. (d) The empty pUC19Δ vector of 2.3 kb containing (e) the *acpm1* insert of 2.7 kb, (f) the *acpm1* deletion construct (*acpm1::URA3*) of 3.4 kb and (g) the *acpm2* deletion construct (*acpm2::URA3*) of 3.5 kb, all digested with *EcoRI*. (h) The empty pUB44 vector of 3.9 kb digested with *HindIII* into hygromycin B resistance gene (*HygB<sup>R</sup>*) of 1.6 kb and 2.3 kb fragment. (i) The pUB44 vector of 3.9 kb containing an *acpm1* deletion construct (*acpm1::URA3*) of 3.4 kb digested with *HindIII* yielding *HygB<sup>R</sup>* of 1.6 kb and 5.8 kb restriction fragment. (j) The pUB44 vector of 3.9 kb containing an *acpm2* deletion construct (*acpm2::URA3*) of 3.5 kb cut with *HindIII* yielding *HygB<sup>R</sup>* of 1.6 kb and fragment of 5.9 kb. Size of the fragments of the molecular weight marker (M) is indicated on the left side of the figure in kilobase pairs (kb).

To exclude ligation of multiple inserts and assure proper orientation of cloned fragments, plasmids were test digested with a number of restriction enzymes. The resulting final constructs were linearized with *NotI* and transformed into the diploid *Y. lipolytica* strain GB14 (*Figure 3.2*). Heterozygous deletion strains in which one of the chromosomal copies of either *ACPM1* or *ACPM2* had been replaced with the *URA3* marker by double homologous recombination were selected for their ability to grow in the absence of uracil and their inability to grow in the presence of hygromycin B. Sporulation, followed by random spore selection was performed both in the presence and absence of 10 μg/ml lipoic acid (see 2.2.19,



materials and methods). Deletion strains transformed with a functional copy of the respective *ACPM* genes on replicative plasmid pUB4 [196] were used as controls and will be referred to as parental strains here.

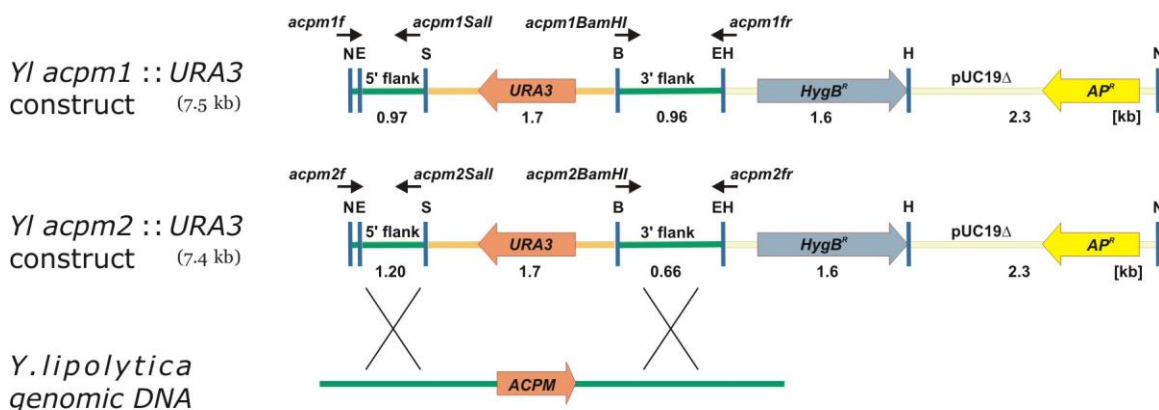


**Figure 3.2** Deletion strategy for *ACPMs*

A *NotI* linearized construct containing the *URA3*-marked *ACPM* deletion allele (orange), the hygromycin B resistance gene (*HygB<sup>R</sup>*), grey and the rest of the pUC19Δ plasmid with ampicillin resistance gene (*AP<sup>R</sup>*), yellow used for deletion of *ACPM* genes by double homologous recombination (indicated by crosses). The *ACPM* deletion (*ACPM/acpmΔ*) strains were selected for their ability to grow in the absence of uracil and their inability to grow in the presence of hygromycin B. Protein coding regions are represented by thick arrows, flanking DNA from the *Y. lipolytica* *ACPM* locus by green lines. The location of primers is indicated by black thin arrows above the construct. The following restriction sites are shown: E, *EcoRI*; H, *HindIII*; N, *NotI*; S, *Sall*; B, *BamHI*.

To ensure proper integration of the deletion constructs into genomic locus of *ACPM* genes, *Y. lipolytica* transformants were tested in a PCR reaction using primers: *acpmckf/acpmchkr* that bind to the chromosomal gene locus outside of the *ACPM* gene; *ura3ds2/ura3us2* binding to the deletion construct and *acpmseq3/acpmseq4* binding to the *ACPM* gene (Figure 3.3).

Proper integration of the *acpm1Δ* construct into the chromosomal locus of the *acpm1* gene was confirmed using primer pairs *acpm1chkf/ura3ds2* and *acpm1chkr/ura3us2*, since products of 1.080 kb and 1.075 kb, respectively were obtained. This indicated presence of the *URA3* gene on the chromosome in the genomic locus of *ACPM1* in the *acpm1Δ* strain (Figure 3.3a, b). In case of *acpm2Δ* strain presence of the *ACPM2* gene was excluded in a PCR reaction using primers *acpm2seq3/acpm2seq4*, in which no product was formed

(Figure 3.3c). Presence of the *URA3* gene in the *acpm2Δ* strain was confirmed using primers *acpm2chkr/ura3us2*, which resulted in a product of 1.050 kb (Figure 3.3f).

As control strains, carrying wild-type copies of the *ACPM2* gene, GB14 and a diploid *acpm2Δ* strain, complemented with the plasmid version of a functional copy of the *ACPM2* gene (2n *acpm2Δ/ACPM2*) were used. Presence of the *ACPM2* gene in the GB14 and the *acpm2Δ/ACPM2* was confirmed in a PCR reaction using primers *acpm2seq3/acpm2seq4*, which yielded a product of 1.000 kb in both strains (Figure 3.3d, e). Absence of the *URA3* gene in the *acpm2Δ/ACPM2* strain was confirmed using primers *acpm2chkf/ura3ds2*, since no product was obtained (Figure 3.3g). Presence of the *URA3* gene in the *acpm2Δ/ACPM2* strain was confirmed using primers *acpm2chkr/ura3us2*, since a 1.050 kb band was observed (Figure 3.3h).

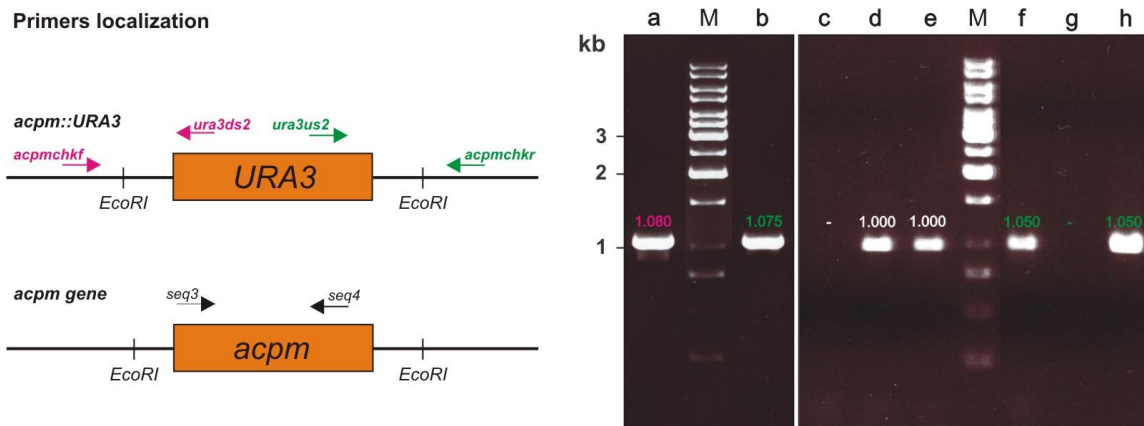


### Figure 3.3 The PCR test for the deletion of *ACPM* genes

The localization of primers in the deletion construct (*acpm::URA3*) and in the genomic locus of the *ACPM* gene are indicated with arrows (left panel). The transformants carrying a properly integrated *URA3* gene into the chromosome of the diploid GB14 strain of *Y. lipolytica* were isolated and checked by PCR (right panel). The *acpm1Δ* strain was tested using primers *acpm1chkf/ura3ds2* (magenta) and *acpm1chkr/ura3us2* (green) that yielded products of (a) 1.080 kb and (b) 1.075 kb, respectively, which confirmed presence of the *URA3* gene in this strain. The *acpm2Δ* strain was verified using primers (c) *acpm2seq3/acpm2seq4* (black) that yielded no product thus excluded presence of the *ACPM2* gene and (f) *acpm2chkr/ura3us2* (green) that yielded a product of 1.050 kb, which confirmed presence of the *URA3* gene in *acpm2Δ*. (d) The GB14 and (e) the *acpm2Δ/ACPM2* strains were both checked using primers *acpm2seq3/acpm2seq4* (black). In both strains, the PCR reaction yielded a product of 1.000 kb, which confirmed presence of *ACPM2* in both strains. (g) The GB14 strain was also confirmed to lack the *URA3* gene using primers *acpm2chkf/ura3ds2* (magenta), since no PCR product was obtained. (h) The *acpm2Δ/ACPM2* strain was confirmed to contain the *URA3* gene using primers *acpm2chkr/ura3us2* (green) since a 1.050 kb band was observed. Size of the fragments of the molecular weight marker (M) is indicated on the left side of the agarose gel in kilobase pairs (kb).

### 3.1.2 Generation of strains with exchanged serines binding the phosphopantethein moiety

Open reading frames (ORFs) together with flanking regions of *ACPM* genes were amplified in the pCR2.1 vector as described in 3.1.1 and cloned into the *EcoRI* site of the vector pUB4 (Figure 3.4A). Mutations leading to the exchange of the phosphopantethein binding serines for alanines were carried out by PCR using primer pairs *acpm1S66Af/ acpm1S66Ar*, *acpm2S88Af/ acpm2S88Ar* for *ACPM1-S66A* and *ACPM2-S88A*, respectively. The resulting products were test digested with *EcoRI* restriction enzyme (Figure 3.4B) and sequenced on an Applied Biosystems 310 genetic analyzer (Figure 3.5). Plasmids pUB4 carrying the mutated genes were transformed into *ACPM1/ acpm1Δ* and *acpm2Δ* strains, respectively and checked by PCR (Figure 3.6).

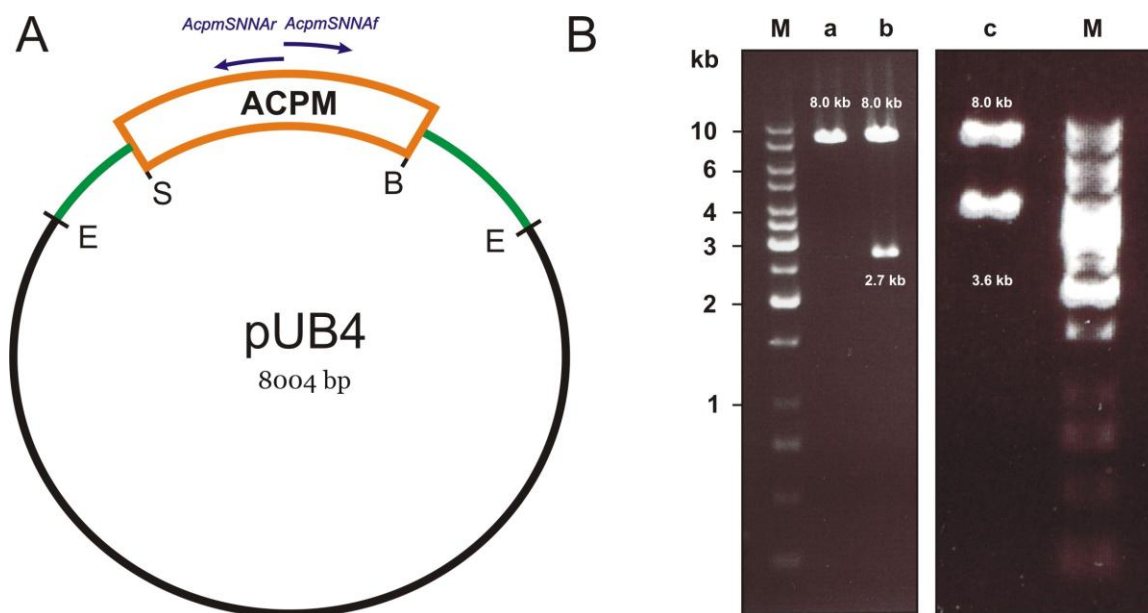


**Figure 3.4** Plasmid *pUB4* containing mutated versions of *ACPMs*

(A) The localization of mutagenesis primers (violet arrows) used for exchange of serines to alanines in *ACPM1-S66A* and *ACPM2-S88A* proteins indicated on the *ACPM* protein coding region (orange). The *ACPM* ORFs were cloned, including their flanking DNA (green lines), into the *EcoRI* site of the pUB4 vector (black). *NN* denotes in primer names position of the serine, 66 in case of *ACPM1* and 88 in case of *ACPM2*. The following restriction sites are shown: E, *EcoRI*; S, *SalI*; B, *BamHI*. (B) *EcoRI* restriction cut of (a) an empty pUB4 plasmid, (b) the plasmid containing a 2.7 kb insert of *ACPM1-S66A* and (c) a 3.6 kb insert of *ACPM2-S88A*. Size of the fragments of the molecular weight marker (M) is indicated on the left side of the agarose gel in kilobase pairs (kb).

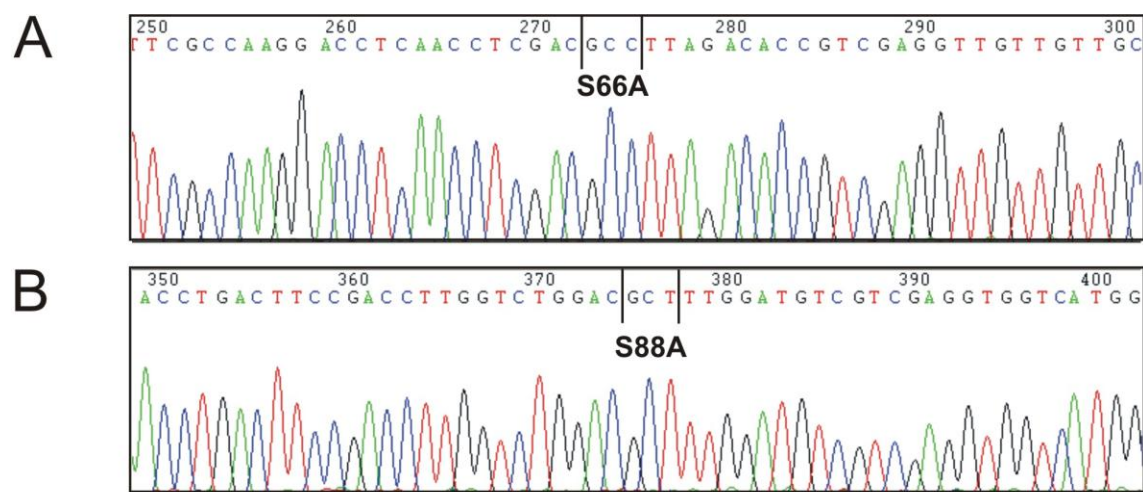


**Figure 3.5 Sections of DNA sequence pherograms from ACPM point mutants**

Mutations leading to the exchange of the phosphopantethein binding serines for alanines in (A) *acpm1Δ,pACPM1-S66A* and (B) *acpm2Δ,pACPM2-S88A* strains were verified by sequencing using primers *acpm1seq1* and *acpm2seq1*, respectively on an Applied Biosystems 310 genetic analyzer.

While the *acpm2Δ,pACPM2-S88A* strain could be generated no *acpm1Δ,pACPM1-S66A* spores were obtained. The *acpm2Δ,pACPM2-S88A* transformants and three control strains, the GB 14, the *acpm2Δ* and a diploid *acpm2Δ* strain, complemented with the plasmid version of a functional copy of the *ACPM2* gene ( $2n$  *acpm2Δ,pACPM2*) were checked by PCR using two primer pairs *acpm2chkf/acpm2S88Ar* and *acpm2f/acpm2S88Ar*, here referred to as (1) and (2), respectively. Localisation of the primers is indicated in (Figure 3.6, left panel). The *acpm2chkf* primer binds outside of the *ACPM2* gene, *acpm2f* binds on the flanking DNA of *ACPM2* gene and *acpm2S88Ar* binds on the ORF of the *ACPM2*. The diploid GB14 strain was confirmed in a PCR reaction using primer pairs (1) and (2) to carry two alleles of *ACPM2* gene, since products of 1.48 kb (magenta) and 1.46 kb (green) respectively, were obtained (Figure 3.6a). The diploid *acpm2Δ,pACPM2* was confirmed to lack a chromosomal copy of the *ACPM2*, since no product with primers (1) could be generated, and it was shown to contain a plasmid-borne copy of the *ACPM2*, since a product of 1.46 kb (green) was obtained with primers (2) (Figure 3.6b). The *acpm2Δ* strain was proven to lack both chromosomal and plasmid versions of the *ACPM2* gene using primer pairs (1) and (2), since no PCR products could be obtained (Figure 3.6c). Finally, the *acpm2Δ,pS88A* strain was confirmed to lack the chromosomal copy of the *ACPM2* gene,

since no product with primers (1) were formed and it was proved to carry a plasmid-borne copy of the *ACPM2-S88A* gene, since a product of 1.46 kb (green) was obtained with primers (2) (*Figure 3.6d*).

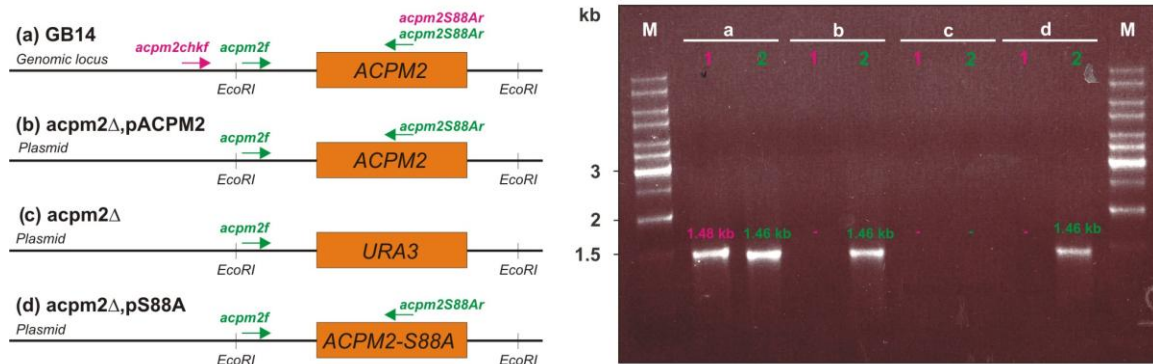


**Figure 3.6 PCR test for presence of *ACPM2-S88A* gene**

In the PCR test for the presence of the *ACPM2-S88A* gene using two primer pairs: (1) *acpm2chkf/acpm2S88Ar* (magenta) and (2) *acpm2f/acpm2S88Ar* (green) strains (a) GB14, (b) *acpm2Δ,pACPM2*, (c) *acpm2Δ* and (d) *acpm2Δ,pS88A* were checked. In these PCR reactions using primers (1) and (2) the following products were obtained, respectively: (a) 1.48 kb and 1.46 kb; (b) no product, 1.46 kb; (c) no product for both primer pairs; (d) no product, 1.46 kb. Size of the fragments of the molecular weight marker (M) is indicated on the left side of the agarose gel in kilobase pairs (kb).

### 3.1.3 The tagged versions of ACPMs

Open reading frames (ORFs) of *ACPM* genes together with flanking regions were amplified in the pCR2.1 vector as described in 3.1.1 and cloned into the *EcoRI* site of the vector pUC19Δ. For generation of the *ACPM1-strepII* and *ACPM2-flag* strains primer pairs *acpm1strepIIIf/acpm1strepIIr* and *acpm2flagf/acpm2flagr*, respectively were used. As a result *ACPM* ORFs were extended by 8 amino acids at the C-termini: *ACPM1* by WSHPQFEK and *ACPM2* by DYKDDDDK. Tagged versions of *ACPM* genes were transferred to the *EcoRI* site of the pUB4 vector and checked by test digestion with restriction enzymes *EcoRI*, and following with *NheI* and *NdeI* to assure cloning of only one insert of tagged *ACPM* gene (*Figure 3.7*). Subsequently, plasmids were confirmed by sequencing (*Figure 3.8*) and transformed into diploid strains carrying one wild-type (*ACPM*) and one *acpm::URA3* allele (*ACPM/acpmΔ*) (*Figure 3.7*). Complemented haploid deletion

strains were obtained by sporulation and random spore selection (2.2.19, materials and methods).

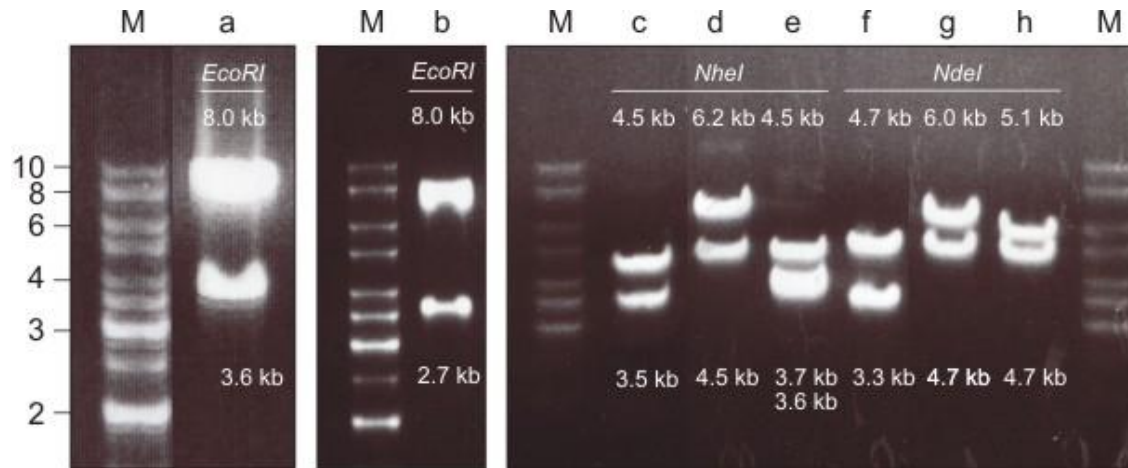


**Figure 3.7 Test digest of pUB4 plasmid containing tagged versions of ACPMs**

The 8.0 kb pUB4 plasmid digested with *EcoRI* containing (a) a 3.6 kb *ACPM1-strepII* insert and (b) a 2.7 kb *ACPM2-flag* insert. To assure presence of only one copy of *ACPM* insert per pUB4 plasmid (c, f) the empty plasmid and (d, g) the plasmid containing the *ACPM1-strepII* and (e, h) the *ACPM2-flag* insert was digested with *NheI* and *NdeI*, respectively resulting in two restriction fragments each. The only exception is (e) the pUB4 vector containing the *ACPM2-S88A* insert, which harbours an additional *NheI* site in the *ACPM2-S88A* fragment. As a result, three restriction fragments (3.6, 3.7 and 4.5 kb) are formed, although on the gel 3.5 kb and 3.6 kb are visible as one thick band. Size of the fragments of the molecular weight marker (M) is indicated on the left side of the agarose gel in kilobase pairs (kb).

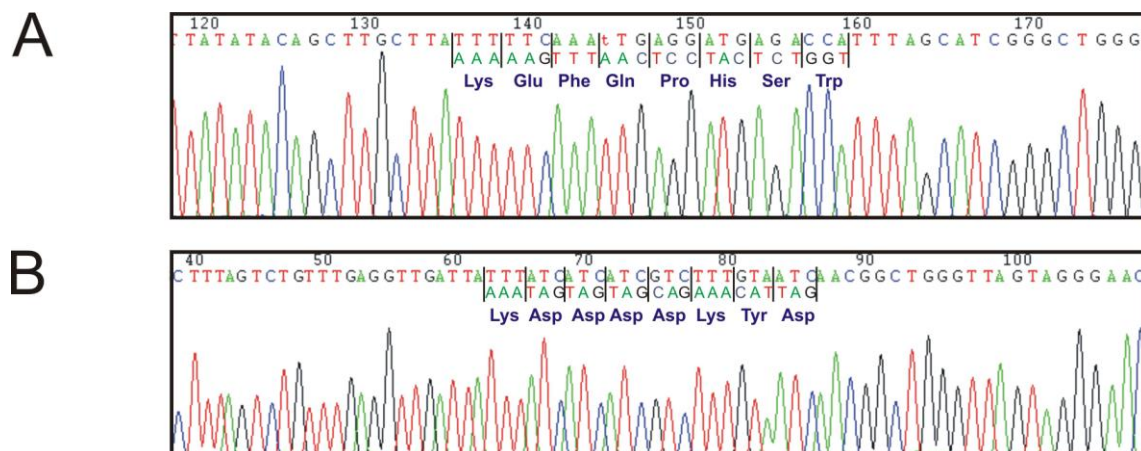


**Figure 3.8 Sections of DNA sequence pherograms from ACPM tagged versions**

*ACPM* ORFs were extended by 8 amino acids at the C-termini: (A) *ACPM1* by WSHPQFEK (StrepII-tag) and (B) *ACPM2* by DYKDDDDK (Flag-tag) as verified by sequencing using primers (A) *acpm1seq4* and (B) *acpm2seq4*, respectively. For localization of primers see 9.1, appendix.

### 3.1.4 Consequence of the deletion of ACPM1 and ACPM2 genes

In order to investigate the function of the ACPMs the two homologues of the *S. cerevisiae* gene for the mitochondrial acyl carrier protein (YKL192c) that had been identified in the *Y. lipolytica* genome as YALI0D14850g (*ACPM1*) and YALI0D24629g (*ACPM2*) were deleted as described in 3.1.1. To minimize the risk of selection for second site repressors during homologous recombination, the linearized deletion constructs were transformed into the diploid *Y. lipolytica* strain GB14 (Figure 3.2). In the case of *ACPM2*, the desired diploid strain that was confirmed to be heterozygous for the deletion allele could be sporulated to yield the desired haploid *acpm2::URA3* deletion strain.

While a diploid *ACPM1/ acpm1::URA3* deletion strain was successfully generated, subsequent extensive sporulation attempts failed to generate haploid strains carrying the *ACPM1* deletion allele. However, when a plasmid-borne, functional copy of the *ACPM1* gene was introduced into the *ACPM1/ acpm1::URA3* strain prior to the sporulation, haploid *acpm1Δ,pACPM1* strains could be isolated. This demonstrated successful complementation of the deletion allele and excluded that second-site genetic defects in the diploid heterozygous deletion strain had prevented formation of viable haploid deletion spores. This experiment indicates that *ACPM1* is an essential gene in *Y. lipolytica*. To discriminate whether the ACPM1 protein as a whole or just its functional group was required for survival serine-66 of ACPM1 with alanine was exchanged. This serine is conserved in all acyl-carrier proteins and known to bind the phosphopantethein moiety. A plasmid-borne copy of *ACPM1-S66A* was transformed into the heterozygous *ACPM1/ acpm1::URA3* strain, but in contrast to the wild-type copy it failed to complement the deletion phenotype and no *acpm1Δ,pACPM1-S66A* spores were obtained. Thus the single amino acid exchange seemed to have the same effect as complete removal of the *ACPM1* gene.

In contrast, *ACPM2* was found to be not essential in a strain carrying NDH2i to complement for complex I deficiency and a haploid *ACPM2* deletion strain (*acpm2Δ*) was obtained. To test whether complex I was affected by deletion of the *ACPM2* gene, first its activities in mitochondrial membranes prepared from the deletion strain were measured and compared to the parental strain (Table 3.1).

	parental	<i>acpm2Δ</i>	<i>acpm2Δ,pS88A</i>	<i>ACPM1-strepII</i>	<i>ACPM2-flag</i>
	$\mu\text{mol min}^{-1}\text{mg}^{-1}$				
<i>Mitochondrial membranes</i>					
NADH:HAR oxidoreductase	0.75	0.18	0.17	0.81	0.77
dNADH:DBQ oxidoreductase	0.27	<0.1	<0.1	0.31	0.30
<i>Purified complex I</i>					
NADH:HAR oxidoreductase	45.2	n.d <sup>6</sup>	n.d	49.5	48.0
dNADH:DBQ oxidoreductase	3.4	n.d	n.d	3.1	3.0

**Table 3.1 Catalytic activities of mitochondrial membranes and complex I**

Specific inhibitor sensitive dNADH:DBQ oxidoreductase activity was lost completely. A strong decrease in dNADH:HAR oxidoreductase activity down almost to a level typically observed with other complex I deficient strains suggested that the loss of complex I activity was due to a very low content of complex I. Remarkably, essentially the same loss in activity was observed when a mutated copy of the *ACPM2* gene was introduced on a plasmid in which the phosphopantethein binding serine-88 was replaced by alanine. The loss of complex I was confirmed when mitochondrial membranes from the *acpm2Δ* strain and the parental strain were analyzed by two-dimensional BN/SDS-PAGE (Figure 3.9A, B). In contrast to the parental strain no complex I could be detected by silver staining in the *ACPM2* deletion strain (Figure 3.9B). The same result was obtained with the mutant version lacking serine-88 (Figure 3.9C). The pattern of the other respiratory chain complexes V<sub>D</sub>, V<sub>M</sub>, III, IV, II and the presence of small amounts of subcomplex F<sub>1</sub>, corresponding to the matrix part of complex V [218] were not affected by the deletion (Figure 3.9).

<sup>6</sup> Not determined



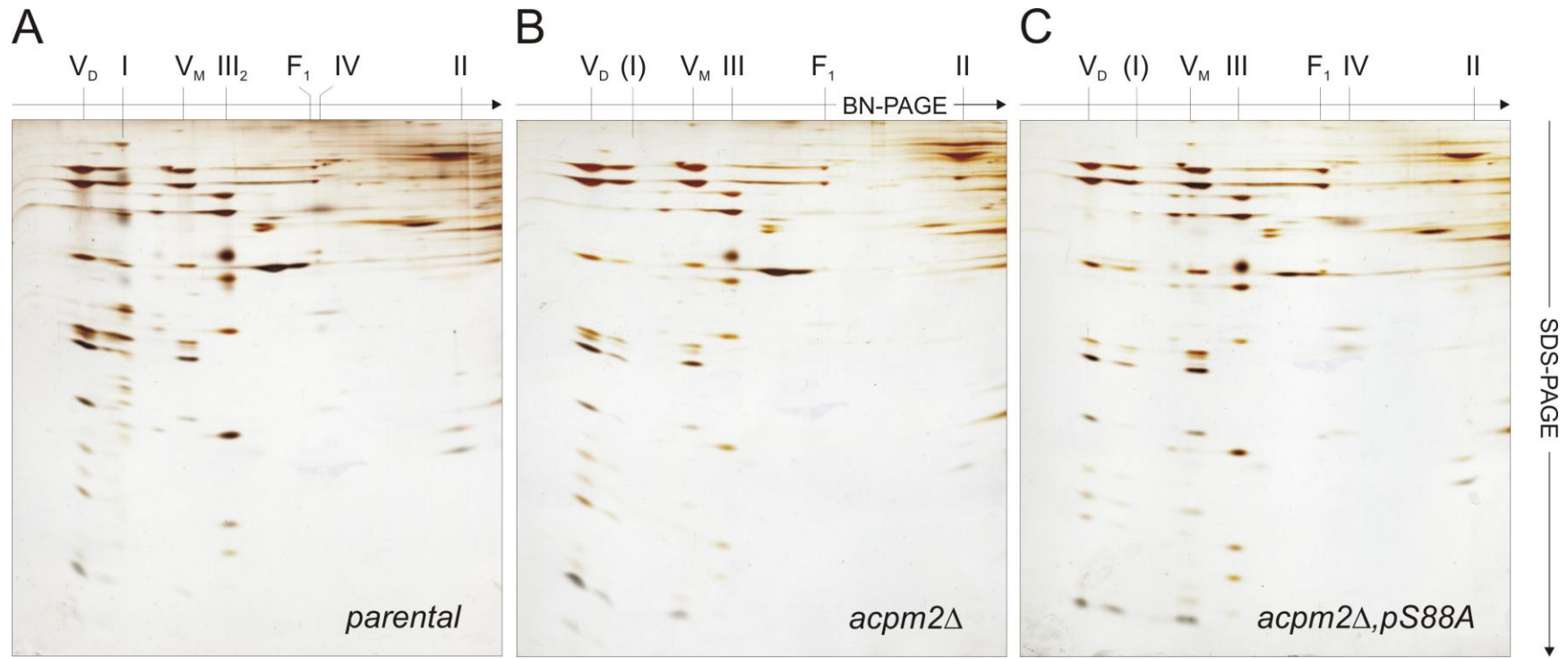


**Figure 3.9 2D-BN/SDS PAGE analysis of *Y. lipolytica* mitochondrial membranes**

Protein complexes were resolved by BN-PAGE in the first and by 16 % SDS-PAGE in the second dimension. (A) A typical pattern of the parental strain respiratory chain complexes visible from left to right with decreasing molecular weight: ATP synthase dimer (V<sub>D</sub>), complex I, complex V monomer (V<sub>M</sub>), complex III, complex IV and complex II. (B) *acpm2Δ* strain and (C) *acpm2Δ,pACPM2-S88A* strain exhibit lack of complex I assembly. Other respiratory complexes appear to assemble normally.

---

For higher sensitivity and to detect low amounts of possible subcomplexes of complex I mitochondrial membranes from the *acpm2Δ* strain were further analyzed by Western blotting of two dimensional (Blue Native/SDS) gels with different antibodies directed against subunits of complex I (Figure 3.10). In membranes from the parental strain fully assembled complex I was found to be the dominant form. In addition, several supercomplexes containing complex I together with complexes III and/or complex IV were detected as described recently [219]. Most likely these are (from left to right with decreasing molecular weight): complex I dimer; I<sub>1</sub>III<sub>2</sub>IV<sub>2</sub>, I<sub>1</sub>III<sub>2</sub>IV<sub>1</sub>, I<sub>1</sub>III<sub>2</sub>, I<sub>1</sub>IV<sub>2</sub>, I<sub>1</sub>IV<sub>1</sub>. Some disintegration of complex I into subcomplexes was also observed with monoclonal antibodies directed against the 51-kDa and 49-kDa subunits of the peripheral arm and the accessory NESM subunit of the membrane arm. With mitochondria from the *ACPM2* deletion and the S88A mutant strain a very small amount of fully assembled complex I was detected with all three antibodies. However, only with the antibody directed against the NESM subunit pronounced signals of two putative subcomplexes were observed. These subcomplexes migrated in a similar position as the disintegration products observed with the parental strain at about 700 (marked with 1 ❶) and 300 kDa (marked with 2 ❷), but the fact that they were not detectable by the anti-51-kDa and anti-49-kDa antibodies in the *ACPM2*-mutant strains suggested a different composition. Rather, the antibodies directed against the 51-kDa and 49-kDa subunits gave strong signals over a broad range of molecular masses that were even more pronounced in the *ACPM2*-mutants. These signals probably reflected the individual subunits and/or small subcomplexes (up to about 100 kDa in size) containing the respective subunits. Unfortunately, due to the very small amounts available, it was not possible to analyze the subunit composition of the subcomplexes any further.

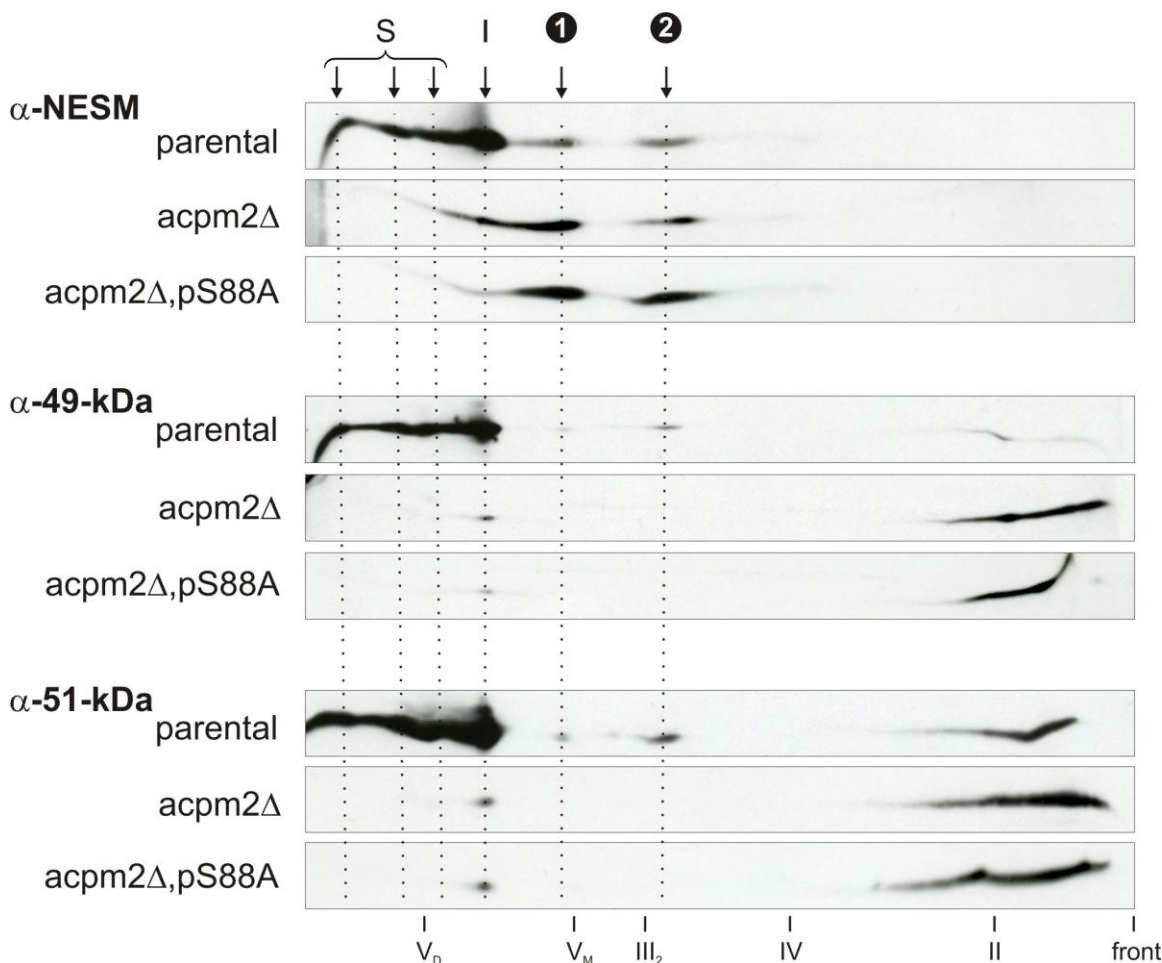


**Figure 3.10 Complex I subcomplexes in *acpm2* $\Delta$  and the *acpm2* $\Delta$ pACPM2-S88A strains**

Western Blot analysis of mitochondrial membranes from the parental strain and strains *acpm2* $\Delta$  and *acpm2* $\Delta$ , pACPM2-S88A is shown. Subcomplexes were detected at positions marked above the picture with 1 ❶ and 2 ❷ by antibodies against the 51-kDa, the 49-kDa and the NESM subunit in the parental strain. In strains *acpm2* $\Delta$  and pACPM2-S88A only the antibody against the membrane arm subunit NESM indicated subcomplexes in these positions suggesting that different subcomplexes of similar size but different composition were detected. In strains *acpm2* $\Delta$  and pACPM2-S88A the majority of the 49-kDa and 51-kDa subunits of the peripheral arm were detected close to the front of the gel and only minute amounts of fully assembled complex I denoted with (I) were identified. Several supercomplexes (S) of complex I associated with complex III and complex IV as described recently in [219] were detected as indicated (S). Positions of the respiratory chain complexes are denoted from left to right with decreasing molecular weight: ATP synthase dimer ( $V_D$ ), complex V monomer ( $V_M$ ), complex  $III_2$ , complex IV and complex II.

### 3.1.5 The mitochondrial lipid composition analysed by thin layer chromatography

To see whether deletion and mutagenesis of ACPM2 had affected the lipid composition, the phospholipid content of extracts (2.4.1, materials and methods) from intact mitochondria of parental, *acpm2Δ* and *acpm2Δ,pACPM2-S88A* strains were analyzed by the thin layer chromatography (TLC), (2.4.2, materials and methods). Phospholipids separated in the chromatography run were visualized either by molybdenum dye staining or by scanning the TLC sheets containing fluorescent dye F<sub>254</sub> with Typhoon Imager. Regardless of the staining method only limited number of phospholipids, phosphatidyl-choline (PC) and phosphatidyl-ethanolamine (PE) (*Figure 3.11A*) or PC, PE and cardiolipin (CL) (*Figure 3.11B*) could be identified, respectively. Also, no difference in the phospholipid composition could be observed among the analyzed strains.

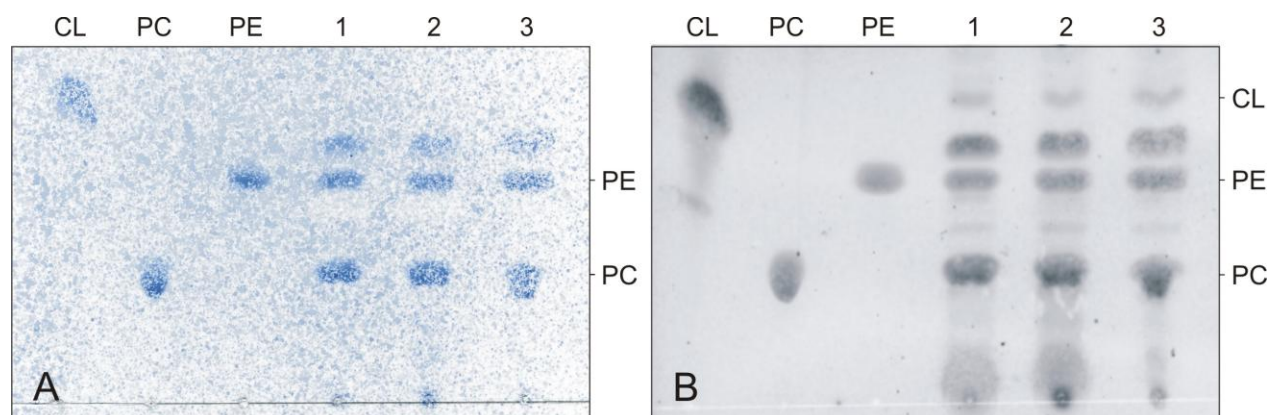


**Figure 3.11 Thin layer chromatography (TLC) of lipids extracted from intact mitochondria**

The TLC analysis of mitochondrial lipids extracted from the (1) parental, (2) *acpm2Δ* and (3) *acpm2Δ::pS88A* strains. The following reference phospholipids were used: CL, cardiolipin; PC, phosphatidyl-choline and PE, phosphatidyl-ethanolamine. (A) Two bands corresponding to phospholipids PE and PC, as well as one unidentified band were detected by visualisation of the TLC sheet with Molybdenum Blue Spray Reagent; (B) Bands corresponding to all reference phospholipids CL, PC and PE, as well as several unidentified bands were detected in the TLC sheet containing a fluorescent dye F<sub>254</sub> scanned with Typhoon Imager in the blue laser light at 488 nm. No difference in the lipid composition among analysed strains both in (A) and (B) could be observed.

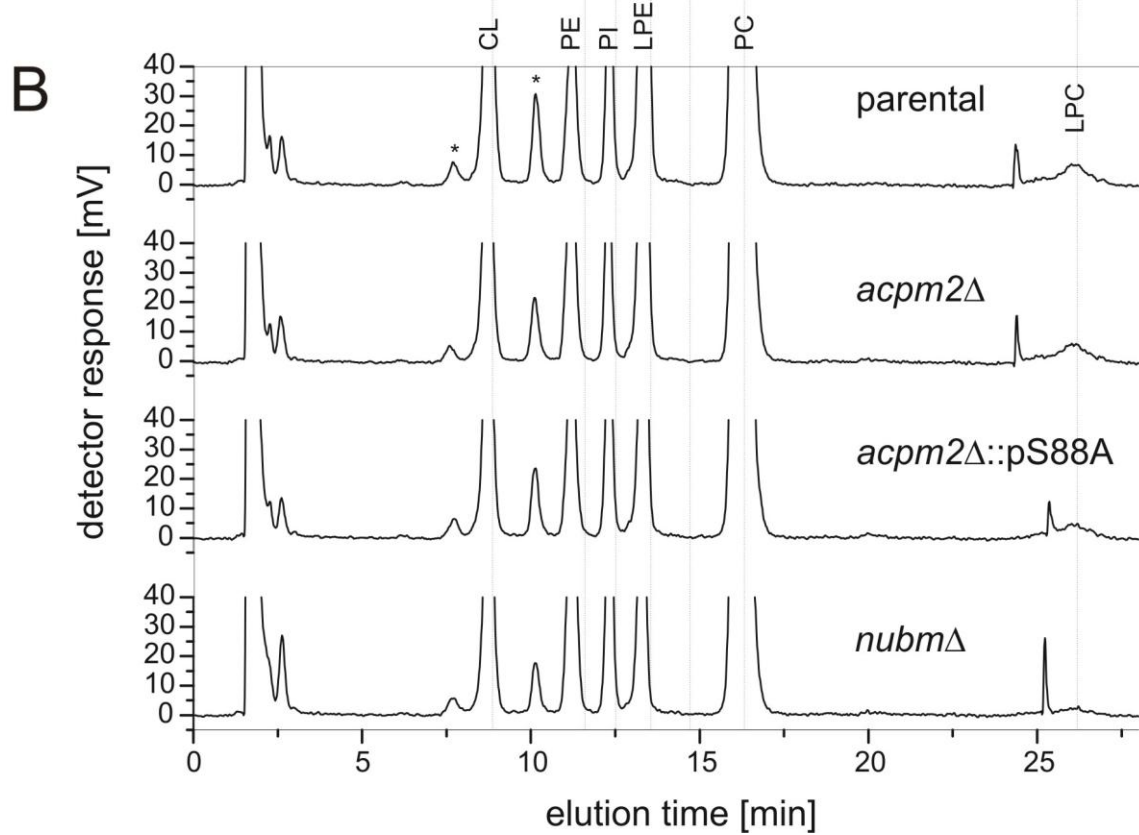
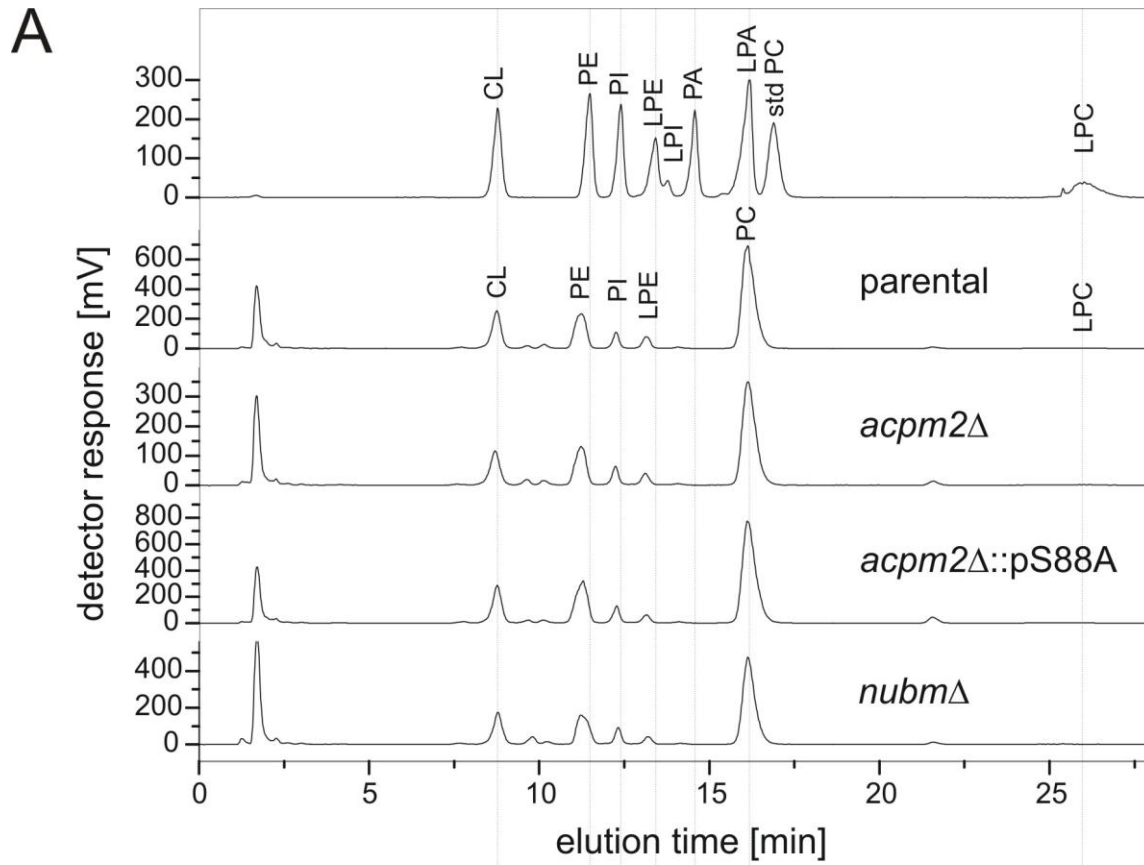
### 3.1.6 The mitochondrial lipid composition analysed by HPLC

*The analysis was performed by Dr. Sebastian Richers.*

In order to detect and compare greater spectrum of mitochondrial phospholipids, extracts (2.4.3, materials and methods) from intact, sucrose gradient-purified mitochondria of parental, *acpm2Δ*, *acpm2Δ,pACPM2-S88A* and the *nubmΔ* strains were analyzed by HPLC. The *nubmΔ* strain carrying a deletion of the central 51-kDa subunit of complex I was included as additional control because of its severe complex I assembly defect [220]. In addition to phospholipids identified in the TLC (3.1.5), phosphatidyl-inositol (PI), lyso-phosphatidyl-ethanolamine (LPE) and lyso-phosphatidyl-choline (LPC) were identified in the HPLC by comparison to the commercially available standards (*Figure 3.12*). All lipids were detected at very similar ratios in mitochondria from all strains, such that PC constituted almost a half, PE and CL roughly 20% each, whereas PI, LPE and LPC less than 10 % each (*Figure 3.13*). Also the protein to phospholipid ratio was nearly identical in mitochondria from all strains (*Figure 3.14*). In addition, the analysis was performed with whole cells, mitochondrial membranes and crude intact mitochondria yielding very similar results.

#### ***Figure 3.12 HPLC profiles of phospholipids extracted from Y. lipolytica mitochondria***

(See the next page) The extracts from intact, sucrose gradient-purified mitochondria (0.5 mg/ml) of the parental, *acpm2Δ*, *acpm2Δ,pACPM2-S88A* and *nubmΔ* strains were analyzed. No significant difference in phospholipid composition among analysed strains was found. Two different HPLC profiles for two different analyzed batches are shown. (A) Profile of a lower magnification. (B) Chromatogram of another extract shown in higher magnification revealed additional unidentified peaks (\*), though their amounts did not vary among analyzed samples. The first prominent peak, which elutes after approximately 2 minutes contains the pass through. Abbreviations used: CL, cardiolipin; PE, phosphatidyl-ethanolamine; PI, phosphatidyl-inositol; LPE, lyso-phosphatidyl-ethanolamine; LPI, lyso-phosphatidyl-inositol; PA, phosphatidic acid; LPA, lyso-phosphatidic acid; PC, phosphatidyl-choline; LPC, lyso-phosphatidyl-choline.



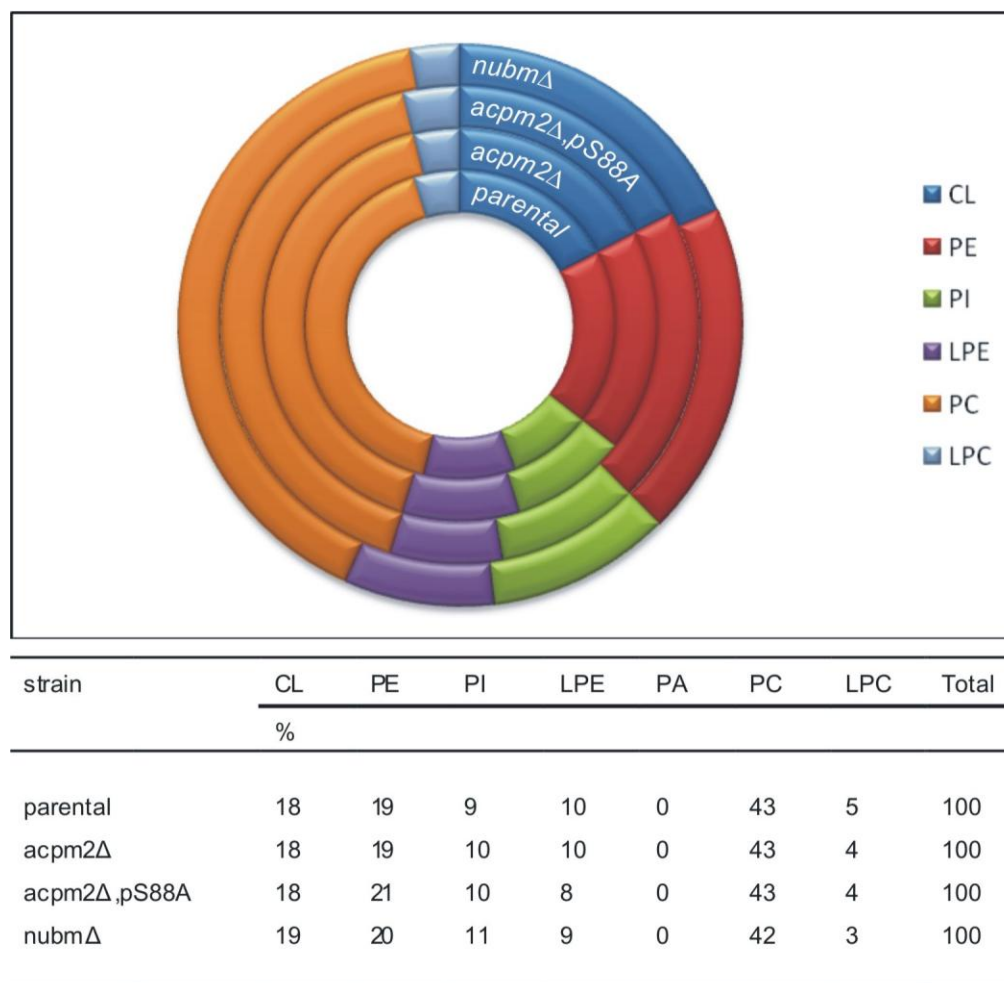
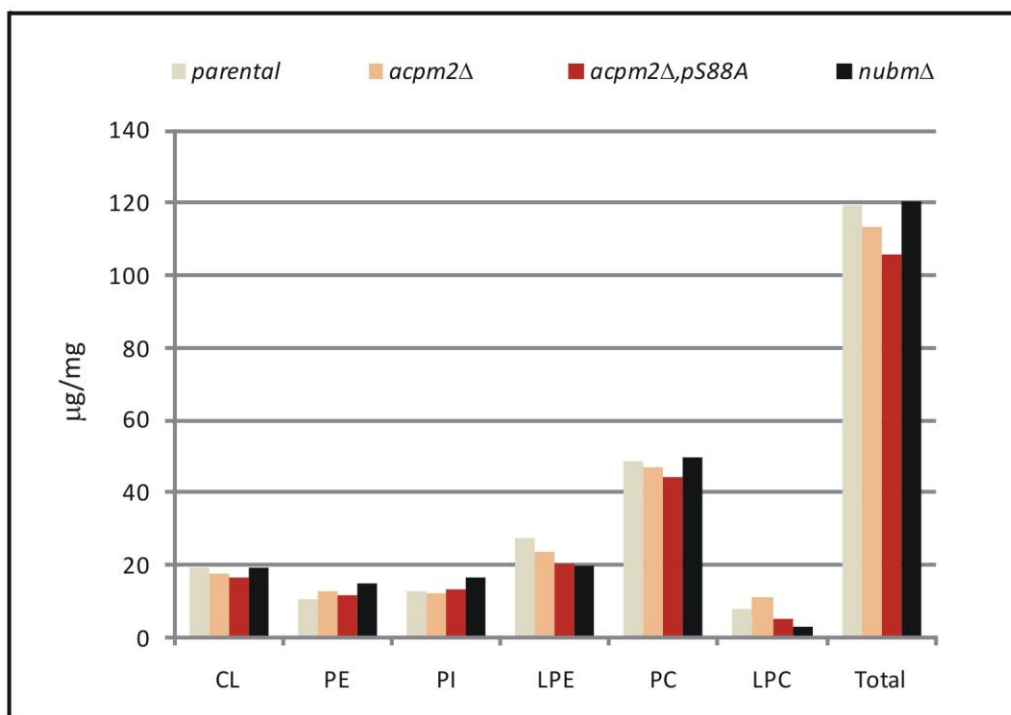


**Figure 3.13** *The phospholipid composition of purified intact mitochondria*

The relative amount (w/w) of individual phospholipids to the total mass of all phospholipids isolated from the intact, sucrose gradient-purified mitochondria of the parental, *acpm2Δ*, *acpm2Δ,pS88A* and the *nubmΔ* strains were determined by HPLC analysis. The detected phospholipids are: CL, cardiolipin; PE, phosphatidyl-ethanolamine; PI, phosphatidyl-inositol; LPE, lyso-phosphatidyl-ethanolamine; PC, phosphatidyl-choline; LPC, lyso-phosphatidyl-choline.



strain	CL	PE	PI	LPE	PA	PC	LPC	Total
	<i>μg/mg</i>							
<i>parental</i>	19	11	13	28	0	49	8	119
<i>acpm2Δ</i>	17	13	12	24	0	47	11	113
<i>acpm2Δ,pS88A</i>	17	11	13	20	0	45	5	106
<i>nubmΔ</i>	19	15	17	20	0	50	3	121

**Figure 3.14 The phospholipid to protein ratio in intact mitochondria**

The concentration of individual phospholipids relative to the protein concentration in intact mitochondria is nearly constant as determined in the HPLC analysis. The detected phospholipids are: CL, cardiolipin; PE, phosphatidyl-ethanolamine; PI, phosphatidyl-inositol; LPE, lyso-phosphatidyl-ethanolamine; PC, phosphatidyl-choline; LPC, lyso-phosphatidyl-choline.

### 3.1.7 Identification of mitochondrial phospholipids with MALDI-TOF-MS

*The analysis was performed by Dr. Sebastian Richers.*

Phospholipids extracted from intact, sucrose gradient-purified mitochondria of *Y. lipolytica* strains were separated on the HPLC column using the standard run as described in 2.4.4, materials and methods. Fractions were collected every 30 seconds beginning with time 0 seconds and were analysed with the matrix-assisted laser desorption ionization time-of-flight



mass spectrometry (MALDI-TOF-MS) (2.4.5, materials and methods). All prominent peaks of the HPLC chromatogram (*Figure 3.13*) were identified using MS (for spectra see 9.5, appendix). It has been shown that CL was found to be present in fraction (fr) 18 (*Figure 9.14*, appendix) and fr 19 (*Figure 9.15*, appendix), PE in fr 24 (*Figure 9.16*, appendix), PI in fr 28 (*Figure 9.17*, appendix), LPE in fr 28 (*Figure 3.15*), phosphatidic acid (PA) in fr 30 (*Figure 9.18*, appendix), LPC in fr 52 (*Figure 9.19*, appendix). It should be noted that the peak for LPE was found at a mass of 454.33 Da indicating substitution with a palmitoyl-chain (16:0; theoretical mass 454.29 Da) rather than an unsaturated acyl-chain (*Figure 3.15*). All phospholipids were measured in the negative charged mode with an exception of LPE and LPC, which were measured in the positive mode.

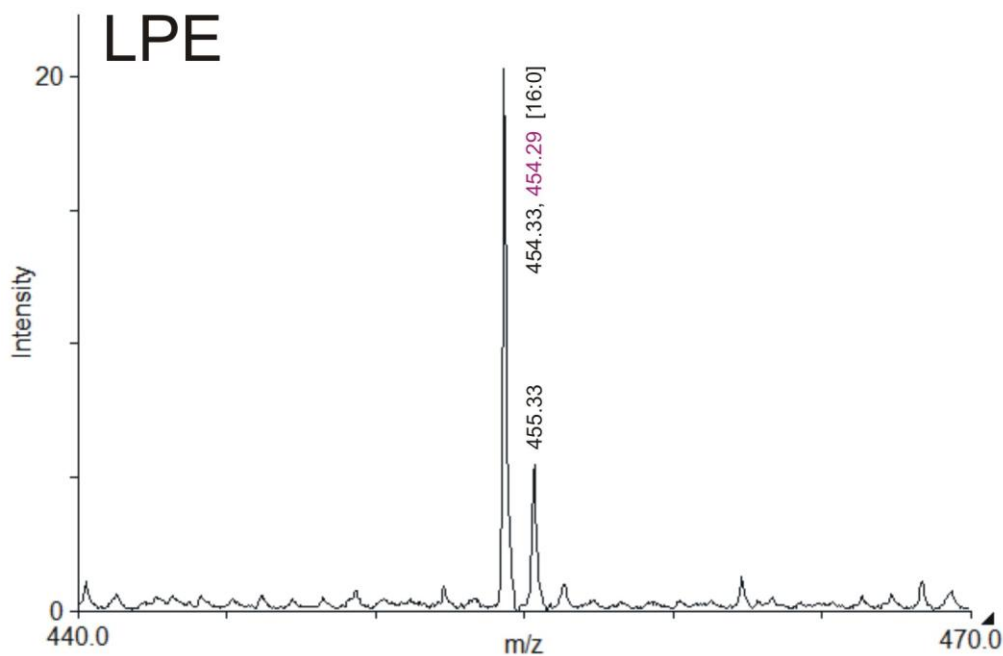


**Figure 3.15** The MALDI-MS spectrum of lyso-phosphatidyl-ethanolamine identified in fraction 28

Phospholipids isolated from intact mitochondria and separated with HPLC (fraction 28) were identified using MALDI-MS. The peak corresponding to LPE obtained in the positive charged mode was found at a mass of 454.33 Da indicating substitution with a palmitoyl-chain (16:0; theoretical mass 454.29 Da) rather than an unsaturated acyl-chain. Masses of the phospholipids determined experimentally are indicated above the spectra in black, whereas the theoretical values in violet. Numbers in brackets separated by a colon indicate the number of carbon atoms in the acyl-chains (first number) and the number of carbon atoms involved in the double bond formation in unsaturated chains (second number).

---

### 3.1.8 ACPM1 and ACPM2 are *bona fide* subunits of *Y. lipolytica* complex I

The next addressed question was whether one or both of the ACPM-proteins in *Y. lipolytica* were bound to complex I as accessory subunits. In a previous proteomic approach aimed at the identification of the accessory subunits of *Y. lipolytica* complex I ACPM1 had already been identified as a component of the purified enzyme by MALDI-TOF mass spectrometry [37]. However, the almost complete loss of fully assembled complex I caused by the deletion of the *ACPM2*-gene suggested a tight link between complex I and ACPM2 as well. Indeed, thorough analysis of the double-spot in dSDS-PAGE that had previously been shown to contain ACPM1 (*Figure 3.17A*) allowed the unambiguous identification of both ACPM1 and ACPM2 by MALDI-MS/MS sequencing of peptides from both proteins (*Figure 3.16*).

To confirm this assignment we introduced tagged versions of the two proteins into the ACPM deletion strains. Both constructs appeared to be functional, since ACPM1-strepII permitted survival of strain *acpm1* $\Delta$  (*Figure 3.17A*) and ACPM2-flag restored normal assembly of complex I (*Figure 3.17C*). Also NADH:HAR oxidoreductase and dNADH:DBQ oxidoreductase activities of mitochondrial membranes from both complemented strains were restored to parental strain levels (*Table 3.1*). Moreover, also the purified complexes from both tagged strains exhibited wild-type catalytic activities indicating normal stability of the multiprotein complex. This allowed dSDS-PAGE analysis of the tagged complexes. Molecular mass shifts of ACPM1-strepII (*Figure 3.17B*, red arrow) and ACPM2-flag (*Figure 3.17C*, blue arrow) subunits as compared to the untagged parental strain (*Figure 3.17A*) confirmed the assignment of the two proteins that thus have both to be considered *bona fide* subunits of complex I from *Y. lipolytica*.

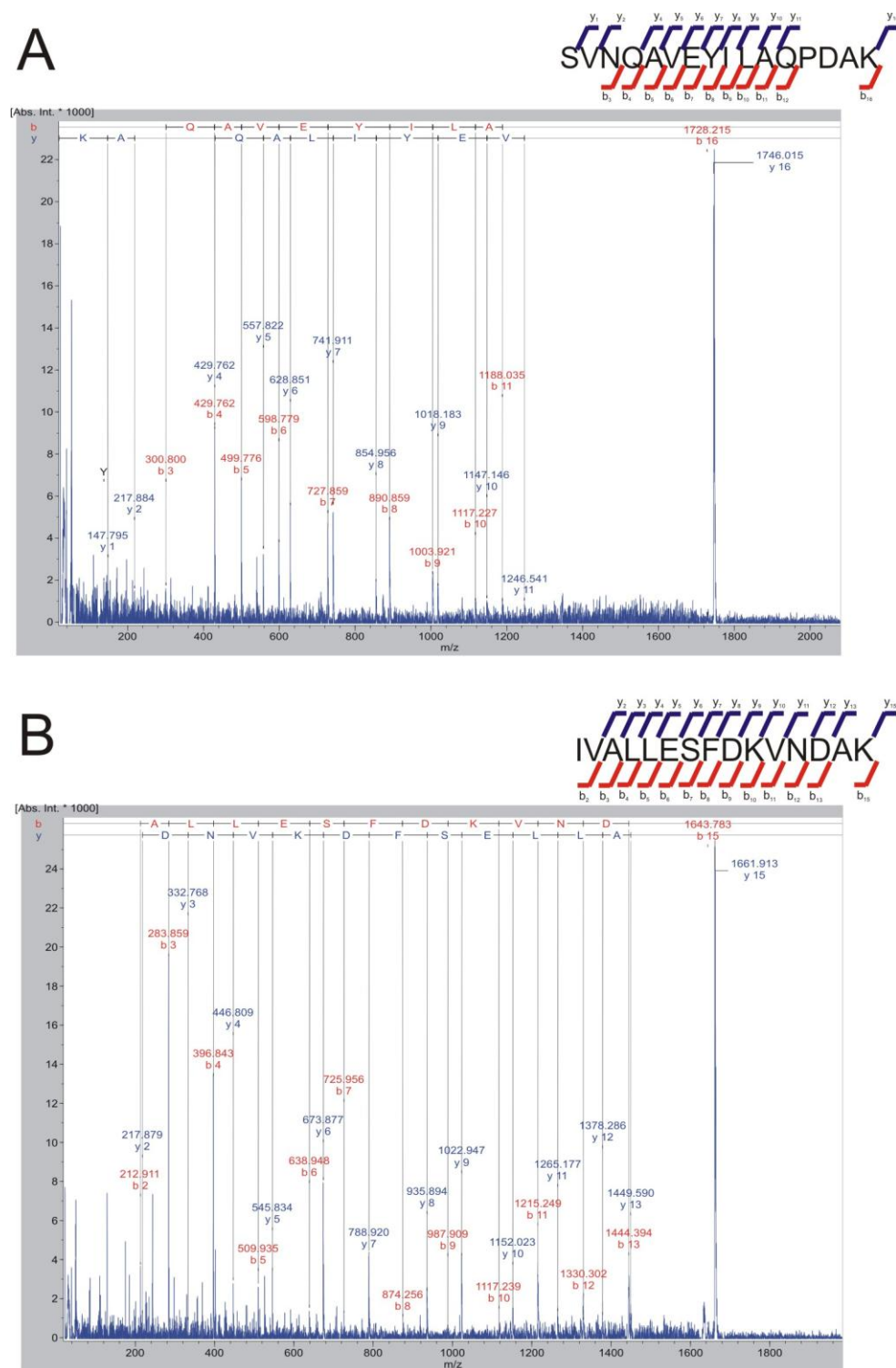


**Figure 3.16 Mass Spectra of ACPM subunits**

MALDI-post-source decay spectra of peptides identified by using  $y$ - and  $b$ -ions. Identification of (A) the C-terminal peptide (position 94-109) SVNQAVEYILAQPDAK ( $MH^+$  1745.907) of the ACPM1 protein (Mascot Score 42) and (B) the peptide (position 59-73) IVALLESFDKVNDAK ( $MH^+$  1661.911) of the ACPM2 protein (Mascot Score 76).

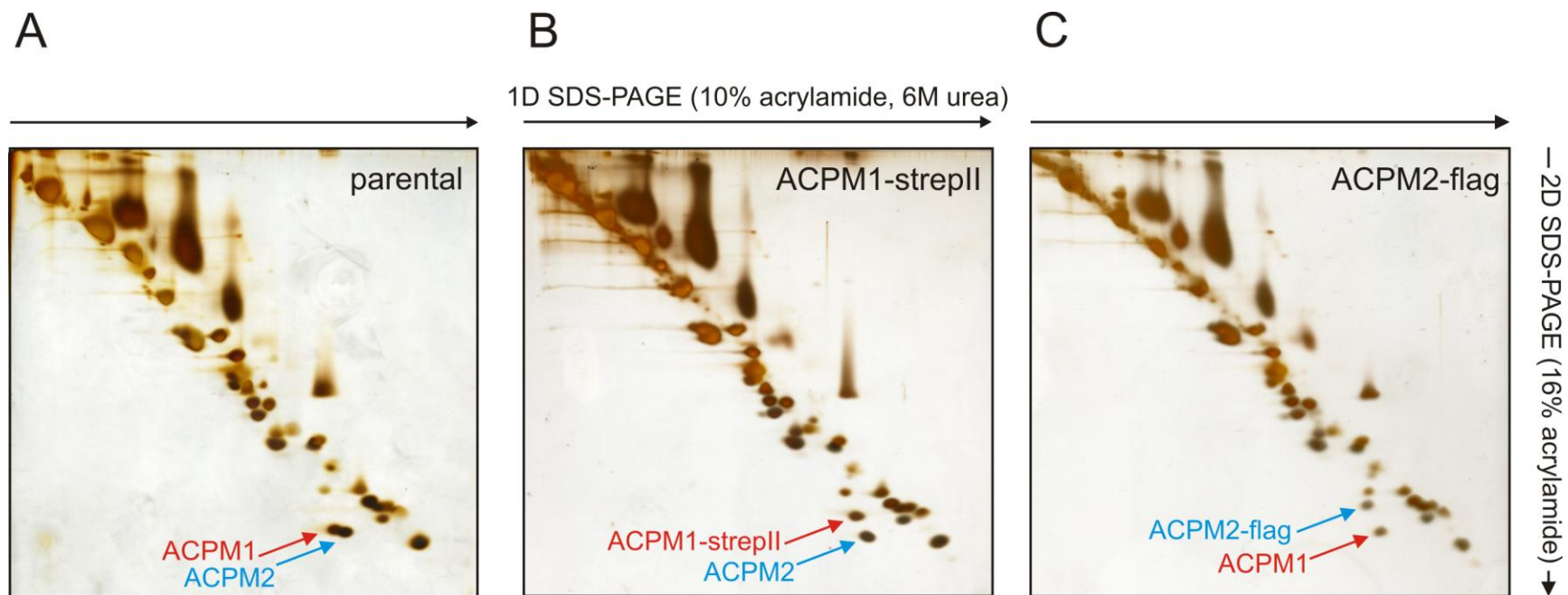


**Figure 3.17 Analysis of tagged versions of ACPMs in dSDS-PAGE**

Both *ACPM* genes were deleted and replaced with plasmid-borne copies encoding tagged versions of the two proteins. Molecular mass shifts as compared to the parental strain (A) are visible in dSDS-PAGE in (B) ACPM1-strepII (red arrow) and (C) ACPM2-flag (blue arrow) complex I.

### 3.1.9 Sub-mitochondrial localization of ACPM1 and ACPM2

The next open question was whether the two ACPMs were exclusively present as complex I subunits in *Y. lipolytica* mitochondria. To answer this question intact mitochondria from the *Y. lipolytica* strains containing the tagged versions of ACPM1 and ACPM2 were isolated and soluble and membrane fractions were analyzed by Western blotting (Figure 3.18). As controls for the identity and purity of the individual fractions aconitase for the mitochondrial matrix, hexokinase for the cytosol and the complex I subunit NESM for the mitochondrial membranes were used. Both ACPMs were exclusively detectable in the membrane fraction but absent in the soluble fraction of mitochondria and the cytosolic fraction (PMS). This strongly suggested that all ACPM1 and ACPM2 in mitochondria were completely bound to complex I in the inner mitochondrial membrane of *Y. lipolytica*.

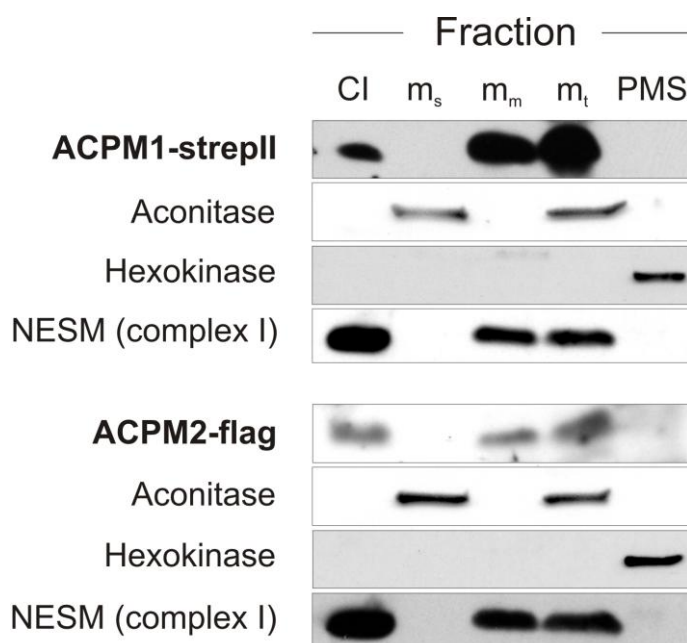


**Figure 3.18 Localization of tagged versions of ACPM in mitochondrial fractions**

Intact mitochondria were fractionated into soluble (m<sub>s</sub>) and membrane (m<sub>m</sub>) part and analyzed for ACPM presence with antibodies specific to strepII- and flag-tags. Neither of them could be detected in the soluble fraction of mitochondria nor in the cytosolic (PMS) fraction. Both ACPMs were detectable in the membrane fraction. Purified complex I (CI) and whole mitochondria (m<sub>t</sub>) were used as controls. Antiserum specific to representative proteins of each fraction were used: aconitase (soluble fraction), hexokinase (cytosol) and NESM (complex I, membrane fraction).



### 3.2 Exploration of the *st1* subunit of complex I from *Y. lipolytica*

#### 3.2.1 Identification of a rhodanese-like protein in purified complex I

Upon gel filtration chromatography, His-tagged *Y. lipolytica* complex I, as Ni<sup>2+</sup>-affinity purified from n-dodecyl- $\beta$ -D-maltoside solubilised mitochondrial membranes, elutes as a single, symmetrical peak, indicating excellent purity and homogeneity (Figure 3.19A). A protein with an apparent molecular mass of 34.6 kDa (Figure 3.19B) previously not detected in complex I from other sources was found to be consistently present even in the purest preparations.

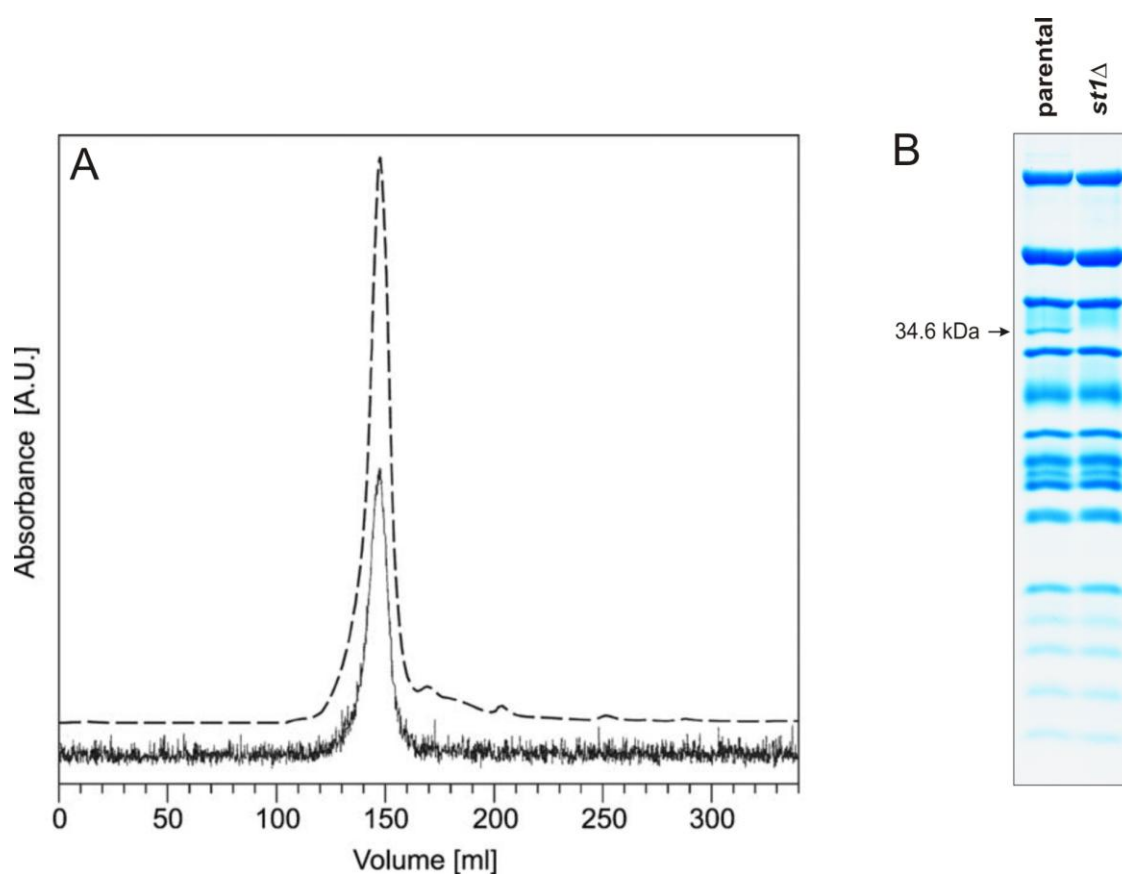


**Figure 3.19** Gel filtration purified complex I contains rhodanese-like protein

(A) Elution profile of *Y. lipolytica* complex I purified by Ni<sup>2+</sup> affinity chromatography. The elution profile of a TSK4000 column run with purified complex I was monitored by measuring A280 for protein (upper trace) and A415 for flavine mononucleotide and iron-sulfur clusters (lower trace). Experimental details were as described in [221]. (B) SDS-PAGE of purified *Y. lipolytica* complex I. Coomassie stained 16% tricine-SDS gel with 30  $\mu$ g of complex I from the parental and the sulfurtransferase deletion (*st1* $\Delta$ ) strains. The band corresponding to the sulfurtransferase protein is marked with an arrow. The sulfurtransferase seems to be present in substoichiometric amounts in the parental strain and is clearly absent in the deletion strain.

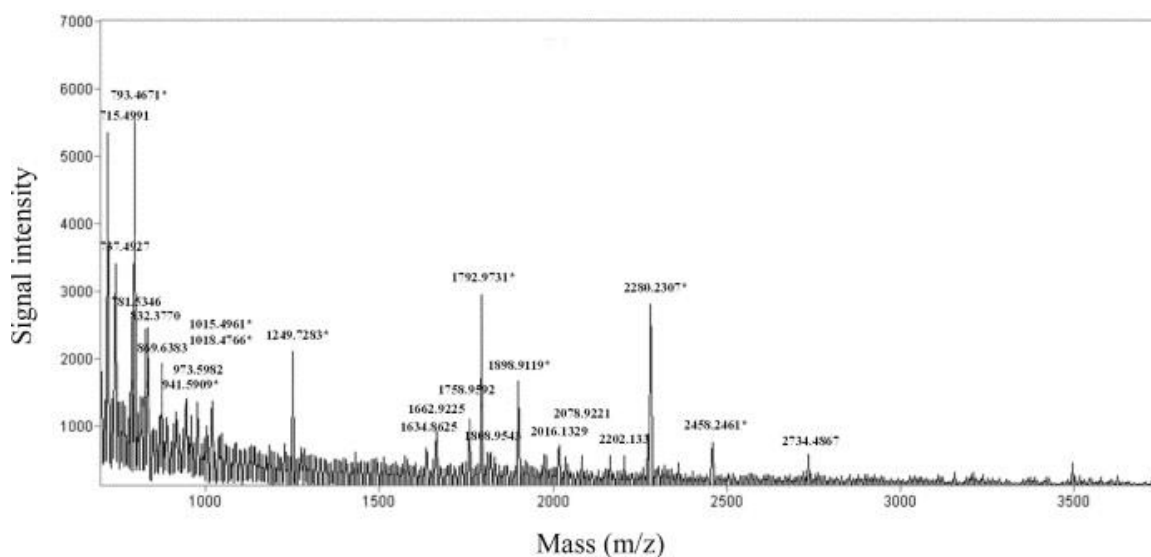


**Figure 3.20 MALDI-TOF mass spectrum of in-gel digested 34.6 kDa protein of *Y. lipolytica* complex I**

The protein spot was excised from a dSDS gel and digested with trypsin. The peptide mixture was analyzed by MALDI-TOF mass spectrometry using peptide mass fingerprinting (PMF). Sequence coverage was 38% using 50 ppm error margin. Tryptic peptides identified by MALDI-TOF MS are marked with asterisks. The analysis was performed by Dr. Albina Abdrakhmanova.

Peptide residues <sup>7</sup>	Expected mass <sup>8</sup> (MH <sup>+</sup> )	Observed mass	Sequence
4 – 12	941.5666	941.5909	LISPAELAK
21 – 36	1792.9268	1792.9731	IFDATWYLPTPANVGK
37 – 44	1018.4298	1018.4766	NAYDNYMK
81 – 102	2280.1506	2280.2307	LGVSSDSPIVVYDTQGVFSGPR
103 – 108	793.4607	793.4671	LVWTFK
150 – 158	1015.5094	1015.4961	IDPADPPYK
169 – 179	1249.6674	1249.7283	SFEDVLAIVEK
211 – 234	2458.2248	2458.2461	AELSSGHVPGAYSIAFPEVVENGK
282 – 297	1898.8303	1898.9119	DTNAVYDGSWTEWAQR

**Table 3.2 Tryptic peptides of the 34.6 kDa protein identified by MALDI-TOF MS**

Its content relative to other complex I proteins seemed variable and appeared substoichiometric in most preparations. Using dSDS-PAGE [205], followed by MALDI-TOF mass spectroscopic analysis (*Figure 3.20*) of tryptic fragments (*Table 3.2*) enabled identification of this protein.

<sup>7</sup> residue numbers refer to the mature amino acid sequence

<sup>8</sup> the monoisotopic single protonated mass of the peptides is shown.



Species, enzyme, NCBI accession	Similarity (%)	Identity (%)	Probability of mitochondrial import (%)
<i>E. coli</i> MST (JX0320)	47	39	not applicable
<i>A. vinelandii</i> MST (ZP_00415650)	45	35	not applicable
<i>A. vinelandii</i> TST (S62187)	35	26	not applicable
<i>S. tokodaii</i> TST1 (BAB66874)	38	31	not applicable
<i>S. tokodaii</i> TST2 (BAB67675)	38	30	not applicable
<i>Y. lipolytica</i> MST (CAG78604)	(100)	(100)	27
<i>S. cerevisiae</i> MST (NP_014894)	48	37	5
<i>N. crassa</i> MST (XP_325872)	50	38	99
<i>P. anserina</i> MST (CAD60606)	54	42	100
<i>T. aestivum</i> MST (AAK64575)	48	39	1
<i>A. thaliana</i> MST1 (AAC17062)	46	37	99
<i>A. thaliana</i> MST2 (AAM61125)	46	39	1
<i>C. elegans</i> MST (NP_501461)	38	28	17
<i>D. rerio</i> MST (AAH74047)	51	35	91
<i>G. gallus</i> MST (XP_416283)	53	41	60
<i>G. gallus</i> TST (XP_416284)	51	42	86
<i>B. taurus</i> TST (NP_803455)	53	36	83
<i>B. taurus</i> MST (NP_001029463)	52	34	75
<i>H. sapiens</i> TST (Q16762)	54	36	82
<i>H. sapiens</i> MST (P25325)	50	37	75

**Table 3.3. Similarity and identity scores for pairwise comparisons between *Y. lipolytica* sulfurtransferase and tandem rhodanese domain repeat enzymes from other organisms**

The alignments were created using the GAP programme from the HUSAR ([genius.embnet.dkfz-heidelberg.de](http://genius.embnet.dkfz-heidelberg.de)) program package in standard mode. The probability of mitochondrial import was calculated using MitoProt II software (<http://ihg.gsf.de/ihg/mitoprot.html>).

The recently identified protein corresponds to NCBI protein data base entry CAG78604, TrEMBL entry Q6C0L9\_YARLI and to open reading frame YALIOF23551g in the *Y. lipolytica* genomic sequence as deposited at the Genolevures site (<http://cbi.labri.fr/Genolevures/index.php>). Sequence coverage was 38% using a 50 ppm error margin. Predicted protein CAG78604 exhibits no homology to any other known subunit of complex I from other organisms but shows up to about 50% sequence

similarity and 40% sequence identity to members of the sulfurtransferase family, in particular to tandem rhodanese domain repeat enzymes like thiosulfate:cyanide sulfurtransferases (TSTs) and 3-mercaptopyruvate: cyanide sulfurtransferases (MSTs) from various sources (Table 3.3).

### 3.2.2 Generation of the *st1* deletion strain (*st1Δ*)

To determine role of the sulfurtransferase (*st1*) associated with *Y. lipolytica* complex I the corresponding gene was deleted. The intronless open reading frame (ORF) encoding a protein of 315 amino acids, together with its flanking DNA was replaced by homologous recombination with *URA3*-marked deletion allele (Figure 3.23).

First, the region encompassing the entire ORF and roughly 1100 bp of upstream and 600 bp of downstream sequence was amplified in the PCR reaction with *Taq* DNA polymerase using primers *st1f/ st1r*. Subsequently, the fragment was cloned into the pCR2.1 vector (Figure 3.21a, b), amplified in *E. coli* cells and transferred to *EcoRI* site of the pUC19Δ vector.

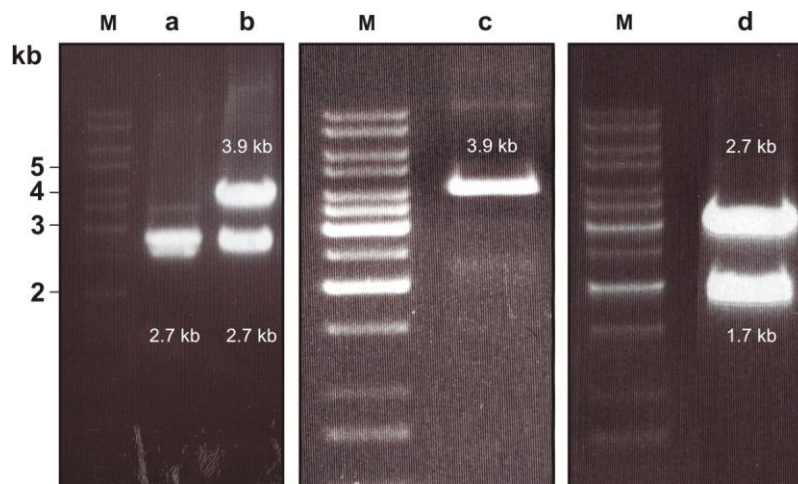


**Figure 3.21 Steps of *st1Δ* strain generation**

(a) A 2.7 kb fragment composed of *st1* gene ORF with its flanking regions produced by PCR using primer pair *st1f/ st1r*; (b) A 3.9 kb pCR2.1 plasmid containing the *st1* insert excised with *EcoRI* restriction enzyme; (c) A construct of 3.9 kb composed of the plasmid pUC19Δ and flanking regions of the *st1* gene generated by PCR using primers *st1SalI/ st1BamHI*; (d) A 2.7 kb pUC19Δ plasmid containing a 1.7 kb *URA3* fragment excised with *BamHI* and *SalI* enzymes; Size of the fragments of the molecular weight marker (M) is indicated on the left side of the agarose gel in kilobase pairs (kb).

For generation of genetically marked *st1* deletion allele a gap comprising the entire open reading frame and 55 bp of upstream sequence was created by PCR using primers *st1Sall/ st1BamHI* (Figure 3.21c). The resulting product was digested with *Sall* and *BamHI* and ligated with a 1.7 kb *Sall/ BamHI* fragment containing the *Y. lipolytica URA3* gene, which had been generated by PCR using primers *ura3f/ ura3r* (Figure 3.21d). In the deletion construct, orientation the *URA3* was opposite to the orientation of *st1* gene.

In order to improve selection efficiency, in addition to *URA3* gene, another selection marker, the hygromycin B resistance gene (*HygB<sup>R</sup>*) was cloned into the *HindIII* site of the deletion construct (*pUC19Δ, st1::URA3*), (Figure 3.23). To assure incorporation of a single *HygB<sup>R</sup>* insert, length of the constructed vector was checked by linearization with *BamHI* (Figure 3.22). The final construct was sequenced and transformed into haploid *Y. lipolytica* GB10 cells. Subsequently, strains were selected on minimal plates for their ability to grow in the absence of uracil and their inability to grow in the presence of hygromycin B.

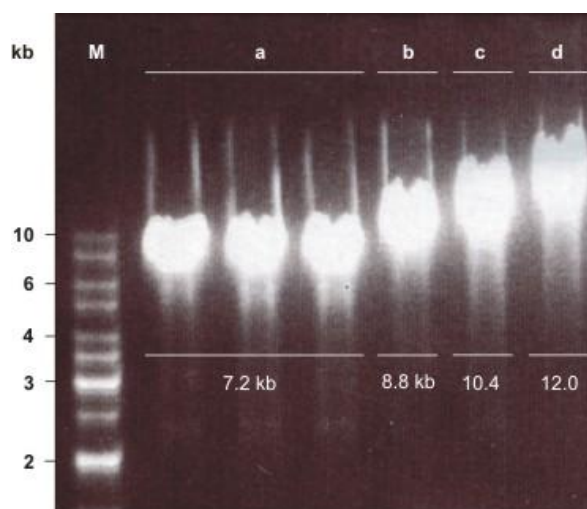


**Figure 3.22 Test digest for the number of hygromycin B inserts**

In order to assure incorporation of only one hygromycin B resistance gene (*HygB<sup>R</sup>*) into the *HindIII* site of the *st1* deletion construct (*pUC19Δ, st1::URA3, HygB<sup>R</sup>*), the vector was linearized with *BamHI* enzyme. A strain carrying (a) single copy of *HygB<sup>R</sup>* gene was verified by sequencing and transformed into GB10 cells. Plasmids that incorporated multiple copies of *HygB<sup>R</sup>* genes: (b) 2, (c) 3 and (d) 4 were discarded. Size of the fragments of the molecular weight marker (M) is indicated on the left side of the agarose gel in kilobase pairs (kb).

To ensure proper integration of the deletion constructs into genomic locus of *st1* gene, transformants were tested by PCR using primers: *st1f* and *st1r*, which bind to the flanking DNA upstream and downstream to *st1* ORF, respectively; *ura3ds2*, *ura3us2* binding to the deletion construct and *st1seq2*, *st1seq5* binding to the ORF of *st1* gene (Figure 3.24). The GB10 strain carrying a wild-type copy of the *st1* gene was used as a control. Presence of the *st1* gene in the GB10 was confirmed in a PCR reaction using primer pairs *st1f*/*st1r* and *st1seq2*/*st1seq5*, which yielded products of 2.8 kb and 0.7 kb, respectively (Figure 3.24a, d). Absence of the *URA3* gene in the GB10 strain was confirmed using primers *st1f*/*ura3ds*, *ura3us*/*st1r*, since no product with any of the primers was obtained (Figure 3.24b, c).

Proper integration of the *st1Δ* construct into the chromosomal locus of the *st1* gene was confirmed using primer pairs *st1f*/*st1r*, *st1f*/*ura3ds*, *ura3us*/*st1r* and *st1seq2*/*st1seq5*, since products of 3.4 kb, 1.2 kb, 0.8 kb and no product, respectively were obtained. This indicated presence of the *URA3* gene on the chromosome in the genomic locus of *st1* in the *st1Δ* strain (Figure 3.24e, f, g) and confirmed absence of the *st1* gene (Figure 3.24h).

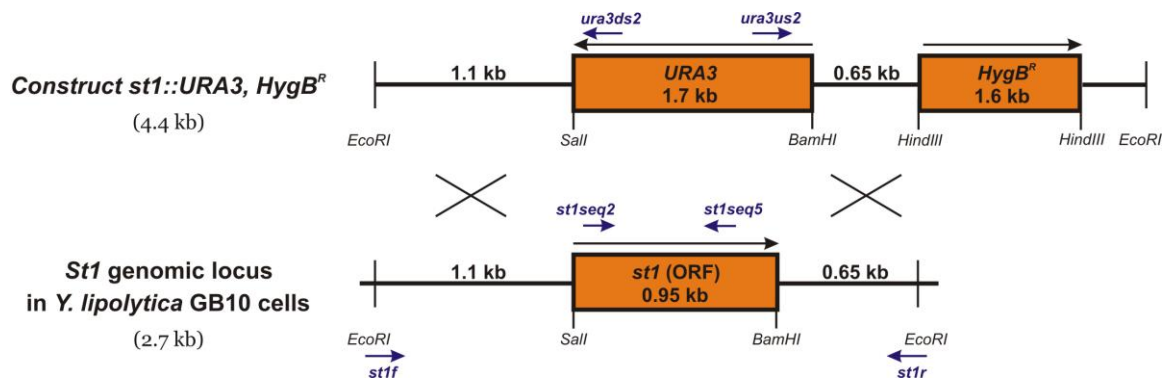


**Figure 3.23 Strategy for generation of the *st1Δ* strain**

A *EcoRI* linearized construct containing the *URA3*-marked *st1* deletion allele and the hygromycin B resistance gene (*HygB<sup>R</sup>*) used for deletion of *st1* gene by double homologous recombination (indicated by crosses). The *st1* deletion (*st1Δ*) strains were selected for their ability to grow in the absence of uracil and their inability to grow in the presence of hygromycin B. The location of PCR primers is indicated by violet arrows.

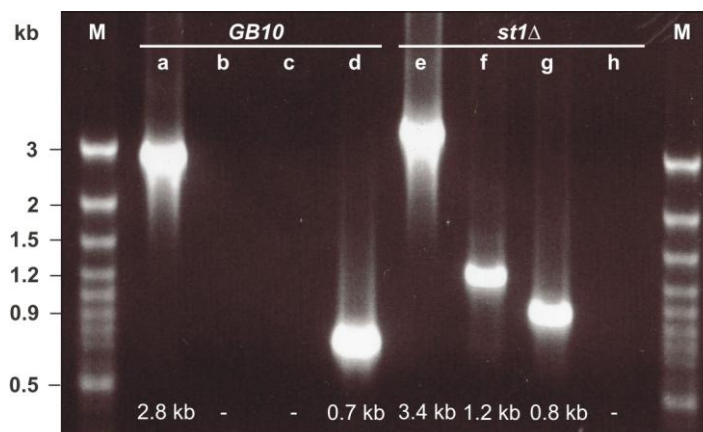


**Figure 3.24 PCR test for deletion of the *st1* gene**

PCR test for proper integration of the *URA3*-marked deletion construct into the genomic locus of the *st1* gene. Genomic DNA isolated from *Y. lipolytica* GB10 and *st1Δ* strains was verified in the PCR reaction using primers (a, e) *st1f/ st1r*; (b, f) *st1f/ ura3ds*; (c, g) *ura3us/ st1r* and (d, h) *st1seq2/ st1seq5*. In case of GB10 strain containing the *st1* gene fragments of (a) 2.8 kb and (d) 0.7 kb were created, whereas in (b) and (c) no products were obtained. The *st1Δ* strain, containing an integrated *URA3* gene replacing the *st1* gene resulted in PCR products of (e) 3.4 kb, (f) 1.2 kb and (g) 0.8 kb, whereas no product in (h) was obtained. For localization of primers see *Figure 3.23* and 9.1.1, appendix. Size of the fragments of the molecular weight marker (M) is indicated on the left side of the agarose gel in kilobase pairs (kb).

### 3.2.3 Complementation of *st1Δ* strain with a plasmid carrying *st1-strepII*

The *st1Δ* strain complemented with a plasmid-borne strepII-tagged version of the *st1* gene (*st1Δ,pst1-strepII*) was generated by PCR amplification of the *st1* ORF with flanking regions (see *Figure 3.23*) integrated in the pCR2.1 vector using primers *st1strepIIIf/ st1strepIIr*. As a result the *st1* ORF was extended by 8 amino acids WSHPQFEK at the C-terminus. The *st1-strepII* gene was cloned into the *EcoRI* site of the replicative plasmid pUB4 [196] and the orientation and number of incorporated inserts was checked by test digestion with *EcoRI*, *NheI* and *NdeI* restriction enzymes (*Figure 3.25*). Verified vector was sequenced (*Figure 3.26*) and transformed into *Y. lipolytica st1Δ* cells. Strains were selected on minimal plates for their ability to grow in the absence of uracil and their inability to grow in the presence of hygromycin B. Furthermore, *st1Δ* strain transformed with a functional copy of the *st1* gene on plasmid pUB4 (*st1Δ,pst1*) was generated and will be referred to as parental strain here.

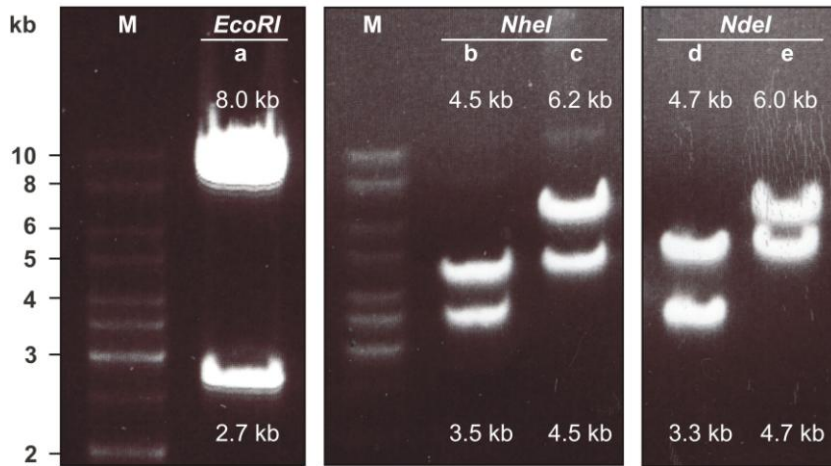


**Figure 3.25 Test digest of the pUB4 plasmid containing the *st1-strepII* insert**

The test digest of the pUB4 plasmid carrying the *st1-strepII* gene with (a) *EcoRI* results in fragments of 8.0 kb and 2.7 kb. To assure integration of a single *st1-strepII* insert the pUB4 plasmids were test digested with *NheI* and *NdeI* enzymes. The *NheI* digestion of (b) an empty pUB4 plasmid and (c) the plasmid containing the *st1-strepII* insert, results in (a) 3.5, 4.5 kb and (b) 4.5, 6.2 kb fragments, respectively. Whereas, the *NdeI* digestion of (d) an empty pUB4 plasmid and (e) the plasmid carrying the *st1-strepII* insert, results in (d) 3.3, 4.7 kb and (e) 4.7, 6.0 kb fragments, respectively. See also map of pUB4 plasmid in **See next page for description.**

*Figure 2.1*, materials and methods. Size of the fragments of the molecular weight marker (M) is indicated on the left side of the agarose gel in kilobase pairs (kb).

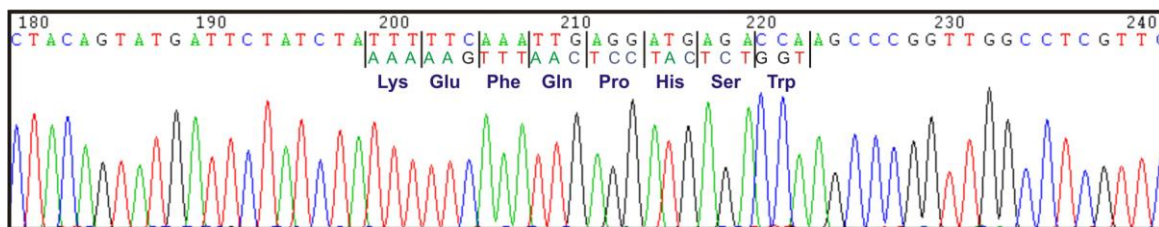


**Figure 3.26 Section of DNA sequence pherogramm from the *st1-strepII* strain**

The *st1* ORF was extended by 8 amino acids WSHPQFEK (*strepII*-tag) at the C-terminus as verified by sequencing using primer *st1seq6*. For localization of the primers see 9.1.1, appendix.

### 3.2.4 Purified *Y. lipolytica* complex I displays rhodanese activity

To find out whether the rhodanese-homologue present in the complex I preparation was functional thiosulfate: cyanide sulfurtransferase activity was measured. A specific rhodanese activity of  $12.1 \text{ nmol min}^{-1} \text{ mg}^{-1}$  was measured for complex I purified from *Y. lipolytica* strain GB10 (Table 3.4). Assuming that each molecule of *Y. lipolytica* complex I with a molecular mass of around 900 kDa is associated with 0.5 molecules of the sulfurtransferase subunit a turnover number of  $\sim 27 \text{ min}^{-1}$  was estimated for the rhodanese activity associated with complex I. Negligible rates of thiocyanate formation ( $<0.1 \text{ nmol min}^{-1} \text{ mg}^{-1}$ ) were observed when complex I was replaced by bovine serum albumin. Also, no rhodanese activity ( $<0.1 \text{ nmol min}^{-1} \text{ mg}^{-1}$ ) was detected with purified complex I from bovine heart mitochondria [222]. This is consistent with the fact that no sulfurtransferase orthologue was found to be associated with the purified mammalian enzyme [35]. Thus, although the observed rate is rather low as compared to rhodanese from bovine heart [210], it was clearly specific for the newly identified protein.

### 3.2.5 The rhodanese deletion strain

To test whether the sulfurtransferase activity of the newly identified protein was required for complex I biogenesis or the synthesis of its iron-sulfur clusters, the entire open reading frame of the corresponding gene was deleted from the *Y. lipolytica* genome by homologous recombination replacing it by the *URA3* marker gene. The *st1Δ* strain was fully viable, moreover yielded considerably higher cell mass than the GB10 wild-type strain, regardless whether grown in minimal- or YPD complete-medium (Figure 3.27). The growth rate difference was more pronounced as cells were grown in the complete medium (for composition of media see 2.1.4, materials and methods).

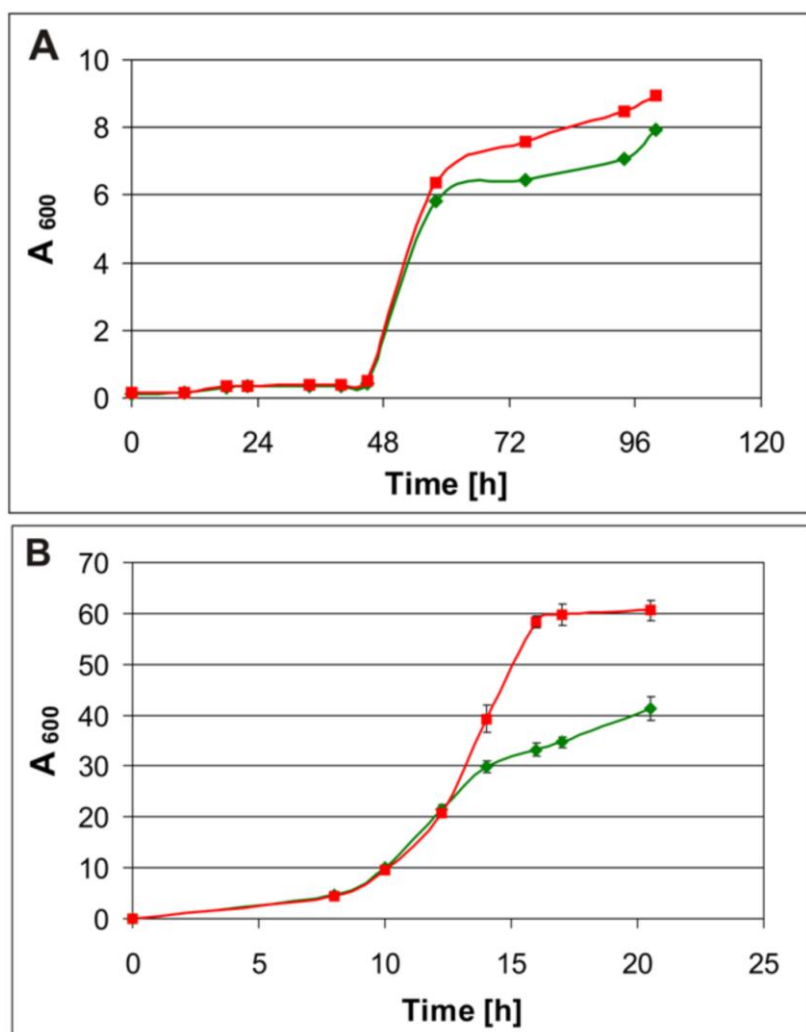


**Figure 3.27** Growth curves of the *st1Δ* strain of *Y. lipolytica*

*Y. lipolytica* strain deprived of rhodanese – *st1Δ* (red trace) yielded considerably higher cell mass than the GB10 wild-type strain (green trace) regardless whether grown in (A) minimal synthetic- or (B) YPD-medium, both supplemented with 2% glucose as carbon source. The growth rate difference is more pronounced as cells were grown in the YPD, full medium.

Mitochondrial membranes of the *st1Δ* strain contained fully assembled complex I at near wild type expression levels, as judged by BN-PAGE (Figure 3.28). NADH:HAR oxidoreductase activities of the membranes also indicated that the deletion did not reduce complex I expression (Table 3.4). In fact, we observed a slight tendency for increased complex I contents in membranes from the *st1Δ* strain, but further studies will be required to test whether this difference is significant.



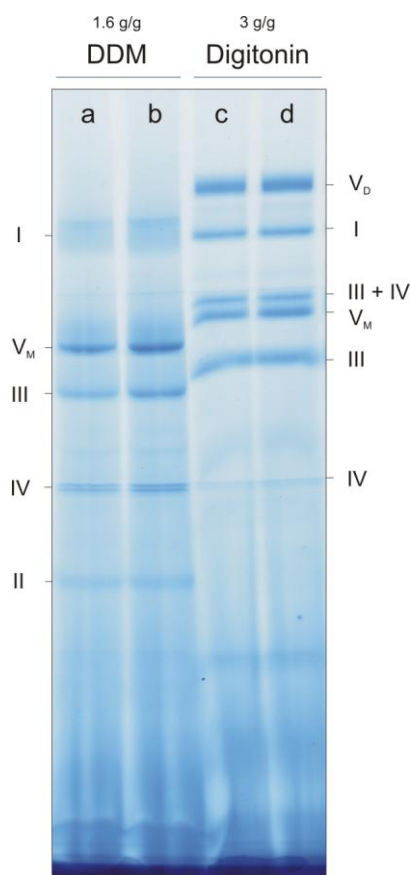


**Figure 3.28 BN-PAGE of mitochondrial membranes from *st1Δ* strain**

Mitochondrial membranes isolated from GB10 and *st1Δ* strains were solubilised with 1.6 gram *n*-dodecyl- $\beta$ -D-maltoside per 1 gram of protein (1.6 g/g DDM) and 3 g/g digitonin and visualized in BN-PAGE. (a) GB10 1.6 g/g DDM, (b) *st1Δ* 1.6 g/g DDM, (c) GB10 3 g/g digitonin, (d) *st1Δ* 3 g/g digitonin. Mitochondrial membranes of the *st1Δ* strain contained fully assembled complex I at near wild type expression levels. This result could be confirmed regardless of the detergent used for solubilisation of the membranes.

Except for the 34.6 kDa band that was missing in the deletion strain, complex I purified from the *st1Δ* strain exhibited the same subunit pattern in standard tricine SDS-PAGE as the parental strain (*Figure 3.19B*). More detailed analysis of the subunit composition by dSDS-PAGE [205] confirmed this finding suggesting that the stability of complex I was not significantly affected.

Although, upon gel filtration chromatography *st1* subunit remained bound to complex I (*Figure 3.19A*), association of the subunit to complex I is not strong enough to resist BN-PAGE. *St1* subunit dissociated from complex I even if the mild detergent digitonin was used for mitochondrial membrane solubilisation, as demonstrated using the tagged version of the protein (*st1-strepII*) specifically detected with alkaline phosphatase-conjugated streptavidin (*Figure 3.29*).

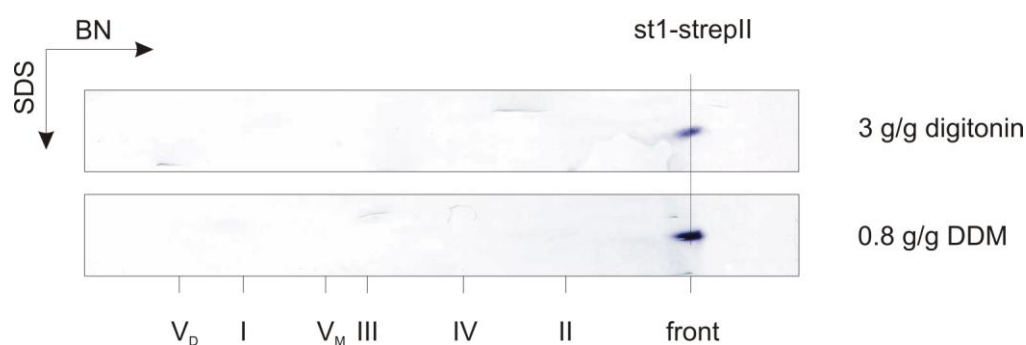


**Figure 3.29 St1 subunit dissociates from complex I in BN-PAGE**

Mitochondrial membranes isolated from the st1-strepII strain were solubilised with 3 g/g digitonin or 0.8 g/g *n*-dodecyl- $\beta$ -D-maltoside (DDM) and resolved in two dimensional BN-SDS PAGE (2.3.9, materials and methods). After transferring proteins to a polyvinylidene difluoride membrane and probing with alkaline phosphatase-conjugated streptavidin (2.3.7, materials and methods) the st1-strepII protein was detected at the front of BN-PAGE indicating migration of dissociated protein.

As expected if the deleted gene coded for the sulfurtransferase associated with complex I, rhodanese activity was not detectable in purified complex from the deletion strain (Table 3.4). Inhibitor sensitive dNADH:DBQ activities in mitochondrial membranes and purified, lipid-reactivated complex I were very similar for the parental and the deletion strain (Table 3.4) and were within the range of typical variations between preparations.

	NADH:HAR oxidoreductase ( $\mu\text{mol min}^{-1}\text{mg}^{-1}$ )	dNADH:DBQ oxidoreductase ( $\mu\text{mol min}^{-1}\text{mg}^{-1}$ )	Rhodanese activity ( $\text{nmol min}^{-1}\text{mg}^{-1}$ )
<i>Parental strain</i>			
Mitochondrial membranes	1.1	0.4	See text
Purified complex I	45	3.5	12.1
<i>st1<math>\Delta</math> strain</i>			
Mitochondrial membranes	1.0	0.4	See text
Purified complex I	53	3.2	<0.1

**Table 3.4 Activities of mitochondrial membranes and purified complex I from *Y. lipolytica***

EPR spectra of iron sulfur clusters N1, N2, N3 and N4 of purified complex I revealed that neither the signal intensities nor the positions of characteristic g values differed between the parental and the deletion strain (*Figure 3.30*). EPR spectra were recorded by Dr. Klaus Zwicker.

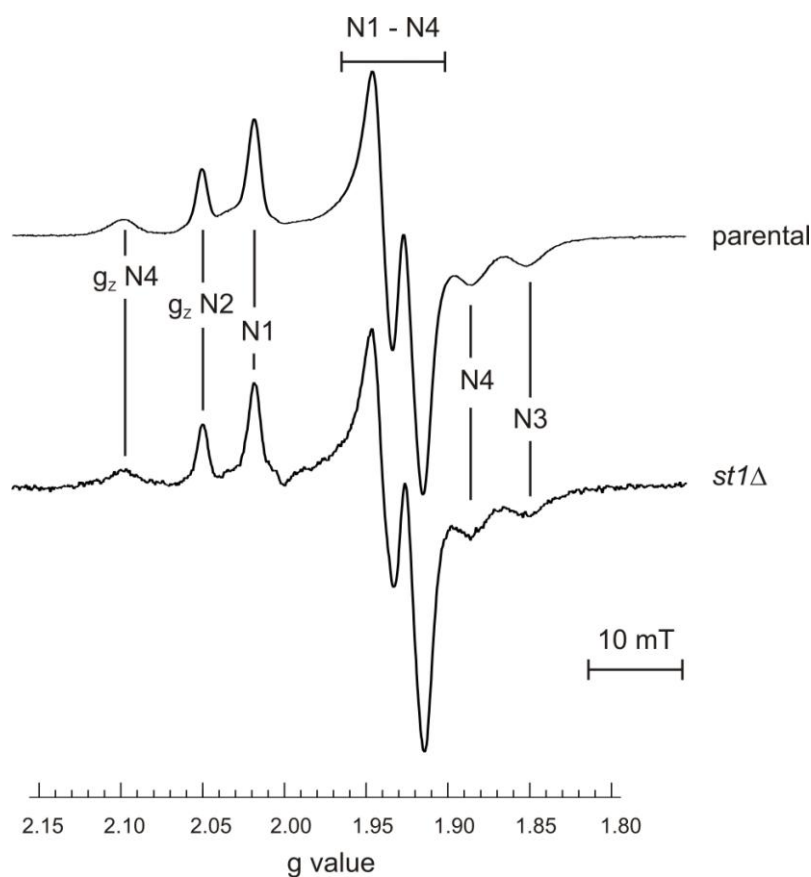


**Figure 3.30** EPR spectra of complex I from the parental and the deletion strains

Complex I was reduced with NADH and spectra were recorded under the following conditions: microwave frequency 9.47 GHz, modulation amplitude 0.64 mT, microwave power 1 mW, sample temperature 12 K. Spectra show contributions from clusters N1, N2, N3 and N4 [58]. No changes could be observed in EPR spectra of the mutant in comparison with the parental strain enzyme.

To test for the presence of other sulfurtransferases in *Y. lipolytica*, also rhodanese activities in mitochondrial membranes were measured. Activities were found to vary considerably between 3 and 9 nmol min<sup>-1</sup> mg<sup>-1</sup> between different batches of membranes from both the parental and the deletion strain. By comparing the increase from membranes to purified complex I in NADH:HAR oxidoreductase and rhodanese specific activities, it can be estimated that the sulfurtransferase associated with complex I contributed no more than about 5% of the total rhodanese activity present in mitochondrial membranes.



## 4 DISCUSSION

### 4.1 Acyl carrier proteins

Individual deletion of the genes for the two mitochondrial acyl-carrier protein homologues ACPM1 and ACPM2 revealed that both proteins serve important functions in *Y. lipolytica*. While in the absence of ACPM2 only trace amounts of fully assembled complex I could be detected in mitochondrial membranes, ACPM1 even seems to be indispensable for survival. This clear difference is quite remarkable considering that the mature forms of the two proteins are of very similar size [110] and exhibit a sequence similarity of 81% with 63% identical amino acids (*Figure 4.1*). Also, predicted 3D-structures of both proteins are almost identical (*Figure 4.2*). Despite of this similarity, no or only partial cross-complementation between the two genes was observed. The fact that ACPM1 turned out to be essential for survival of *Y. lipolytica* indicated an important role for viability that could not be compensated by ACPM2. In return the role of ACPM2 in assembly and stability of mitochondrial complex I could not be taken over by ACPM1. Two scenarios could accommodate these findings. On one hand it could be envisioned that the two mitochondrial acyl-carrier proteins have entirely different and independent functions. However, this seems unlikely considering their very high similarity and the fact that neither of the proteins seems to contain functional domains not present in the other.

YL_ACPM1	<u>MLR-NVSR</u> <b>LALRSNFARQA</b> ----- <b>TMQRFYS</b> --- <b>VARPDAEKRIA</b>	37
YL_ACPM2	<u>MLRQSVLR</u> <b>LS-RAAVAR</b> <b>PALSRSFVTA</b> <b>VARPQ</b> <b>LVRAAPV</b> <b>SFIRHYSSAHVLT</b> <b>KDMIQERIV</b>	60
	*** . * ** : * : : * * . *	
YL_ACPM1	<b>AVLESFDKISN</b> <b>PAAITPTASFAKDLN</b> <b>LDSLD</b> <b>TV</b> <b>EVVVAIEE</b> <b>FGIEIPDKEADEIKSVNQA</b>	98
YL_ACPM2	<b>ALLESFDKVN</b> <b>DAKNITATAN</b> <b>LTSDLGLD</b> <b>SLDV</b> <b>VEVVMAIEE</b> <b>FGLEIPD</b> <b>HDADEIKTVQQA</b>	121
	* : ***** : : . * * . * * . : : * * . ***** . ***** : ***** : ***** : * : *	
YL_ACPM1	<b>VEYILAQPDAK</b> 109	
YL_ACPM2	<b>IDYVSAQPAAV</b> 132	
	:: * : * * * *	

*Figure 4.1 Sequence alignment of ACPM1 and ACPM2 from Y. lipolytica*

The protein sequences were aligned using the CLUSTALW software (<http://www.ebi.ac.uk/clustalw/index.html>) and adjusted manually in the presequence region to reduce the number of large gaps. \* - identical amino acids; : - conservative substitutions; . - semi-conservative substitutions. Small and hydrophobic amino acids are represented in red, acidic residues in blue, basic residues in magenta; hydroxyl and basic residues in green. The mitochondrial presequences predicted with the MitoProt II software (<http://ihg2.helmholtz-muenchen.de/ihg/mitoprot.html>) are underlined and the site of processing is indicated by a black triangle.

---

Alternatively, the two proteins could operate together e.g. by forming a heterodimer responsible for both functions. In this case, one would have to postulate that in the deletion strains a homodimer of ACPM1 but not of ACPM2 could be formed to take over the function essential for survival and that on the other hand, both proteins would be necessary for complex I assembly and stability. In agreement with a similar function for ACPM1 and ACPM2, we also found that removal of the conserved phosphopantethein carrying serines in either of the two proteins had the same effect as deletion of the complete reading frame. It should be noted here that it has been shown in a previous study using laser induced liquid beam ion desorption mass spectrometry (LILBID-MS) that both proteins carry an additional mass of about 560 Da consistent with the binding of phosphopantetheine-hydroxy-tetradecanoate [110].

Before LILBID-MS was used to prove the post-translational modification of ACPMs, a modification could be suspected from anomalous migration of both ACPMs in the dSDS-PAGE, namely all hydrophilic subunits localize on the diagonal of the dSDS gel, whereas ACPMs were always present slightly underneath it (*Figure 4.4A*). Tetradecanoate has been previously detected on *N. crassa* ACPM [150], moreover the same acyl intermediate has been reported to confer a post-translational modification to ND5 subunit of complex I from this organism. Thus, ACPM was postulated to be involved in the synthesis or delivery of myristic acid [223], which could enhance proper assembly of complex I by anchoring the ND5 subunit to the membrane and thus stabilizing its interaction with the rest of the complex I. This hypothesis seems to be supported by the fact that deletion of ACPM from *N. crassa* indeed results in destabilization of complex I [98]. Although, no myristoyl post-translational modification of ND5 subunit in *Y. lipolytica* complex I could be predicted<sup>9</sup>, lack of the ACPM2 subunit had even more severe effects on the complex assembly, since mostly subcomplexes and only trace amounts of fully assembled complex I could be detected (*Figure 3.10*, results). Another reason for detection of 3-hydroxytetradecanoate modification bound to the ACPM in mass spectrometric analysis could be the fact that this particular modification is one of the most stable intermediates of the fatty acid synthetic pathway.

---

<sup>9</sup> N-terminal myristoylation sites could not be predicted with the ExPASy Tool Myristoyl CoA:Protein N-myristoyltransferase

In addition to the phosphopantetheine-binding domain both proteins contain a region, which is similar to the calcium-binding domain, however, it turned out to that it is not capable of ion binding.

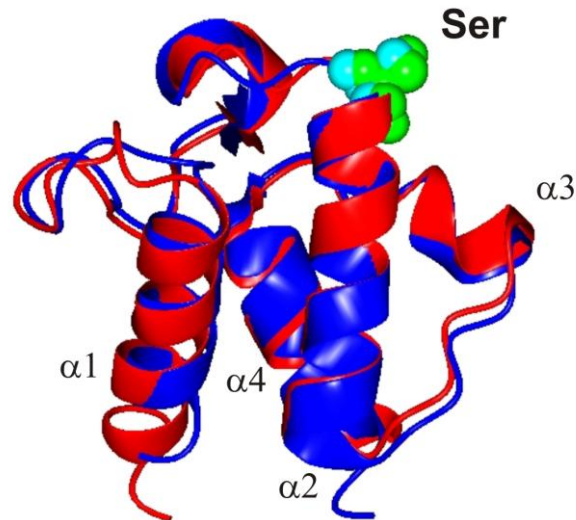


**Figure 4.2 Predicted structures of ACPMs from *Y. lipolytica***

The ribbon representation of mature ACPM1 (red) superimposed with mature ACPM2 subunit (blue). The phosphopantetheine-binding serines are represented in sphere models, the Ser66 of ACPM1 (green) and the Ser88 of ACPM2 (cyan) in *Y. lipolytica* nomenclature. Both structures were predicted by comparison to the *Toxoplasma gondii* apicoplastal ACP, which exhibited 39% sequence identity to the ACPM1 and 27% to the ACPM2. Models were prepared using QuickPhyre software [224] and superimposed with CCP4 Molecular graphics software [158].

The observation that the residue binding the phosphopantethein moiety is of critical importance was in line with the postulated role of the ACPMs in the lipid metabolism of mitochondria. Indeed, it has been reported that disruption of the ACPM subunit of complex I from *N. crassa* results in a four-fold increase of lysophospholipids in mitochondrial membranes [98]. However, in the ACPM2 deletion strain of *Y. lipolytica* no changes in the phospholipid composition of the mitochondria could be observed (Figure 3.12 and Figure 3.13, results).

In *Y. lipolytica* both ACPMs were found to be tightly and exclusively associated with complex I and no protein was detected in any mitochondrial compartment other than the mitochondrial membranes (Figure 3.18, results). This in striking contrast to the situation in other organisms analyzed so far. In mammalian mitochondria, where the ACPM protein was first identified as the SDAP subunit of complex I [152], the major

portion of this protein is detectable in the mitochondrial matrix [124]. In *Arabidopsis* none of the three ACPM isoforms seems to bind tightly to complex I [123].

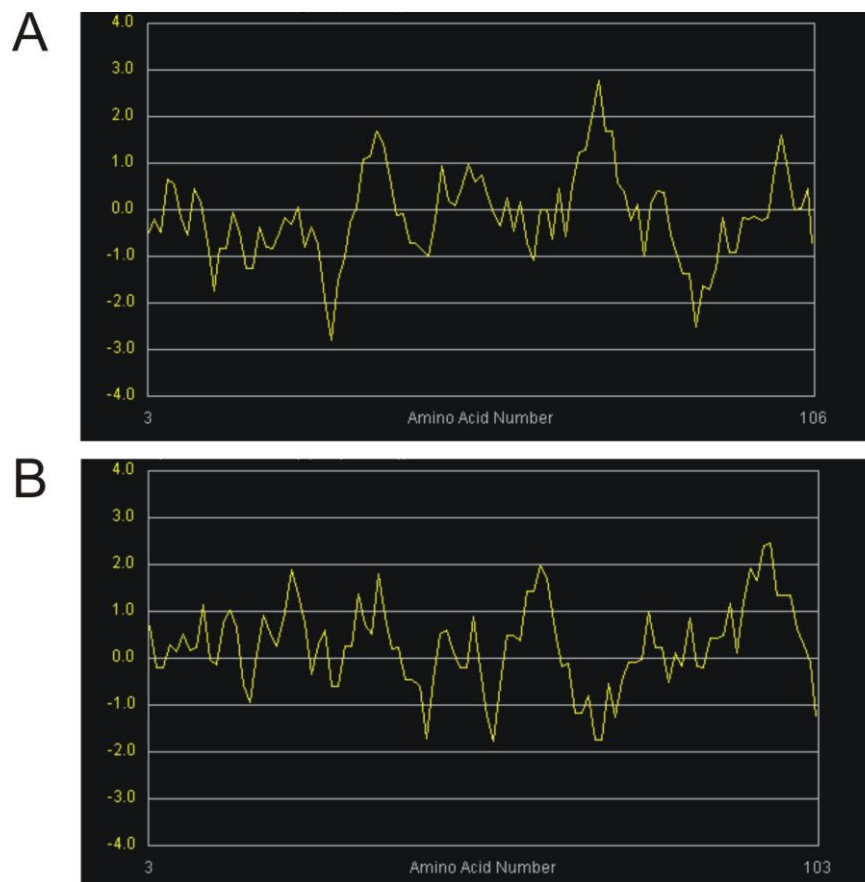


**Figure 4.3 Hydropathy plots of ACPM subunits**

The hydrophobicity plots of (A) the ACPM1 and (B) the ACPM2 subunits were simulated using the Software Hydropobicity Plots (Molecular Toolkit, Colorado State University, USA; <http://www.vivo.colostate.edu/molkit/hydropathy/index.html>). The y-axis represents the Kyte-Doolittle hydrophobicity scale, where the positive values represent hydrophobic, whereas negative hydrophilic character of the amino acids. On the x-axis the amino acid number is indicated. The window size, which is the number of amino acids examined at a time to determine the point of hydrophobic character, was set to 7.

This suggests that the functionality of the ACPMs is independent of their location, i.e. whether they are bound as subunits to complex I or reside in the mitochondrial matrix. Notably, ACPM is also found in *S. cerevisiae* which does not contain mitochondrial complex I and is devoid of all other complex I genes [83].

While *ACPM1* seems to be an essential gene in *Y. lipolytica*, *N. crassa* carrying a disrupted *acp-1* gene - the only gene coding for an ACPM protein in this organism [225] - is viable. The functional basis of this observation remains unclear. With respect to assembly of complex I the effects are similar in both organisms. Disruption of the *acp-1*



gene in *N. crassa* results in lack of assembly of the peripheral arm and improper assembly of the membrane part [98] and deletion of the *ACPM2* gene in *Y. lipolytica* results in a severe assembly defect of complex I and generation of subcomplexes (*Figure 3.30*, results). In line with a role in the stabilization of complex I, evidence exists that ACPM1 and ACPM2 seem to be located at the interface between the peripheral and the membrane arm of complex I, because both proteins were not found in either of these fragments that can be prepared by treating purified complex I with the chaotropic detergent lauryl-dimethylamine-oxide [37]. Furthermore, when incubated with this detergent also bovine heart complex I splits into subcomplexes I $\alpha$  and I $\beta$  (*Figure 1.5*, introduction) that both contain the ACPM homologous subunit SDAP [35]. Additional evidence indicating that ACPMs reside on two different subcomplexes is provided by an experiment, where complex I from *Y. lipolytica* was deprived of the NUJM subunit. This deletion resulted in generation of two subcomplexes roughly corresponding to I $\beta$  – a 300 kDa large distal part of the membrane arm and I $\alpha$  – a 700 kDa large remaining part of the complex (Kaiser, Krack et al, unpublished). Purified I $\alpha$  analyzed with dSDS was shown to contain ACPM1, however, it lacked among others the ACPM2 subunit (*Figure 4.4*). If the assumption that ACPMs form a dimer is correct, one has to conclude that the interaction between these two proteins is not strong enough to hold both subcomplexes together.

Moreover, lack of predicted transmembrane helices<sup>10</sup> in ACPMs (for hydrophaty plots see *Figure 4.3*), as well as the fact that assembly of complex I was not affected by attaching C-terminal affinity-tags to ACPMs (*Figure 3.17*, results) may suggest localization of these proteins close to the surface of the complex.

---

<sup>10</sup> Predicted using servers <http://www.enzim.hu/hmmtop/> and <http://www.cbs.dtu.dk/services/TMHMM/>

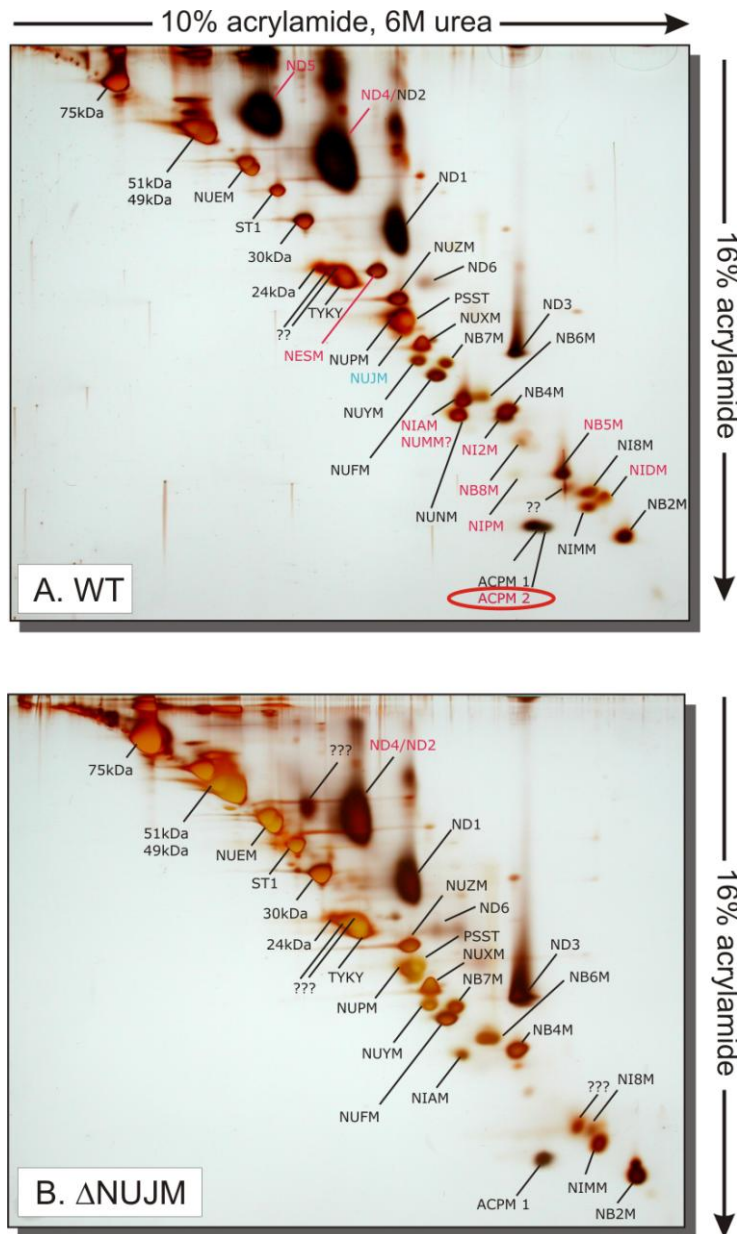


**Figure 4.4 Deletion of the NUJM complex I subunit leads to formation of subcomplexes**

Doubled SDS-PAGE of *Y. lipolytica* complex I isolated from (A) wild-type and (B) *nujm* $\Delta$  strain. Deletion of single transmembrane domain subunits (STDs) – NUJM or NIAM (not shown) results in destabilisation of complex I and formation of subcomplexes of approximately 300 kDa and 700 kDa. The larger subcomplex is composed of complex I lacking the distal part of the membrane embedded arm, whereas the smaller constitute two central hydrophobic core subunits ND4 and ND5 and several neighbouring accessory subunits NIAM (STD), NESM (STD), NIDM, NI2M, NB8M and ACPM2. Subunits belonging to the 700 kDa complex are denoted in black, to the 300 kDa in red and the NUJM subunit in green (Figure provided by Silke Kaiser, unpublished).

Following the assumption that ACPMs are involved in the synthesis of octanoic acid as a precursor for lipoic acid, sporulation of the *ACPM1/acpm1::URA3* strain was performed in the presence of 10 µg/ml lipoic acid, but again, no viable *acpm1Δ* spores could be isolated. However, the significance of this result is unclear since it has been reported that *N. crassa* mitochondria are not able to take up exogenously added lipoic acid [166].

The reason of ACPM association with complex I is not clear, however, many other accessory subunits are also involved in various metabolic pathways. It is possible that some of the enzymatic activities are associated to complex I because the corresponding proteins use the complex as a tether to the inner membrane. One may speculate that the immobilisation of a soluble FAS component could confer an evolutionary intermediate stage of the FAS type I complex, where all enzymatic activities reside on one or two polypeptide chains in multi-domain biosynthetic machinery.

Further studies will be required to better understand why the deletion of the *ACPM1* gene is essential for survival and why the highly similar *ACPM2* gene is not. Differences between species seem to suggest that the exact role of ACPMs in mitochondrial fatty acid metabolism and complex I assembly may vary among species.

---

## 4.2 *Rhodanese*

A protein associated with *Y. lipolytica* complex I has been identified as a functional sulfurtransferase. The additional protein was not only present in complex I purified by Ni<sup>2+</sup> affinity chromatography, but a protein band of the same molecular mass had also been detected before in *Y. lipolytica* complex I purified by ion exchange chromatography [58]. This suggests that although the protein was usually found in substoichiometric amounts, it may be considered as a bona fide subunit of *Y. lipolytica* complex I. Specific interaction with complex I is also suggested by the fact that some mutants of the 39 kDa subunit of *Y. lipolytica* complex I significantly affect sulfurtransferase levels in purified complex I [226], (*Figure 4.5*). Moreover, partial loss of subunits upon purification has also been observed for the 42 kDa subunit of bovine complex I [35]. In mammals and probably also in complex I from other species that were subjected to proteomic analysis [38;39], a sulfurtransferase subunit was not identified so far. This may suggest that in these organisms the interaction is too weak to detect the protein in the purified complex.

Deletion of the gene encoding the sulfurtransferase associated with complex I from the *Y. lipolytica* genome had no effect on complex I assembly, catalytic activity and its EPR detectable iron-sulfur clusters. This indicated that it is not essential for complex I biosynthesis.

The relatively low sulfurtransferase activity of the st1 subunit of *Y. lipolytica* complex I (*Table 3.4*, results), can be explained by comparison of its active site-loop sequence to the typical active-site of TSTs and MSTs enzymes (*Figure 4.6*), (*Figure 9.6*, appendix). The st1 subunit sequence exhibits a classic MST active-site loop, whereas the sulfurtransferase activity of the st1 subunit was assayed using thiosulfate as substrate, against which the enzyme could have had lower affinity.

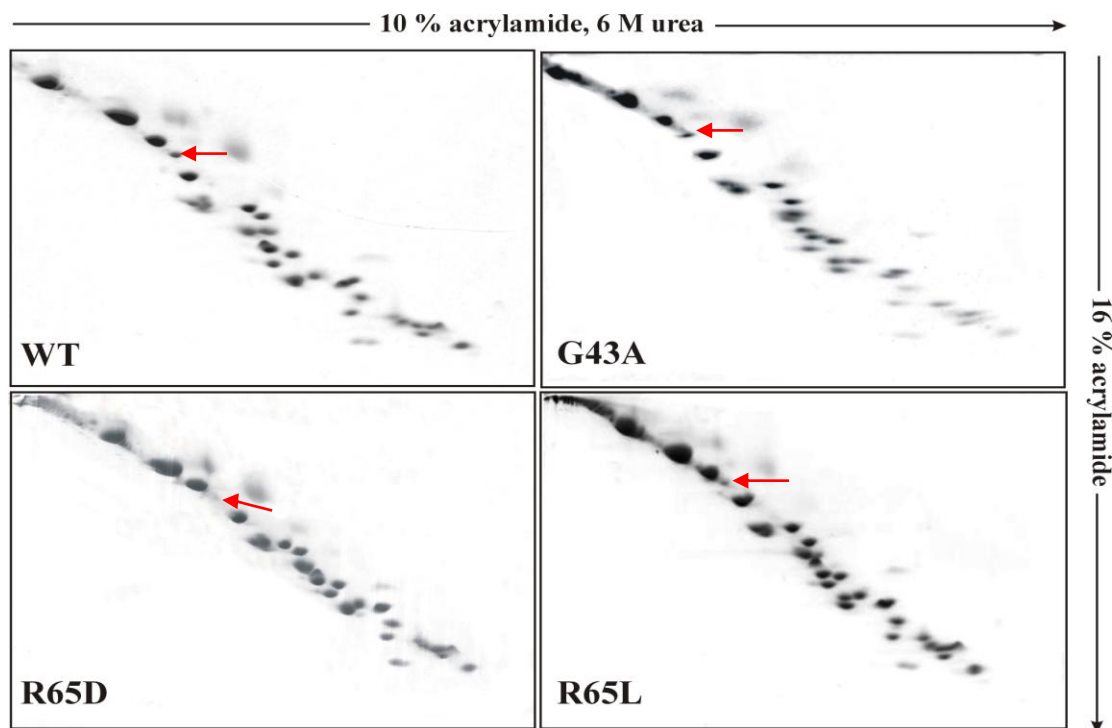


**Figure 4.5** *Doubled SDS-PAGE of complex I isolated from 39kDa subunit mutant strains*

Coomassie stained dSDS-gels with 70-80 $\mu$ g complex I isolated from 39kDa subunit mutant strains. All complex I subunits, with the exception of st1, are present in stoichiometric amounts. Variations in the amount of the st1 subunit from normal in the parental strain to completely missing subunit in the R65D strain are indicated with red arrows. Reprinted from [227].

<i>TST</i>	CR X GX[R/T]
<i>MST</i>	CG[S/T]GV T
<i>STI</i>	CG S GV T

**Figure 4.6** *Sequence comparison of the st1 active-site loop with typical TST and MST loops*

The st1 subunit represents a typical 3-mercaptopyruvate:cyanide sulfurtransferase (MST) active-site loop. Typical MSTs are able to catalyse the same reaction as thiosulfate:cyanide sulfurtransferases (TSTs) but show higher affinity for 3-mercaptopyruvate as sulfur donor. Small and hydrophobic amino acids are represented in red; acidic in blue; basic in magenta; hydroxyl, amine and basic in green.

---

Other sulfurtransferase activities were detectable in mitochondrial membranes from *Y. lipolytica* and may have complemented the loss of the enzyme associated with complex I. No second tandem rhodanese domain-type sulfurtransferase (*Figure 4.6*) could be identified in the *Y. lipolytica* or the genomes of other yeasts or fungi suggesting that the additional activity was due to the presence of single rhodanese domain-type enzymes of which two candidate open reading frames (CAG82611.1 and CAG78833), referred here as to st2 and st3, respectively, could be identified in the *Y. lipolytica* genome (*Figure 9.6*, appendix). An alternative explanation for the absence of a deletion phenotype for the complex I associated sulfurtransferase may be the fact that rather than being involved in iron-sulfur biosynthesis, this enzyme may be important for the repair, regulation or quality control [191] of the iron-sulfur proteins of complex I.

It is tempting to speculate that st1 subunit functions as a sort of ‘molecular break’ of the cell growth rate since a strain deprived of the protein yields higher cell mass than the GB 10 wild-type strain (*Figure 3.27*, results). On the other hand, the *st1Δ* strain possess the *URA3* gene encoding orotidine 5-phosphate decarboxylase, an enzyme involved in the synthesis of uracil, which replaced the *st1* gene by homologous recombination in the deletion strategy. The more feasible explanation for the increased growth rate seems to be the fact that *URA3* selection marker allows the *st1Δ* strain to reach higher OD values, whereas the GB10 wild-type strain ceases to grow at the time point where all the uracil available in the growth medium is expended. Verification of the growth curves by supplementation of the media with sufficient amount of uracil or comparing growth rates of the *st1Δ* strain and the *st1Δ* strain complemented with a plasmid version of the *st1* gene is to be assayed.

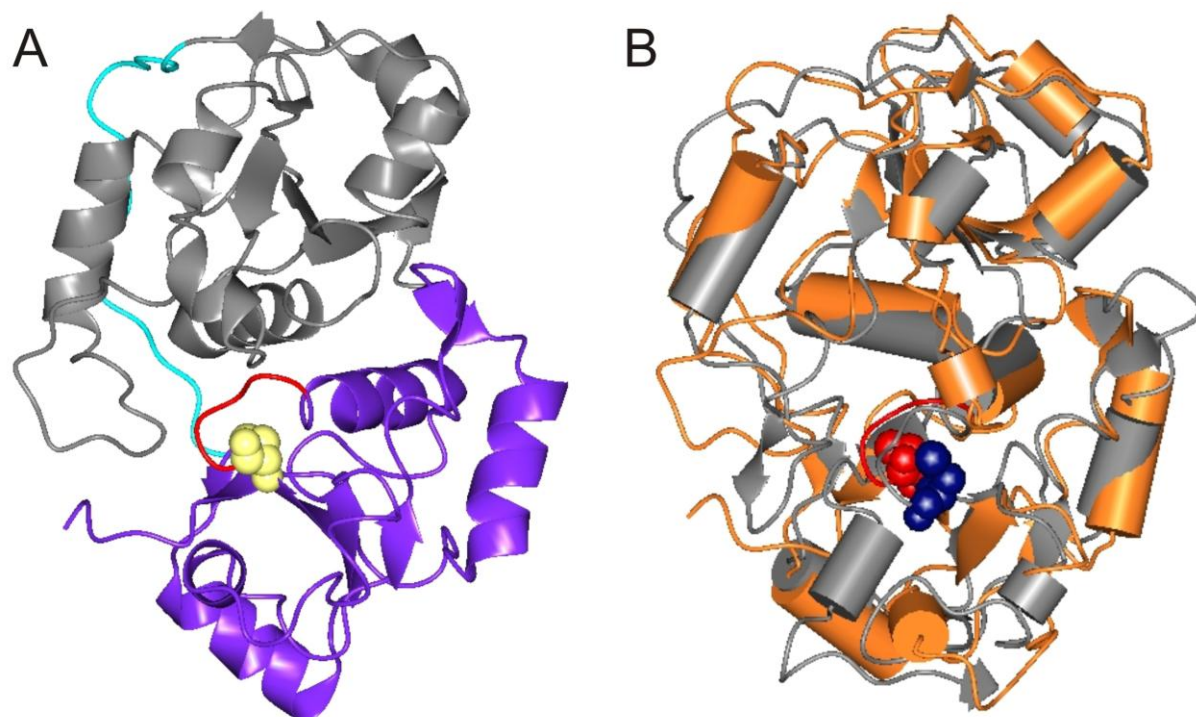


**Figure 4.7** Predicted structure of the *st1* sulfurtransferase from *Y. lipolytica*

(A) Predicted structure of the *st1* subunit of *Y. lipolytica* complex I was predicted by comparison to the x-ray structure of 3-mercaptopyruvate sulfotransferase from *E. coli* that share 35% sequence identity. In this ribbon representation N- and C-terminal domains are represented in grey and purple, respectively; the linker peptide in blue; the active-site loop in red; the catalytic residue, Cys260 (*Y. lipolytica* nomenclature) is represented in sphere model (yellow); (B) The predicted structure of the *st1* subunit of *Y. lipolytica* complex I (orange) superimposed with an x-ray structure of sulfurtransferase RhdA from *A. vinelandii* (grey). *Y. lipolytica* active-site loop and the catalytic cysteine residue is shown in red (sphere model). The catalytic cysteine residue of *A. vinelandii* is represented in sphere model (dark blue). The structure prediction was performed with QuickPhyre [224] and models were superimposed using CCP4 Molecular graphics [158].

Although *st1* was predicted<sup>1</sup> to lack transmembrane helices, its exact position in complex I is not known (for the hydropathy plot of the *st1* see *Figure 4.8*). Weak association of the *st1* subunit with complex I was shown not only by investigation of the 39kDa subunit mutants (*Figure 4.5*), but also *st1* is known to dissociate from the complex in BN-PAGE even if the mild detergent digitonin is used for mitochondrial membrane solubilisation (*Figure 3.29*, results).

<sup>1</sup> Predicted using servers <http://www.enzim.hu/hmmtop/> and <http://www.cbs.dtu.dk/services/TMHMM/>.

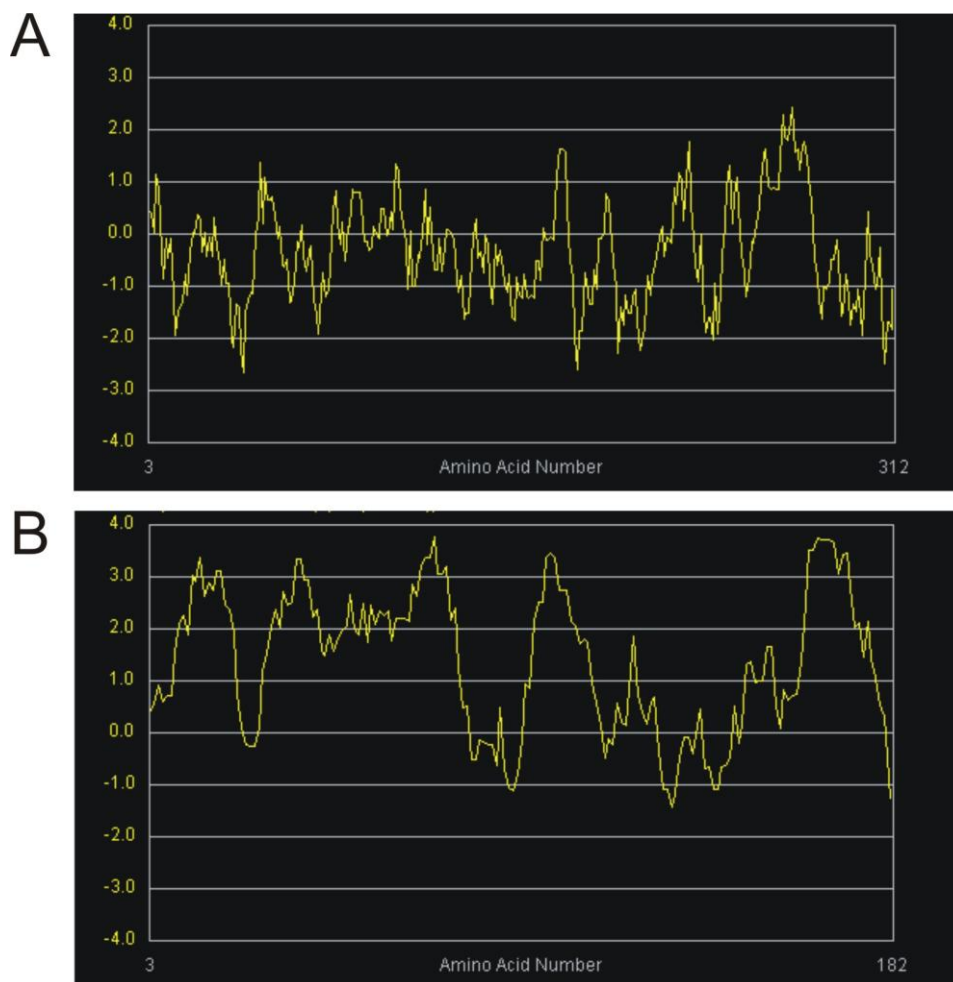


**Figure 4.8 Hydrophobicity plots of *st1* and *ND6* subunits**

The hydrophobicity plots of (A) the *st1* subunit and (B) the *ND6* subunit, the most hydrophobic of all complex I subunits were simulated using the Software Hydrophobicity Plots (Molecular Toolkit, Colorado State University, USA; <http://www.vivo.colostate.edu/molkit/hydrophathy/index.html>). The y-axis represents the Kyte-Doolittle hydrophobicity scale, where the positive values represent hydrophobic, whereas negative hydrophilic character of the amino acids. On the x-axis the amino acid number is indicated. The window size, which is the number of amino acids examined at a time to determine the point of hydrophobic character, was set to 7.

### **4.3 Biosynthetic module of complex I - link between ACPMs and *st1* subunit**

It is tempting to speculate that one or both ACPM subunits operate together with the *st1* sulfurtransferase in a functional biosynthetic domain. Also, the 39 kDa subunit of complex I, a member of the short-chain dehydrogenase/ reductase (SDR) family was postulated to be a



---

part of the same biosynthetic module [35]. Furthermore, two homologues of the SDR family the enoyl-acyl carrier protein reductase (mENR1 and mENR2) closely related to mitochondrial FASII component the trans-2-enoyl-CoA, were recently identified in addition to the ACPM as complex I subunits in *Trypanosoma brucei* [228].

ACPMs from several organisms are known to provide octanoic acid as a precursor for the lipoic acid synthesis. Although, it is known that in octanoic acid synthesis pathway the sulfur insertion is usually catalyzed by lipoic acid synthase it cannot be ruled out that the st1 subunit could take over or support this function, especially, as sulfurtransferase has been shown to bind lipoate at its active site [229]. Therefore, lipoic acid levels of the parental, *acpm2* $\Delta$  and the *acpm2* $\Delta$ ,pS88A and *st1* $\Delta$  strains were determined in a turbidimetric assay using suspensions of lipoic acid-deficient *E. coli* strain [230]. Unfortunately, it was not possible to assess significance of these enzymes in the lipoic acid synthetic pathway due to the high variability in the measured values (data not shown).

Possibly, the biosynthetic module could also play a regulatory role within the respiratory chain by managing the production of specialized fatty acids, as well as managing sulfur supply for iron-sulfur and lipoic acid biosynthesis, as well as control of the lipoylation status of Krebs cycle enzymes. The possible localization of the biosynthetic module in complex I is the speculated localization of ACPMs, which is the interface between domains I $\alpha$  and I $\beta$ . The st1 protein is predicted to lack transmembrane helices (*Figure 4.7, Figure 4.8*) and is known to dissociate from the complex I, if the 39-kDa (NUEM) subunit is absent, therefore one could speculate that these two subunits remain in contact in complex I.

Modules associated with complex I that are organism specific and confer certain functions were described before. A plant complex I contains additional subunits  $\gamma$ -carbonic anhydrases, associated with specific plant function of reversible interconversion of CO<sub>2</sub> and HCO<sub>3</sub> [76;77]. The theoretical biosynthetic module of *Y. lipolytica* may be functionally linked to certain specialized function of *Yarrowia* in a similar way, for instance with unusual lipid metabolism [3]. Further studies will be needed to elucidate possible interactions among sulfurtransferase and ACPMs associated with *Y. lipolytica* complex I.



## 5 SUMMARY

The nicotinamide-adenine-dinucleotide (NADH):ubiquinone oxidoreductase (complex I) from the strictly aerobic yeast *Y. lipolytica* contains at least 26 “accessory” subunits however the significance of most of them remains unknown. The aim of this study was to characterize the role of three accessory subunits of complex I, recently identified: two mitochondrial acyl carrier proteins, ACPM1 and ACPM2 and a sulfurtransferase (st1) subunit.

ACPMs are small (approx. 10 kDa) acidic proteins that are homologous to the corresponding central components of prokaryotic fatty acid synthase complexes. Genomic deletions of the two genes *ACPM1* and *ACPM2* resulted in strains that were not viable or retained only trace amounts of assembled mitochondrial complex I, respectively, as assessed using two-dimensional blue native/sodium dodecyl sulfate polyacrylamide gel electrophoresis (BN/SDS) PAGE. This suggested different functions for the two proteins that despite high similarity could not be complemented by the respective other homolog still expressed in the deletion strains. To test whether complex I was affected by deletion of the *ACPM2* gene, its activities in mitochondrial membranes were measured. Consequently, specific inhibitor sensitive dNADH: decylubiquinone (DBQ) oxidoreductase activity was lost completely and a strong decrease in dNADH: hexa-ammine-ruthenium (HAR) oxidoreductase activity was measured.

Remarkably, the same phenotypes were observed if just the conserved serine carrying the phosphopantethein moiety was exchanged with alanine. Although this suggested a functional link to the lipid metabolism of mitochondria, using HPLC chromatography no changes in the lipid composition of the organelles were found. Proteomic analysis revealed that both ACPMs were tightly bound to purified mitochondrial complex I. Western blot analysis revealed that the affinity tagged ACPM1 and ACPM2 proteins were exclusively detectable in mitochondrial membranes but not in the mitochondrial matrix as reported for other organisms. Hence it has been concluded that the ACPMs can serve all their possible functions in mitochondrial lipid metabolism and complex I assembly and stabilization as subunits bound to complex I.

---

A protein exhibiting rhodanese (thiosulfate:cyanide sulfurtransferase) activity was found to be associated with homogenous preparation of complex I. From a rhodanese deletion strain, functional complex I that lacked the additional protein but was fully assembled and displayed no functional defects or changes in EPR signature was purified. In contrast to previous suggestions, this indicated that the sulfurtransferase associated with *Y. lipolytica* complex I is not required for assembly of its iron–sulfur clusters.

---

## 6 OUTLOOK

In the future, it is expected that the tagged versions of ACPMs will facilitate their isolation from purified complex I and analysis of the acyl rests attached to them, thus providing better insight to the role of ACPMs. Mutagenesis studies of regions with significant differences in the amino acid sequence between ACPM1 and ACPM2 can indicate regions responsible for specific functions (*Figure 4.1*, discussion), for instance dimerization regions, the ACP-binding motif, which was shown to interact strongly and specifically to allow using it as a bait in the affinity purification of partner FAS components [118]. Moreover, a strategy has been developed to swap larger fragments of the ACPM proteins and to assign specific parts of the protein sequence to their functions. The most notable difference between ACPMs of *Y. lipolytica* is with the organelle targeting sequences. Although both presequences direct these proteins to mitochondria, the ACPM1<sup>1</sup> presequence is considerably shorter (*Figure 4.1*, discussion) and it is predicted to direct the protein also to other cellular compartments, where ACPM1 might confer additional functions. Performed Western-blot analysis does not support the view that the tagged versions of ACPMs are present in other compartments than in the inner mitochondrial membrane (*Figure 3.18*, results). However, concentration of the strepII-tagged version of ACPM1 in fractions used for analysis could have been below the antibody detection sensitivity, therefore isolation of individual cellular compartments will be required to confirm this statement.

It is already known that the ACPM2 cannot complement the function of the ACPM1. A remaining open question is whether the presequence of ACPM1 fused with the ACPM2 protein can rescue the vital function of ACPM1. Potentially interesting effects on complex I might be observed with a double deletion mutant deprived of both ACPM1 and ACPM2. Since ACPMs were postulated to be an important link in the lipoic acid biosynthetic pathway, it would be important to perform activity assays of Krebs cycle enzymes (pyruvate and  $\alpha$ -ketoglutarate dehydrogenase), which utilise lipoate as a cofactor.

Tagged versions of ACPMs and st1 subunit make it possible to label these subunits by immuno-gold and localize them using electron microscopy. Alternatively, an immune-

---

fluorescent-dye labelling can be applied to determine distances among these subunits by means of the FRET method. Complex I deprived of ACPM2 subunit dissociates into subcomplexes, whose composition could be analysed using the newly developed and highly sensitive LILBID mass spectrometry [110].

Rhodanese activity of the st1 subunit has been measured with the thiosulfate as a sulfur donor. It would be interesting to check if st1, which possesses a typical MST catalytic loop, exhibits higher sulfurtransferase activity, when 3-mercaptopyruvate is used as substrate.

---

<sup>1</sup> The protein is recognized as a secretory protein, which might be directed to Endoplasmic reticulum or microsomes

## 7 AUSFÜHRLICHE DEUTSCHSPRACHIGE ZUSAMMENFASSUNG

### 7.1 *Komplex I*

Komplex I (NADH: Ubichinon Oxidoreduktase) ist der erste elektronentransferierende Proteinkomplex der mitochondrialen Atmungskette, und stellt einen der größten und kompliziertesten membrangebundenen Proteinkomplexe dar [25]. Das L-förmige Molekül besteht aus einem Segment, das sich in der Lipiddoppelschicht der inneren Membran befindet, sowie einem peripheren Teil, der in den Matrix-Raum hineinragt und alle bekannten Resdoxzentren enthält. Die atomare Struktur des hydrophilen Teils des homologen Enzyms aus *Thermus thermophilus* wurde gelöst [17]. Der genaue, katalytische Mechanismus von Komplex I ist jedoch noch nicht verstanden. Komplex I katalysiert die Übertragung von zwei Elektronen von reduziertem Nicotinamidadenindinucleotid (NADH) über Flavin mononucleotid (FMN) und acht Eisen-Schwefel-Cluster auf Ubichinon. An diesen Transfer ist die Translokation von vier Protonen über die innere mitochondrielle Membran gekoppelt. Die minimale Anzahl von 14 zentralen Untereinheiten, aus denen sich das prokaryotische Enzym zusammensetzt, ist in Eukaryonten um bis zu 31 akzessorische Untereinheiten erweitert, was sich auf eine Masse von 1 MDa summiert [35;36].

### 7.2 *Acyl-Carrier-Proteine*

Acyl-Carrier-Proteine (ACPs) sind kleine (~10 kDa), saure Proteine mit hochkonservierten Sequenzbereichen. Sie sind zentrale Bestandteile der prokaryotischen und mitochondrialen sowie der Chloroplasten-Fettsäure-Synthase (FAS II) Komplexe. ACPs enthalten ein zentral lokalisiertes, an Serin gebundenes Pantethein-4'-Phosphat als prosthetische Gruppe, die post-translational angefügt wird und als Plattform für die Acyl Zwischenprodukte während der Fettsäure-Synthese dient. Zusätzlich wird für die bakteriellen ACPs eine Beteiligung an der Synthese von Polyketiden [141], von Peptid-Antibiotika [143] und der Acylierung von Toxinen [147] postuliert. In der Regel werden ein oder mehrere ACPs vom Typ II FAS in den Mitochondrien verschiedener Spezies gefunden, und aufgrund ihrer Lokalisation als

---

ACPM (M=Mitochondrial) bezeichnet. Seit der Entdeckung und Identifizierung von ACPMs haben weitere Studien angedeutet, dass Mitochondrien alle notwendigen Enzyme für die Fettsäure-Biosynthese enthalten. Sie sind in der Lage, kurze [159;160] und möglicherweise sogar langkettige [162;163] Fettsäuren zu synthetisieren. Es wird ihnen außerdem eine Rolle bei der Herstellung von Oktansäure zugeschrieben, einem Vorläufer der Liponsäure. Letzere ist die prosthetische Gruppe einiger mitochondrialer Enzyme, die an wichtigen zellulären Prozessen beteiligt sind [162];[163];[164;165]; [166];[176], wie die Pyruvat-Dehydrogenase- und 2-Oxoglutarat-Dehydrogenase-Komplexe [148;167]. Es wurde auch spekuliert, dass die Aktivität der ACPMs eine wesentliche Rolle bei der Reparatur von mitochondrialen Lipiden spielt [159].

### ***7.3 Rhodanese (Thiosulfat:Cyanid Sulfurtransferase)***

Sulfurtransferasen sind ubiquitäre Enzyme, die in allen lebenden Organismen gefunden wurden, von Bakterien bis zum Menschen [177]. Bei Säugetieren sind dies zwei eng miteinander verwandte Enzyme, die Thiosulfat: Cyanid Sulfurtransferase, auch bezeichnet als Rhodanese, und die 3-Mercaptopyruvat: Cyanid Sulfurtransferase. Beide sind vorwiegend in den Mitochondrien lokalisiert [178]. *In vitro* katalysiert Thiosulfatsulfurtransferase (TST) die Übertragung eines Sulfan-Schwefelatoms von Thiosulfat auf Cyanid, wodurch Thiocyanat und Sulfit entstehen. 3-Mercaptopyruvat Sulfurtransferase (MST) ist in der Lage, die gleiche Reaktion zu katalysieren, zeigt aber eine höhere Affinität für 3-Mercaptopyruvat als Schwefeldonor [179]. Der Schwefel-Transfer findet durch einen doppelten Verdrängungsmechanismus statt, der die Bildung eines persulfidhaltigen Zwischenproduktes mit einem invarianten katalytischen Cystein beinhaltet [177]. Die tatsächliche biologische Rolle von TST und MST ist allerdings weitgehend unklar, da ihre *in vivo* Substrate immer noch nicht bekannt sind. Vorgeschlagene Funktionen beinhalten die Cyanid-Entgiftung [187], die Erhaltung des Sulfan Pools [188], den Selen-Stoffwechsel [189] und die Thiamin-Biosynthese [190]. Aufgrund ihrer Eigenschaft, Schwefelatome zu übertragen, und ihrer mitochondrialen Lokalisation wurde vorgeschlagen, dass die Rhodanese die Bildung von Eisen-Schwefel-Zentren katalysieren könnte.



## 7.4 Zielsetzungen

Das Ziel dieser Studie war es, die Funktion von drei kürzlich charakterisierten akzessorischen Untereinheiten von Komplex I der strikt aeroben Hefe *Yarrowia lipolytica* zu charakterisieren. Es handelt sich um zwei mitochondriale Acyl-Carrier-Proteine, ACPM1 und ACPM2, sowie um die Sulfurtransferase (St1) Untereinheit.

Die Bedeutung der beiden ACPMs für die strukturelle Integrität und die Aktivität von Komplex I wurde untersucht. Der Phosphopantetheine-bindende Serin-Rest der ACPMs wurde mutiert, um feststellen zu können, ob die Bedeutung der ACPMs in ihrer enzymatischen Aktivität begründet ist oder ob ihre Anwesenheit als strukturelle Komponente von Komplex I von Bedeutung ist. Außerdem wurden die Auswirkungen der ACPM-Deletion und des Serinaustauschs auf die Atmungsketten-Komplex Assemblierung und Aktivität überprüft. Da postuliert wird, dass ACPMs an der mitochondrialen Fettsäure-Synthese beteiligt sind, wurde die mitochondriale Lipid-Zusammensetzung der *Yarrowia* Stämme, in denen der Pantethein-4'-Phosphat-Kofaktor fehlte bzw. in dem das Acyl Carrier Protein komplett entfernt worden war, bestimmt. Da ACPMs in anderen Organismen sowohl in der Mitochondrien-Matrix als auch assembliert mit Komplex I nachgewiesen wurden, wurde die submitochondriale Verteilung der ACPMs in *Y. lipolytica* überprüft.

Einem Protein, das Rhodanese -(Thiosulfat: Cyanid Sulfurtransferase) Aktivität aufwies und mit einer homogenen Komplex I Präparation assoziiert war, wurde eine mögliche Rolle in der Eisen-Schwefel-Zentren Assemblierung zugesprochen. Daher wurde in einem Rhodanese-negativen *Y. lipolytica* Stamm sowohl die Assemblierung und Aktivität von Komplex I als auch die Assemblierung der Eisen-Schwefel-Cluster untersucht.

## 7.5 Ergebnisse

Neueste massenspektrometrische Analysen von *Y. lipolytica* Komplex I hatten die Anwesenheit von zwei mitochondrialen Acylcarrierproteinen, ACPM1 und ACPM2, gezeigt. Um die Funktion der ACPMs zu untersuchen, wurden die entsprechenden Gene durch homologe Rekombination deletiert.

Die Deletion des als *ACPM1* bezeichneten Gens in einem diploiden Stamm (*ACPM1/acpm1::URA3*) und die anschließende Sporulation ergab keine haploiden Deletions-

---

Stämme. Wurde jedoch eine Plasmid-kodierte, funktionsfähige Kopie des *ACPM1* Gens in den *ACPM1/acpm1::URA3* Stamm eingeführt, konnten haploide *acpm1Δ*, *pACPM1* Stämme isoliert werden. Somit wurde festgestellt, dass es sich bei *ACPM1* um ein essentielles Gen in *Y. lipolytica* handelt. Um zu unterscheiden, ob das *ACPM1* Protein als Ganzes oder nur seine funktionelle Gruppe für das Überleben erforderlich sind, wurde das Serin-66 von *ACPM1* durch Alanin ausgetauscht. Dieses konservierte Serin ist in allen Acyl-Carrier-Proteinen enthalten und bindet kovalent die prosthetische Gruppe, das Phosphopantethein. Im Unterschied zur wildtypischen *ACPM1* Kopie konnte diese mutierte Version des *ACPM1* Gens den Deletions-Phänotyp nicht komplementieren. Folgerichtig konnten keine *acpm1Δ*, *pACPM1-S66A* Sporen erhalten werden. Somit scheint der Austausch einer einzigen Aminosäure die gleiche Wirkung zu haben wie die vollständige Entfernung des *ACPM1* Gens.

Im Gegensatz dazu ist das zweite *ACPM2* Protein, *ACPM2*, nicht essentiell für das Überleben, da haploide *ACPM2* Deletions-Stämme (*acpm2Δ*) mit derselben Strategie wie für *ACPM1* angewandt hergestellt werden konnten. Um zu überprüfen, ob Komplex I von der Deletion des *ACPM2* Gens beeinträchtigt wird, wurde zuerst die Aktivität in mitochondrialen Membranen aus Deletions-Stämmen gemessen und mit den Werten des Wildtyps verglichen. Die spezifische, Inhibitor-sensitive dNADH:DBQ Oxidoreduktase Aktivität war völlig verschwunden. Ein starker Rückgang der dNADH:HAR Oxidoreduktase Aktivität auf ein Niveau, das häufig bei anderen Komplex I-defizienten Stämmen beobachtet wurde, ließ darauf schließen, dass der Verlust der Komplex I-Aktivität auf einen sehr geringen Anteil an intaktem Komplex I zurückzuführen ist. Bemerkenswert ist, dass ähnlich reduzierte Aktivitäten beobachtet wurden, wenn ein Plasmid mit mutiertem *ACPM2* in die Zellen eingeführt worden war. Dieses *ACPM2* enthielt eine Mutation, durch die das Phosphopantethein-bindende Serin-88 im *ACPM2* durch Alanin ersetzt wurde. Der Verlust von Komplex I wurde durch zwei-dimensionale BN/SDS-PAGE bestätigt, in der mitochondriale Membranen aus dem *acpm2Δ* Stamm und dem Wildtyp-Stamm analysiert wurden. Im Gegensatz zum Wildtyp konnte im *ACPM2* Deletions-Stamm kein Komplex I durch Silberfärbung nachgewiesen. Das gleiche Ergebnis wurde mit dem Stamm erzielt, der die mutierte Version von *ACPM2* exprimiert, in der Serin-88 durch Alanin ersetzt worden war.

Mitochondriale Membranen aus dem *acpm2Δ* Stamm wurden durch Western Blot Analyse von nativen Gelen untersucht, um etwaige geringe Mengen von Komplex I-Subkomplexen zu detektieren. Während in den Membranen aus dem parentalen Stamm komplett assemblierter Komplex I als die vorherrschende Form gefunden wurde, war in den Mitochondrien der *acpm2Δ* und S88A Mutanten nur eine sehr kleine Menge an vollständig assembliertem Komplex I zu finden. Stattdessen wurden zwei Subkomplexe von etwa 700 und 300 kDa erkannt, die leider aufgrund der sehr geringen verfügbaren Menge an Probenmaterial nicht weiter bezüglich ihrer Untereinheiten-Zusammensetzung analysiert werden konnten.

Um zu sehen, ob die Deletion bzw. die Mutagenese von ACPM2 die Lipid-Zusammensetzung der mitochondrialen Membranen beeinflusst hatte, wurden mitochondriale Membranen des Wildtyp Stammes und der Stämme *acpm2Δ* sowie *acpm2Δ, pACPM2-S88A* auf ihren Phospholipidgehalt untersucht. Alle Lipide waren in sehr ähnlichen Verhältnissen in den intakten, mittels Saccharose Gradient gereinigten Mitochondrien aus allen Stämmen vorhanden. Prominente Peaks wurden mittels MALDI-MS als Cardiolipin, Phosphatidyl-Ethanolamin, Phosphatidyl-Inositol, Lyso-Phosphatidyl-Ethanolamin, und Phosphatidyl-Cholin identifiziert.

In früheren Berichten wurde eine Lokalisierung der ACPMs in der mitochondrialen Matrix vorgeschlagen. Um die submitochondriale Verteilung der ACPMs in *Y. lipolytica* zu untersuchen, wurden die lösliche und die Membran-Fraktion der Mitochondrien analysiert. Die Fraktionierung wurde mit *Yarrowia* Stämmen durchgeführt, die die getaggten Versionen der ACPMs, ACPM1-strepII und ACPM2-flag, exprimierten, um sie nach der SDS-PAGE im Western-Blot nachweisen zu können. Beide ACPMs waren ausschließlich in der mitochondrialen Membran-Fraktion nachweisbar und fehlten sowohl in der löslichen Fraktion der Mitochondrien als auch in der cytosolischen Fraktion.

Ein Rhodanese-ähnliches Protein mit einer molekularen Masse von ca. 34,6 kDa war auch in den reinsten Präparationen aus *Y. lipolytica* dauerhaft vorhanden. Das Protein wies Thiosulfat:Cyanid Sulfurtransferase Aktivität auf, die zuvor nie in Komplex I aus anderen Quellen aufgetreten war. Der Gehalt des St1 benannten Proteins schien im Vergleich zu anderen Komplex I Proteinen variabel zu sein und tauchte substöchiometrisch in den meisten Komplex I-Präparationen auf. Um zu testen, ob die Sulfurtransferase Aktivität von St1 für

---

die Komplex I Biogenese oder die Synthese von Eisen-Schwefel-Zentren erforderlich ist, wurde das Gen durch homologe Rekombination entfernt. Der *St1Δ* Stamm war voll lebensfähig, und durch BN-PAGE konnte nachgewiesen werden, dass seine mitochondrialen Membranen vollständig assemblierten Komplex I mit ähnlichem Expressionsmuster wie im Wildtyp enthalten

Die NADH:HAR Oxidoreduktase-Aktivitäten der mitochondrialen *St1Δ* Membranen deuten ebenfalls daraufhin, dass die Deletion die Komplex I Aktivität nicht reduzierte. Abgesehen von der 34,6 kDa Bande, die in dem Deletions-Stamm fehlte, zeigte der gereinigte Komplex I aus dem *St1Δ* Stamm das gleiche Untereinheiten Muster wie der Wildtyp unter Standard Tricin-SDS-PAGE Bedingungen. Dies deutet darauf hin, dass die Stabilität von Komplex I nicht wesentlich beeinträchtigt wurde. Die Inhibitor-sensitiven dNADH:DBQ Aktivitäten von mitochondrialen Membranen und gereinigtem Komplex I waren sehr ähnlich im Wildtyp und dem *St1Δ* Stamm. Die EPR-Spektren der Eisen-Schwefel-Cluster N1, N2, N3 und N4 des gereinigten Komplex I zeigten, dass sich weder die Signalintensitäten noch die Positionen der charakteristischen g-Werte zwischen dem parentalen und dem Deletions-Stamm unterschieden.

## 7.6 Fazit

Die genomischen Deletionen der beiden Gene ACPM1 and ACPM2 in *Y. lipolytica* führten zu Stämmen, die entweder, wie im Fall von *acpm1*Δ, nicht lebensfähig waren oder, wie beim *acpm2*Δ Stamm, nur Spuren von assembliertem mitochondriellen Komplex I enthalten. Dies deutete auf unterschiedliche Funktionen der beiden ACPMs hin. Denn trotz ihrer hohen Sequenz-Ähnlichkeit konnten die Funktionen des jeweiligen deletierten ACPMs nicht durch das andere ACPM-Homolog, das ja noch in den Deletions-Stämmen exprimiert wurde, übernommen werden.

Bemerkenswert ist, dass der gleiche Phänotyp beobachtet wurde, wenn nur das konservierte Serin, das die Phosphopantethein-Gruppe trägt, gegen Alanin ausgetauscht wurde. Obwohl dies eine funktionale Querverbindung zum Lipidstoffwechsel der Mitochondrien andeutete, wurden keine Veränderungen in der Lipid-Zusammensetzung der Organellen gefunden. Die Proteomanalyse ergab, dass die beiden ACPMs eng mit dem gereinigten mitochondrialen Komplex I verbunden waren. Die Western-Blot Analyse zeigte, dass die affinitätsmarkierten Versionen der ACPM1 und ACPM2 Proteine ausschließlich in der mitochondrialen Membran nachweisbar waren und nicht in der mitochondrialen Matrix wie bei einigen anderen Organismen. Daraus wurde gefolgert, dass die ACPMs ihre möglichen Funktionen wie z.B. im mitochondrialen Lipidstoffwechsel und in der Komplex I Assemblierung und Stabilisierung, gebunden als Untereinheiten von Komplex I ausüben können.

Der Rhodanese-Deletions Stamm ( $\Delta$ St1) enthielt vollständig assemblierten, funktionsfähigen Komplex I, und zeigte keine funktionellen Defekte oder Veränderungen in der EPR Signatur. Im Gegensatz zu früheren Vorschlägen, dass St1 für die Assemblierung der Eisen-Schwefel-Zentren des Komplex I erforderlich ist, lassen die Ergebnisse mit dem Deletionsstamm darauf schließen, dass dies für die mit Komplex I assoziierte Sulfurtransferase in *Y. lipolytica* nicht gilt.

---

## 7.7 *Ausblick*

Es ist vorstellbar, dass die affinitätsmarkierten Versionen der ACPMs ihre Isolierung aus gereinigtem Komplex I ermöglichen. Hierdurch würde die Analyse der mit ihnen verbundenen Acyl Reste erleichtert werden, um einen besseren Einblick in die Rolle der ACPMs zu bekommen.

Es ist bereits bekannt, dass ACPM2 die Funktion des ACPM1 nicht übernehmen kann, obwohl die reifen Proteine eine hohe Sequenzähnlichkeit aufweisen. Eine verbleibende offene Frage ist, ob die durch die Präsequenz der ACPMs vermittelte Lokalisation eine Rolle für die Funktion spielt, da hier die größten Unterschiede zwischen beiden Proteinen bestehen. Daher könnte die ACPM1 Präsequenz mit der Sequenz des reifen ACPM2 Proteins fusioniert werden, um zu überprüfen, ob ACPM2 anschließend die lebensnotwendige Funktion des ACPM1 übernehmen kann.

Da angenommen wird, dass mitochondriale Acyl Carrier Proteine eventuell eine wichtige Rolle in der Liponsäure Biosynthese spielen, wäre es wichtig, Aktivitäts-Tests von Krebs-Zyklus Enzymen (Pyruvat- und  $\alpha$ -Ketoglutarat-Dehydrogenase) durchzuführen, die Lipoat als Cofaktor benötigen.

Die Rhodanese Aktivität der St1 Untereinheit wurde mit Thiosulfat als Schwefelspender gemessen. Es wäre interessant zu überprüfen, ob St1, das eine für MST Enzyme typische katalytische Schleife besitzt, eine höhere Sulfurtransferase-Aktivität aufweist, wenn 3-Mercaptopyruvat als Substrat verwendet wird.

---

## 8 REFERENCES

- [1] P.Mitchell. Coupling of phosphorylation to electron and hydrogen transfer by a chemi-osmotic type of mechanism, *Nature* 191 (1961) 144-148.
- [2] S.Kerscher. Diversity and origin of alternative NADH:ubiquinone oxidoreductases, *Biochim.Biophys.Acta* 1459 (2000) 274-283.
- [3] S.Kerscher, S.Dröse, K.Zwicker, V.Zickermann, U.Brandt. *Yarrowia lipolytica*, a yeast genetic system to study mitochondrial complex I, *Biochim.Biophys.Acta - Bioenerg.* 1555 (2002) 83-91.
- [4] J.L.Guler, E.Kriegova, T.K.Smith, J.Lukes, P.T.Englund. Mitochondrial fatty acid synthesis is required for normal mitochondrial morphology and function in *Trypanosoma brucei.*, *Mol.Microbiol.* 67 (2008) 1125-1142.
- [5] I.Fridovich. The biology of oxygen radicals, *Science* 201 (1978) 875-880.
- [6] J.F.Turrens. Mitochondrial formation of reactive oxygen species, *J.Physiol.* 552 (2003) 335-344.
- [7] S.Dröse, U.Brandt. The mechanism of mitochondrial superoxide production by the cytochrome bc1 complex, *J.Biol.Chem.* 283 (2008) 21649-21654.
- [8] Y.Bai, P.Hájek, A.Chomyn, B.B.Seo, A.Matsuno-Yagi, T.Yagi, G.Attardi. Lack of complex I activity in human cells carrying a mutation in MtDNA-encoded ND4 subunit is corrected by the *Saccharomyces cerevisiae* NADH-quinone oxidoreductase (NDI1) gene, *J.Biol.Chem.* 276 (2001) 38808-38813.
- [9] J.Smeitink, L.Van den Heuvel. Human mitochondrial complex I in health and disease, *Am.J.Hum.Genet.* 64 (1999) 1505-1510.
- [10] V.Yankovskaya, R.Horsefield, S.Tomroth, C.Luna-Chavez, C.Leger, B.Byrne, G.Cecchini, S.Iwata. Architecture of succinate dehydrogenase and reactive oxygen species generation., *Science* 299 (2003) 700-704.
- [11] S.Iwata, J.W.Lee, K.Okada, J.K.Lee, M.Iwata, B.Rasmussen, T.A.Link, S.Ramaswamy, B.K.Jap. Complete structure of the 11-subunit bovine mitochondrial cytochrome *bc<sub>1</sub>* complex, *Science* 281 (1998) 64-71.
- [12] C.Hunte, J.Koepke, C.Lange, H.Michel. Structure at 2.3 angstrom resolution of the cytochrome bc(1) complex from the yeast *Saccharomyces cerevisiae* co-crystallized with an antibody Fv fragment, *Structure* 8 (2000) 669-684.

- 
- [13] S.Iwata, C.Ostermeier, B.Ludwig, H.Michel. Structure at 2.8 Å resolution of cytochrome *c* oxidase from *Paracoccus denitrificans*, *Nature* 376 (1995) 660-669.
- [14] C.Ostermeier, A.Harrenga, U.Ermler, H.Michel. Structure at 2.7 Å resolution of the *Paracoccus denitrificans* two- subunit cytochrome *c* oxidase complexed with an antibody FV fragment, *Proc.Natl.Acad.Sci.USA* 94 (1997) 10547-10553.
- [15] J.P.Abrahams, A.G.W.Leslie, R.Lutter, J.E.Walker. Structure at 2.8 Å resolution of F<sub>1</sub>-ATPase from bovine heart mitochondria, *Nature* 370 (1994) 621-628.
- [16] Y.Hatefi, A.G.Haavik, D.E.Griffiths. Studies on the Electron Transfer System. XL. Preparation and properties of mitochondrial DPNH-coenzyme Q reductase, *J.Biol.Chem.* 237 (1962) 1676-1680.
- [17] L.A.Sazanov, P.Hinchliffe. Structure of the hydrophilic domain of respiratory complex I from *Thermus thermophilus*, *Science* 311 (2006) 1430-1436.
- [18] H.Schägger, K.Pfeiffer. Supercomplexes in the respiratory chains of yeast and mammalian mitochondria, *EMBO J.* 19 (2000) 1777-1783.
- [19] I.Wittig, R.Carrozzo, F.M.Santorelli, H.Schägger. Supercomplexes and subcomplexes of mitochondrial oxidative phosphorylation, *Biochim.Biophys.Acta* 1757 (2006) 1066-1072.
- [20] P.Paumard, J.Vaillier, B.Coulary, J.Schaeffer, V.Soubannier, D.M.Mueller, D.Brethes, J.P.di Rago, J.Velours. The ATP synthase is involved in generating mitochondrial cristae morphology, *Embo J* 21 (2002) 221-230.
- [21] Strauss.M, Hofhaus.G, R.R.Schröder, W.Kühlbrandt. Dimer ribbons of ATPsynthase shape the inner mitochondrial membrane., *EMBO J.* 27 (2008) 1154-1160.
- [22] B.J.Bultema, H.P.Braun, E.J.Boekema, R.Kouril. Megacomplex organization of the oxidative phosphorylation system by structural analysis of respiratory supercomplexes from potato., *Biochim.Biophys.Acta* 1787 (2009) 60-67.
- [23] I.Wittig, H.Schägger. Supramolecular organization of ATP synthase and respiratory chain in mitochondrial membranes, *Biochim.Biophys.Acta* 46205 (2009).
- [24] R.D.Allen. Membrane Tubulation and Proton Pumps, *Protoplasma* 189 (1995) 1-8.
- [25] U.Brandt. Energy converting NADH : Quinone oxidoreductase (Complex I), *Annu.Rev.Biochem.* 75 (2006) 69-92.
- [26] M.K.F.Wikström. Two protons are pumped from the mitochondrial matrix per electron transferred between NADH and ubiquinone., *FEBS Lett.* 169 (1984) 300-304.
- [27] T.Ohnishi, K.Kawaguchi, B.Hagihara. Preparation and some properties of yeast mitochondria, *J.Biol.Chem.* 241 (1966) 1797-1806.



- 
- [28] W.X.Balcavag, J.R.Mattoon. Properties of *Saccharomyces Cerevisiae* Mitochondria Prepared by A Mechanical Method, *Biochim.Biophys.Acta* 153 (1968) 521-&.
- [29] R.Büschges, G.Bahrenberg, M.Zimmermann, K.Wolf. NADH: ubiquinone oxidoreductase in obligate aerobic yeasts., *Yeast* 10 (1994) 475-479.
- [30] S.Kerscher. Diversity and origin of alternative NADH:ubiquinone oxidoreductases., *Biochim.Biophys.Acta - Bioenerg.* 1459 (2000) 274-283.
- [31] A.G.Rasmusson, A.S.Svensson, V.Knoop, L.Grohmann, A.Brennicke. Homologues of yeast and bacterial rotenone-insensitive NADH dehydrogenases in higher eukaryotes: two enzymes are present in potato mitochondria, *Plant J.* 20 (1999) 79-87.
- [32] C.M.Gomes, T.M.Bandeiras, M.Teixeira. A New Type-II NADH Dehydrogenase from the Archaeon *Acidianus ambivalens*: Characterization and in vitro Reconstitution of the Respiratory Chain, *J.Bioenerg.Biomembr.* 33 (2001) 1-8.
- [33] J.Smeitink, L.Van den Heuvel, S.DiMauro. The genetics and pathology of oxidative phosphorylation, *Nat.Rev.Genet.* 2 (2001) 342-352.
- [34] J.A.M.Smeitink, L.W.P.J.van den Heuvel, W.J.H.Koopman, L.G.J.Nijtmans, C.Ugalde, P.H.G.M.Willems. Cell biological consequences of mitochondrial NADH: Ubiquinone oxidoreductase deficiency, *Current Neurovascular Research* 1 (2004) 29-40.
- [35] J.Hirst, J.Carroll, I.M.Fearnley, R.J.Shannon, J.E.Walker. The nuclear encoded subunits of complex I from bovine heart mitochondria, *Biochim.Biophys.Acta* 1604 (2003) 135-150.
- [36] J.Carroll, I.M.Fearnley, R.J.Shannon, J.Hirst, J.E.Walker. Analysis of the subunit composition of complex I from bovine heart mitochondria, *Mol.Cell.Proteomics* 2 (2003) 117-126.
- [37] A.Abdrakhmanova, V.Zickermann, M.Bostina, M.Radermacher, H.Schägger, S.Kerscher, U.Brandt. Subunit composition of mitochondrial complex I from the yeast *Yarrowia lipolytica*, *Biochim.Biophys.Acta* 1658 (2004) 148-156.
- [38] I.Marques, M.Duarte, J.Assuncao, A.V.Ushakova, A.Videira. Composition of complex I from *Neurospora crassa* and disruption of two "accessory" subunits, *Biochim.Biophys.Acta* 1707 (2005) 211-220.
- [39] P.Cardol, F.Vanrobaeys, B.Devreese, J.Van Beeumen, R.F.Matagne, C.Remacle. Higher plant-like subunit composition of mitochondrial complex I from *Chlamydomonas reinhardtii*: 31 conserved components among eukaryotes, *Biochim.Biophys.Acta* 1658 (2004) 212-224.
- [40] J.L.Heazlewood, K.A.Howell, A.H.Millar. Mitochondrial complex I from *Arabidopsis* and rice: orthologs of mammalian and fungal components coupled with plant-specific subunits, *Biochim.Biophys.Acta* 1604 (2003) 159-169.

- 
- [41] T.Yagi, A.Matsuno-Yagi. The proton-translocating NADH-quinone oxidoreductase in the respiratory chain: the secret unlocked, *Biochem.* 42 (2003) 2266-2274.
- [42] T.Friedrich. The NADH:ubiquinone oxidoreductase (complex I) from *Escherichia coli*, *Biochim.Biophys.Acta* 1364 (1998) 134-146.
- [43] P.Hinchliffe, J.Carroll, L.A.Sazanov. Identification of a novel subunit of respiratory complex I from *Thermus thermophilus*, *Biochem.* 45 (2006) 4413-4420.
- [44] U.Brandt. Structural and functional insights into mitochondrial complex I, *Biochimica et Biophysica Acta-Bioenergetics* (2006) 70.
- [45] V.D.Sled, N.I.Rudnitzky, Y.Hatefi, T.Ohnishi. Thermodynamic analysis of flavin in mitochondrial NADH: ubiquinone oxidoreductase (complex I), *Biochem.* 33 (1994) 10069-10075.
- [46] W.Fecke, V.D.Sled, T.Ohnishi, H.Weiss. Disruption of the gene encoding the NADH-binding subunit of NADH: ubiquinone oxidoreductase in *Neurospora crassa*. Formation of a partially assembled enzyme without FMN and the iron-sulphur cluster N-3, *Eur.J.Biochem.* 220 (1994) 551-558.
- [47] D.Voet, J.G.Voet. Elektronentransport und oxidative Phosphorylierung, in: A.Maelicke, W.Müller-Esterl (Eds.), *Biochemie*, VCH Verlagsgesellschaft mbH, Weinheim, New York, Basel, Cambridge, 1992, pp. 527-560.
- [48] T.Rasmussen, D.Scheide, B.Brors, L.Kintscher, H.Weiss, T.Friedrich. Identification of two tetranuclear FeS clusters on the ferredoxin-type subunit of NADH:ubiquinone oxidoreductase (complex I), *Biochem.* 40 (2001) 6124-6131.
- [49] T.Ohnishi. Iron-sulfur clusters semiquinones in Complex I, *Biochim.Biophys.Acta* 1364 (1998) 186-206.
- [50] D.-C.Wang, S.W.Meinhardt, U.Sackmann, H.Weiss, T.Ohnishi. The iron-sulfur clusters in the two related forms of mitochondrial NADH: ubiquinone oxidoreductase made by *Neurospora crassa* , *Eur.J.Biochem.* 197 (1991) 257-264.
- [51] T.Ohnishi, E.Nakamaru-Ogiso. Were there any "misassignments" among iron-sulfur clusters N4, N5 and N6b in NADH-quinone oxidoreductase (complex I)?, *Biochimica.et Biophysica.Acta (BBA.) - Bioenergetics.* 1777 (2008) 703-710.
- [52] G.Yakovlev, T.Redda, J.Hirst. Reevaluating the relationship between EPR spectra and enzyme structure for the iron-sulfur clusters in NADH: quinone oxidoreductase, *Proceedings of the National Academy of Sciences of the United States of America* 104 (2007) 12720-12725.
- [53] T.Clason, V.Zickermann, T.Ruiz, U.Brandt, M.Radermacher. Direct localization of the 51 and 24 kDa subunits of mitochondrial complex I by three-dimensional difference imaging, *J.Struct.Biol.* 159 (2007) 433-442.

- 
- [54] M.Radermacher, T.Ruiz, T.Clason, S.Benjamin, U.Brandt, V.Zickermann. The three-dimensional structure of complex I from *Yarrowia lipolytica*: A highly dynamic enzyme, *J.Struct.Biol.* 154 (2006) 269-279.
- [55] L.A.Sazanov, J.E.Walker. Cryo-electron Crystallography of Two Sub-complexes of Bovine Complex I Reveals the Relationship between the Membrane and Peripheral Arms, *J.Mol.Biol.* 392 (2000) 455-464.
- [56] N.Grigorieff. Three-dimensional structure of bovine NADH:ubiquinone oxidoreductase (Complex I) at 22 Å in ice, *J.Mol.Biol.* 277 (1998) 1033-1046.
- [57] K.Leonard, H.Haiker, H.Weiss. Three-dimensional structure of NADH:ubiquinone reductase (complex I) from *Neurospora* mitochondria determined by electron microscopy of membrane crystals, *J.Mol.Biol.* 194 (1987) 277-286.
- [58] R.Djafarzadeh, S.Kerscher, K.Zwicker, M.Radermacher, M.Lindahl, H.Schägger, U.Brandt. Biophysical and structural characterization of proton-translocating NADH-dehydrogenase (complex I) from the strictly aerobic yeast *Yarrowia lipolytica*, *Biochim.Biophys.Acta* 1459 (2000) 230-238.
- [59] M.Finel. Organization and evolution of structural elements within complex I, *Biochim.Biophys.Acta* 1364 (1998) 112-121.
- [60] T.Friedrich, H.Weiss. Modular evolution of the respiratory NADH:ubiquinone oxidoreductase and the origin of its modules, *J.theor.Biol.* 187 (1997) 529-540.
- [61] A.Tran-Betcke, U.Warnecke, C.Böcker, C.Zaborosch, B.Friedrich. Cloning and nucleotide sequences of the genes for the subunits of NAD-reducing hydrogenase of *Alcaligenes eutrophus* H16, *J.Bacteriol.* 172 (1990) 2920-2929.
- [62] R.Böhm, M.Sauter, A.Böck. Nucleotide sequence and expression of an operon in *Escherichia coli* coding for formate hydrogenlyase components, *Mol.Microbiol.* 4 (1990) 231-243.
- [63] S.P.J.Albracht. Intimate relationships of the large and the small subunits of all nickel hydrogenases with two nuclear-encoded subunits of mitochondrial NADH:ubiquinone oxidoreductase, *Biochim.Biophys.Acta* 1144 (1993) 221-224.
- [64] I.M.Fearnley, J.E.Walker. Conservation of sequences of subunits of mitochondrial complex I and their relationships with other proteins. [Review], *Biochim.Biophys.Acta* 1140 (1992) 105-134.
- [65] C.Mathiesen, C.Hagerhall. Transmembrane topology of the NuoL, M and N subunits of NADH : quinone oxidoreductase and their homologues among membrane- bound hydrogenases and bona fide antiporters, *Biochimica et Biophysica Acta-Bioenergetics* 1556 (2002) 121-132.

- 
- [66] V.Zickermann, S.Kerscher, K.Zwicker, M.A.Tocilescu, M.Radermacher, U.Brandt. Architecture of complex I and its implications for electron transfer and proton pumping., *Biochimica et Biophysica Acta* (2009).
- [67] M.Finel, J.M.Skehel, S.P.J.Albracht, I.M.Fearnley, J.E.Walker. Resolution of NADH:ubiquinone oxidoreductase from bovine heart mitochondria into two subcomplexes, one of which contains the redox centers of the enzyme, *Biochem.* 31 (1992) 11425-11434.
- [68] L.A.Sazanov, S.Y.Peak-Chew, I.M.Fearnley, J.E.Walker. Resolution of the membrane domain of bovine complex I into subcomplexes: implications for the structural organization of the enzyme, *Biochem.* 39 (2000) 7229-7235.
- [69] J.Carroll, R.J.Shannon, I.M.Fearnley, J.E.Walker, J.Hirst. Definition of the nuclear encoded protein composition of bovine heart mitochondrial complex I - Identification of two new subunits, *J.Biol.Chem.* 277 (2002) 50311-50317.
- [70] J.Carroll, I.M.Fearnley, J.M.Skehel, R.J.Shannon, J.Hirst, J.E.Walker. Bovine complex I is a complex of 45 different subunits, *J.Biol.Chem.* 281 (2006) 32724-32727.
- [71] U.Brandt, A.Abdrakhmanova, V.Zickermann, A.Galkin, S.Dröse, K.Zwicker, S.Kerscher. Structure–function relationships in mitochondrial complex I of the strictly aerobic yeast *Yarrowia lipolytica*, *Biochem.Soc.Trans.* 33 (2005) 840-844.
- [72] Y.M.Galante, Y.Hatefi. Purification and molecular and enzymatic properties of mitochondrial NADH dehydrogenase, *Arch.Biochem.Biophys.* 192 (1979) 559-568.
- [73] Y.M.Galante, Y.Hatefi. Resolution of complex I and isolation of NADH dehydrogenase and an iron-sulfur protein, *Methods Enzymol.* 53 (1978) 15-21.
- [74] C.I.Ragan, Y.M.Galante, Y.Hatefi, T.Ohnishi. Resolution of mitochondrial NADH dehydrogenase and isolation of two iron-sulfur proteins, *Biochem.* 21 (1982) 590-594.
- [75] J.E.Walker. The NADH:ubiquinone oxidoreductase (complex I) of respiratory chains, *Q.Rev.Biophys.* 25 (1992) 253-324.
- [76] M.Perales, H.Eubel, J.Heinemeyer, A.Colaneri, E.Zabaleta, H.P.Braun. Disruption of a nuclear gene encoding a mitochondrial gamma carbonic anhydrase reduces complex I and supercomplex I+III<sub>2</sub> levels and alters mitochondrial physiology in *Arabidopsis*, *J.Mol.Biol.* 350 (2005) 263-277.
- [77] N.V.Dudkina, H.Eubel, W.Keegstra, E.J.Boekema, H.P.Braun. Structure of a mitochondrial supercomplex formed by respiratory-chain complexes I and III, *Proceedings of the National Academy of Sciences of the United States of America* 102 (2005) 3225-3229.
- [78] A.Videira. Complex I from the fungus *Neurospora crassa*, *Biochim.Biophys.Acta* 1364 (1998) 89-100.

- 
- [79] C.Brockmann, A.Diehl, K.Rehbein, H.Strauss, P.Schmieder, B.Korn, R.Kuhne, H.Oschkinat. The oxidized subunit B8 from human complex I adopts a thioredoxin fold, *Structure (Camb)* 12 (2004) 1645-1654.
- [80] N.Wiedemann, A.E.Frazier, N.Pfanner. The protein import machinery of mitochondria, *J.Biol.Chem.* 279 (2004) 14473-14476.
- [81] R.M.Chen, I.M.Fearnley, S.Y.Peak-Chew, J.E.Walker. The phosphorylation of Subunits of complex I from bovine heart mitochondria, *J.Biol.Chem.* 279 (2004) 26036-26045.
- [82] B.Schilling, R.Aggeler, B.Schulenberg, J.Murray, R.H.Row, R.A.Capaldi, B.W.Gibson. Mass spectrometric identification of a novel phosphorylation site in subunit NDUFA10 of bovine mitochondrial complex I, *FEBS Lett.* 579 (2005) 2485-2490.
- [83] T.Gabaldon, D.Rainey, M.A.Huynen. Tracing the evolution of a large protein complex in the eukaryotes, NADH : Ubiquinone oxidoreductase (Complex I), *J.Mol.Biol.* 348 (2005) 857-870.
- [84] I.M.Fearnley, J.Carroll, R.J.Shannon, M.J.Runswick, J.E.Walker, J.Hirst. GRIM-19, a cell death regulatory gene product, is a subunit of bovine mitochondrial NADH:ubiquinone oxidoreductase (complex I), *J Biol Chem* 276 (2001) 38345-38348.
- [85] J.E.Angell, D.J.Lindner, P.S.Shapiro, E.R.Hofmann, D.V.Kalvakolanu. Identification of GRIM-19, a novel cell death-regulatory gene induced by the interferon- $\beta$  and retinoic acid combination, using a genetic approach, *J.Biol.Chem.* 275 (2000) 33416-33426.
- [86] C.Lufei, J.Ma, G.Huang, T.Zhang, V.Novotny-Diermayr, C.T.Ong, X.Cao. GRIM-19, a death-regulatory gene product, suppresses Stat3 activity via functional interaction, *EMBO J.* 22 (2003) 1325-1335.
- [87] G.C.Huang, H.Lu, A.J.Hao, D.C.H.Ng, S.Ponniah, K.Guo, C.C.Lufei, Q.Zeng, X.M.Caoj. GRIM-19, a cell death regulatory protein, is essential for assembly and function of mitochondrial complex I, *Mol.Cell.Biol.* 24 (2004) 8447-8456.
- [88] A.N.Gubin, J.M.Njoroge, G.G.Bouffard, J.L.Miller. Gene expression in proliferating human erythroid cells, *Genomics* 59 (1999) 168-177.
- [89] J.Murray, S.W.Taylor, B.Zhang, S.S.Ghosh, R.A.Capaldi. Oxidative damage to mitochondrial complex I due to peroxynitrite - Identification of reactive tyrosines by mass spectrometry, *J.Biol.Chem.* 278 (2003) 37223-37230.
- [90] U.Schulte, V.Haupt, A.Abelmann, W.Fecke, B.Brors, T.Rasmussen, T.Friedrich, H.Weiss. A reductase/isomerase subunit of mitochondrial NADH:ubiquinone oxidoreductase (complex I) carries an NADPH and is involved in the biogenesis of the complex, *J.Mol.Biol.* 292 (1999) 569-580.
- [91] A. Abdrakhmanova, V. Zickermann, S. Kerscher, U. Brandt, NADPH binding to the accessory 39 kDA subunit of complex I from *Yarrowia lipolytica*. *Biochimica et Biophysica Acta - Bioenergetics* 1658, Supplement, 133. 2004. Abstract

- 
- [92] M.E.Baker, W.N.Grundy, C.P.Elkan. A common ancestor for a subunit in the mitochondrial proton-translocating NADH:ubiquinone oxidoreductase (complex I) and short-chain dehydrogenases/reductases, *Cell.Mol.Life Sci.* 55 (1999) 450-455.
- [93] A.Videira, M.Tropschüg, E.Wachter, H.Schneider, S.Werner. Molecular cloning of subunits of complex I from *Neurospora crassa*. primary structure and *in vitro* expression of a 22-kDa polypeptide., *J.Biol.Chem.* 265 (1990) 13060-13065.
- [94] P.Cardol, R.F.Matagne, C.Remacle. Impact of mutations affecting ND mitochondria-encoded Subunits on the activity and assembly of complex I in chlamydomonas. Implication for the structural organization of the enzyme, *J.Mol.Biol.* 319 (2002) 1211-1221.
- [95] M.Duarte, A.Videira. Respiratory chain complex I is essential for sexual development in neurospora and binding of iron sulfur clusters are required for enzyme assembly, *Genet.* 156 (2000) 607-615.
- [96] C.Ugalde, R.Vogel, R.Huijbens, L.Van den Heuvel, J.Smeitink, L.Nijtmans. Human mitochondrial complex I assembles through the combination of evolutionary conserved modules; a framework to interpret complex I deficiencies, *Hum.Mol.Genet.* 13 (2004) 659-667.
- [97] G.Tuschen, U.Sackmann, U.Nehls, H.Haiker, G.Buse, H.Weiss. Assembly of NADH:ubiquinone reductase (complex I) in *Neurospora* mitochondria. Independent pathways of nuclear-coded and mitochondrially encoded subunits, *J.Mol.Biol.* 213 (1990) 845-857.
- [98] R.Schneider, M.Massow, T.Lisowsky, H.Weiss. Different respiratory-defective phenotypes of *Neurospora crassa* and *Saccharomyces cerevisiae* after inactivation of the gene encoding the mitochondrial acyl carrier protein., *Curr.Genet.* 29 (1995) 10-17.
- [99] A.Videira, M.Duarte. On complex I and other NADH : Ubiquinone reductases of *Neurospora crassa* mitochondria, *J.Bioenerg.Biomembr.* 33 (2001) 197-203.
- [100] R.Küffner, A.Rohr, A.Schmiede, C.Krüll, U.Schulte. Involvement of Two Novel Chaperones in the Assembly of Mitochondrial NADH:Ubiquinone Oxidoreductase (Complex I), *J.Mol.Biol.* 283 (1998) 409-417.
- [101] R.Janssen, J.Smeitink, R.Smeets, L.Van den Heuvel. CIA30 complex I assembly factor: a candidate for human complex I deficiency?, *Hum.Genet.* 110 (2002) 264-270.
- [102] I.Bourges, C.Ramus, B.M.de Camaret, R.Beugnot, C.Remacle, P.Cardol, G.Hofhaus, J.P.Issartel. Structural organization of mitochondrial human complex I: role of the ND4 and ND5 mitochondria-encoded subunits and interaction with prohibitin, *Biochem.J.* 383 (2004) 491-499.

- 
- [103] U.Nehls, T.Friedrich, A.Schmiede, T.Ohnishi, H.Weiss. Characterization of Assembly Intermediates of NADH:Ubiquinone Oxidoreductase (Complex I) Accumulated in *Neurospora crassa* Mitochondria by Gene Disruption, *J.Mol.Biol.* 227 (1992) 1032-1042.
- [104] S.Scacco, V.Petruzzella, S.Budde, R.Vergari, R.Tamborra, D.Panelli, L.P.Van den Heuvel, J.A.Smeitink, S.Papa. Pathological mutations of the human NDUFS4 gene of the 18-kDa (AQDQ) subunit of complex I affect the expression of the protein and the assembly and function of the complex, *J.Biol.Chem.* 278 (2003) 44161-44167.
- [105] G.Barth, C.Gaillardin. *Yarrowia lipolytica*, in: K.Wolf (Ed.), *Non-conventional yeasts in biotechnology*, Springer, Berlin-Heidelberg, 1996, pp. 313-388.
- [106] G.Barth, C.Gaillardin. Physiology and genetics of the dimorphic fungus *Yarrowia lipolytica*, *FEMS Microbiol.Rev.* 19 (1997) 219-237.
- [107] S.de Vries, C.A.M.Marres. The mitochondrial respiratory chain of yeast. Structure and biosynthesis and the role in cellular metabolism, *Biochim.Biophys.Acta* 895 (1987) 205-239.
- [108] A.G.Rasmusson, V.Heiser, E.Zabaleta, A.Brennicke, L.Grohmann. Physiological, biochemical and molecular aspects of mitochondrial complex I in plants, *Biochim.Biophys.Acta* 1364 (1998) 101-111.
- [109] S.Kerscher, J.G.Okun, U.Brandt. A single external enzyme confers alternative NADH:ubiquinone oxidoreductase activity in *Yarrowia lipolytica*, *J.Cell Sci.* 112 (1999) 2347-2354.
- [110] N.Morgner, V.Zickermann, S.Kerscher, I.Wittig, A.Abdrakhmanova, H.D.Barth, B.Brutschy, U.Brandt. Subunit mass fingerprinting of mitochondrial complex I, *Biochimica et Biophysica Acta-Bioenergetics* 1777 (2008) 1384-1391.
- [111] S.Kerscher, N.Kashani-Poor, K.Zwicker, V.Zickermann, U.Brandt. Exploring the catalytic core of complex I by *Yarrowia lipolytica* yeast genetics, *J.Bioenerg.Biomembr.* 33 (2001) 187-196.
- [112] S.Rafi, P.Novichenok, S.Kolappan, X.Zhang, C.F.Stratton, R.Rawat, C.Kisker, C.Simmerling, P.J.Tonge. Structure of acyl carrier protein bound to FabI, the FASII enoyl reductase from *Escherichia coli.*, *J.Biol.Chem.* (2006).
- [113] A.K.Joshi, L.Zhang, V.S.Rangan, S.Smith. Cloning, expression and characterisation of a human 4'-phosphopantetheinyl transferase with broad substrate specificity, *J.Biol.Chem.* 278 (2003) 33142-33149.
- [114] G.Y.Xu, A.Tam, L.Lin, J.Hixon, C.C.Fritz, R.Powers. Solution structure of *B. subtilis* acyl carrier protein, *Structure* 9 (2001) 277-287.
- [115] K.H.Mayo, J.H.Prestegard. Structural characterisation of short-chainacylated acyl carrier proteins by NMR, *Biochem.* 24 (1985) 7838.

- 
- [116] A.Roujeinikova, C.Baldock, W.J.Simon, J.Gilroy, D.W.Rice, A.R.Slabas, J.B.Rafferty. X-ray crystallographic studies on butyryl-ACP reveal flexibility of the structure around a putative acyl chain binding site, *Structure* 10 (2002) 825-835.
- [117] M.A.Reed, M.Schweizer, A.E.Szafranska, C.Arthur, T.P.Nicholson, R.J.Cox, J.Crosby, M.P.Crump, T.J.Simpson. The type I rat fatty acid synthase ACP shows structural homology and analogous biochemical properties to type II ACPs, *Org Biomol Chem* 1 (2003) 463-471.
- [118] Y.M.Zhang, B.Wu, J.Zheng, C.O.Rock. Key residues responsible for acyl carrier protein and  $\beta$ -ketoacyl-acyl carrier protein reductase (FabG) interaction, *J.Biol.Chem.* 278 (2003) 52935-52943.
- [119] M.P.Crump, J.Crosby, C.E.Dempsey, J.A.Parkinson, M.Murray, D.A.Hopwood, T.J.Simpson. Solution structure of the actinorhodin polyketide synthase acyl carrier protein from *Streptomyces coelicolor* A3, *Biochem.* 36 (1997) 6000-6008.
- [120] Q.Li, C.Khosla, J.D.Puglisi, C.W.Liu. Solution structure and backbone dynamics of the holo form of the frenolicin acyl carrier protein, *Biochem.* 42 (2003) 4648-4657.
- [121] Y.M.Zhang, M.S.Rao, R.J.Heath, A.C.Price, A.J.Olson, C.O.Rock, S.W.White. Identification and analysis of the acyl carrier protein (ACP) docking site on beta-ketoacyl-ACP synthase III, *J Biol Chem* 276 (2001) 8231-8238.
- [122] A.D.Showalter, T.P.Smith, G.L.Bennett, K.W.Sloop, J.A.Whitsett, S.J.Rhodes. Differential conservation of transcriptional domains of mammalian Prophet of Pit-1 proteins revealed by structural studies of the bovine gene and comparative functional analysis of the protein, *Gene* 291 (2002) 211-221.
- [123] E.H.Meyer, J.L.Heazlewood, A.H.Millar. Mitochondrial acyl carrier proteins in *Arabidopsis thaliana* are predominantly soluble matrix proteins and none can be confirmed as subunits of respiratory Complex I, *Plant Mol.Biol.* DOI 10.1007/s11103-007-9156-9 (2007).
- [124] J.E.Cronan, I.M.Fearnley, J.E.Walker. Mammalian mitochondria contain a soluble acyl carrier protein, *FEBS Lett.* 579 (2005) 4892-4896.
- [125] G. Bunkoczi, A. Joshi, E. Papagrigoriu, C. Arrowsmith, A. Edwards, M. Sundstrom, J. Weigelt, F. Von Delf, S. Smith, U. Oppermann, Structure of aminoadipate-semialdehyde dehydrogenase-phosphopantetheinyl transferase in complex with cytosolic acyl carrier protein and CoA. 2006. Internet Communication
- [126] S.Smith, S.C.Tsai. The type I fatty acid and polyketide synthases: a tale of two megasynthases, *Nat Prod Rep.* 24 (2007) 1041-1072.
- [127] C.O.Rock, J.E.Cronan. *Escherichia coli* as a model for the regulation of dissociable (type II) fatty acid biosynthesis, *Biochim.Biophys.Acta* 1302 (1996) 1-16.



- 
- [128] S.W.White, J.Zheng, Y.M.Zhang, C.O.Rock. The structural biology of type II fatty acid biosynthesis, *Annu.Rev.Biochem.* 74 (2005) 791-831.
- [129] J.W.Campbell, J.E.Cronan. Bacterial fatty acid biosynthesis: targets for antibacterial drug discovery, *Annu Rev Microbiol.* 55 (2001) 305-332.
- [130] E.Schweizer, J.Hofmann. Microbial type I fatty acid synthases (FAS): major players in a network of cellular FAS systems, *MMBR* 68 (2004) 501-517.
- [131] S.Smith, A.Witkowski, A.K.Joshi. Structural and functional organisation of the animal fatty acid synthase, *Prog Lipid Res* 42 (2003) 289-317.
- [132] S.Jenni, M.Leibundgut, T.Maier, N.Ban. Architecture of a Fungal Fatty Acid Synthase at 5 Å Resolution, *Science* 311 (2006) 1263-1267.
- [133] T.Maier, S.Jenni, N.Ban. Architecture of Mammalian Fatty Acid Synthase at 4.5 Å Resolution, *Science* 311 (2006) 1258-1262.
- [134] S.Smith. The animal FAS: one gene, one polypeptide, seven enzymes., *FASEB J.* 8 (1994) 1248-1259.
- [135] S.L.Wang, X.Q.Liu. The plastid genome of *Cryptomonas phi* encodes an hsp70-like protein, a histone-like protein, and an acyl carrier protein, *Proc.Natl.Acad.Sci.USA* 88 (1991) 10783-10787.
- [136] M.Reith. A  $\beta$ -ketoacyl-ACP-synthase III gene (*fabH*) is encoded on the chloroplast genome of the red alga *Porphyra umbilicalis*, *Plant Mol.Bio.* 21 (2004) 185-189.
- [137] F.Fichtlscherer, C.Wellein, M.Mittag, E.Schweizer. A novel function of yeast fatty acid synthase. Subunit alpha is capable of self-pantetheinylation, *Eur J Biochem* 267 (2000) 2666-2671.
- [138] S.Jenni, M.Leibundgut, T.Maier, N.Ban. Architecture of a fungal fatty acid synthase at 5Å resolution, *Science* 311 (2006).
- [139] T.Maier, S.Jenni, N.Ban. Architecture of mammalian fatty acid synthase at 4.5 Å resolution., *Science* 311 (2006).
- [140] S.Jenni, M.Leibundgut, D.Boehringer, C.Frick, B.Mikolásek, N.Ban. Structure of fungal fatty acid synthase and implications for iterative substrate shuttling., *Science* 316 (2007).
- [141] D.A.Hopwood, D.H.Sherman. Molecular genetics of polyketides and its comparison to fatty acid biosynthesis, *Annual Review of Genetics* 24 (1990) 37-66.
- [142] B.Shen, R.G.Summers, H.Gramajo, M.J.Bibb, C.R.Hutchinson. Purification and characterisation of the acyl carrier protein of the *Streptomyces glaucescens* tetracenomycin C polyketide synthase, *J.Bacteriol.* (1992) 3818-3821.

- 
- [143] F.Lipmann. Bacterial production of antibiotic polypeptides by thiol-linked synthesis on protein templates, *Advances in Microbial Physiology* 21 (1980) 266.
- [144] I.Sanyal, S.L.Lee, D.H.Flint. Biosynthesis of pimeloyl-CoA, a biotin precursor in *Escherichia coli*, follows a modified fatty acid synthesis pathway: <sup>13</sup>C-labeling studies, *J.Am.Chem Soc.* (1994) 2637-2638.
- [145] H.Therisod, A.C.Weissborn, E.P.Kennedy. An essential function for acyl carrier protein is the biosynthesis of membrane-derived oligosaccharides of *Escherichia coli*, *Proc.Natl.Acad.Sci.USA* 83 (1986) 7236-7240.
- [146] M.Frentzen, E.Heinz, T.A.McKeon, P.K.Stumpf. Specificities and selectivities of glycerol-3-phosphate acyl transferase and monoacylglycerol-3-phosphate acyl transferase from pea and spinach chloroplasts, *Eur.J.Biochem.* (1983) 629-636.
- [147] J.P.Issartel, V.Koronakis, C.Hughes. Activation of *Escherichia coli* prohaemolysin to the mature toxin by acyl carrier protein-dependent fatty acylation, *Nature* 351 (1991) 759-761.
- [148] S.W.Jordan, J.E.Cronan. The acyl carrier protein of lipid synthesis donates lipoic acid to the pyruvate dehydrogenase complex in *Escherichia coli*, *J.Biol.Chem.* 272, No. 29 (1997) 17903-17906.
- [149] C.E.Barry, R.E.Lee, K.Mdluli, A.E.Sampson, B.G.Schroeder, R.A.Y.Y.Slayden. Mycolic acids: structure, biosynthesis and physiological functions, *Prog Lipid Res* 37 (1998) 143-179.
- [150] S.Brody, S.Mikolajczyk. *Neurospora* mitochondria contain an acyl-carrier protein, *Eur.J.Biochem.* 173 (1988) 353-359.
- [151] U.Sackmann, R.Zensen, D.Roehlen, U.Jahnke, H.Weiss. The acyl-carrier protein in *Neurospora crassa* mitochondria is a subunit of NADH: ubiquinone reductase (complex I), *Eur.J.Biochem.* 200 (1991) 463-469.
- [152] M.J.Runswick, I.M.Fearnley, J.M.Skehel, J.E.Walker. Presence of an acyl carrier protein in NADH:ubiquinone oxidoreductase from bovine heart mitochondria, *FEBS Lett.* 286 (1991) 121-124.
- [153] K.Shintani, J.B.Ohlogge. The characterization of a mitochondrial acyl carrier protein isoform isolated from *Arabidopsis thaliana*, *Plant Physiol.* 104 (1994) 1221-1229.
- [154] T.Abe, H.Hirota, C.Kurosaki, M.Yoshida, S.Yokohama. Solution structure of RSGI RUH-059, an ACP domain of acyl carrier protein, mitochondrial [precursor] from human cDNA, *Genomics/Proteomics Initiative (RSGI)* (2006).
- [155] A.K.Wernimont, A.Dong, C.Yang. Crystal structure of toxoplasma specific mitochondrial acyl carrier protein, *Structural Genomic Consortium* 59.m03510 (2008).

- 
- [156] J.L.Moreland, A.Gramada, O.V.Buzko, Q.Zhang, P.E.Bourne. The molecular biology toolkit (MBT): a modular platform for developing molecular visualization applications, *BMC Bioinformatics* 6 (2005).
- [157] X.Qiu, C.A.Janson. Structure of apo acyl carrier protein and a proposal to engineer protein crystallization through metal ions, *Acta Crystallogr.,Sect.D* 60 (2004) 1545-1554.
- [158] E.Potterton, S.McNicholas, E.Krissinel, K.Cowtan, M.Noble. The CCP4 molecular-graphics project 2, *Acta Crystallographica Section D-Biological Crystallography* 58 (2002) 1955-1957.
- [159] M.Focke, E.Gieringer, L.Jansch, S.Binder, H.S.Braun. Fatty Acid Biosynthesis in Mitochondria of Grasses: Malonyl-Coenzyme A Is Generated by a Mitochondrial-Localized Acetyl-Coenzyme A Carboxylase1, *Plant Physiol.* 133 (2003) 875-884.
- [160] J.K.Hiltunen, F.Okubo, V.A.S.Kursu, K.J.Autio, A.J.Kastaniotis. Mitochondrial fatty acid synthesis and maintenance of respiratory competent mitochondria in yeast , *Biochem.Soc.Trans.* 33 (2005).
- [161] R.Schneider, B.Brors, M.Massow, H.Weiss. Mitochondrial fatty acid synthesis: a relic of endosymbiotic origin and a specialized means for respiration, *FEBS Lett.* 407 (1997) 249-252.
- [162] V.Gueguen, D.Macherel, M.Jaquinod, R.Douce, J.Bourguignon. Fatty acid and lipoic acid biosynthesis in higher plant mitochondria, *J.Biol.Chem.* 275, No. 7 (2000) 5016-5025.
- [163] R.Yasuno, P.Wettstein-Knowles, H.Wada. Identification and molecular characterization of the -ketoacyl-[acyl carrier protein] synthase component of the *Arabidopsis* mitochondrial fatty acid synthase, *J.Biol.Chem.* 279, No.9 (2004) 8242-8251.
- [164] S.W.Jordan, J.E.Cronan. A new metabolic link. The acyl carrier protein of lipid synthesis donates lipoic acid to the pyruvate dehydrogenase complex in *Escherichia coli* and mitochondria, *J.Biol.Chem.* 272 (1997) 17903-17906.
- [165] H.Wada, D.Shintani, J.Ohlogge. Why do mitochondria synthesize fatty acids? Evidence for involvement in lipoic acid production, *Proc.Natl.Acad.Sci.USA* 94 (1997) 1591-1596.
- [166] S.Brody, C.Oh, U.Hoja, E.Schweizer. Mitochondrial acyl carrier protein is involved in lipoic acid synthesis in *Saccharomyces cerevisiae* , *FEBS Lett.* 408 (1997) 217-220.
- [167] R.N.Perham. Domains, motifs, and linkers in 2-oxo acid dehydrogenase multienzyme complexes: a paradigm in the design of a multifunctional protein., *Biochem.* 30 (1991) 8501-8512.
- [168] K.E.Reed, J.E.Cronan. Lipoic acid metabolism in *Escherichia coli*: sequencing and functional characterization of the *lipA* and *lipB* genes, *J.Microbiol* 175 (1993) 1325-1336.

- 
- [169] T.W.Morris, K.E.Reed, J.E.Cronan. Lipoic acid metabolism in *Escherichia coli*: the *lplA* and *lipB* genes define redundant pathways for ligation of lipoyl groups to apoprotein, *J.Microbiol.* 177 (1995) 1-10.
- [170] J.R.Miller, R.W.Busby, S.W.Jordan, J.Cheek, T.F.Henshaw, G.W.Ashley, J.B.Broderick, J.E.Cronan, M.A.Marletta. *Escherichia coli* LipA is a lipoyl synthase: in vitro biosynthesis of lipoylated pyruvate dehydrogenase complex from octanoyl-acyl carrier protein., *Biochem.* 49 (2000) 15166-15178.
- [171] K.J.Autio, A.J.Kastaniotis, H.Pospiech, I.J.Miinalainen, M.S.Schonauer, C.L.Dieckmann, J.K.Hiltunen. An ancient genetic link between vertebrate mitochondrial fatty acid synthesis and RNA processing, *FASEB J.* 22 (2008) 569-578.
- [172] M.S.Schonauer, A.J.Kastaniotis, J.K.Hiltunen, C.L.Dieckmann. Intersection of RNA processing and the type II fatty acid synthesis pathway in yeast mitochondria, *Mol Cell Biol.* 28 (2008) 6646-6657.
- [173] J.K.Hiltunen, M.S.Schonauer, J.A.Kaija, T.M.Mittelmeier, A.J.Kastaniotis, C.L.Dieckmann. Mitochondrial fatty acid synthesis type II: More than just fatty acids, *J.Biol.Chem.* 284 (2008) 9011-9015.
- [174] R.Zensen, H.Husmann, R.Schneider, T.Peine, H.Weiss. *De novo* synthesis and desaturation of fatty acids at the mitochondrial acyl carrier protein, a subunit of NADH:ubiquinone oxidoreductase in *Neurospora crassa*., *FEBS Lett.* 310 (1992) 179-181.
- [175] U.Schulte. Biogenesis of respiratory complex I, *J.Bioenerg.Biomembr.* 33 (2001) 205-212.
- [176] J.L.Stephens, S.H.Lee, K.S.Paul, P.T.Englund. Mitochondrial Fatty Acid Synthesis in *Trypanosoma brucei*, *J.Biol.Chem.* 282, NO. 7 (2007) 4427-4436.
- [177] D.Bordo, P.Bork. The rhodanese/Cdc25 phosphatase superfamily - Sequence-structure-function relations, *Embo Reports* 3 (2002) 741-746.
- [178] N.Nagahara, T.Ito, H.Kitamura, T.Nishino. Tissue and subcellular distribution of mercaptopyruvate sulfurtransferase in the rat: confocal laser fluorescence and immunoelectron microscopic studies combined with biochemical analysis, *Histochem.Cell.Biol.* 110 (1998) 243-250.
- [179] N.Nagahara, T.Nishino. Role of amino acid residues in the active site of rat liver mercaptopyruvate sulfurtransferase. cDNA cloning, overexpression, and site-directed mutagenesis, *J.Biol.Chem.* 271 (1996) 27395-27401.
- [180] J.H.Ploegman, G.Drent, K.H.Kalk, W.G.Hol. Structure of bovine liver rhodanese. I. Structure determination at 2.5 Å resolution and a comparison of the conformation and sequence of its two domains., *J.Mol.Biol.* 123 (1978) 557-594.

- 
- [181] D.Bordo, D.Deriu, R.Colnaghi, A.Carpen, S.Pagani, M.Bolognesi. The crystal structure of a sulfurtransferase from *Azotobacter vinelandii* highlights the evolutionary relationship between the rhodanese and phosphatase enzyme families, *J.Mol.Biol.* 298 (2000) 691-704.
- [182] W.K.Ray, G.Zeng, B.Potters, A.M.Mansuri, T.J.Larson. Characterization of a 12-kilodalton rhodanese encoded by *glpE* of *Escherichia coli* and its interaction with thioredoxin, *J.Bacteriol.* 182 (2000) 2277-2284.
- [183] A.Spallarossa, J.Donahue, T.J.Larson, M.Bolognesi, D.Bordo. *Escherichia coli* GlpE is a prototype sulfurtransferase for the single-domain rhodanese homology superfamily, *Structure* 9 (2001) 1117-1125.
- [184] M.G.Claros, P.Vincens. Computational method to predict mitochondrially imported proteins and their targeting sequences, *Eur.J.Biochem.* 241 (1996) 779-786.
- [185] P.J.Kraulis. MOLSCRIPT: a program to produce both detailed and schematic plots of protein structures, *J.Appl.Cryst.* 24 (1991) 946-950.
- [186] E.A.Merrit, M.E.P.Murphy. Raster3d, a program for photorealistic molecular graphics., *Acta Crystallographica Section D-Biological Crystallography* 50 (1994) 869-873.
- [187] B.Sorbo. Sulfite and complex-bound cyanide as sulfur acceptors for rhodanese, *Acta Chem.Scand.* 11 (1957) 628-633.
- [188] J.Westley. Mammalian cyanide detoxification with sulfane sulfur, *Ciba Foundation Symposia* 140 (1988) 201-218.
- [189] Y.Ogasawara, G.Lacourciere, T.C.Stadtman. Formation of a selenium-substituted rhodanese by reaction with selenite and glutathione: Possible role of a protein perselenide in a selenium delivery system, *Proceedings of the National Academy of Sciences of the United States of America* 98 (2001) 9494-9498.
- [190] P.M.Palenchar, C.J.Buck, H.Cheng, T.J.Larson, E.G.Mueller. Evidence that ThiI, an enzyme shared between thiamin and 4-thiouridine biosynthesis, may be a sulfurtransferase that proceeds through a persulfide intermediate, *J.Biol.Chem.* 275 (2000) 8283-8286.
- [191] K.Ogata, M.Volini. Mitochondrial Rhodanese - Membrane-Bound and Complexed Activity, *J.Biol.Chem.* 265 (1990) 8087-8093.
- [192] F.Bonomi, S.Pagani, P.Cerletti, C.Cannella. Rhodanese-Mediated Sulfur Transfer to Succinate-Dehydrogenase, *Eur.J.Biochem.* 72 (1977) 17-24.
- [193] S.Pagani, F.Bonomi, P.Cerletti. Enzymic synthesis of the iron-sulfur cluster of spinach ferredoxin, *Eur.J.Biochem.* 142 (1984) 361-366.
- [194] S.Pagani, Y.M.Galante. Interaction of rhodanese with mitochondrial NADH dehydrogenase, *Biochim.Biophys.Acta* 742 (1983) 278-284.

- 
- [195] K.Ogata, X.Dai, M.Volini. Bovine Mitochondrial Rhodanese Is A Phosphoprotein, *J.Biol.Chem.* 264 (1989) 2718-2725.
- [196] S.Kerscher, A.Eschemann, P.M.Okun, U.Brandt. External alternative NADH:ubiquinone oxidoreductase redirected to the internal face of the mitochondrial inner membrane rescues complex I deficiency in *Yarrowia lipolytica*, *J.Cell Sci.* 114 (2001) 3915-3921.
- [197] D.-C.Chen, J.-M.Beckerich, C.Gaillardin. One-step transformation of the dimorphic yeast *Yarrowia lipolytica*, *Appl.Biochem.Biotechnol.* 48 (1997) 232-235.
- [198] J.Sambrook, E.F.Fritsch, T.Manias. Molecular cloning. A Laboratory Manual, Cold Spring Harbor Laboratory Press, Cold Spring Harbor, NY, 1989.
- [199] Current protocols in molecular biology. Ausubel, F. M., Brent, R., Kingston, R. E., Moore, D. D., Seidman, J. G., Smith, J. A., and Struhl, K. 2000. New York. Ref Type: Serial (Book,Monograph)
- [200] C.Zhou, Y.Yang, A.Y.Jong. Mini-prep in ten minutes, *BioTechniques* 8 (1990) 172-173.
- [201] K.Zwicker, A.Galkin, S.Dröse, L.Grgic, S.Kerscher, U.Brandt. The redox-Bohr group associated with iron-sulfur cluster N2 of complex I, *J.Biol.Chem.* 281 (2006) 23013-23017.
- [202] O.H.Lowry, N.R.Rosebrough, A.L.Farr, R.J.Randall. Protein measurement with the folin phenol reagent, *J.Biol.Chem.* 193 (1951) 265-275.
- [203] A.Helenius, K.Simons. The binding of detergents to lipophilic and hydrophilic proteins, *J.Biol.Chem.* 247 (1972) 3656-3661.
- [204] H.Schägger. Tricine-SDS-PAGE, *Nat.Protoc.* 1 (2006) 16-22.
- [205] I.Rais, M.Karas, H.Schägger. Two-dimensional electrophoresis for the isolation of integral membrane proteins and mass spectrometric identification., *Proteomics* 4 (2004) 2567-2571.
- [206] H.Schägger. Blue Native Electrophoresis, in: C.Hunte, G.von Jagow, H.Schägger (Eds.), *Membrane Protein Purification and Crystallization: A Practical Guide*, Academic Press, San Diego, 2003, pp. 105-130.
- [207] V.D.Sled, A.D.Vinogradov. Reductive inactivation of the mitochondrial three subunit NADH dehydrogenase., *Biochim.Biophys.Acta* 1143 (1993) 199-203.
- [208] E.V.Gavrikova, V.G.Grivennikova, V.D.Sled, T.Ohnishi, A.D.Vinogradov. Kinetics of the mitochondrial three-subunit NADH dehydrogenase interaction with hexammineruthenium(III), *Biochim.Biophys.Acta* 1230 (1995) 23-30.
- [209] B.Sörbo. Rhodanese, *Methods Enzymol.* 2 (1955) 334-337.

- 
- [210] J.Westley. Thiosulfate: cyanide sulfurtransferase (rhodanese), *Methods Enzymol.* 77 (1981) 285-291.
- [211] N.Kashani-Poor, S.Kerscher, V.Zickermann, U.Brandt. Efficient large scale purification of his-tagged proton translocating NADH:ubiquinone oxidoreductase (complex I) from the strictly aerobic yeast *Yarrowia lipolytica*, *Biochim.Biophys.Acta* 1504 (2001) 363-370.
- [212] B.A.van Montfort, M.K.Doeven, B.Canas, L.M.Veenhoff, B.Poolman, G.T.Robillard. Combined in-gel tryptic digestion and CNBr cleavage for the generation of peptide maps of an integral membrane protein with MALDI-TOF mass spectrometry, *Biochimica et Biophysica Acta-Bioenergetics* 1555 (2002) 111-115.
- [213] A.Marchler-Bauer, J.B.Anderson, C.DeWeese-Scott, N.D.Fedorova, L.Y.Geer, S.He, D.I.Hurwitz, J.D.Jackson, A.R.Jacobs, C.J.Lanczycki, C.A.Liebert, C.Liu, T.Madej, G.H.Marchler, R.Mazumder, A.N.Nikolskaya, A.R.Panchenko, B.S.Rao, B.A.Shoemaker, V.Simonyan, J.S.Song, R.A.Thiessen, S.Vasudevan, Y.Wang, R.A.Yamashita, J.J.Yin, S.H.Bryant. CDD: a curated Entrez database of conserved domain alignments, *Nucleic Acids Res.* 31 (2003) 383-387.
- [214] E.G.Bligh, W.J.Dyer. A rapid method for total lipid extraction and purification., *Can.J.Biochem.Physiol.* 37 (1959) 911-917.
- [215] C.Meisinger, T.Sommer, Pfanner, N. Purification of *Saccharomyces cerevisiae* mitochondria devoid of microsomal and cytosolic contaminations , *Anal.Biochem* 287 (2000) 339-342.
- [216] J.Folch. A simple method for the isolation and purification of total lipids from animal tissues, *J Biol Chem.* 226 (1957) 497-509.
- [217] J.Becart, C.Chevalier, J.F.Biesse. Quantitative Analysis of Phospholipids by HPLC with a Light Scattering Evaporating Detector - Application to Raw Materials for Cosmetic Use, *Journal of High Resolution Chromatography* 13 (1990) 126-129.
- [218] R.Carrozzo, I.Wittig, F.M.Santorelli, E.Bertini, S.Hofmann, U.Brandt, H.Schägger. Subcomplexes of human ATP synthase mark mitochondrial biosynthesis disorders, *Ann.Neurol.* 59 (2006) 265-275.
- [219] E. Nübel, I. Wittig, S. Kerscher, U. Brandt, H. Schägger, Two-dimensional native electrophoretic analysis of respiratory supercomplexes from *Yarrowia lipolytica*. *Proteomics* 2009.  
Ref Type: In Press
- [220] K.Bych, S.Kerscher, D.J.Netz, A.J.Pierik, K.Zwicker, M.A.Huynen, R.Lill, U.Brandt, J.Balk. The iron-sulphur protein Ind1 is required for effective complex I assembly, *EMBO J.* 27 (2008) 1736-1746.

- 
- [221] N.Kashani-Poor, S.Kerscher, V.Zickermann, U.Brandt. Efficient large scale purification of his-tagged proton translocating NADH : ubiquinone oxidoreductase (complex I) from the strictly aerobic yeast *Yarrowia lipolytica*, *Biochimica et Biophysica Acta-Bioenergetics* 1504 (2001) 363-370.
- [222] J.G.Okun, V.Zickermann, K.Zwicker, H.Schägger, U.Brandt. Binding of detergents and inhibitors to bovine complex I - A novel purification procedure of bovine complex I retaining full inhibitor sensitivity, *Biochim.Biophys.Acta* 1459 (2000) 77-87.
- [223] N.Plesofsky, N.Gardner, A.Videira, R.Brambl. NADH dehydrogenase in *Neurospora crassa* contains myristic acid covalently linked to the ND5 subunit peptide, *Biochim.Biophys.Acta - Bioenerg.* 1495 (2000) 223-230.
- [224] R.M.Bennett-Lovsey, A.D.Herbert, M.J.E.Sternberg, L.A.Kelley. Exploring the extremes of sequence/structure space with ensemble fold recognition in the program Phyre, *Proteins-Structure Function and Bioinformatics* 70 (2008) 611-625.
- [225] J.E.Galagan, S.E.Calvo, K.A.Borkovich, E.U.Selker, N.D.Read, D.Jaffe, W.FitzHugh, L.J.Ma, S.Smirnov, S.Purcell, B.Rehman, T.Elkins, R.Engels, S.Wang, C.B.Nielsen, J.Butler, M.Endrizzi, D.Qui, P.Ianakiev, D.Bell-Pedersen, M.A.Nelson, M.Werner-Washburne, C.P.Selitrennikoff, J.A.Kinsey, E.L.Braun, A.Zelter, U.Schulte, G.O.Kothe, G.Jedd, W.Mewes, C.Staben, E.Marcotte, D.Greenberg, A.Roy, K.Foley, J.Naylor, N.Stange-Thomann, R.Barrett, S.Gnerre, M.Kamal, M.Kamvysselis, E.Mauceli, C.Bielke, S.Rudd, D.Frushman, S.Krystofova, C.Rasmussen, R.L.Metzenberg, D.D.Perkins, S.Kroken, C.Cogoni, G.Macino, D.Catcheside, W.Li, R.J.Pratt, S.A.Osmani, C.P.DeSouza, L.Glass, M.J.Orbach, J.A.Berglund, R.Voelker, O.Yarden, M.Plamann, S.Seiler, J.Dunlap, A.Radford, R.Aramayo, D.O.Natvig, L.A.Alex, G.Mannhaupt, D.J.Ebbole, M.Freitag, I.Paulsen, M.S.Sachs, E.S.Lander, C.Nusbaum, B.Birren. The genome sequence of the filamentous fungus *Neurospora crassa*, *Nature* 422 (2003) 859-868.
- [226] A.Abdrakhmanova, K.Zwicker, S.Kerscher, V.Zickermann, U.Brandt. Tight binding of NADPH to the 39-kDa subunit of complex I is not required for catalytic activity but stabilizes the multiprotein complex, *Biochim.Biophys.Acta* 1757 (2006) 1676-1682.
- [227] A. Abdrakhmanova, Accessory subunits of complex I from *Y. lipolytica*. 2005. Goethe-Universität, Frankfurt am Main, Germany Thesis/Dissertation
- [228] A.K.Panigrahi, A.Zikova, R.A.Dalley, A.Acestor, Y.Ogata, A.Anupama, P.J.Myler, K.D.Stuart. Mitochondrial complexes in *Trypanosoma brucei*. A novel and a unique oxidoreductase complex, *Molecular and cellular proteomics* 7 (2008) 534-545.
- [229] M.Cianci, F.Gliubich, G.Zanotti, R.Berni. Specific interaction of lipoate at the active site of rhodanese, *BBA - Protein Structure and Molecular Enzymology* 1481 (2000) 103-108.
- [230] A.A.Herbert, J.R.Guest. Lipoic Acid Content of *Escherichia coli* and Other Microorganisms, *Arch.Microbiol.* 106 (1975) 259-266.



## 9 APPENDIX

### 9.1 Gene maps

The names and direction of primers used are marked in blue; sequences of the primers are highlighted in yellow. The capital letters in the primer sequence denote unchanged nucleotides; small letters represent mutated nucleotides. The translated exons are shown in green capital letters below the genomic sequence.

#### 9.1.1 The *st1* gene encoding the rhodanese, locus CAG78604, ACC No. YALI0F23551g, ID 2908766

```

                                stickf ▶
                                G GCAATCGAGG CGATATATG
1  gggttggact ctaagagaat gatatggagg gcaatcgagg cgatatatga gagggaatac ttttgtgtgt atgaaaggac catgataata aaatttatca
   cccaacctga gattctctta ctatacctcc cgtttagctcc gctatatact ctcccttatg aaaacacaca tacttttcctg gtactattat tttaaatagt

                                stickf ▶
                                CGA CGATACCGAT GCTAGAG
101 ggtgtggagt ggcgctgcga cgataccgat gctagagatc cgtttgttta gccctcaaga taccacattt acgtttataa gcataatcaa cgaatgctca
   ccacacctca ccgcgacgct gctatggcta cgatctctag gcaacaacaa cggggagtct atagtgtaaa tgcaaatatt cgtattagtt gcttacgagt

201 atgcacgctc aagtaaggga tggatagtag agtattaagc atgattgttt tatgtccggg gagtcgtcca tatcgggtct cgaccgactc tccgcgcttc
   tacgtgcgag ttcattccctt acctateatc tcataatctg tactaacaana atacaggccc ctccagcagg atagcccaga gctggctgag agggcgcaag

301 ggatttggct tctttcaggg ctatgagggt tttcggctga acagtagagc caatggcagg taggaggggg atctgaattt gatatgtaag cgacatgtgt
   cctaaaccga agaaagtccc gatactccaa aaagccgact tgtcatctcg gttaccgtcc atccctcccc tagactataa ctatacttc gctgtacaca

401 caatgcattt tccgggtaaa tgtattaatt cagcatatct caggagcgaa atgaaagggt ttgtgtgtga tttcatagcc tccaactact tctacaggca
   gttacgtaaa agggccattt acataaataa gtcgtataga gtcctcgctt tactttccca aacacacact aaagtatcgg aggttgatga agatgtccgt

501 tatattgaac ttctacgaat cacagcgcac tgagtcggct tatatagact cgagatgatt agcatgtgcc aagaggaagt agctgcagta gctcacacac
   atataacttg aagatgctta gtgtcgcgta actcagccga atatatctga gctctactaa tcgtacacgg ttctccttca tcgacgtcat cgagtgtgtg

601 ttgcacactg tttatgagag gtgaaccgggt cattaaaagt ccgatcgcct gtgttagatc tcggatctgt caaatatgca gtcttattat tcatatatcg
   aacgtgtgac aaatactctc cacttgccca gtaattttca ggtagcggaa cacaactctag agcctagaca gtttatacgt cagaataata agtatatagc

                                sliseq1 ▶
                                CACTTCGC TGACTCAGAA TG
701 gtgatatacc cgactgtaat caccttacta atcacttcgc tgactcagaa tgcacgttta agttgttgaa agacacgtgt ctccatctgt ctgcaatgac
   cactatattg gctgacatta gtggaatgat tagtgaagcg actgagctct acgtgcaaat tcaacaactt tctgtgcaca gaggtagaca gagcttactg

801 ctttgcgaaa gtgcgaaccca cgagatcacc gcttctacat tgtgtactca cccattgaga tgggtgtgtg ccgataatgc gtagggactg ctgacctgac
   gaaacgcttt cagcttgggt gctctagtag cgaagatgta acacatgatt gggtaactct acccaacgac ggctattacg catacctgac cgaggactcg

901 ggggttgcta gagaacagcg tgtcgttcaa actacagcaa ttggagcaat atccacaaa aaaactgttt catatcaaaa taaaatcgc ttagtctaac
   ccccaacgat ctcttctgac acagcaagtt tgatgtcgtt aacctcgtta taagtgggtt tttgacaaa gtatagtttt attttatgac aatcagtatg

1001 agacagatcc cccgccaatc aaacttgctc aaactcatat tttccctcgc tctcattggt ttcacttgtt tcgtttaagc tccacagaca tacttttagt
   tctgtcctaa gggcggttag ttgaaacaag ttgagtata aaagggagcg agagtaacca aagtgaacaa agcaaatctg aggtgtctgt atgaaataca

                                slisall
                                CG TCCTAGTAGT AGCAGcagct ga a
1101 tgcatagggc gtcccacaac acttcacagc aggatcatca tcgtcatctt tacaccttga tattgggtcaa ttgatacact acaggacaca aaaacacaac
   acgtatcccc cagggttgggt tgaagtgtcg tcttagtagt agcagtagaa atgtggaact ataaccagtt aactatgtga tgcctctgtg ttttgtgttg

                                sliseq2 ▶
                                AG ATCTTCGATG CTACCTGG
1201 atgtcgaaac tcatttcccc tgcgcaattg gccaaagcgc tttcttccaa ggaacaacaag atcttcgatg ctacctggta tcttcccacc cctgcccaacg
   tacagctttg agtaaaaggg acggcttaac cggttcgcgtg aaagaaggtt cctttgggtc tagaagctac gatggacct agagggttg gggaggttca aggggttgc
   >>.....st1.....>>
   M S K L I S P A E L A K R L S S K E T K I F D A T W Y L P T P A N

1301 ttggtaagaa cgcttacgac aattacatga agaagcggat tcccggcgct ctctactttg acatcgatgc cgtaacacc cctccaagt tccccacat
   aaccattctt gcgaatgctg ttaatgtact tcttcgcta agggccgcca gagatgaaac tgtagctacg gcagttgtgg gggaggttca aggggttga
   >.....st1.....>
   V G K N A Y D N Y M K K R I P G A L Y F D I D A V N T P S K F P H

```

```

                                                                    ◀ st1seq4
GAAGAGGCCT
1401 gcttccctct cctcagacct ttgaaaacga gctcacgaag ctgggtgttt cctctgactc tcccactgtg gtctacgaca cacaaggcgt cttctccgga
cgaagggaga ggagctctga aacttttctc cgagtgcttc gaccacaaa ggagactgag agggtagcac cagatgctgt gtgttccgca gaagaggcct
>.....st1.....>
M L P S P Q T F E N E L T K L G V S S D S P I V V Y D T Q G V F S G

st1seq4
GGAGCTGAAC
1501 cctcgacttg tgtggacctt taaggtcttt ggccatgaca acgtccagtt cctcaatggc tttgaggctt acaccagct ccttggtatc cccagcagac
ggagctgaac acacctggaa attccagaaa ccggtactgt tgcaggtaaa ggagttaccg aaactccgaa tgtgggtcga gggaccatag ggtctgtctg
>.....st1.....>
P R L V W T F K V F G H D N V Q F L N G F E A Y T Q L P G I P S R

1601 cggatgccta cacctggggc atctgggaca cacaagtcc tggtaaagtc gatcccgcgc atcctccta caaggtgacc aaggcccgc cagactggtt
gcctacggat gtggaccccg tagaccctgt gtgttcaagg accattctag ctaggccgcg taggaggat gttccactgg ttccggctg ggctcgacca
>.....st1.....>
P D A Y T W G I W D T Q V P G K I D P A D P P Y K V T K A R P E L

                                                                    ▶ st1seq3
GAG GTCACCTTCA TTGATGC
1701 caagtccttt gaagacgtgc tggccactgt cgagaaacac aacggtgacg gagccaagt tcgaaacgag gtcaccttca ttgatgcccg acccaacgga
gttcaggaaa cttctgcacg accggtagca gctctttgtg ttgccactgc ctccggttcta agctttgctc cagtggaggt aactacgggc tgggttgctt
>.....st1.....>
V K S F E D V L A I V E K H N G D G A K I R N E V T F I D A R P N G

1801 cgattcacag gcaaggacgc tgaacctcga gccgagctgt cctcgggcca tgttcccgga gcttactcca tgccttccc cgagggtggtc gagaatggaa
gctaagtgtc cgttctcgcg acttggagct cggctcgaca ggagcccgtt acaagggcct cgaatgaggt agcgggaagg gctccaccag ctcttacctt
>.....st1.....>
R F T G K D A E P R A E L S S G H V P G A Y S I A F P E V V E N G

                                                                    ◀ st1seq5
TACACA CCTAGGCCAC AGTG
1901 aattcaaatc tctgaggag ctcaaggctc tgtttgcttc caagggcatt gatggctcta agcccacat ctccatgtgt ggatccgggtg tcactgctct
ttaagtttag aggactcctc gagttccgag aaaaacgaag gttcccgtaa ctaccgagat tcgggtagta gaggtacaca ctagggccac agtgacggac
>.....st1.....>
K F K S P E E L K A L F A S K G I D G S K P I I S M C G S G V T A

2001 tgtcattgac ctggctctgg agattgccgg cattggttct cgagacacca atgctgtcta cgatggatct tggaccgagt gggcccagcg agctcccaca
acagtaactg gaccgagacc tctaacggcc gtaaccaaga gctctgtggt tacgacagat gctacctaga acctggctca cccgggtcgc tcgagggtgt
>.....st1.....>
C V I D L A L E I A G I G S R D T N A V Y D G S W T E W A Q R A P T

                                                                    ◀ st1repIIr
CTTG CTCGGTTGG CCCGAAccag agtagga
                                                                    st1repIIr ▶
caatttg aaaaaTAGAT AGAATCATACTGTAG
stIBamHI ▶
GGAGGA tccCTTGAAC GAGGCCAACC
2101 aagtacattg tcaaggagga gaacttgaac gaggccaacc gggcttagat agaatcatac tgtagatcaa tgaaacatg aaattagaca aagggaggga
ttcatgtaac agttcctcct ctggaacttg ctccggttgg cccgaateta tcttagtatg acatctagtt accttggtag ttaatatctg ttccctcctc
>.....st1.....>
K Y I V K E E N L N E A N R A -

```

```

2201 ggaaaagtt taagtgggat aatttgtgca aatctgttac atttgagtgt accccgtact tcttgtacgc agaagaatat atagaatacc ggtatatatg
    ccttttcaaa attcacccta ttaaacacgt ttagacaatg taaactcaca tggggcatga agaacatgcg tcttcttata tatcttatgg ccatatatac

                                     ◀ st1seq6
                                     TGAACGTC TCTCTAGGAA GG
2301 tttagtatgt aaatcgccact aatagtacaa tgtttcagcc caggtctact atacttgcag agagatcctt ccgctcatgg ggccttgttt aagacttcct
    aaatcataca tttagcgtga ttatcatggt acaaagtcgg gtgcagatga tatgaacgtc tctctagtaa ggcgagtacc ccgggacaaa ttctgaagga

2401 tgctaggcac gattagaata caagaaattg tataccacct ccaatatttc attctctgtt aagataactg tttccactta cccttttaca acagctacag
    acgatccgtg ctaatcttat gttctttaac atatgtggca ggttataaag taagagacaa ttctatgac aaagtggaat gggaaaatgt tgtcgatgtc

2501 tacccttctc atcttaaata atcatgtgag agataaatc acattcgcag aagtgttttg tgaaccaggg ttcaagaacg agtatcttgc gcttttttag
    atgggaagga tagaatttat tagtacactc tctattatag tgtaagcgtc ttcacaaaca actttgggtcc aagtcttctg tcatagaacg cgaaaacatc

2601 tattcaatca tattaatgt agttttgttg gccaatatgg attatatac acagtgaaga gtctctgact taaaaagcac acccagttct acatttcgcc
    ataagttagt ataatttaca tcaaaaacac cggttatacc taatataag tgtcacttct cagagactga attttctgtg tgggtcaaga tgtaaagcgc

                                     ◀ st1r
                                     GACATCTCC
2701 tctacagtaa atcttggaga acaacaacat gcctctgtga ttaagcaact tgaccagtga agatgaatat ctaattacag tatatcagtt gctgtagagg
    agatgtcatt tagaacctct tgttgttgta cggagacact aattcgttga actggctact tctacttata gattaatgtc atatagtcaa cgacatctcc

                                     ◀ st1ckr
                                     GTGAC CAGCGTACCA GTATT
                                     st1r
ACGGACACTT
2801 tgccctgtgaa acaggagtac ttgtactgtg tagtgtaaag tattgcaact gtcgcatggt cataaattct atatacagtt ttcggacctc tacctcgtca
    acggacactt tgtcctcatg aacatgacac atcacatttc ataactgtac cagcgtacca gtatttaaga tatatgtgca aagcctggag atggagcgtat

2901 gcagcatgct gaatatccac tcttcttaac atcgccttgc tccaaattca gctgctgagc tcctccagta gtcggtgac gaactccata tctcttatca
    cgtcgtacga cttataggtg agaagaattg tagcgggaagc aggtttaagt cgacgactcg aggaggtcat cagcaactg cttgaggtat agagaatagt

3001 ttgatattgg tcttgccagt cttgatattg gactggatct tctgagccac ccgctgatac gcctctagta cctggctctc tgtcttggct gacgtttcaa
    aactataacc agaacggtca gaactataac ctcacctaga agactcggtg ggcgactatg cggagatcat ggaccagagg acagaaccga ctgcaaaagt

3101 tgaacccggc tagaccattt tcatctgccc attttcgggc ttcctcagcc tccacctgac gcgctccaac gtcggtcttg ttgccacca gcatgatgat
    acttgggccc atctggtaaa agtagacggg taaaagcccc aaggagtcgg aggtggactg cgcgaggttg caggcagaac aacgggttgg cgtactacta

3201 gatatcttgc tcagcctgat ccgcaactc ccccagccac atttgcactg tggcaaacgt cttggggcgc gtgatatcgt agaccagcaa gcagcccgca
    ctatagaagc agtcggacta gggcgttgag ggggtcggtg taaacgtgca accgtttgca gaaccccgcg cactatagca tctgggtcgt cgtcgggcgt

3301 gcggttcgga aatcagaccg ggtcacggcc cgaaaatgct cctgccc
    cgcaacgct ttatgctggc ccagtgccgg gcttttacga ggacggg

```

**Figure 9.1** The fragment of *stI* gene encoding rhodanese

Primers for generation of the *stI* deletion strain, *stI*-strepII tagged version, *Bam*HI and *Sal*I enzyme cleavage sites, PCR check primers and sequencing primers are shown.

## 9.1.2 The ACPM1 gene, locus CAG81024.1, ACC. No. YALI0D14850g, ID 2911329.

```

1 caacaggagc gggacctcac cgcacgactc cgtcaggagc aggaggagc ctacgagcga tcgctcgccc aggatcgagc ccgagaccaa caacgagccc
                                     acpm1chkf ▶
                                     AAGCCGAG CGACACAAGG AG
101 gggaaacggga ggcagtgccc gaagccgaac gtgcggcagc cgaagccgag cgacacaagg agctccagc ccaaaaaact cagcagtgga tcaaatggcc
                                     acpm1f ▶
                                     TA CTCGGCTGAA CTGCAAG
201 ggctggaaa atcaaggaga agaaggaaga tgatgcctcc acccctactg cccgagtggtg tttctgtgtg ccttccggta ctgggctgaa ctgcaagtcc
301 cccgcctatt cgactctgga ggcactctac gcctatgtgg agtgtcacga cgtgttgaac ggcgatgacg acttttcgga cgtggagaaa cccgaagact
401 acgacatga gtactccttt gagctggttt caccatgccc ccgaaagtg atcaagccgg tgacggatgt gactgttcag gaggagcctg ccatttgccc
501 caacggagca ttgaacgtgg aggtggttga cgaggaagag gactaagaga cagcaacatc caatactttg aagaagctga caatctagt tactgtacct
601 gatgtgtctc aaagtgcgaa gtacatcttt ggggtgtccc gtggcaggag ctcacgggtgc tcttcgctaa caggtacatg tgtgtatag cgcagtcgcg
701 tattgtatcg taaagtactt tcaaatatta aagactgtat atataatgaa gtatacggca gttcttgcaa ggtgtgtagt ggcattcaag cgttgactct
801 aagttgaatc tctcaagcat tgttgcgggt tcaagttttt gtctttggac gtcacgtttg tagaaatggc atcgaacaat cattctaagt tgctttgagg
901 tgtctagaat ggcaatattt gagaaaagtc atgatttttg ttgtttttt atcgcggaag tttcgatttt ttacatcatg tataagccca aaaaactcaa
                                     ◀ acpm1sall
                                     CAA GCTTAGGACA
                                     acpm1seq1 ▶
                                     GTTAGCT GTCAGGCAGT GG
1001 aaaatatctt ccgtcccggg ggcagagtg ttaaggcgtt gccctgctaa tttgttagct gtcaggcagt gggttttgcc cgcgcaggtt cgaatcctgt
                                     acpm1sall
                                     GGCACaGCTg a a
1101 ccgtgacgat tttttgctgg atttcgggat ttaagcttc cctacttgag ggttaccggg ccgaacactt ccaacaattt gcctttacca atgaaagttg
1201 acaatattac acacttgtaa ggaacacaac cccacacagt acctgacaat gcttcgaaac gtttcccgac tcgctctgcg atccaacttt gcccgacagg
                                     >>.....Exon1.....>>
                                     M L R N V S R L A L R S N F A R Q
                                     ◀ acpm1_1-2r1
                                     GCT ACGGCTCTTC GCTTA
                                     acpm1_2-1f1 ▶
                                     CGAATTGCTG CTGTTCTCG
1301 ccaccatggg ccagcgatc tactcggctg ctcgaccgga tgcgagagaag cgaattgctg ctgttctcga gtcttttgac aagtgagtt ttgaccaaga
                                     >.....Exon1.....>>
                                     A T M G Q R F Y S V A R P D A E K R I A A V L E S F D K
1401 caagctggat gaggatgatt cagagagaga ggcacattga ggatgtcgca gtgatagcga tgaacgaatg gacttgtgat tgagagcaat cagcacagag
                                     acpm1seq2
                                     GATCCACAG
1501 aagacctccg gccgtgtggt ttggttgagg ggcggtatca ttaactggtat gtctgaatgt ctgaagaagg caccactttc cgateccacag
                                     ◀ acpm1seq3
                                     CGTAAGTGGA CACCGTAAG
                                     acpm1seq2 ▶
                                     ACGCACAAATG
1601 acgcacaatg tetctgccat ctatccacgc aggtcgatgt cgggtgcttt gtcgctgttg agctctcatt gcattcacct ttggcattca atagcactga
1701 ggggtctttg ccaccacagc tgccaccacac cgtgccaccc accgtgccac ccacaaagtt atgttactgt cgtttgctca gatcaaacgg gtgtacagct

```

```

acpm1S66AF
g c C T TAGACACCGT

acpm1S66Ar
GGT T CCTGGAGTTG GAGCTG

acpm1_1-2r2
GTTGGGGCG ACGGTAGTGG

acpm1_2-1f2
CATCACC CCCACCGCTT CC

1801 cccccagct teacctacta acctagatct ccaaccccg cgcctcacc cccaccgctt ccttcgcaa ggacctcaac ctgcacagct tagacaccgt
>>.....Exon2.....>>
I S N P A A I T P T A S F A K D L N L D S L D T

acpm1_1-2r3
CTCAA GCCGTAGCTC TAG

acpm1_2-1f3
GAG ATCCCCGACA AGGAG

acpm1S66AF
CGAGGTTG

1901 cgaggttgtt gttgccatcg aggaggagt cggcatcag atccccgaca aggaggctga cgagatcaag tctgtcaacc aggccctcga gtacattctc
>.....Exon2.....>
V E V V V A I E E E F G I E I P D K E A D E I K S V N Q A V E Y I L

acpm1BamHI
atgga tccAGCGTTA AGGCCACAG

acpm1strepIIr
GGTCGGGC TACGATTTAc cagagtagga

acpm1strepIIF
caat ttgaaAAATA AGCAAGCTGT ATATAATAG

2001 gccccagccg atgctaaata agcaagctgt atataataga ttgagcgta aggccacaga ttggtgtagt agtttgtaac cgtgtttcac tgcacagagct
>.....Exon2.....>
A Q P D A K -

acpm1seq4
GAAC CTCGAGATCC ATCCG

2101 gaagtggagc cttgataga agctgtcagt acctgtcag accgacatgt gggagctcta ggagcccttg gagctctagg taggccccca aggtggctgt
2201 acggcggcac ggatacaata ctaaaagtag acgcccgtctc tatacggact gcagagatga ataactcttg ctgcacatag taccaccggg gccaaaggctg
2301 gtgcatttct ggtctcgcta aactgtccgt tttctgcctt atcagcaccg cctccagctg tcagatcaga agggccgtat cggaagatgt cacgcttgcc
2401 ctacctgaca ccccagggcc atggggggag tgctcgcgag catctgggtt ccagggggca acaaaaaaca aaacaaaaa acatgttctgg aaacttggag
2501 gaagtcgatt cccgaaagcc gatccccaca gcgctctgtc tcaggagaca gtcaagcggg caacttgaaa catgcaccgg gcaactgttc acaatgtgct
2601 atacgagggc ggccgaaacg agcgtcaggt gaactcagg cggactcagg ggtgcatggt gtcagagaaa aaagtacgga taaaagcaat tctgaaactc
2701 gagatctttt cctccacacc ccagttggtt ggtctctgct tcttgacaaa gggggggtca gaggcgtatg aagagaagga atcaggccat ggcggaacgg
2801 tttcagtttg ggggtagttc acgtcaaac atcacctccc caacaaacag ttttctact tgtagacgat acaccggact tatactctgt gtaccaagtc

acpm1chr
GAG

acpm1r
G CAACACTTCG GCACTCTA

2901 cggagttata acaaaacag gtttggcgga gaaggggtgc tttccgtgga gatatcagac gttgtgaagc cgtgagataa gtgatagtta tctttatctc

acpm1chr
AGACCGACAC TGACCGA

3001 tctggctgtg actggctgtg ttgcaatgga gattcacaag acgattcgac gccttgtaga cattgtgtaa gacgagggtt tcttcaggct actgctgtac
3101 agtacatgct tgcagctctc cgtccactaa tagcatgtct aatagtttta gtaccagttc caccatcacc aacagttaac tagagccctt ctgggtctag
3201 tgcccgtgcy agtetcaagt tggaccacg aatgtctcat gttcagctct catggtcggg ttaggaaagc agacgttggg ctgaaacggc aaagcgaag

```

**Figure 9.2** The ACPM1 gene used for generating the mutants

Primers for generation of the ACPM1 deletion strain, ACPM1-strepII tagged version, for the swap strategy, for generation of *Bam*HI and *Sal*I enzyme cleavage sites, PCR check primers and sequencing primers are shown.

### 9.1.3 The ACPM2 gene, locus CAG81441.2, fusion of loci YALI0D24629g and YALI0D24643g, ACC. No. YALI0D24629g, ID 2910510.

```

acpm2f ▶
CACGCACCAG TTACTCTGTC
1 cacgcaccag ttactctgtc cattaaaca actcttagta gacaatacat agtattgggc cgggtgtgag aaggacgtca catttgacaa gccggtaatg
101 ggcgtttttg tgttgggga agacaattgt gcaactcaca tgcaagactc tgtactttga ggaaccagta gtccgcaggt ctcctcatct ctccgggtgt
201 tcctctctgc gtgtggacca gggctctcct tccagccta gctcgggagt cctgaggtaa ttcttttcag ggcaatccat gacgactggt atcggcgaca
301 ggaggagtta ggttggcggg gcctggagat gtccacacta gactggggcg gctccttctc cagcgggtcca actcagcgag gcttccatca tctctcatt
401 tggcggtttt tgggtctctc accatcagcg gtaactgttg acaatgtctc aatcttacta tgtgggtcat tgggtgtatc aatcaaacat caatcaaaaa

acpm2fnew ▶
GTA CAGAAGTGTC GGCGCAG
501 agtaatctgt acagtatgta ctgtacagta cagaagtgtc ggcgcagatt tcggcaaatg tgctggttgc tttcaattaa aatgatgaaa tgaatgtgag
601 agaagcgaac aacgggttca gttgtcggcg tagatcagcc acttggtcag tgtaacagcg gcgagagact cttacggcga ctgtacctgg attggtgaca
701 agaagcagag gaacgaagat aactaaaggt aaatgaggat gataagacca agtattgtaa gtgcttgaga ctcacttata tactttggct ttcgtgtctg
801 tgtaacatgt ggactatggt tggccatgca agtgattaga agtgaagatc tgtagcaatc agcttgagta aaaagtgagc attactttga tctgcagttt
901 aaagtattcc aaaattcaag aaatttattt ggaatgtcaa tcagctcaaa atcgggtcatt ataagatctc caacggcgtc agggccgagg tcacaataaa

acpm2seq1 ▶
CTGAGCA ATATCTCCGC ACC
1001 acatctgggt atattttatt ccaccaagtc tcccgaatcc aatgatacca accacttccc gaactgagca atatctccgc acctttgctc tcgtcccaaa

acpm2Sall
GGTG TGGTAGGAGG TGTGACagct gaa
1101 acctctcaca gttagtaac acaattaaag ttaacctccc caaccagtaa aaagacggca atatatcccac accatcctcc acactacaca tttctggaaa
1201 atgtcccagc agtccgttct ccgtctttct cgagccggcg ttgccgggcc cgtctgtctg cgatcgttcg tgaccgccgt cgcccgacc cagctcgtgc
>>.....Exon1.....>
M L R Q S V L R L S R A A V A R P A L S R S F V T A V A R P Q L V

acpm2_2-1r1
GT ACTAAGTCCT CGCTTA
acpm2_1-2f1 ▶
GAATCGTG GCTCTTCTGG
1301 gagcggcccc cgtgtcgttc atccgacact actcctcgcc ccacgtgctg accaaggaca tgattcagga gcgaatcgtg gctctctcgg agtcggttga
>.....Exon1.....>
R A A P V S F I R H Y S S A H V L T K D M I Q E R I V A L L E S F

acpm2S88Af ▶
gcTTTG GATGTCGTCG AGGTG
acpm2S88Ar
GAAGGC TGGAAACCAGA CCTG
acpm2_2-1r2
CTGCGGTTCT TGTAGTGG
1401 caaggtcaat gacgccaaga acatcaccgc caccgccaac ctgacttccg accttggctc ggacagtttg gatgtcgtcg aggtggtcat ggccattgag
>.....Exon1.....>
D K V N D A K N I T A T A N L T S D L G L D S L D V V E V V M A I E

acpm2seq2 ▶
GTA CTAGTGACTG ACCGAAG
1501 gaggtgagta ctagtgactg accgaagatc aggttcggac cctgacgcgg ccaactgtcgc tgtccggttg gaaacagact gcatatgtga cctgaatcgt
>>> Exon1
E
1601 ggcagaatat cgcggcagaa tatcgtggca gaatctcgtg attgtatcta tacagtttac gatgggctgc atcagataga ctgcccgac ctaagctgta
1701 ccgccacgtc tgatcagatg aggtatgagc tcaggttggg agtagatgac agttggtgag gaccgcgtgg tgccctgatg gagtacctga atgactcaag
1801 gacagacaga cccactgaaa ctaatttttc tgcttgaagt cagcacttga tcgaccactc gactctttag cagctcttcc tgccctacct ttatgtctca
1901 aaacgtggga agtagctctg gcgatcattt caccagttgc aattgtgcgt cccatgcttt cagacaacgc attactctac tgtttcttca aacattctac

```

```

                                acpm2seq3 ▶
                                GAGTCTGCAT ACAGTCTGAG
2001 agtctatcaa actgtctgct acagttgctc tggtaacata gagtctgcat acagttgag ccatgtttaa ttaccaagct gttccgctc gacctatgag
2101 tgagcaccca gttcggctta ccgccgactt gctgcatcct tagcgtctta ctaaccagg aatttggcct cgagatcccc gaccacgatg ctgacgagat
                                >>.....Exon2.....>
                                E F G L E I P D H D A D E
2201 caagaccgtc cagcaggcca ttgactacgt ctctgccag cccgcagggt agtatgagag atataagaat cattgggaag acgccatgag gtgcagtcac
>.....Exon2.....>
I K T V Q Q A I D Y V S A Q P A
2301 acgaaaaaga cgcgataaca gcatgagaag atagcgtaaa caccacgaca ggacaagaac cgataacaca tggcccagct tgacacagct tgaccagcgc
2401 taacctctca caccatgaca ctggcaagat tcacgggtgt tgggggatgg cagtacgga aagggcgaca caagttagtg atgtgctatt tttctggtag
2501 aagatagctt tatcacacc actgtgttca tttaccgcc actagtacc cagcccctca tggatgcaca cgctatctcc attccgtag ctccgttttc
2601 ttaccacaca gcctacagcc catctttacc gaatggggca tcttagtggc actggccgcy taccacacag cacgtgtctg acgtcgatgg acatccgctt
2701 atgccttacc gtgtgaaact tagataccgc cttgggtggg ggtttggtt ttgggggttt atatgaagcg gtcttgtgtt gttatctta tcgtcatgct
2801 gagtcatgac taaaaaacta tgtgcgatgg gtccttacc ttatcttat cgcagggtg agtcatgact gaaaactgtg ttgcagatgg gttgtccgct

                                acpm2BamHI ▶
                                aa ggatCCTCAA ACAGACTAAA GCCCT
                                acpm2Ragf ▶
                                galga tgalaaaTAA TCAACCTCAA ACAGAC
                                ◀ acpm2Ragr
                                G GATGATTGGG TCGGCAActa atgtttctg
2901 cagacatggt tcgcttgctc tcgccgttcc ctactaacc agccgtttaa tcaacctcaa acagactaaa gccctgtaca taaaaataca tctccacca
                                >>Exon3>>
                                A V -

                                ◀ acpm2seq4
                                STAGAG GAAGACGCAG CAGC
3001 cagcggctaa attgcacttc cttctgctc gtcgtctctt atctgtctc ttcatagagt tgactggcgc agaaagtatc gtgtagagct actaatcgat
3101 agagcttggg ccggaatagc aacgtactgt accatgtact gtaaccacg cacagtggca gagaagcgca tcagcatggt cattgattgc gacagtcgat
3201 agccgatggt aacacttctg gcccacgtga ccgggcgact ggcagaccgg gcgactgaca ggccgagcag ggcgcaacac ctgttggtca ccgtctcttg
3301 tggcccacgg cacatatctc ctttttggga gtcctaacte tgacgtetaa aatcgacgta aaatcgactg aaaaatcgac taaacctacc cttctgctga
3401 cgcgaccgaa tctacagtgc cttctgagtt gaggtttagt cgggttttagt gttttgatgc cgcttgtgtg agggtaaaaa aaaagtgttg ccaaaaaaat

                                ◀ acpm2r
                                CTCA TGCCGCAATC
3501 atgcagctct ttttttttac cgggtcaaaa tgaaaaaccg acttaaagat ttgaaattt gggtttgccg ctaattttgg agtggggagt acggcgttag

                                acpm2r
                                TCGCTC
3601 agcgagctgt gggggcggtt agagactgtc ttgggggat ggaccctgt ctgggggttg taaggagcct ggtttatggt tgcagagctc atttggggct

                                ◀ acpm2chkr
                                CAAGGTAGGA CGGTTACGC
3701 ctttttttagc cgctgtcggt ttttttggcc cggcgtttaa gttccatctt gccaaagtgc ttatcttggg tttactcaa agtgcctggg cccatgaaat
gaaaaaatcg gcgacagcca aaaaaaccgg gccgcaaat caaggttaga cggttcacgc aatagaacca aaatgagtt tcacgacca gggacttta
3801 tgaaaattct ttattatccg ccagccagaa cttttcaacg ggacatggcc tggagactga gacgctgaga ctcgaccggg atttcattgg cgaccacaga
acttttaaga aataatagcg ggtcgttctt gaaaagtgc cctgtaccgg acctctgact ctgcgactct gagctggccc taaagtaacc cgtggtgtct
3901 catctttgga agtatttgcg accacaaca gacgacagcg gcccgacaac agacaagcag acgacagaca agcagagcgc cgacaagcag acggccgaca
gtagaaacct tcataaacgc tgggtgttgt ctgctgtccg ccggctgttg tctgtctgtc tgctgtctgt tcgtctgccc gctgtctgct tggcggctgt
4001 agcagacagc agcagcgaga caagtagaca accaccagaa gaccatacga ccattcgaac atccacacgt ccacacttcc acagctccac acttccacac
tcgtctgtcg tctgcccgtc gttcatctgt tgggtgtctt ctggtatgct ggtaagcttg taggtgtgca ggtgtgaagg tgtgcaggtg tgaaggtgtg
4101 gtccacacgt ccacacaacc tcattatgga cacaactctc ctgcatccgg aatacatccc gggaacggtc caaatcatcg gacagcatga cgacgactcg
caggtgtgca ggtgtgttgg agtaatacct gtgttagaag gagctaggcc ttatgtaggg cccttgccag gtttagtagc ctgtcgtact gctgctgagc
4201 atgctgatca aggacgaaaa ggaacgggtg ctgcttcccc aaccaccctc gtcgcaaac gaccgctca aatggctgctg gagcagaaaa ctctggcaca
tacgactagt tctgtctttt cccttgccac gacgaagggg ttgggtggag cagcgggttg ctggggcagat ttaccagcac ctgctctttt gagaccgtgt
4301 ctctcttggg gtgtttcacc accgatttca cagcagccac ctccaacgac
gagagaacca cacaaagtag tggcctaagt gtcgtcggtg gaggttgcgt

```

**Figure 9.3** The ACPM2 gene used for generating the mutants

Primers for generation of the ACPM2 deletion strain, ACPM2-flag tagged version, *Bam*HI and *Sal*I enzyme cleavage sites, PCR check primers and sequencing primers are shown.

## 9.2 Oligonucleotides

The capital letters in the primer sequence denote unchanged nucleotides; small letters represent mutated nucleotides. Recognition sites of the restriction enzymes are underlined. Nucleotides coding for mutated serine are bold.

### 9.2.1 Oligonucleotides for the *st1* gene

name	sequence	binding site
st1f	5'-CGACGATACCGATGCTAGAG-3'	118-137
st1BamHI	5'-GGAGG <u>Atcc</u> CTTGAACGAGGCCAACC-3'	2115-2140
st1SalI	5'-aag <u>tegac</u> GACGATGATGATCCTGC-3'	1153-1129
st1r	5'-TTCACAGGCACCTCTACAGC-3'	2810-2792

**Table 9.1 Oligonucleotides for generation of the *st1* deletion strain**

name	sequence	binding site
st1ckf	5'-GGCAATCGAGGCGATATATG-3'	30-49
st1ckr	5'-TTATGACCATGCGACCAGTG-3'	2865-2846

**Table 9.2 Oligonucleotides for checking of the deletion via PCR**

name	sequence	binding site
st1strepII <sub>f</sub>	5'-caattgaaaaTAGATAGAATCATACTGTAG-3'	2134-2165
st1strepII <sub>r</sub>	5'-aggatgagaccAAGCCCGGTTGGCCTCGTTC-3'	2157-2127

**Table 9.3 Oligonucleotides for creating the *strepII*-tagged version of *st1* gene**

name	sequence	binding site
st1seq1	5'-CACTTCGCTGACTCAGAATG-3'	733-752
st1seq2	5'-AGATCTTCGATGCTACCTGG-3'	1259-1278
st1seq3	5'-GAGGTCACCTTCATTGATGC-3'	1768-1787
st1seq4	5'-CAAGTCGAGGTCGGGAGAAG-3'	1510-1491
st1seq5	5'-GTGACACCGGATCCACACAT-3'	1994-1975

**Table 9.4 Oligonucleotides for sequencing of the *st1* gene**



## 9.2.2 Oligonucleotides for ACPM1 gene

name	sequence	binding site
acpm1f	5'-TACTCGGCTGAACTGCAAG-3'	279-297
acpm1BamHI	5'-atggatccAGCGTTAAGGCCACAG-3'	2036-2059
acpm1r	5'-ATCTCACGGCTTCACAACG-3'	2978-2960
acpm1SalI	5'-aagTCGaCACGGACAGGATTCTGAAC-3'	1112-1088

**Table 9.5 Oligonucleotides for generation of the ACPM1 deletion strain**

name	sequence	binding site
acpm1chkf	5'-AAGCCGAGCGACACAAGGAG-3'	143-162
acpm1chkr	5'-AGCCAGTCACAGCCAGAGAG-3'	3017-2998

**Table 9.6 Oligonucleotides for checking of the deletion via PCR**

name	sequence	binding site
acpm1strepII <sub>f</sub>	5'-caatttgaaAAATAAGCAAGCTGTATATAATAG-3'	2007-2039
acpm1strepII <sub>r</sub>	5'-aggatgagaccATTTAGCATCGGGCTGG-3'	2030-2003

**Table 9.7 Oligonucleotides for creating the strepII-tagged version of ACPM1 gene**

name	sequence	binding site
acpm1seq1	5'-GTTAGCTGTCAGGCAGTGG-3'	1054-1072
acpm1seq2	5'-GATCCACAGACGCACAATG-3'	1592-1610
acpm1seq3	5'-GAATGCCACAGGTGAATGC-3'	1689-1671
acpm1seq4	5'-GCCTACCTAGAGCTCCAAG-3'	2185-2165

**Table 9.8 Oligonucleotides for sequencing of the ACPM1 gene**

name	sequence	binding site
acpm1S66Af	5'-gcCTTAGACACCGTCGAGGTTG-3'	1887-1907
acpm1S66Ar	5'-GTCGAGGTTGAGGTCCTTGG-3'	1886-1867

**Table 9.9 Oligonucleotides for mutating the phosphopantetheine-binding serine (S66A)**

### 9.2.3 Oligonucleotides for the ACPM2 gene

name	sequence	binding site
acpm2fnew	5'-GTACAGAAGTGTCGGCGCAG-3'	528-547
acpm2BamHI	5'-aaggatCCTCAAACAGACTAAAGCCCT-3'	2949-2975
acpm2SalI	5'-aagTCGacAGTGTGGAGGATGGTGTGG-3'	1193-1167
acpm2r	5'-CTCGCTCTAACGCCGTA-3'	3606-3587

**Table 9.10 Oligonucleotides for generation of the ACPM2 deletion strain**

name	sequence	binding site
acpm2f	5'-CACGCACCAGTTACTCTGTC-3'	1-20
acpm2chkr	5'-CGCACTTGGCAGGATGGAAC-3'	3760-3741

**Table 9.11 Oligonucleotides for checking of the deletion via PCR**

name	sequence	binding site
acpm2flagf	5'-gatgatgataaaTAATCAACCTCAAACAGAC-3'	2939-2966
acpm2flagr	5'-gtctttgtaatcAACGGCTGGGTTAGTAGG-3'	2959-2930

**Table 9.12 Oligonucleotides for creating the flag-tagged version of ACPM2 gene**

name	sequence	binding site
acpm2seq1	5'-CTGAGCAATATCTCCGCACC-3'	1064-1083
acpm2seq2	5'-GTACTAGTGACTGACCGAAG-3'	1508-1527
acpm2seq3	5'-GAGTCTGCATACAGTCTGAG-3'	2041-2060
acpm2seq4	5'-CGACGACGCAGAAGGAGATG-3'	3034-3015

**Table 9.13 Oligonucleotides for sequencing of the ACPM2 gene**

name	sequence	binding site
acpm2S88Af	5'-gcTTTGGATGTCGTCGAGGTG-3'	1465-1485
acpm2S88Ar	5'-GTCCAGACCAAGGTCGGAAG-3'	1464-1445

**Table 9.14 Oligonucleotides for mutating the phosphoantethine-binding serine (S88A)**

### 9.2.4 Oligonucleotides for ACPM1 and ACPM2 genes swap strategy

name	sequence	binding site
acpm1_2-1f1	5'-CGAATGCTGCTGTTCTCG-3'	1351-1369
acpm1_2-1f2	5'-CATCACCCCCACCGCTTCC-3'	1844-1862
acpm1_2-1f3	5'-GAGATCCCCGACAAGGAG-3'	1938-1955
acpm1_1-2r1	5'-ATTCGCTTCTCGGCATCG-3'	1355-1338
acpm1_1-2r2	5'-GGTGATGGCAGCGGGGTTG-3'	1850-1832
acpm1_1-2r3	5'-GATCTCGATGCCGAACTC-3'	1943-1926

*Table 9.15 Oligonucleotides for swap strategy of ACPM1 gene*

name	sequence	binding site
acpm2_1-2f1	5'-GAATCGTGGCTCTTCTGG-3'	1373-1390
acpm2_1-2f2	5'-GTAGTGGCGGTGGCGGTTGG-3'	1422-1441
acpm2_2-1r1	5'-ATTCGCTCCTGAATCATG-3'	1376-1359
acpm2_2-1r2	5'-GGTGATGTTCTTGGCGTC-3'	1428-1411

*Table 9.16 Oligonucleotides for swap strategy of ACPM2 gene*

### 9.2.5 Oligonucleotides for URA3 gene

name	sequence	binding site
ura3f	5'-GTCGACAAAGGCCTGTTTC-3'	outside of the gene
ura3r	5'-GAGGATCCGTCTGACTCGTCATTGC-3'	outside of the gene
ura3us2	5'-CACAGCCTCCAACGAAGAATG-3'	105-86
ura3ds2	5'-CCTGGAGGCAGAAGAACTTG-3'	1587-1606

*Table 9.17 Oligonucleotides for URA3 gene*

### 9.3 Complex I subunits of *Yarrowia lipolytica*

<i>Procaryotes</i>		<i>Eucaryotes</i>						
<i>E. coli</i>		<i>P. denitrificans</i>	<i>Y. lipolytica</i>			<i>B. taurus</i>		
		<i>T. thermophilus</i>						
Subunit NUO	Subunit NQO	Subunit	Mr <sup>1</sup> [Da]	TMDs <sup>2</sup>	Subunit	M <sub>r</sub> [kDa]	Remarks /modification/ Cofactor <sup>3</sup>	
<i>Central nuclear coded</i>								
G	3	NUAM	75,198.7	0/0	75-kDa	77.0	Δ1-23/[2Fe-2S],2x[4Fe-S]	
F	1	NUBM	51,660.0	0/0	51-kDa	48.5	Δ 1-20/[4Fe-4S], FMN	
D <sup>4</sup>	4	NUCM	49,945.0	0/0	49-kDa	49.2	Δ 1-33/[4Fe-4S]	
C <sup>4</sup>	5	NUGM	30,476.2 <sup>5</sup>	0/0	30-kDa	26.4	Δ 1-38	
E	2	NUHM	24,068.6	0/0	24-kDa	23.8	Δ 1-32/[2Fe-2S]	
I	9	NUIM	22,321.3	1/0	TYKY	20.1	Δ 1-36/2x[4Fe-4S]	
B	6	NUKM	20,425.6	0/0	PSST	20.2	Δ 1-37/[4Fe-4S]	
<i>Central mitochondrially coded</i>								
H	8	NU1M	38,347.7	10/10	ND1	36	-	
N	14	NU2M	53,331.9	14/13	ND2	39	-	
A	7	NU3M	14,470.5	3/3	ND3	13	-	
M	13	NU4M	54,481.2	13/12	ND4	52	-	
L	12	NU5M	73,705.4	18/16	ND5	67	-	
J	10	NU6M	20,758.3	5/5	ND6	19	-	
K	11	NULM	9810.9	2/2	ND4L	11	-	

*Accessory nuclear coded*

NUEM	40,434.0	0/0	39-kDa	39.1	Short-chain dehydrogenase, NADPH
ST1	34,621.2	0/0	n.p.	n.p.	n.p.
NESM	23,438.1	1/0	ESSS	14.5	STMD <sup>6</sup> , phosphorylation
NUJM	20,827.6	2/2	B14.7	14.8	TIM17/22 family, -Met +Ac
NUZM	19,749.6	0/0	n.p.	n.p.	n.p.
NUPM	19,196.0	0/0	PGIV	20.0	Cystein-rich motif, -Met
NUXM	18,565.2	3/2	n.p.	n.p.	n.p.
N7BM	16,153.2	0/0	B17.2	17.1	+Ac, nitration
NUYM	15,939.9	0/0	AQDQ	15.3	Phosphorylation
NUFM	15,572.7	0/0	B13	13.2	-Met+Ac
NIAM	14,642.3	1/1	ASHI	18.7	STMD, Δ1-28
NB4M	14,626.7	0/0	B14	15.0	-Met+Ac, nitration
NUMM	14,257.0	0/0	13-kDa	10.5	Δ1-28
NB6M	13,960.2	1/1	B16.6	16.6	STMD, proapoptotic factor, -Met+Ac
NUNM	13,300.9	1/1	n.p.	n.p.	n.p.
NI2M	12,879.8	0/0	B22	21.7	-Met+Ac
NB8M	11,067.8	0/0	B18	16.5	Cystein-rich motif -Met +Myr
NIDM	10,890.1	0/0	PDSW	20.8	Cystein-rich motif, -Met
NB5M	10,347.7	1/1	B15	15.1	STMD, -Met+Ac
ACPM2 <sup>7</sup>	9526.7	0/0	SDAP	10.7	Phosphopantetheine <sup>8</sup>
NIPM	10,018.6	0/0	PFFD	12.5	Cystein-rich motif, -Met
NIMM	9662.1	1/1	MWFE	8.1	STMD, phosphorylation
ACPM1 <sup>7</sup>	9071.2	0/0	SDAP	10.7	Phosphopantetheine <sup>8</sup>

NI8M	9472.8	0/0	B8	11.0	Thioredoxin fold, - Met +Ac
NI9M	7704.8	1/1	B9	9.3	STMD, -Met+Ac
NB2M	6804.7	1/1	B12	11.1	STMD, -Met+Ac (partial)
NEBM <sup>9</sup>	7900	1/1	n.p.	n.p.	n.p.

*Mammal specific subunits*

KFYI	5.8	STMD, Δ1-27
MNLL	7.0	STMD, -Met
AGGG	8.5	STMD, Δ1-36
MLRQ	9.3	STMD
10-kDa	8.4	Δ1-34
B14.5a	12.6	-Met+Ac
B14.5b	14.1	STMD, +Ac(partial)
SGDH	16.7	STMD, Δ1-46
B17	15.4	STMD, -Met+Ac
42-kDa	36.7	Δ1-23, phosphorylation

**Table 9.18 Central and accessory subunits of *Yarrowia lipolytica* complex I**

Nomenclature for subunits NESM (formerly called NUWM), NB5M (formerly called NUVM) and NUNM (newly identified, with no significant homology to proteins from other organisms) was introduced in [71]. Information to bovine complex I was adapted from [35]. Abbreviations: n.p: not present; - Met: N-terminal methionine is removed post-translationally; + Ac: N-terminal residue is acetylated; + Myr: N-terminal residue is myristoylated. Δa – b: known mitochondrial import sequence (residues a to b) are removed.

<sup>1</sup> Average molecular masses of mature proteins, excluding cofactors, calculated using the “compute pI/Mw” tool at [http://www.expasy.ch/tools/pi\\_tool.html](http://www.expasy.ch/tools/pi_tool.html).

<sup>2</sup> Predicted using servers <http://www.enzim.hu/hmmtop/> and <http://www.cbs.dtu.dk/services/TMHMM/>.

<sup>3</sup> *Y. lipolytica* posses the same composition of FeS clusters, a FMN, NADPH and phosphopantetheine as bovine complex I

<sup>4</sup> NuoC and NuoD are fused in a single subunit in *E. coli*

<sup>5</sup> Including hexa-histidine tag and hexa-alanine spacer

<sup>6</sup> Single transmembrane domain (STMD)

<sup>7</sup> Including phosphopantetheine and hydroxy-tetradecanoate

<sup>8</sup> By means of LILBID spectrometry, a phosphopantetheine-hydroxy-tetradecanoate modification to both acyl carrier proteins of *Y. lipolytica* complex I was identified.

<sup>9</sup> Nübel *et al*, unpublished. Exact mass of the subunit has not been determined yet.

## 9.4 Protein alignments

The protein sequences were aligned using the CLUSTALW software (<http://www.ebi.ac.uk/clustalw/index.html>). \* - conserved amino acids; : - conserved substitutions; · - semi-conserved substitutions. Small and hydrophobic amino acids are represented in red, acidic in blue, basic in magenta; hydroxyl + amine + basic in green. The mitochondrial presequences predicted with the MitoProt II software (<http://ihg2.helmholtz-muenchen.de/ihg/mitoprot.html>) are underlined.

### 9.4.1 Alignment of ACPs from different species

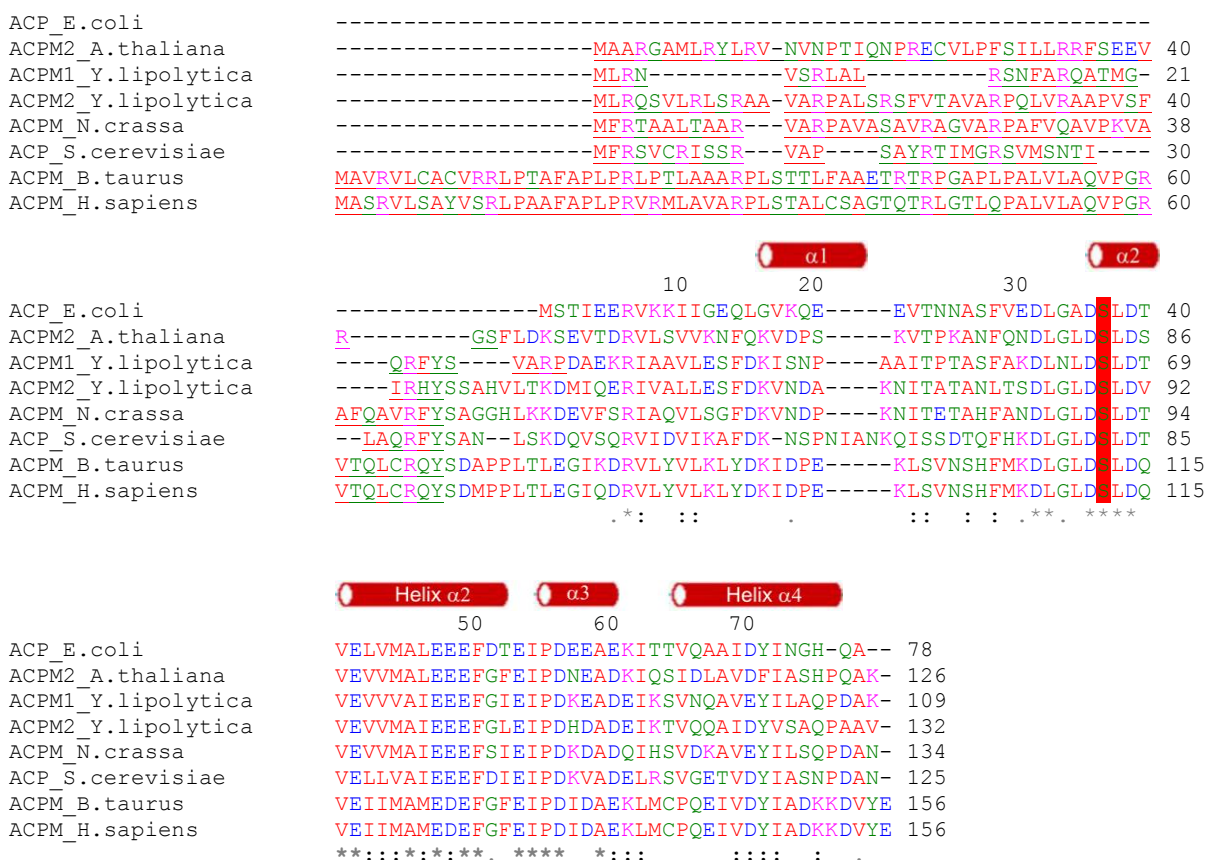


**Figure 9.4** Alignment of ACPM1 and ACPM2 subunits with acyl carrier proteins from other species

Four  $\alpha$ -helices ( $\alpha$ I-IV) denoted in red and positions of amino acids according to *E. coli* nomenclature are indicated above the sequence alignment. The phosphopantetheine-binding serine residue conserved among different species is highlighted in red.

## 9.4.2 Alignment of ACPM1 and ACPM2 subunits from *Y. lipolytica*

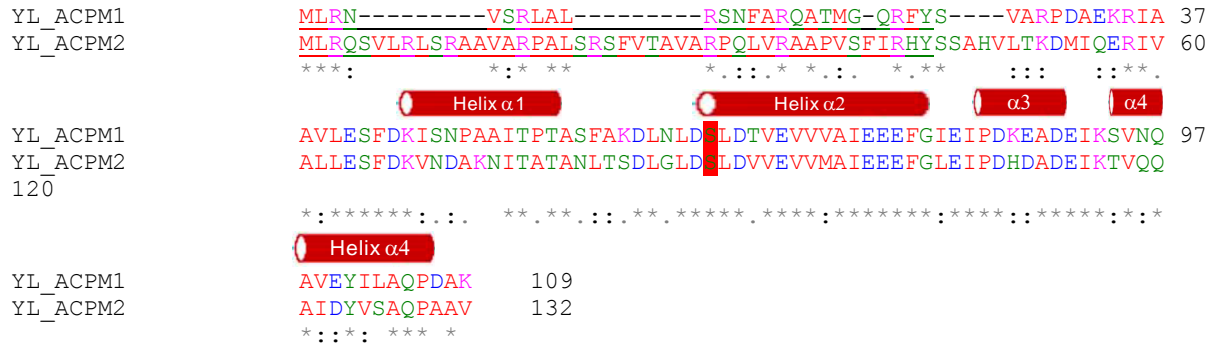
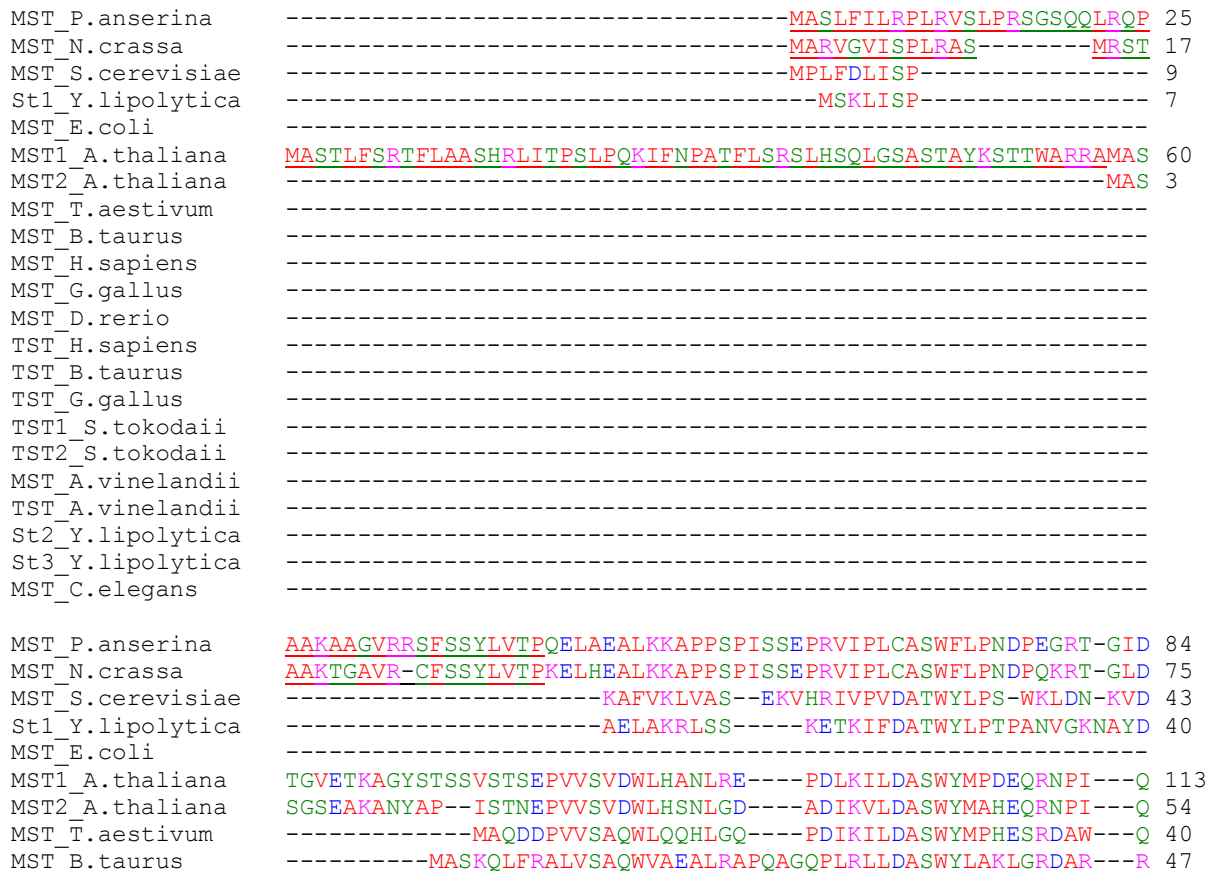


**Figure 9.5** Alignment of *Y. lipolytica* ACPM1 and ACPM2 subunits

The pantetheine-4'-phosphate-binding serine residue is highlighted in red. Localisation of four  $\alpha$ -helices ( $\alpha$ I-IV) is denoted in red above the aligned sequences.

## 9.4.3 Alignment of the st1 subunit





MST_H.sapiens	-----MASPOLCRALVSAQWVAEALRAPRAGQPLQLLDASWYLPKLGDRAR---	R	47
MST_G.gallus	-----MSQQLLYRALVSAKWLSEAIKSKQTGQALKVVVDASWYLPKMKRDPK---	Q	47
MST_D.rerio	-----MAAQT--RALVAARWLADAVKSNRVGNLRILDASWYLPKMKRNPR---	A	45
TST_H.sapiens	-----MVHQVLYRALVSTKWLAESIRTGKLGPLRVLDASWYSPGT-REAR---	K	46
TST_B.taurus	-----MVHQVLYRALVSTKWLAESVRAGKVGPLRVLDASWYSPGT-REAR---	K	46
TST_G.gallus	-----MAAQALGRALVSAKWLSEAVRAGRVGAGLRVLDASWYPPQE-RNAR---	Q	46
TST1_S.tokodaii	-----MLVSVKWLZENLN-----EVKILEIDFDPEIN-----		27
TST2_S.tokodaii	-----MSQTIQQQVVVDTKWLEHLKD---PNVRIVEVDYDNTA-----		37
MST_A.vinelandii	-----MSHAQLLDPARLAERLDQ---PDLRILDRCFALEDPAYGAR---		38
TST_A.vinelandii	-----MDDFASLPLVIEPADLQARLSA---PELILVDLTSAAAR-----		35
St2_Y.lipolytica	-----		
St3_Y.lipolytica	-----		
MST_C.elegans	-----MAVDMIVEPKVVVQNFNIRILLDASWTFKPKADIAEYKAKYYNKFVGMNELKNP		55
MST_P.anserina	VFREKRIPKARFFDLKVIDKHSEYPHML-----PTPKGFAAAMSELGIRHEDTVVYDS		139
MST_N.crassa	VFIEKRIPKARFFDLKVIDKRSYPHML-----PSSKDFAAAMSELGIRREDTVVIYDS		130
MST_S.cerevisiae	FLTTPRIPNSIFFDIDAIKDKKSPYHMF-----PTKKVDDAMSNGVQKDDILVYDR		98
St1_Y.lipolytica	NYMKKRIPGALYFDIDAVN-TPSKFPHML-----PSPQTFENELTKLGVSSDSPVVYDT		94
MST_E.coli	---MDIFPAQCFLISKRFLDHTSPLPHML-----PRPETFAVAMLELGVNQDKHLIVYDE		52
MST1_A.thaliana	EYQVAHIPGALFFDLGIDSRKTSPLHML-----PTEEFAAGCSALGIDNKDEVVYDG		168
MST2_A.thaliana	EYQVAHIPGALFFDLNGIADRKTNLRHML-----PSEEFAAGCSALGIDNNDGVVYDG		109
MST_T.aestivum	EYQVAHIPGALYFDIDGIDSRDTTHLPHML-----PLEEFAAAVSAALGIDSNHDKVIVYDG		95
MST_B.taurus	EFEERHIPGAAFFDIDQCSDRTPSYDHML-----PSAAHFSEYAGRLGVGAATHVVYDA		102
MST_H.sapiens	EFEERHIPGAAFFDIDQCSDRTPSYDHML-----PGAHFHFAEYAGRLGVGAATHVVYDA		102
MST_G.gallus	EFEERHIPGAVFFDIDQCSDRTPSYDHMM-----PKANEFHFAEYVGLGVGNDSHVVYDG		102
MST_D.rerio	EFEQTHIPGASFFDIDCCDKSSEFDHML-----PTKGEFADYVGNLGIIGNTHVVYDA		100
TST_H.sapiens	EYLERHVPGASFFDIEECRDTASPYEMML-----PSEAGFAEYVGRIGISNHTHVYDG		101
TST_B.taurus	EYLERHVPGASFFDIEECRDKASPYEVML-----PSEAGFADYVGSIGISNHTHVYDG		101
TST_G.gallus	EFKERHIPGASFFDIEECRDKSSPYDFML-----PSEAHFADYVGRIGVSNHTHVYDG		101
TST1_S.tokodaii	-YYEGHIPSALLLPWKS-LLHDKIRDFAP-----PEK--FSKVLGNLGVKEDDLIVLYSD		78
TST2_S.tokodaii	-YNVWHIQGAVLIRWREDLRHPVIRDFIE-----PSD--FEKLMESKIGISNNTTVVLYGD		89
MST_A.vinelandii	SYAEAHIPGARFADLERDLG-PVHKVGTGRHPLDPVLLTERLRWGIIDNSQVVLYDD		97
TST_A.vinelandii	-YAEGHIPGARFVDPKR TQLGQPPAPGLQ-----PPREQLSFLGELGHRPEAVYVVYDD		89
St2_Y.lipolytica	-----		
St3_Y.lipolytica	-----MMFRITPVARRVIARDASK-----HALGIRGRALRPIVNS		36
MST_C.elegans	EYLAEHINGAAHFNFIDAIYPSENERFTLY-----TPEEFSSYVKRLGVFNGDHLVIYGR		110
MST_P.anserina	K-ELGIFSAPRVGWTLKTFGHPR-VHILNN-FRLWVEQG-LPTE-----SGNVW		184
MST_N.crassa	Q-ELGIFSAPRVGWTMKVFGHPK-VHILNN-FKLWIEEG-LPTE-----SGNVW		175
MST_S.cerevisiae	---VGNFSSPRCAWTFKVMGHPK-VYLLNN-FNQYREFK-YPLD-----SSKVA		141
St1_Y.lipolytica	---QGVSFSGPRLVWTFKVFQHDN-VQFLNG-FEAYTQLPGIPSRPDA-----YTWGIW		142
MST_E.coli	---GNLFSAPRAWMLRFTFVEK-VSILGGLAGWQRDLLLLLEEG-----		93
MST1_A.thaliana	---KGFISAARVWMMFRVFGHEK-VWVLDGGLPWRASGYDVESASGDAILKASAASEA		224
MST2_A.thaliana	---MGLFSAARVWMMFRVFGHDK-VWVLDGGLPKWRASGYDVESVSNDAILKASAATEA		165
MST_T.aestivum	---KGFYSAPRVWMMFRILGHDK-VWVLDGGFPQWQASGFNIGSSCPDDAVLKSKAANIA		151
MST_B.taurus	S-DQGLYAAPRVWMMFRVFGHRT-VSLDGGLRNWLRLQGLPLSSGKS-----		147
MST_H.sapiens	S-DQGLYSAPRVWMMFRVFGHHA-VSLDGGLRHWLRQNLPLSSGKS-----		147
MST_G.gallus	S-DQGLFSAPRVWMMFRVFGHEA-VSLDGGLRNWLREGFPLSSGKT-----		147
MST_D.rerio	S-DFGSFSAPRVWMMFRVFGHSS-VSVLDGGFKNWLKEGHPVSQQYS-----		145
TST_H.sapiens	E-HLGSFYAPRVWMMFRVFGHRT-VSVLNGGFRNWLKEGHPVTSEPS-----		146
TST_B.taurus	D-DLGSFYAPRVWMMFRVFGHRT-VSVLNGGFRNWLKEGHPVTSEPS-----		146
TST_G.gallus	D-ELGTFYAPRAWMMFRVFGHRE-VSVLNGGFKNWWKEGHPVTSEPS-----		146
TST1_S.tokodaii	---MGNRYAFYTYWLMKAYGHEN-VAILNGGIYKWLKEGYPVENEPT-----		121
TST2_S.tokodaii	---YNNWFAVYTFWLFKAYGHED-VRIILNGGRTKWAENLPTEQGPK-----		132
MST_A.vinelandii	---GPGAFARAWLLLAWLGRDGVFLLDGGLNAWRAAGLPLSGEPP-----		141
TST_A.vinelandii	---EGGWAGRFIWLLDVIQQQR-YHYLNGGLTAWLAEDRPLSRELP-----		132
St2_Y.lipolytica	-----		
St3_Y.lipolytica	-----MKLSTLFSTFVCVTLG-----		16
MST_C.elegans	-----ITTRKVHVSQVLSARVALAAVPHNFHTQLL-----		67
	GKDGGMAAASRAYWTFRYYGTYT-VSVLNGGIEAFKLAQGVVQSGES-----		156

\*

MST\_P.anserina TVECG---TYPIPEMDEAK-----VAHFEDVREVALDYNKEGAE-----VQILDARSYG 231  
MST\_N.crassa TIECG---TYPIPEMNEDK-----VASFEEVRQVAIDSSKEGSKS-----VQILDARSPG 222  
MST\_S.cerevisiae AFSPYPKSHYESSSESFDQKE---IVDYEMFQLVK--SGELAKK-----FNAFDARS LG 190  
St1\_Y.lipolytica DTQVPGKIDPADPPYKVTKARPELVKSFEDVLAIVEKHNGDGAKIRN--EVTFIDARPNG 200  
MST\_E.coli -----AVELPEGEFNAAFN-----PEAVVKVTDVLLASHENT-----AQIIDARPA 135  
MST1\_A.thaliana IEKIYQGQTVSPITFQTKFQ-----PHLVWTLQVKNMEDPT---YQHIDARSKA 272  
MST2\_A.thaliana IEKIYQGQTI SPITFQTKFR-----PHLVLALDQVKENIEDKT---YQHIDARSKA 213  
MST\_T.aestivum VETAYNGELANAATFQTEFR-----HQLLWTLKVKHNVAKA----HQQVVDARVKG 199  
MST\_B.taurus -----RPQPAEFHAVLD-----PAYIKTYEDIKENLESRR---FQVVDARAAG 187  
MST\_H.sapiens -----QPAPAEFRAQLD-----PAFIKTYEDIKENLESRR---FQVVDARATG 187  
MST\_G.gallus -----QVAPSDFHATLD-----KCMVKTYEDILDNLDSHR---FQVVDARVEG 187  
MST\_D.rerio -----KPAPVDFNASFK-----ESWVKTYEDVLNNIKTKE---FQVVDARANG 185  
TST\_H.sapiens -----RPEPAVFKATLD-----RSLLKTYEQVLENLESKR---FQLVDSRSQG 186  
TST\_B.taurus -----RPEPAIFKATLN-----RSLLKTYEQVLENLESKR---FQLVDSRAQG 186  
TST\_G.gallus -----QPAQAVFKATLD-----KTLKTFEEMMENVGSKK---FQVVDARFAG 186  
TST1\_S.tokodaii -----FPSK-KSNYIVKRVD-----WSS-RILLWELLSKLN-----SIELIDARNRE 161  
TST2\_S.tokodaii -----EPQYPKGSYKVKKVD-----WGSRAFFWEVLQVTKGEVVKTTILVDVRS PK 180  
MST\_A.vinelandii -----APAAGTFRGQPD-----ASLLVDAQDLLARLGAR---LTLDDARALP 181  
TST\_A.vinelandii -----APAGGPVALSLH-----DEPTASRDYLLGRLGAAD---LAIWDARSPQ 172  
St2\_Y.lipolytica -----VASSAK-----EYSYFDVKKLSSESLVDGSAPADTILIDVR--- 51  
St3\_Y.lipolytica -----KRRYSALSSECR-----ELTYPDIKALS DNILKGDN--DNVILVDVR--- 107  
MST\_C.elegans -----MISSGNYEAKSVDN-----NILAKMADIPFDNLASIK-----YLDARSKE 196

\* \*

MST\_P.anserina RWSGKDEPRP-----GLSSGHMPGSINIPFDAVLDPQTKAFLPVDKPKQVFKEKG---- 282  
MST\_N.crassa RWSGTEPEPRE-----GLSSGHMPGSINIPFSAVLDSSTKAFLPADKPKLKEVFARAG---- 273  
MST\_S.cerevisiae RFEGTEPEPRS-----DIPSGHIPGTQPLPYGSLLDPETKTYPEAGEAIHATLEKALKDF 245  
St1\_Y.lipolytica RFTGKDAEPRA-----ELSSGHVPGAYSIAFPEVVE--NGKFKSPEELKALFASKG---- 249  
MST\_E.coli RFNAEVDEPRP-----GLRRGHIPGALNVPWTELVR--EGELKTTDELDAIFFGRG---- 184  
MST1\_A.thaliana RFDGTAPRPRK-----GIRSGHIPGSKCIPFPQMF--SCNTLLPAEELKRRFDQED---- 322  
MST2\_A.thaliana RFDGIAPEPWK-----GLPSGHIPGSKCVFPPLMFD--SSQTLPAEELKQFEQED---- 263  
MST\_T.aestivum RFDGVMPEPRE-----GVRSGHIPGTKCVFPPEMSD--GAQTLPADEL SKKFEQAG---- 249  
MST\_B.taurus RFRGTEPEPRD-----GIEPGHIPGTINIPFTDFLT--EDGLEKSPPEIRRLFQDKK---- 237  
MST\_H.sapiens RFRGTEPEPRD-----GIEPGHIPGTINIPFTDFLS--QEGLEKSPPEIRHLFQEKK---- 237  
MST\_G.gallus RFRGIEPEPRD-----GIEPGHIPGTINIPFTDFLT--ESGLEKTPPEQIRSLFQEKK---- 237  
MST\_D.rerio RFRGVEPEPRA-----NTEPGHIPASLNMPFSPFMDPESGLERPVEELTKLFQAG---- 236  
TST\_H.sapiens RFLGTEPEPDAV---GLDSGHIRGAVNMPFMDFLT--EDGFEEKPEELRALFQTKK---- 237  
TST\_B.taurus RYLGTEPEPDAV---GLDSGHIRGAVNMPFMNFLT--EDGFEEKSPEELRAMFEAKK---- 237  
TST\_G.gallus RFQGTTELDQ-----GLESGHIPGAVNMPFSTFLT--ESGHEKSI EBIQQMFHEKK---- 234  
TST1\_S.tokodaii EYEGLTSAPPEHKCEQTQVSGHIPNAKNIPWTLFN--EDGTLKGREELKIFSS----- 214  
TST2\_S.tokodaii EYTGIEIRAPPEYADEQTQVGGHIPGATSPWSQAVNPE TGEFKPIEELRRLVSSG---- 236  
MST\_A.vinelandii RFRGVEPEPLD-----VAGHIPGARCAPFTDNLG--ADGRFLPADELRAFARFGLG--- 230  
TST\_A.vinelandii EYRGE-KVLAA-----KGGHIPGAVNFEWTAAMD--PSRALRIRTDIAGRLE--ELG--- 219  
St2\_Y.lipolytica -----EPSE-----YAAGFIPGAFNMPLKTQSF---ALCKSPEEFETAMGFPK---- 91  
St3\_Y.lipolytica -----EPDE-----FKAGHIPGAINIPVKSTPG---ALSLSAEEFEGTFGFPK---- 147  
MST\_C.elegans EFIGKVPYIGYP-----DSKAEGVRCKDAIHFPPIGEVCAAKGFKKKTDCDQAFAAKG---- 247

:

MST\_P.anserina ---VDPKPIISSG GTGVTACVLETALNEAQYGSPE TRKVDYDGSWTEWAQRVKPSSDLIR 339  
MST\_N.crassa ---VDPSKPIISSG GTGVTACVLETALNEAQFGSPEKSKVYDGSWTEWAQRVKSSSESLIE 330  
MST\_S.cerevisiae HCTLDPSKPTICSGTGVSGVVIKTALELA--GVPNVR--LYDGSWTEWVLKSGP--EWIAE 301  
St1\_Y.lipolytica ---IDGSKPIISSG GSGVTACVIDLLEIAGIGSRD TNNAVYDGSWTEWAQRAPTKYIVKE 306  
MST\_E.coli ---VSYDKPIIVSG GSGVTA AVVLLALATLD---VPNVKLYDGAWEW GARADLPVEPVK 238  
MST1\_A.thaliana ---ISLDKPIMASG GTGVTACILAMGLHRLG---KTDVPIYDGSWTEWATQP--DLPIES 374  
MST2\_A.thaliana ---ISLDSPIAASG GTGVTACILALGLYRLG---KTNVAIYDGSWTEWATAP--NLPIVG 315  
MST\_T.aestivum ---ISLDGPVILTASGVTACILALGLYRIG---KHDVPVYDGSWTEWEALPDNDYPIVT 303  
MST\_B.taurus ---VDLSLPLVATG GSGVTACHVALGAYLCG---KPDVPIYDGSWVEWYMRAPEDIISE 291  
MST\_H.sapiens ---VDLSKPLVATG GSGVTACHVALGAYLCG---KPDVPIYDGSWVEWYMRARPEDIISE 291  
MST\_G.gallus ---VDLSKPLVATG GSGVTACHVALGAYLCG---KPDVAVYDGAWEWYMRAPENIISE 291  
MST\_D.rerio ---VDLQKPFVVTG GSGVTACHIALAAHLCG---HPGVSLYDGAWEWFTKAAPHEHIISE 290  
TST\_H.sapiens ---VDLSQPLIATG GSGVTACHVALAAYLCG---KPDVAVYDGSWEWFRAPPESRVSQ 291

TST_B.taurus	---VDLT <b>KPLIAT</b> <b>RR</b> <b>RGVT</b> ACHIALAAYLCG---KPDVAIYDGSWFEWFH <b>RAPPETWVSQ</b> 291
TST_G.gallus	---VDLSKPLTAT <b>RR</b> <b>RGVT</b> ACHIALAAYLCG---KPDVAIYDGSWFEWFH <b>RAPPQYKVTE</b> 288
TST1_S.tokodaii	---IN <b>KDKE</b> IIVVY <b>CR</b> TGAPASAVWYVL <b>KEVLS</b> --YK <b>NVRL</b> YDGSWVEYGNLVGV <b>PIER</b> -- 267
TST2_S.tokodaii	---IS <b>QDKE</b> IITY <b>CR</b> IGEPAAHTWFVL <b>KYLLG</b> --YPAVRVYDGSWAEWGNIVGAPV <b>KKGN</b> 291
MST_A.vinelandii	---ERP <b>VER</b> LVAYCGSGVTACHNLFAL <b>SLAG</b> ---YPLAPLYAGSWSEWLTDRSRPVATGD 284
TST_A.vinelandii	---ITPD <b>KE</b> IIVTH <b>CR</b> THH <b>S</b> GLTYLIAKALG---YPRV <b>KGY</b> AGSWGEGWGNHPDT <b>PVEL</b> -- 271
St2_Y.lipolytica	---PSK <b>NM</b> HVV <b>FY</b> <b>Q</b> SGV <b>F</b> ARMAEK <b>Q</b> GE <b>Q</b> CG---YEN <b>R</b> GIYLG <b>S</b> WKE <b>S</b> QY <b>E</b> TE <b>V</b> GG <b>Q</b> C-- 143
St3_Y.lipolytica	---PDIN <b>DEL</b> V <b>FY</b> <b>Q</b> AG <b>I</b> SAKAES <b>L</b> A <b>E</b> TCG---YQLRAN <b>Y</b> PGSYNDWLA <b>HQ</b> K----- 194
MST_C.elegans	---IKV <b>G</b> DT <b>V</b> VIG <b>G</b> IGLSASAIWLAAAR <b>S</b> G---IVAKLYNGG <b>V</b> HELAY <b>K</b> AP <b>Q</b> HL <b>N</b> TK <b>G</b> 300
	* . * * . :
MST_P.anserina	TVEQHSE-- 346
MST_N.crassa	KAE----- 333
MST_S.cerevisiae	NRD----- 304
St1_Y.lipolytica	ENLNEANRA 315
MST_E.coli	-----
MST1_A.thaliana	VESSS----- 379
MST2_A.thaliana	SSS----- 318
MST_T.aestivum	STGS----- 307
MST_B.taurus	GRGKI <b>H</b> --- 297
MST_H.sapiens	GRGK <b>TH</b> --- 297
MST_G.gallus	GKGK <b>TV</b> --- 297
MST_D.rerio	GKGK <b>QP</b> --- 296
TST_H.sapiens	GKSE <b>KA</b> --- 297
TST_B.taurus	GKGG <b>KA</b> --- 297
TST_G.gallus	LKR <b>NK</b> G--- 294
TST1_S.tokodaii	-----
TST2_S.tokodaii	EP----- 293
MST_A.vinelandii	-----
TST_A.vinelandii	-----
St2_Y.lipolytica	-----
St3_Y.lipolytica	-----
MST_C.elegans	-----

**Figure 9.6** Alignment of the *st1* subunit with tandem rhodanese domain repeat enzymes from other organisms

*Y. lipolytica* *st1* subunit exhibits the highest similarity to a sulfurtransferase of another *Ascomycota* fungus *Podospora anserina*. The 3-mercaptopyruvate:cyanide sulfurtransferase (MST) catalytic modules containing six-amino-acid active-site loop are highlighted in grey; the conserved cysteine residue is highlighted in red; the thiosulfate:cyanide sulfurtransferase (TST) active sites are highlighted in blue; the active site of the *st1* subunit is highlighted in green; the active site of single rhodanese domain-type enzymes of which two candidate open reading frames CAG82611.1 (*st2* - theoretical protein) and CAG78833 (*st3* - theoretical protein) were identified in the *Y. lipolytica* genomic sequence are highlighted in yellow. For the cladogram of tandem rhodanese domain repeat enzymes see *Figure 9.7*

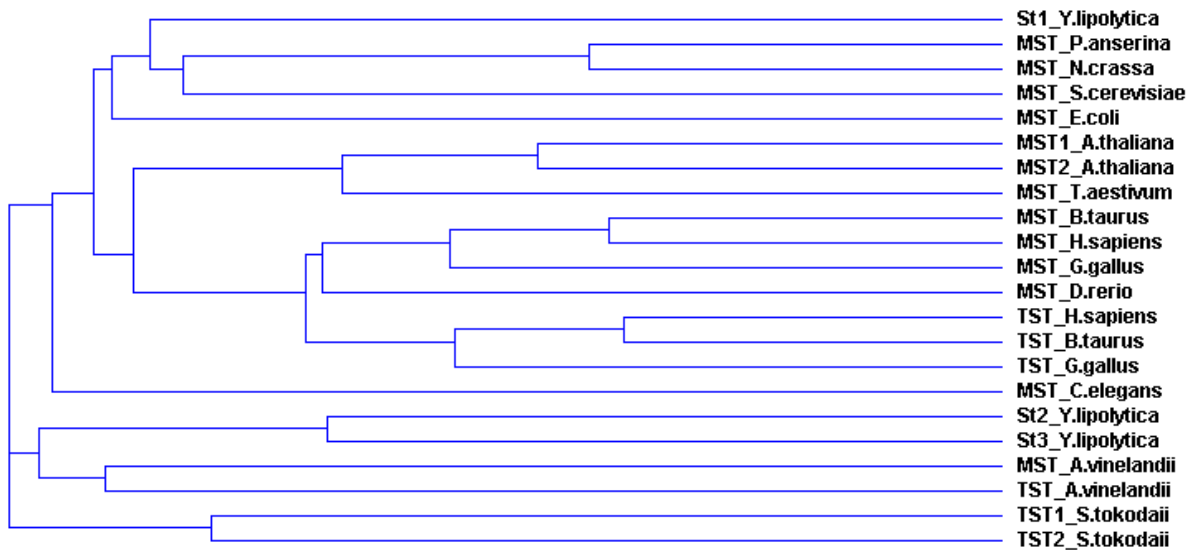


**Figure 9.7** The cladogram of tandem rhodanese domain repeat enzymes aligned in 9.4.3

The cladogram was predicted with the CLUSTALW software (EMBL-EBI, Heidelberg, Germany).

#### 9.4.4 Alignment of *S. cerevisiae* and *Y. lipolytica* mitochondrial FASII enzymes

The protein sequences of the mitochondrial fatty acid synthase type II enzymes from *Y. lipolytica* were obtained using BLAST search in Genolevures database <http://www.genolevures.org>. by comparison to the *S. cerevisiae* (Sc) FASII enzymes. *Y. lipolytica* (YAL) protein sequences are denoted with the accession number.

```

Sc_CEM1          MSRRVVI TGLGCVT PLGRSL SESWGNLL SSKNGLT PITSLPNYNEDY KLRKSI PSTITV 60
YALI0F30679g    MTR-VVVTGLGLVSP LGVGVKQAWNRLIAGKSG---IVALDERFDALSCRVG----- 48
*:* **:*:*:* *:*:* .:.*:*..*:*:* *:* * : : . * : : :

Sc_CEM1          GKIPENFQENSAINKLLFTSQDERRTSSFIKLALRTTYEALHNAGLLNPNDITINTSLC 120
YALI0F30679g    GVVPQDEWSEASSAN---LAAGEIKRVPLFAQYAMVAAQEAVNDSKLLADAGESAKH--- 102
* :*:: . * * : * : : : : : * . * : * : : * : : : * * . : : :

Sc_CEM1          NLDHFGCLIGSGIGSIQDIYQTSLQFHNDNKR-INPYFVPKILT NMAAGNVSIKFNLRGL 179
YALI0F30679g    --TDIGCSI GTGIANMAELADTVTAFNNK GPRGISPLFVPRIIANMGAGHVSMRFLQGP 160
: .:* **:*:*..: : : * * : * . * * * * : : : * * : * : * *

Sc_CEM1          SHSVSTACATGNNSIGDAFN FIRLGMQD ICVAGASETSLHPLSLAGFIRAKSITNG--- 236
YALI0F30679g    NHSVSTACATGAHSIGDAANFIRLGYAKAMIAGSTEACMHPIALGGFARAKSVATKW NDS 220
.***** :***** ***** . :*:*:*:*:*:*:* * * : * : * : *

Sc_CEM1          ---ISRPFDTQRSGFVLGEGCGMIVMESLEHAQKR NANIISELVGYGLSSDACHITSPPA 293
YALI0F30679g    PSEASRPFDKDRGGFVMGEGSAVLVLEEYEHAVARGAPIYAEVCGYGLSGDAHHTAPPD 280

```

```

          *****:*.***:***.:::*. ** * * *: : *****.* ** **:*
Sc_CEM1      DNGAKRAIEMALKMARLEPTDVDYVNAHATSTLLGDKAECLAVASALLPGRSKSKPLYI 353
YALI0F30679g DNGAYRAMKQALKQANVSAVKIDYVNAHATSTPLGDAENAALT-QLFEGRNLS-DIAV 338
          ***** *: : ** * * : . . . . : ***** ** * * *: : * : ** . * : :

Sc_CEM1      SSNKAIGHLLGARGAVESIFTICSLKDDKMPHTLNLNDNVLTLENNEADKLFHFRDKPIV 413
YALI0F30679g SSTKGAIGHLLGGAGSVEALFTIKALETGDLPTLNLN---ELSDPDVFKFNFVP-KETQ 394
          **_*****_ *: **: **: *: : . : * *****: : : * . : . * : : : *

Sc_CEM1      GANPKYALCNSFGFGGVNTSLLFKKWEGS 442
YALI0F30679g HRDVRVYALNNSFGFGGTNSSLFGKV--- 420
          : : ** * *****_* : ***** *

```

### Figure 9.8 Mitochondrial beta-keto-acyl synthase (CEM1)

*Cem1* posses possible role in fatty acid synthesis and is required for mitochondrial respiration.

#### ETR1 homologue YALI0C19624g

```

Sc_ETR1      KTLAFPINPSDINQLQGVYPSRPEKTYDYSTDEPAAIAGNEGVFEVVSLSGSSKGDLLK 114
YALI0C19624g KSLGFTINPADINQLEGVYPSVPPKSQVINNED-AAIGGNEGLFQVLDP---GAKSGLKK 116
          *: *_**_* : *****: ***** * * : : . : : : ** * . *****: *: : . . : * . **

Sc_ETR1      GDRVIPLQANQGTWSNYRVFSSSSDLIKVN--DLDFSAATVSVNGCTGFQLVSDYIDWN 172
YALI0C19624g GDWVLPKTCFGTWRSHALVEADT-VVKIDNTDLTKVQATTVSVNPSTAYEMLKDLKEG- 174
          ** * : * : : ** * . : . . . . : : * : : ** * . * : *****_* . * : : : : * :

Sc_ETR1      SNGNEWIIQNAGTSSVSKIVTQVAKAKGIKTLVIRDRDNFDEVAKVLEDKYGATKVISE 232
YALI0C19624g ----DWFIQNGGNSGVRAAIQIGHIRLKSISVVRDRPDLEVLKKELT-DLGATHVITE 229
          : * : ** * . * . * . : . * : : : * : : : : ** * : : : : * * * * * : : * : * :

Sc_ETR1      SQNNDKTFAKEVLSKIILGENARVRLALNSVGGKSSASIAARKLENNALMLTYGGMSKQPVT 292
YALI0C19624g EEASDKLFSKQIKSWTGGK---IKLALNCIGGKSATSIMRQLGAGGSIVTYGGMSKKPLT 286
          . : * ** * : * : : * * : : * : : * : : : * : * : * . : : : *****_* : * :

Sc_ETR1      LPTSLHIFKGLTSKGYWVTEKNKKNPQSKIDTISDFIKMYNYGHIISPRDEIETLTWN-T 351
YALI0C19624g FPTGPFIFKDI TAKGYWLTWRADKHPBEKAKTIENIFKFYREKKFVAPPVNI STLDFSKG 346
          : ** . * ** . : : *****_* . * : : : * . * . : : : * . : : : * : * * * : .

Sc_ETR1      NTTTDEQLLELVKKGITGKGGKKMVVLEW- 380
YALI0C19624g NDVVLSEFLDALGKAQKGGKKQLVQWVEY 376
          * . . . : * : : * . * * * : : *

```

#### ETR1 homologue YALI0B12386g

```

Sc_ETR1      MLPTFKRYMSSSAHQIPKHFKSLIYSTHEVEDCTKVLVSVKNYTPKQDLSQSIVLKTLAFF 60
YALI0B12386g -----MKSVQVKDDKGAENLYIGEGPTPNPQNGQ-LLVKTEYVFG 39
          : : : : : : . : . : . : . : ** : : * : : * *

Sc_ETR1      INPSDINQLQGVYPSRPEKTYDYSTDEPAAIAGNEGVFEVVSLSGSSKGDLLKLDGDRVIP 120
YALI0B12386g LNRMDLLQRLGNYPPLPQAPKTLGVFEFGTIEKSE-----SDKFAVGDKVFG 86
          : * * : * * ** * : . . : . : * . * : : : . . . : ** : * :

Sc_ETR1      LQANQGTWSNYRVFSSSSDLIKVNDLDFSAATVSVNGCTGFQLVSDYIDWNSNGNEWII 180
YALI0B12386g LVYG-GAYAEYVVAEETLIKVPDLSMEVAAGLPEVWF TGIQVLT TVGKFKQKGS--VL 143
          * . * : : : * * . . : : * : : * * . . * : * : : : . : . . . . : :

```

```

Sc_ETR1      QNAGTSSVSKIVTQVAKAKGIKTLVIRDRDNFDEVAKVLEDKYGATKVISESQNNDKTF 240
YALI0B12386g FHAGASSVGIQAVIQLAASLGASKIFTT VGSDEKCEFVKKLGKNGFVTVVPINYNHED--- 200
      :*:***. * *: * : * . : . . * : * . * * :*: * * * : :*: * :

Sc_ETR1      AKEVLSKIILGEN--ARVRLALNSVGGKSSASIAKLENNALMLTYGGMSKQPVT--LPTS 296
YALI0B12386g FKEVISKHYDASKGEGVNVIIIDPVGQTYFVRNLEIAAKDARIVLMGAMSGPIVKGDVPIG 260
      ***:* * . . * : : : * * . . . . : : * : : * . * * * . : * .

Sc_ETR1      LHIFKGLTSKGYWVTEKNKKNPQSKIDTISDFIKMYNYGHIISPRDEIETLTWNTNTTTD 356
YALI0B12386g LIIYKRLVVQGTTLRSRD---LAYQEKLRDFFVSHVPLILEG--KIDTFVDKLFNFFTT 314
      * * : * * . : * : : : : : * : : : * : . : * : * : . : . *

Sc_ETR1      EQLLELVKKGITGKGGKKKMVVLEW 380
YALI0B12386g EDIVASHKYLESNKSMGKIVIKI- 337
      * : : : * . : . * : : *

```

**Figure 9.9 2-enoyl thioester reductase (ETR1)**

The ETR1 is the member of the medium chain dehydrogenase/reductase family. It is localized into the mitochondria, where it has a probable role in fatty acid synthesis. Two different ETR1 homologues are present in *Y. lipolytica*.

```

Sc_HFA1      -----
YALI0C11407g MRLQLRTLTRFFFSMASGSSTPDVAPLVDPNIHKGLASHFFGLNSVHTAKPSKVKEFVAS 60

Sc_HFA1      -----MRSIRKWAYETFNDEKIIQFVVMATPDDLHANSEYIRM 38
YALI0C11407g HGGHTVINKVLIANNGIAAVKEIRSVRKWAYETFGDERAISFTVMATPEDLAANADYIRM 120
      :*:*****. * : * . * * * : * * * : : * * *

Sc_HFA1      ADQYVQVPGGTNNNNYANIDLILDVAEQTDVDAVWAGWGHASENCPPELLASSQRKILF 98
YALI0C11407g ADQYVEVPGGTNNNNYANVELIVDAERFQVDAVWAGWGHASENPLLPESLAASPRKIVF 180
      ***** : ***** : : * : * * * : . ***** * * * * * * * * * * * *

Sc_HFA1      IGPPGRAMRSLGDKISSTIVAQSAKIPCIWPSGSHIDTIHIDNKTNFVSVPPDDVYVRGCC 158
YALI0C11407g IGPPGAAMRSLGDKISSTIVAQHAKVPCIPWSGTGVDVVVDKSTNLVSVSEEVYTKGCT 240
      ***** ***** * * : * * * * * : : * : : * : . * * : * * * . : : * * : * *

Sc_HFA1      SSPEDALEKAKLIGFPVMIKASEGGGKGIIRVDNEDDFIALYRQAVNETPGSPMFVMKV 218
YALI0C11407g TGPKQGLEKAKQIGFPVMIKASEGGGKGIIRKVEREEDFEAAYHQVEGEPGSPIFIMQL 300
      . : * : . * * * * * * * * * * * * * * * * * * * * * * * * * * * * * * * * * * * * * * * * * *

Sc_HFA1      VTDARHLEVQLLADQYGTNITLFRDCSIQRRHQKIIIEAPVTITKPETFQRMERAAIRL 278
YALI0C11407g AGNARHLEVQLLADQYGNISLFRDCSVQRRHQKIIIEAPVTVAGQQTFTAMEKAAVRL 360
      . : * * * * * * * * * * * * * * * * * * * * * * * * * * * * * * * * * * * * * * * * *

Sc_HFA1      GELVGYVSAGTVEYLYSPKDDKFFYLELNPRLQVEHPTTEMISGVNLPATQLQIAMGIPM 338
YALI0C11407g GKLVGYSAGTVEYLYSHEDDKFFYLELNPRLQVEHPTTEMVTGVNLPAAQLQIAMGIPL 420
      * : * * * * * * * * * * * * * * * * * * * * * * * * * * * * * * * * * * * * * * * * *

Sc_HFA1      HMISDIRKLYGLDPTGTSYIDFKN-----LKRPSPKGHICISCRITSEDPNEGFKPST 390
YALI0C11407g DRIKDIRLFYGVNPHTTTPIDFDFSGEDAKTQRRPVRGHTTACRITSEDPGEGFKPSG 480
      . * . * * * : * : * : * * . * * * . * * * * * * * * * * * * * * * * * * * * * * * *

Sc_HFA1      GKIHELNFRSSSNVWGYFSVGNNGAIHSFSDSQFGHIFAVGNDRQDAKQNMVLALKDFSI 450
YALI0C11407g GTMHELNFRSSSNVWGYFSVGNQGGIHSFSDSQFGHIFAFGENRSASRKHMVVALKELSI 540
      * . : * * * * * * * * * * * * * * * * * * * * * * * * * * * * * * * * * * * * * * * * *

Sc_HFA1      RGEFKTPIEYLIELLETRDFESNNISTGWLLDLILKNLSSDSKLDPTLAIICGAMKAYV 510

```

---

YALI0C11407g	RGDFRTTVEYLKILLETDFEDNITITGWLDELISNKLTAE-RPDSFLAVVCGAATKAHR	599
Sc_HFA1	FTEKVRNKYLELLRRGQVPPKDFLTKFPVDIFDNNRYLFNVAQSSEEQFILSINKSQC	570
YALI0C11407g	ASEDSIATYMASLEKQGVFARDILKTLFPVDFIYEGQRYKFTATRSEDSYTLFINGSRC	659
Sc_HFA1	EVNVQKLSSDCLLISVDGKCHTIVYWKDDIRGTRLSIDSNTIFLEAELNPTQVISPTPGKL	630
YALI0C11407g	DIGVRPLSDGGILCLVGGRSHNVYWKKEVGATRLSVDSKTCLEVENDEPTQLRSPSPGKL	719
Sc_HFA1	VKYLVRSGDHVFAQQYAEIEIMKMOMPLVAKSDGVIELLRQPGSIIEAGDVIAKLTLDS	690
YALI0C11407g	VKFLVENGDHVRANQPYAEIEVMKMYMTLTAQEDGIVQLMKQPGSTIEAGDILGILALDD	779
Sc_HFA1	PSKANESSLYRGELPVLGPPLIEGSRPNHKLRLVINRLENIINGYHENSGETTLKELIK	750
YALI0C11407g	PSKVHAKPFEGLPELGPPTLSGNKPHQRYEHCQNVLHNILLGFDNQVVMKSTLQEMVG	839
Sc_HFA1	ILRDGRLPYSEWDSQISTVVRNLPRQLNEGLGNLVKKSVS----FPAKELHKLTKRYLEE	806
YALI0C11407g	LLRNPELPYLQWAHQVSSLHTRMSAKLDATLAGLIDKAKQGGFFPAKQLLRALKEASS	899
Sc_HFA1	NTNDHVYVALQPLKISERYSEGLANHECEIFLKLKYYAVEKIFENHDIHEERNLLN	866
YALI0C11407g	GEVDALFQQLAPLFDLAREYQDGLAIHELQVAAGLQAYYDSEARFCGPNVRDEDVILK	959
Sc_HFA1	LRRKDLTNLKKILCISLSHANVVAKNKLVTAILHEYEPLCQDSSK-----MSLKFRAV	919
YALI0C11407g	LREENRDSLRKVVMAQLSHSRVGAKNLVLALLDEYKVADQAGTDSPASNVHVAKYLRPV	1019
Sc_HFA1	IHDLASLESKWAKEVAVKARSVLLRGIFPPIKKRKEHIKTLQLHDKDTGAENIHSRNIY	979
YALI0C11407g	LRKIVELESRASAKVSKAREILIQCALPSLKERTDQLEHIRRSSVVEESRYGEVGLHRT	1079
Sc_HFA1	SCMRDFGNLIHSNLIQLQDLFFFQDHTALSSIASEIYARYAYGNYQLSKIKHKG-AP	1038
YALI0C11407g	PRADILKEVVDISKYIVFDVLAQFFAHDDPWIVLAALELYIRRACKAYSILDINYHQSDSL	1139
Sc_HFA1	DLLMSWQF-----SSLRNYLVNSDGESDEFTKLSKPPSTS-----GKSSANSFGLLV	1085
YALI0C11407g	PPVISWRFRLPTMSSALYNSVSSGSKTPSPSVRADSVDFSYTVERDAPARTGAIV	1199
Sc_HFA1	NMRALESLEKTLDEVEEQIHIPEE--RLSSGEN-----SLIV	1120
YALI0C11407g	AVPHLDDLEDALTRVLENLPKRGAGLAI SVGASNKSAASARDAAAAASSVDTGLSNIC	1259
Sc_HFA1	NILSPIRYSEND--LIKTLKIKLHENERGLSKLVNRITFAFIAANAPAVKFYSFDGTT	1178
YALI0C11407g	NVMIGRVDESDDDDTLIARISQVIEDFKEDFEACSLRRITFSFGNSRGTYPKYFTFRGPA	1319
Sc_HFA1	YDEISQIRNMDPSYEAPLELGMKSNYKIRS LPTYDSSIRIFEGISKFTPLDKRFFVRKII	1238
YALI0C11407g	YEEDPTIRHI PALAQLELARLSNFDIKPVHTDNRNIHVY EATGKNAASDKRFFTRGIV	1379
Sc_HFA1	NSFMYNDQKTTEENLKAENAQVVMLEHLGAVDISNSDLNHI FLNFNTV LNIPVHRL EE	1298
YALI0C11407g	RPGRLENIPTSEYLI SEADRLMSDILDALVI GTTNSDLNHI FINFSAVFALKPEEVEA	1439
Sc_HFA1	IVSTILKTHETRLFQERITDVEICISVECLETKKPAPLRLLISN KSGYVVKIETYYEKIG	1358
YALI0C11407g	AFGGFLERFGRLLWRLRV TGA EIRMMVSDPETGSAPPLRAMINNVSGYVVQSELYAEAKN	1499

---

```
Sc_HFA1      KNGNLIILEPCSEQSHYSQKSLSLPYSVKDWLQPKRYKAQFMGTTYVYDFPGLFHQAAIQQ 1418
YALI0C11407g DKGQWIFKSLGKPGSMHRSINTPYPTKEWLQPKRYKAHLMGTTYCYDFPELFRQSIESD 1559
.:*: *::. .: .      :*: . * . .:*****:***** *:* *:*: .:

Sc_HFA1      WKRYFPKHKLNSFFSWVELIEQNGNLIKVNREPLNNIGMVAFEIMVQTPEYPEGRNMI 1478
YALI0C11407g WKKYDYGKAPDDLMTCNELILDEDSGELQEVNREPGANNVGMVAWKFQAKTPEYPRGRSFI 1619
*:* * : . : * * .: * * :***** *:******:: .:***** . * .:

Sc_HFA1      VISNDITYNIGSFGPREDLFFDRVNTYARERGIPRIYLAANSKAKLGAEEIPLFRVAW 1538
YALI0C11407g VVANDITFQIGSFGPAEDQFFFKVTELARKLGIPRIYLSANSGARIGIADELVGKYKVAW 1679
*:******:***** * * * :*: * : *****:*****:***:***: .:***

Sc_HFA1      NDPSDPTKGFQYLYLAPKDMQLLKDSGKNSVVEHKMVYGEERYIIKAIVGFEEGLGVE 1598
YALI0C11407g NDETDPKSGFKYLYFTPELATLKPDTVVVTEIEEEGPNQVEKRHVIDYIVGEKDGGLVE 1739
** :*:*:*:*:*:*:*:*:*: ** . . : : * . *:::* . * * : :*****

Sc_HFA1      CLQGSGLIAGATSKAYRDIPTITAVTCRSVIGSYLVRGQRTIQVEDKPIILTGASAIN 1658
YALI0C11407g CLRGSLIAGATSRAYKDIPTTLTVTCRSVIGAYLVRGQRAIQIEGQPIILTGAPAIN 1799
*:******:***:***:* * * * * * :*****:*****:***:***: .:***** . * *

Sc_HFA1      KVLGTDIYTSNLQIGGTQIMYKNGIAHLTASNDMKAIEKIMTWLSYVPAKRDMSPLLE-E 1717
YALI0C11407g KLLGREVYSSNLQLGGTQIMYNNGVSHLTARDDLNGVHKIMQWLSYIPASRGLPVPLPH 1859
*:** :*:***:*****:***:*** * :::: . : * * * * : * . . . * : * .

Sc_HFA1      TMDRWDRDVFDPKAKQVPYEARWLEIEGKWDENNFSGLFDKDSFFETLSGWAKGVIVGR 1777
YALI0C11407g KTDVWRDVFQPVGRGEQYDVRWLISGRTELDGAFESGLFDKDSFQETLSGWAKGVVGR 1919
. * * * * * * * * . : * . * * * . * : . . . * : * * * * * * * * * * * * * *

Sc_HFA1      ARLGGIPVGVIAVETKTIEEIIIPADPANLDSSEFSVKEAGQVWYPNSAFKTAQTINDFNY 1837
YALI0C11407g ARLGGIPFGVIGVETATVDNTPADPANPDSIEMSTSEAGQVWYPNSAFKTSQAINDFNH 1979
***** . * * . * * * * : : : * * * * * * * * * * * * * * * * * * * * *

Sc_HFA1      GEQLPLIILANWRGFSGGQRDMYNEVLKYGSFIVDALVDYKQPILYIPPFGLRGGSWV 1897
YALI0C11407g GEALPLMILANWRGFSGGQRDMYNEVLKYGSFIVDALVDYKQPIMVYIPPTGLRGGSWV 2039
** * * . :*****:*****:*****:*****:*****:*****:*****:*****:*****

Sc_HFA1      VIDPTINPEQMEMYADVESRGGVLEPDGVVSIKYRKEKMIETMIRLDSTYGHLLRRLTEK 1957
YALI0C11407g VVDPTINSDMMEYADVESRGGVLEPEGMVGIKYRRDKLLDTPMARLDPEYSSLKKQLEES 2099
*:******: * * * * * * * * * * * * * * * * * * * * * * * * * * * * * *

Sc_HFA1      KLSLEKQNDLTKRLKIRERQLIPIYQIISIQFADLHDRSTRMLVKGIVIRNELEWKKSRRF 2017
YALI0C11407g PDSEE----LKVKLSVREKSLMPIYQQISVQFADLHDRAGRMEAKGVIREALVWKDARRF 2155
* * * . : * : * * : * * : * * * * * * * * * * * * * * * * * * * * *

Sc_HFA1      LYWLRRLRNNEGQVIKRLQKKTCDNKTKMKYDDLKIVQSWYNDLDVNDRAVVEFIERN 2077
YALI0C11407g FFWRIRRLRVVEYLITKINSILPS---CTRLECLARIKSWKPATLDQGSDRGVAEWFDEN 2212
:***:*** * : * . : : . . : : * * . * * . . * * . * * . : . *

Sc_HFA1      SKKIDKNIIEFEISLLIDELKKKFE-DRRGNIVLEELTRLVDSKRKR 2123
YALI0C11407g SDAVSARLSELKKDASAQSFAQLRKDRQGTLDQ----- 2245
* . . . . : * : : . : : . : . * * : * . :
```

**Figure 9.10 Mitochondrial acetyl-coenzyme A carboxylase (HFA1)**

HFA1 catalyzes the production of malonyl-CoA in mitochondrial fatty acid biosynthesis.



```

Sc_HTD2      MKSKTWIFRDVLSHRTKAFDSSLCCR-----LPVSKATKHLQLGHEHFLFFPP--SFEK 52
YALI0A19096g MLRQFIRSYSTASSSTASSIAALKARAPWRKLDYVSPVTSQMLKTSISHLFFQQPEKQFQV 60
* :      .. ** ::: : * . *      .. :: * : . . ** * . * :

Sc_HTD2      LDRD-----GYFNYQNPA SLLG-----NPDLYRRRIWGQG--ELVQYLPVTLDQE 96
YALI0A19096g GDAVPPGFHMAYFNPCDEPTLASDGYSEQQAPGEPYVNRMWLGGSVFHKGRQLSMGEQ 120
*      .*** : * . *      * . * . * : * : : : : : : :

Sc_HTD2      YTCHEIKYVKKIR-DEHVVCIERLLQERPENVSSPMDICLFERRVLMYTNSPAN---- 151
YALI0A19096g STCSESLVQVREPGSSTSGDKLLVTIQRDLRNDSAPAEPAVTEKRTLIMKAETGQKRG 180
** ** : * : : . : * : : : : : . . : . : * * * * : : : .

Sc_HTD2      KTAVKMPVGEENYKILKNFTVTDMDIVAYGQMSLNPHRIHWDKEYSRVVEGYDDIIMQGP 211
YALI0A19096g ATFEKIISPFDGATHSVSFVPSSTLLFRYSALTFNGHKIHYDPDYAREVESLPAVIVHGP 240
* * : : . . . * . . . . * . : : * * * * * : * * * * . : * * * *

Sc_HTD2      FSVQLLQKCIQPFLEQPIR-----QLRYRNLNYIYPNTTSLICQSLSSSSGMYTFQIRDL 266
YALI0A19096g LTVTLMLTWMNGVIQKDLPGKRIAFAFEYKNVLPFCNNELTLRCKPLMNSDGYKQVWIENH 300
: * * : . : : : : : : : : : * : * : : . . * . * . * . * :

Sc_HTD2      QKANLVYMKADVFC 280
YALI0A19096g HQSLCMNGTVKVE- 313
: : : : . . . *

```

### Figure 9.11 Mitochondrial 3-hydroxyacyl-thioester dehydratase (HTD2)

HTD2 is involved in the fatty acid biosynthesis and is required for respiratory growth and normal mitochondrial morphology

```

Sc_MCT1      --MKLLTFPGQGTSSISISILKAIIRNKSRFQITLSQNGKESNDLLQYIFQNPSSPGSIA 58
YALI0E18590g MSLRAAFFPQGQLRPRMLQKLWQSAIR--ETLKPALDQLKTEVQEVLLGNSS----- 52
: :      * * * * * . . : * : . * : : : . . : . : : : : : * . * :

Sc_MCT1      VCSNLFYQLYQILSNPDPQDQAPKNMTKIDSPDKKDNEQCYYLLGHSILGELTCLSVNSLF 118
YALI0E18590g --LGEDEQMKLITQTQNAQPGILLSSYASFLANQGASKNYSHLLGHSILGEYSALVCGGYL 110
: .      * : * . . . . . . . : : : : : . : : . : * * * * * * * : * . . :

Sc_MCT1      SLKDLFDIANFRNKLMTVSTEKYLVAHNINRSNKFEMWALSSPRATDLPQEVQKLLNSPN 178
YALI0E18590g TLEQGVQLVQKR-----GYMQRANDESGKETAMVALLLHRTVDINRLVQACEG--- 159
: * : : : : * : : :      * : * : : : : * * * * : * . * : : * * .

Sc_MCT1      LLSSSQNTISVANANSVKQCVVTGLVDDLESRLRTELNLRFPLRITELTNPYNIPFHNST 238
YALI0E18590g -----WNGANVANINSSGQVVLSGERSAINELVAHLKASKLRVLKAIPLN-VSAPFH-SA 212
: :      * . * * * * * * : * : . : : * : * : : * : : * . * * * * :

Sc_MCT1      VLRPVQEPLYDYIWDILKKNHTHTLMELNHPPIIANLDGNISYYIHHALDRFVKCSSRTVQ 298
YALI0E18590g IMAVVSSELDVACQQLKIR---PDFSADKPVVSNASGKPFGSADEMYESMIGSPVHTVN 269
: : * * . *      : : : : : : : : : * * : . . : : : . : * * :

Sc_MCT1      FTMCYDTINSGTPVEIDKSI CFGPGNVIYNLIRRNCPQVDTIEYTSLATIDAYHKA A EEN 358
YALI0E18590g WLASVEYLKHVGVVESDG---YGPVCVDIGKMLVLPGERYD----- 306
: . : : :      * * * : : * * * . : : : * : : : : :

Sc_MCT1      KD 360
YALI0E18590g --

```

### Figure 9.12 Predicted malonyl-CoA:ACP transferase (MCT1)

MCT1 is a putative component of a type-II mitochondrial fatty acid synthase, which produces intermediates for phospholipid remodelling.

**OAR1 homologue YALI0F29975g**

```

Sc_OAR1      -MHYLPVAIVTGATRGIGKAICQKLFQKGLSCIILGSTKESIERTAIDRGQLQSGLSYQR 59
YALI0F29975g MSLRNTTALITGGSGGIGYRISKAFASAGARVIILSHKKEIDTALFALPERLEGEKHHE 60
               . . * : : * : : * * * . * * . * : : : : * . : : .
               . . * : : * : : * * * . * * . * : : : : * . : : .

Sc_OAR1      QCAIAIDFKKWPHWLDYESYDGIIEYFKDRPPLKQKYSTLFDPCKNWSNNERRYVNLIN 119
YALI0F29975g GIVHNVTSIQPPAGVDFSEVD-----VLVN 85
               . : : : * : * . . *
               . : : : * : * . . *

Sc_OAR1      CAGLTQESLSVRTTASQIQDIMNVNFMSPVMTNICKYMMKSQRRWPELSGQS-ARPTI 178
YALI0F29975g CAGISLTGLLSTTSTKDIQNVVNVNLVGTMFMTKFAMEAWQKRYPERAASDRKAENGCCI 145
               * * * : : . * * : : * * : : * * : : . . * . . : : . . *
               * * * : : . * * : : * * : : * * : : . . * . . : : . . *

Sc_OAR1      VNISSILHSGMKKVPGTSVYSASKAALSFRTEVLAAEMEPNIRCFITISPLVKGTDMIQ 238
YALI0F29975g INISSILG-LRAVSPGLSIYAATKTALIMFTKSMCVEGGRMAIRSNAIKCPGYVR-TEMTK 203
               : * * * * * : : * * * : * * : * * * * * * * : : . . * * * : * * * * : * * :
               : * * * * * : : * * * : * * : * * * * * * * : : . . * * * : * * * * : * * :

Sc_OAR1      NLPVEAKEMLERTIGASGTSAPAEIAEEVWSLYSRTALET----- 278
YALI0F29975g AHELSEFKTPLQ-EFGDTGDSVESIANAAAMYFATNPQVSGSILSVDKGICAN 254
               : . * * * : * * : * : . * * : . : : . . : .
               : . * * * : * * : * : . * * : . : : . . : .

```

**OAR1 homologue YALI0C19965g**

```

Sc_OAR1      MHYLPVAIVTGATRGIGKAICQKLFQKGLSCIILGSTKESIERTAIDRGQLQSGLSYQRQ 60
YALI0C19965g MFLRPLQNSQVWINPLVRKYSISASSLSGKTALVTGGSGGIGLVIKLAANG----ARV 56
               * . * : . . : : . . . . . : : . . . * . . : : *
               * . * : . . : : . . . . . : : . . . * . . : : *

Sc_OAR1      CAIAIDFKKWPHWLDYESYDGIIEYFKDRPPLKQKYSTL-FDPCKNWSNNERRY-YVNLIN 118
YALI0C19965g ILLARDETKLNGALEELTHTLTKDEQTORIDITQTAHSTISYDIKATTPPEIDFKMVDLLV 116
               : * * . * * : : : : . : * : : * * : * . : : * : * : * :
               : * * . * * : : : : . : * : : * * : * . : : * : * : * :

Sc_OAR1      NCAGLTQESLSVRTTASQIQDIMNVNFMSPVMTNICKYMMKSQRRWPELSGQSARPTI 178
YALI0C19965g NCAGVTQTSLLMTTKN--IDQIIGTNLAGAIKMSQYAMRPWMKRKSG-----CI 163
               * * * : * * * : * . * : * * : * * : : : * * :
               * * * : * * * : * . * : * * : * * : : : * * :

Sc_OAR1      VNISSILHSGMKKVPGTSVYSASKAALSFRTEVLAAEMEPNIRCFITISPLVKGTDMIQ 238
YALI0C19965g VNISSVLGLRGLTG-GSTVYSAKAGLVGFTKALAVEVGARGIRVNCVCPGLVE-TEMTK 221
               * * * * * : * . * : : * * * : * * * * * * * * : . * * * : . * * * : * * *
               * * * * * : * . * : : * * * : * * * * * * * * : . * * * : . * * * : * * *

Sc_OAR1      NLPVEAKEMLERT-IGASGTSAPAEIAEEVWSLYSRTALET----- 278
YALI0C19965g NVTVQNGFATPLQGMKDNYSVADSVADAVLYLAASEEQTGSILTIDKGLSAV 274
               * : * : : * . . : . . : * * :
               * : * : : * . . : . . : * * :

```

**Figure 9.13 Mitochondrial 3-oxoacyl-[acyl-carrier-protein] reductase (OAR1)**

There are two homologues of OAR1, which are components of the type II mitochondrial fatty acid synthase of *Y. lipolytica*.

### 9.5 *The mass spectrometric analysis of mitochondrial phospholipids*

Masses of phospholipids determined experimentally are indicated above the spectra in black, whereas the theoretical values in violet. Numbers in brackets separated by a colon indicate the number of carbon atoms in the acyl-chains (first number) and the number of carbon atoms involved in the double bond formation in unsaturated chains (second number).

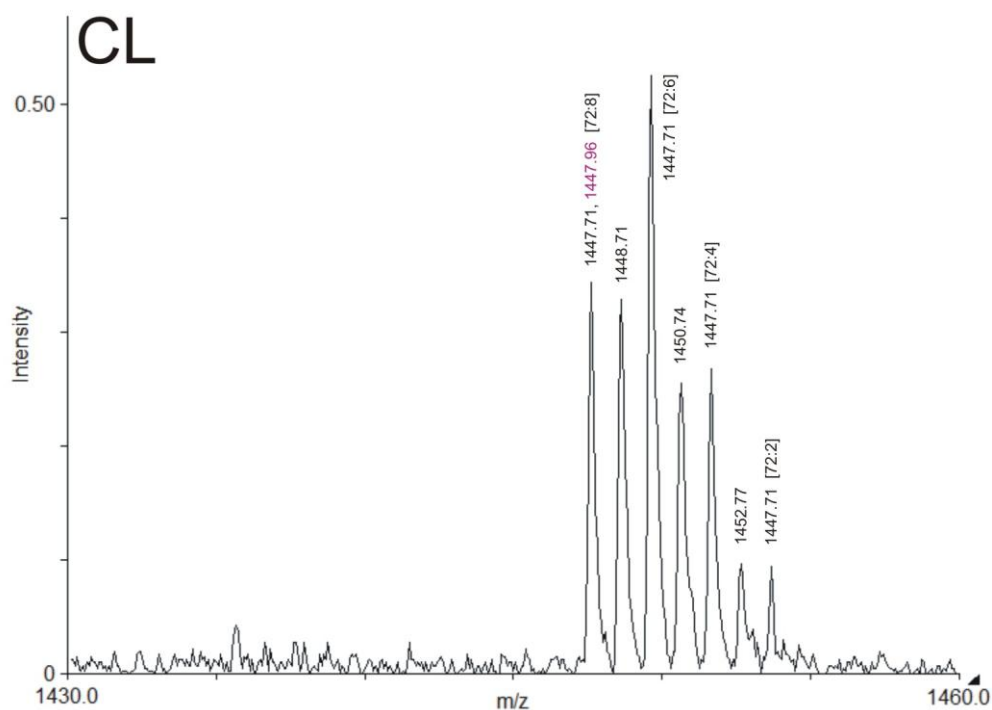


**Figure 9.14** *The MALDI-MS spectrum of cardiolipin identified in fraction 18*

Identification of cardiolipin species substituted with unsaturated acyl-chains containing from 1 to 4 double bonds [72:2-8].

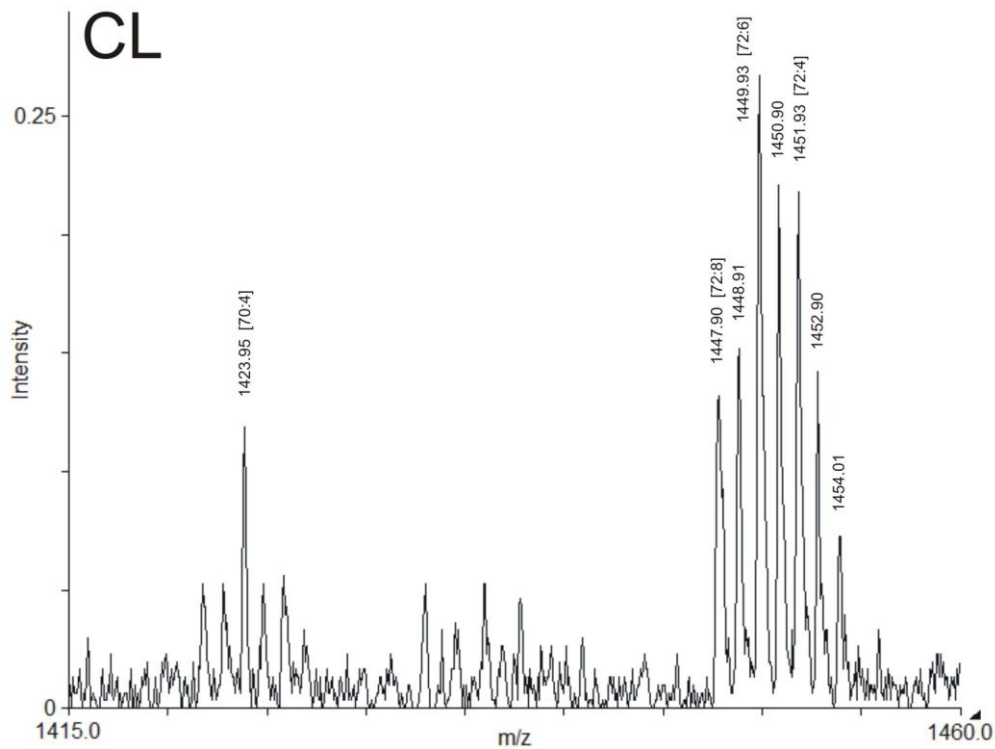


**Figure 9.15** *The MALDI-MS spectrum of cardiolipin identified in fraction 19*

Identification of several cardiolipin species substituted with unsaturated acyl-chains.

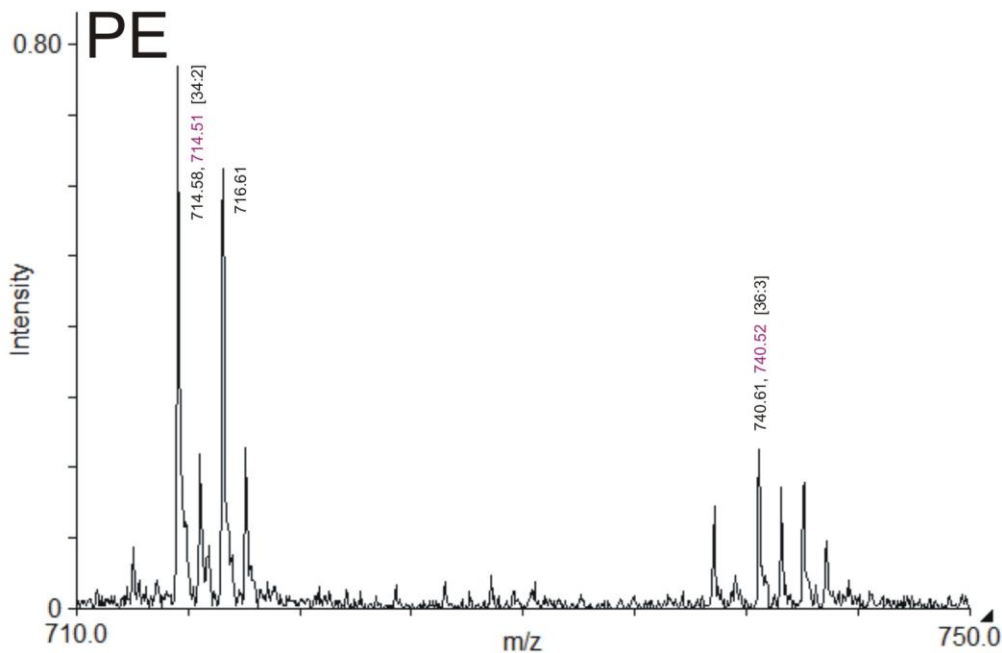


**Figure 9.16** *The MALDI-MS spectrum of phosphatidylethanolamine identified in fraction 24*

Identification of several species of phosphatidylethanolamine substituted with unsaturated acyl-chains.

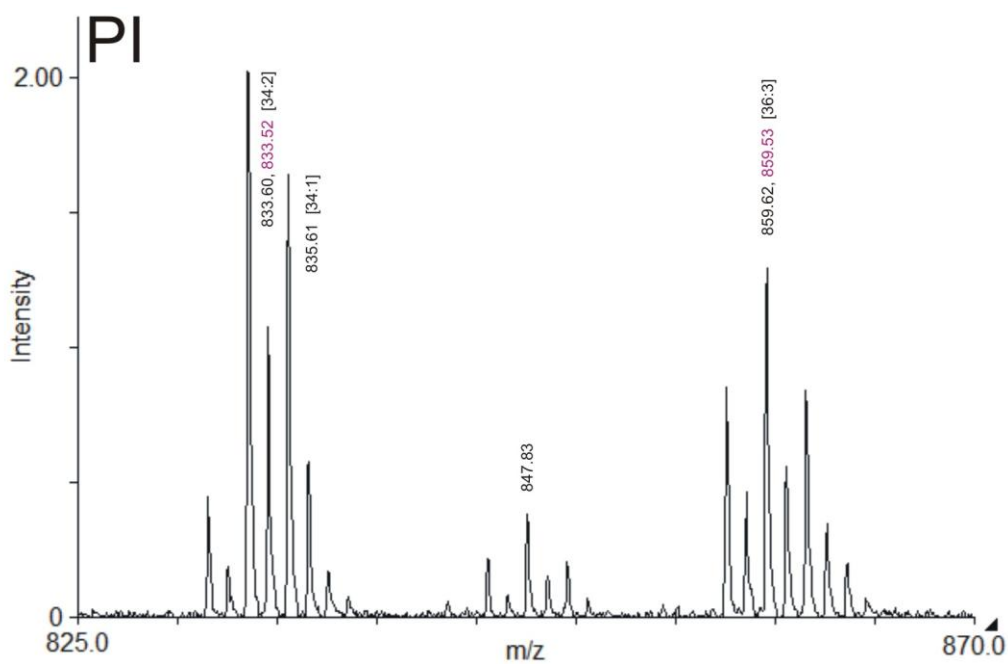


**Figure 9.17** The MALDI-MS spectrum of phosphatidylinositol identified in fraction 28. Identification of several species of phosphatidylinositol substituted with unsaturated acyl-chains.

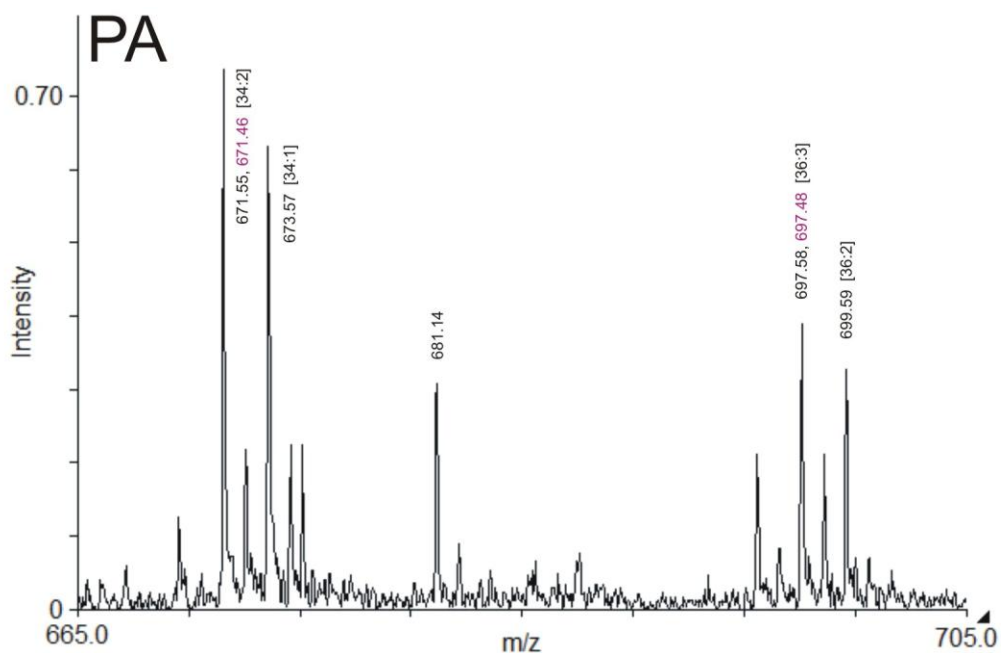


**Figure 9.18** The MALDI-MS spectrum of phosphatidic acid identified in fraction 30. Identification of several species of phosphatidic acid substituted with unsaturated acyl-chains.

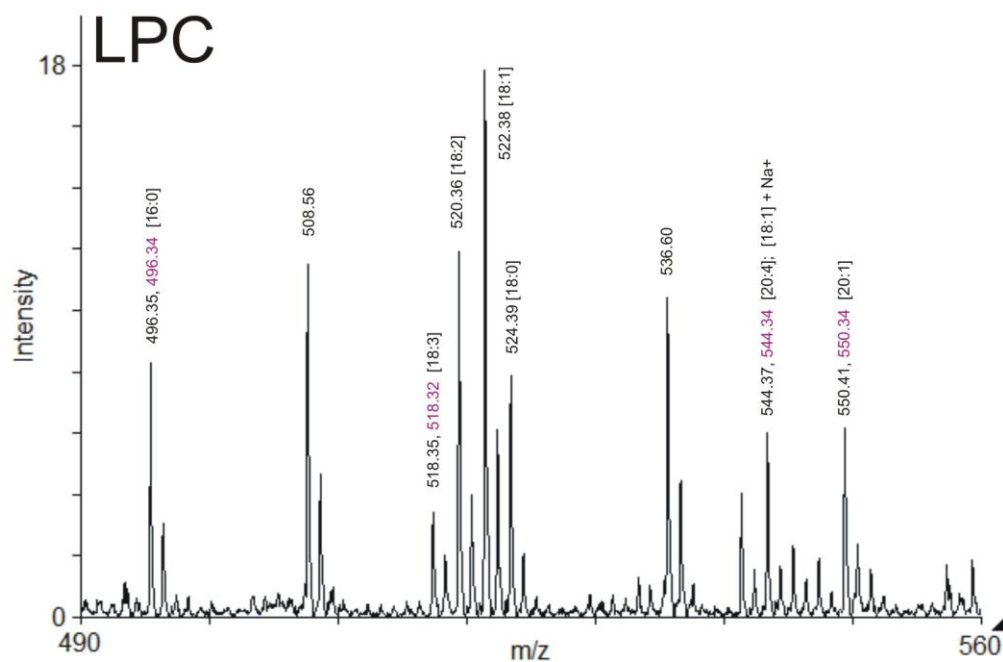


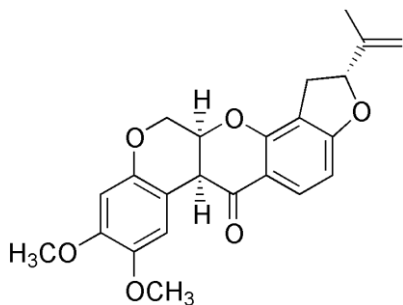
**Figure 9.19** *The MALDI-MS spectrum of lyso-phosphatidylcholine identified in fraction 52*

Identification of several species of lyso-phosphatidylcholine (LPC) substituted with saturated and unsaturated acyl-chains in positive mode. The peak for LPC found at a mass of 496.35 indicates substitution with a palmitoyl-chain (16:0; theoretical mass 496.34 Da), whereas at the mass range 518.35 - 524.39 indicates substitution with different species of stearoyl-chains. Also a peak corresponding to the sodium salt of the stearic acid at a mass of 544.37 was found. This same peak value corresponds to the detected [20:4] acyl-chain (theoretical mass 544.34 Da).

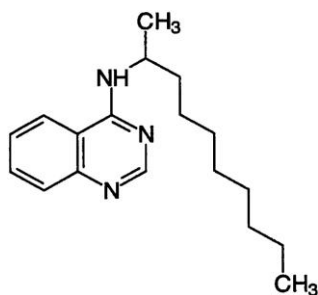
## 9.6 Chemical Structures

### 9.6.1 Complex I Inhibitors

#### 9.6.1.1 Rotenone

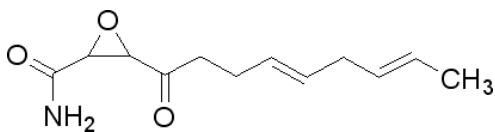


#### 9.6.1.2 2-decyl-4-quinazolinyl amine (DQA)



### 9.6.2 Fatty Acid Synthase Inhibitor

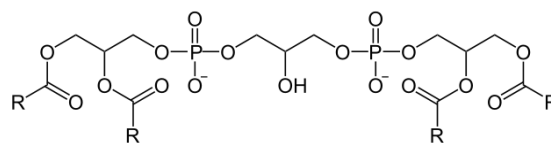
#### 9.6.2.1 Cerulenin



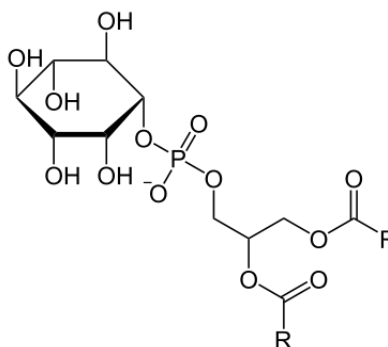
### 9.6.3 Phospholipids

R – hydrocarbon chain

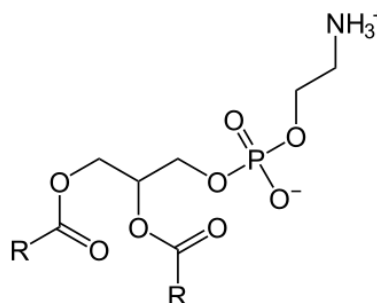
#### 9.6.3.1 Cardiolipin (CL)



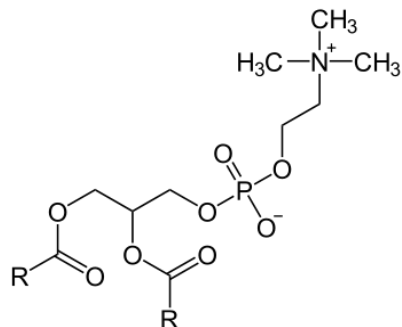
#### 9.6.3.2 Phosphatidylinositol (PI)



#### 9.6.3.3 Phosphatidylethanolamine (PE)

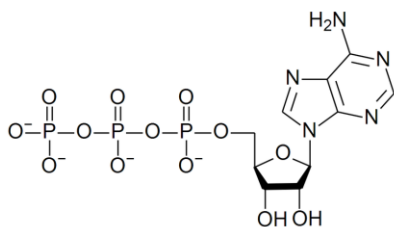


### 9.6.3.4 Phosphatidylcholine (PC), lecithine

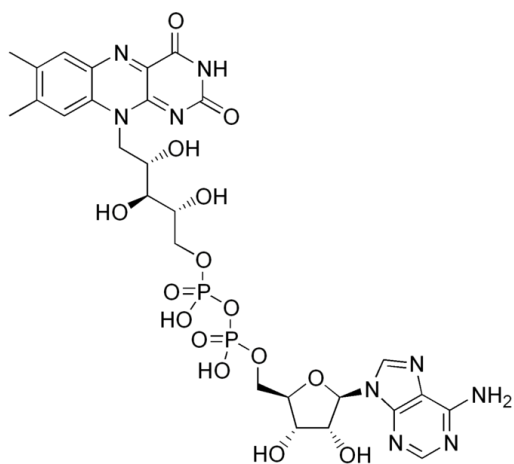


## 9.6.4 Cofactors

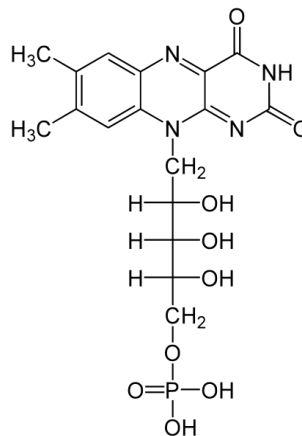
### 9.6.4.1 Adenosine-triphosphate (ATP)



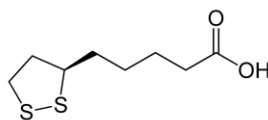
### 9.6.4.2 Flavin-adenine-dinucleotide (FAD)



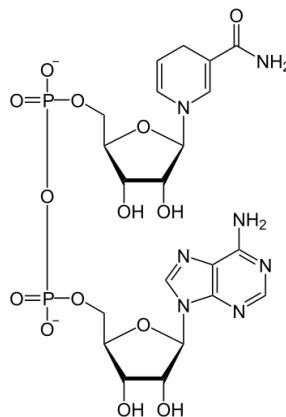
### 9.6.4.3 Flavin-mononucleotide (FMN)



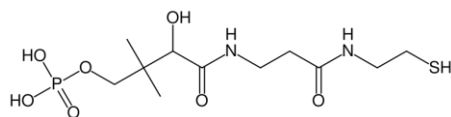
### 9.6.4.4 $\alpha$ -Lipoic acid (LA)



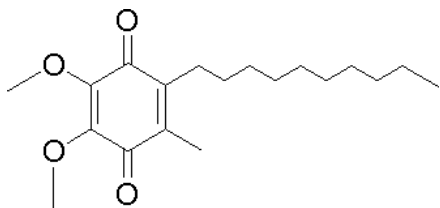
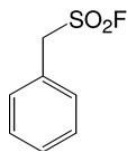
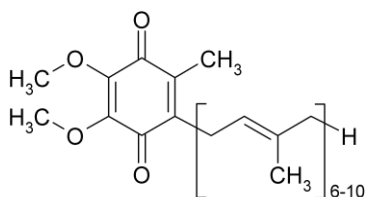
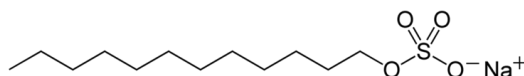
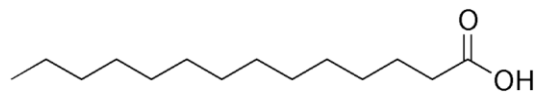
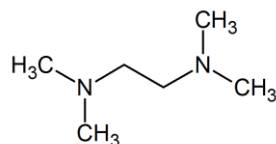
### 9.6.4.5 Nicotinamide-adenine- dinucleotide (NADH)



### 9.6.4.6 Phosphopantetheine





**9.6.4.7 *n*-decylubiquinone (DBQ)****9.6.5.2 Phenylmethylsulfonyl Flouride (PMSF)****9.6.4.8 Ubiquinone****9.6.5.3 Sodium-dodecylsulfate (SDS)****9.6.5 Other Structures****9.6.5.1 Myristic Acid****9.6.5.4 Tetramethylethylenediamine (TEMED)**



---

## 10 ABBREVIATIONS

(mt)DNA	(mitochondrial) deoxy ribonucleic acid
2D BN/SDS PAGE	two dimensional blue native/sodium dodecyl sulfate polyacrylamide gel electrophoresis
ACC. No.	accession number
ACP	acyl carrier protein
ACPM	mitochondrial acyl carrier protein
AT	acyl transferase
ATP	adenosine triphosphate
ADP	adenosine diphosphate
BN-PAGE	blue-native polyacrylamide gel electrophoresis
bp	base pair
BSA	bovine serum albumin
CoA	coenzyme A
DBQ	<i>n</i> -decylubiquinone
DH	dehydratase
dNADH	deamino-nicotinamide-adenine-dinucleotide (reduced form)
DQA	2-decyl-4-quinazolinyl amine
dSDS-PAGE	doubled sodium dodecylsulfate-polyacrylamide gel electrophoresis
EPR	electron paramagnetic resonance
ER	enoylreductase
ESI-MS	electrospray ionization mass spectrometry
ETC	electron transport chain
FAD	flavin adenine dinucleotide
FADH <sub>2</sub>	flavin adenine dinucleotide (reduced form)

---

FAS	fatty acid synthase
FeS	iron-sulphur cluster
FMN	flavin mononucleotide
FP	flavo-protein
HAR	hexa-ammine-ruthenium(III)-chloride
HP	hydrophobic protein
IMM	inner mitochondrial membrane
IP	iron-protein
kb	kilobase
KGDH	$\alpha$ -ketoglutarate dehydrogenase
KR	$\beta$ -ketoreductase
KS	$\beta$ -ketosynthase
LHON	Leber's hereditary optic neuropathy
MALDI-TOF-MS	matrix-assisted laser desorption/ionization-time of flight mass spectrometry
MAT	malonyl-coA-/acetyl-coA-ACP transacylase
MPT	malonyl/palmitoyl transferase
MST	3-mercaptopyruvate sulfurtransferase
NAD <sup>+</sup>	nicotinamide-adenine-dinucleotide (oxidised form)
NADH	nicotinamide-adenine-dinucleotide (reduced form)
NDH-2(i)	external alternative NADH Dehydrogenase (internal)
ORF	open reading frame
OXPPOS	oxidative phosphorylation
PCR	polymerase chain reaction
PDH	pyruvate dehydrogenase
PMSF	phenylmethylsulfonyl flouride

PP	pantetheine-4'-phosphate
PT	phosphopantetheine transferase
Q	ubiquinone
Q <sub>1</sub>	quinone with 1 isoprenyl side chain
QH <sub>2</sub>	ubihydroquinone (Ubiquinol)
ROS	reactive oxygen species
RP-HPLC	reversed-phase high performance liquid chromatography
SDS	dodecylsulfate Na-salt
STMD	single transmembrane domain
TE	thioesterase
TMD	transmembrane domain
TST	thiosulfate sulfurtransferase
V <sub>D</sub>	ATP-ase synthase dimer



## 11 LIST OF FIGURES

<b>Figure 1.1</b>	<i>Schematic representation of the mitochondrial electron transfer chain</i> .....	2
<b>Figure 1.2</b>	<i>Supramolecular molecular structures of the respiratory chain complexes</i> .....	3
<b>Figure 1.3</b>	<i>Schematic representation of a binuclear and a tetranuclear iron-sulfur cluster</i> .....	5
<b>Figure 1.4</b>	<i>Structure of the hydrophilic domain of complex I from <i>T. thermophilus</i> and electron microscopic reconstruction of <i>Y. lipolytica</i> enzyme</i> .....	6
<b>Figure 1.5</b>	<i>Subcomplexes and subunits of bovine heart complex I</i> .....	8
<b>Figure 1.6</b>	<i>dSDS-PAGE of purified complex I from <i>Y. lipolytica</i></i> .....	12
<b>Figure 1.7</b>	<i>The acyl carrier protein structure</i> .....	15
<b>Figure 1.8</b>	<i>Structural formula for the pantetheine-4'-phosphate-ACP</i> .....	16
<b>Figure 1.9</b>	<i>Reaction sequence in fatty acid synthesis</i> .....	17
<b>Figure 1.10</b>	<i>Structure of type I fatty acid synthase complexes</i> .....	18
<b>Figure 1.11</b>	<i>Superimposed NMR structures of ACP from <i>Mycobacterium tuberculosis</i></i> .....	19
<b>Figure 1.12</b>	<i>Structures of the mitochondrial acyl carrier proteins</i> .....	20
<b>Figure 1.13</b>	<i>Reaction sequence of lipoic acid synthesis in mitochondria</i> .....	21
<b>Figure 1.14</b>	<i>Scheme representing the sulfur-transfer reaction catalyzed by rhodanese</i> .....	24
<b>Figure 1.15</b>	<i>Overall structure of <i>A. vinelandii</i> rhodanese</i> .....	25
<b>Figure 2.1</b>	<i>Maps of plasmids</i> .....	34
<b>Figure 3.1</b>	<i>Generation of ACPM deletion constructs</i> .....	58
<b>Figure 3.2</b>	<i>Deletion strategy for ACPMs</i> .....	59
<b>Figure 3.3</b>	<i>The PCR test for the deletion of ACPM genes</i> .....	60
<b>Figure 3.4</b>	<i>Plasmid pUB4 containing mutated versions of ACPMs</i> .....	61
<b>Figure 3.5</b>	<i>Sections of DNA sequence pherograms from ACPM point mutants</i> .....	62
<b>Figure 3.6</b>	<i>PCR test for presence of ACPM2-S88A gene</i> .....	63
<b>Figure 3.7</b>	<i>Test digest of pUB4 plasmid containing tagged versions of ACPMs</i> .....	64
<b>Figure 3.8</b>	<i>Sections of DNA sequence pherograms from ACPM tagged versions</i> .....	64
<b>Figure 3.9</b>	<i>2D-BN/SDS PAGE analysis of <i>Y. lipolytica</i> mitochondrial membranes</i> .....	67
<b>Figure 3.10</b>	<i>Complex I subcomplexes in <i>acpm2</i>Δ and the <i>acpm2</i>Δ,pACPM2-S88A strains</i> .....	69
<b>Figure 3.11</b>	<i>Thin layer chromatography (TLC) of lipids extracted from intact mitochondria</i> ....	70
<b>Figure 3.12</b>	<i>HPLC profiles of phospholipids extracted from <i>Y. lipolytica</i> mitochondria</i> .....	71

---

<b>Figure 3.13</b> The phospholipid composition of purified intact mitochondria.....	73
<b>Figure 3.14</b> The phospholipid to protein ratio in intact mitochondria.....	74
<b>Figure 3.15</b> The MALDI-MS spectrum of lyso-phosphatidyl-ethanolamine identified in fr. 28 ...	75
<b>Figure 3.16</b> Mass Spectra of ACPM subunits .....	77
<b>Figure 3.17</b> Analysis of tagged versions of ACPMs in dSDS-PAGE.....	78
<b>Figure 3.18</b> Localization of tagged versions of ACPM in mitochondrial fractions.....	79
<b>Figure 3.19</b> Gel filtration purified complex I contains rhodanese-like protein .....	81
<b>Figure 3.20</b> MALDI-TOF mass spectrum of in-gel digested 34.6 kDa protein of <i>Y. lipolytica</i> complex I.....	82
<b>Figure 3.21</b> Steps of <i>st1</i> Δ strain generation .....	84
<b>Figure 3.22</b> Test digest for the number of hygromycin B inserts .....	85
<b>Figure 3.23</b> Strategy for generation of the <i>st1</i> Δ strain .....	86
<b>Figure 3.24</b> PCR test for deletion of the <i>st1</i> gene .....	87
<b>Figure 3.25</b> Test digest of the pUB4 plasmid containing the <i>st1-strepII</i> insert.....	88
<b>Figure 3.26</b> Section of DNA sequence pherogramm from the <i>st1-strepII</i> strain.....	88
<b>Figure 3.27</b> Growth curves of the <i>st1</i> Δ strain of <i>Y. lipolytica</i> .....	90
<b>Figure 3.28</b> BN-PAGE of mitochondrial membranes from <i>st1</i> Δ strain .....	91
<b>Figure 3.29</b> <i>St1</i> subunit dissociates from complex I in BN-PAGE.....	92
<b>Figure 3.30</b> EPR spectra of complex I from the parental and the deletion strains.....	93
<b>Figure 4.1</b> Sequence alignment of ACPM1 and ACPM2 from <i>Y. lipolytica</i> .....	95
<b>Figure 4.2</b> Predicted structures of ACPMs from <i>Y. lipolytica</i> .....	97
<b>Figure 4.3</b> Hydropathy plots of ACPM subunits .....	98
<b>Figure 4.4</b> Deletion of the NUJM complex I subunit leads to formation of subcomplexes .....	100
<b>Figure 4.5</b> Doubled SDS-PAGE of complex I isolated from 39kDa subunit mutant strains .....	103
<b>Figure 4.6</b> Sequence comparison of the <i>st1</i> active-site loop with typical TST and MST loops...	103
<b>Figure 4.7</b> Predicted structure of the <i>st1</i> sulfurtransferase from <i>Y. lipolytica</i> .....	105
<b>Figure 4.8</b> Hydropathy plots of <i>st1</i> and ND6 subunits.....	106
<b>Figure 9.1</b> The fragment of <i>st1</i> gene encoding rhodanese .....	141
<b>Figure 9.2</b> The ACPM1 gene used for generating the mutants .....	143
<b>Figure 9.3</b> The ACPM2 gene used for generating the mutants .....	145



---

<b>Figure 9.4</b> Alignment of ACPM1 and ACPM2 subunits with acyl carrier proteins from other species .....	153
<b>Figure 9.5</b> Alignment of <i>Y. lipolytica</i> ACPM1 and ACPM2 subunits .....	154
<b>Figure 9.6</b> Alignment of the <i>st1</i> subunit with tandem rhodanese domain repeat enzymes from other organisms .....	157
<b>Figure 9.7</b> The cladogram of tandem rhodanese domain repeat enzymes aligned in 9.4.3 .....	158
<b>Figure 9.8</b> Mitochondrial beta-keto-acyl synthase ( <i>CEM1</i> ) .....	159
<b>Figure 9.9</b> 2-enoyl thioester reductase ( <i>ETR1</i> ) .....	160
<b>Figure 9.10</b> Mitochondrial acetyl-coenzyme A carboxylase ( <i>HFA1</i> ) .....	162
<b>Figure 9.11</b> Mitochondrial 3-hydroxyacyl-thioester dehydratase ( <i>HTD2</i> ) .....	163
<b>Figure 9.12</b> Predicted malonyl-CoA:ACP transferase ( <i>MCT1</i> ) .....	163
<b>Figure 9.13</b> Mitochondrial 3-oxoacyl-[acyl-carrier-protein] reductase ( <i>OAR1</i> ) .....	164
<b>Figure 9.14</b> The MALDI-MS spectrum of cardiolipin identified in fraction 18 .....	165
<b>Figure 9.15</b> The MALDI-MS spectrum of cardiolipin identified in fraction 19 .....	166
<b>Figure 9.16</b> The MALDI-MS spectrum of phosphatidylethanolamine identified in fraction 24 .....	166
<b>Figure 9.17</b> The MALDI-MS spectrum of phosphatidylinositol identified in fraction 28 .....	167
<b>Figure 9.18</b> The MALDI-MS spectrum of phosphatidic acid identified in fraction 30 .....	167
<b>Figure 9.19</b> The MALDI-MS spectrum of lyso-phosphatidylcholine identified in fraction 52 ...	168



## 12 LIST OF TABLES

<i>Table 1.1. Similarity and identity scores for pairwise comparisons between Y. lipolytica ACPM1 or ACPM2 and ACP from other organisms .....</i>	15
<i>Table 3.1 Catalytic activities of mitochondrial membranes and complex I.....</i>	66
<i>Table 3.2 Tryptic peptides of the 34.6 kDa protein identified by MALDI-TOF MS.....</i>	82
<i>Table 3.3. Similarity and identity scores for pairwise comparisons between Y. lipolytica sulfurtransferase and tandem rhodanese domain repeat enzymes from other organisms .....</i>	83
<i>Table 3.4 Activities of mitochondrial membranes and purified complex I from Y. lipolytica .....</i>	92
<i>Table 9.1 Oligonucleotides for generation of the st1 deletion strain .....</i>	146
<i>Table 9.2 Oligonucleotides for checking of the deletion via PCR.....</i>	146
<i>Table 9.3 Oligonucleotides for creating the strepII-tagged version of st1 gene .....</i>	146
<i>Table 9.4 Oligonucleotides for sequencing of the st1 gene.....</i>	146
<i>Table 9.5 Oligonucleotides for generation of the ACPM1 deletion strain .....</i>	147
<i>Table 9.6 Oligonucleotides for checking of the deletion via PCR.....</i>	147
<i>Table 9.7 Oligonucleotides for creating the strepII-tagged version of ACPM1 gene.....</i>	147
<i>Table 9.8 Oligonucleotides for sequencing of the ACPM1 gene .....</i>	147
<i>Table 9.9 Oligonucleotides for mutating the phosphopantetheine-binding serine (S66A).....</i>	147
<i>Table 9.10 Oligonucleotides for generation of the ACPM2 deletion strain .....</i>	148
<i>Table 9.11 Oligonucleotides for checking of the deletion via PCR.....</i>	148
<i>Table 9.12 Oligonucleotides for creating the flag-tagged version of ACPM2 gene .....</i>	148
<i>Table 9.13 Oligonucleotides for sequencing of the ACPM2 gene .....</i>	148
<i>Table 9.14 Oligonucleotides for mutating the phosphopantetheine-binding serine (S88A).....</i>	148
<i>Table 9.15 Oligonucleotides for swap strategy of ACPM1 gene.....</i>	149
<i>Table 9.16 Oligonucleotides for swap strategy of ACPM2 gene.....</i>	149
<i>Table 9.17 Oligonucleotides for URA3 gene .....</i>	149
<i>Table 9.18 Central and accessory subunits of Yarrowia lipolytica complex I .....</i>	152



---

## 13 CURRICULUM VITAE

### Personal Details

---

Name: **DOBRYNIN, Krzysztof**  
Address: Schossstr. 62, D-60486 Frankfurt am Main  
Tel.: + 49 172 14 75 676  
E-mail: krisdobrynin@gmail.com  
Birth: 05.08.1981, Lodz, Poland  
Nationality: Polish  
Gender: Male  
Family Status: Single



### Education

---

01/2005 – 06/2010 **Ph. D. Thesis**  
Prof. Ulrich Brandt, Molecular Bioenergetics  
Biochemistry, Chemistry and Pharmacy Department  
Goethe University, Frankfurt am Main, Germany  
Focus: Accessory subunits of complex I from aerobic yeast *Y. lipolytica*

07/2004 – 12/2004 **IAESTE Laboratory Internship**  
Prof. Robert Tampe, Institute of Cellular Biochemistry,  
Biocenter Frankfurt, Germany  
Focus: Characterization of ATP-binding cassette transporter proteins

02/2004 – 06/2004 **Master Thesis Project**  
Dr. Thierry Chardot,  
Institute National Agronomique Paris-Grignon, France  
Focus: Oleosins, new emulsifiers from plants

10/1999 – 06/2004 **Technical University of Lodz, Poland**  
Prof. Stanislaw Bielecki, International Faculty of Engineering,  
Molecular Biotechnology and Technical Biochemistry Department  
**Master of Science**

02/2002 – 02/2003 **University of Applied Life Sciences, Vienna, Austria**  
Erasmus Scholarship

08/1998 – 06/1999 **High School Pottsville, AR, USA**  
Secondary School Certificate

09/1996 – 06/1998 High School XXIX, Lodz, Poland

Frankfurt am Main, 08.07.2010